

**THE POTENTIAL ROLE OF
ENDOTHELIAL PROGENITOR CELLS FOR
THERAPEUTIC ANGIOGENESIS**

PETER COLIN RAE

A thesis submitted for the degree of

DOCTOR OF PHILOSOPHY



Centre for Cardiovascular Sciences

*School of Clinical and Experimental Medicine
College of Medical and Dental Sciences
University of Birmingham*

August 2011

UNIVERSITY OF
BIRMINGHAM

University of Birmingham Research Archive

e-theses repository

This unpublished thesis/dissertation is copyright of the author and/or third parties. The intellectual property rights of the author or third parties in respect of this work are as defined by The Copyright Designs and Patents Act 1988 or as modified by any successor legislation.

Any use made of information contained in this thesis/dissertation must be in accordance with that legislation and must be properly acknowledged. Further distribution or reproduction in any format is prohibited without the permission of the copyright holder.

ABSTRACT

The natural angiogenic response of the vasculature to cardiovascular disease has been shown, at least in part, to involve circulating endothelial progenitor cells (EPCs). However, the native response is often insufficient to restore vascularity without additional intervention. In this study the angiogenic activity of EPCs, demonstrated by *in vitro* tubule formation, confirmed the suggested potential of EPCs to be used therapeutically. However, as EPCs are found in limited circulating numbers, embryonic stem cells (ESCs) and induced pluripotent stem cells (iPSCs) were also investigated as sources of donor EPCs for transplantation. Here ESCs, but not iPSCs, were shown to generate cells with a genetic and proteomic profile, as well as an angiogenic potential, identical to natural EPCs. Using an *in vivo* mouse model of hindlimb ischemia, this investigation illustrated the preferential binding of transplanted EPCs at sites of angiogenic stimulation, and revealed the importance of platelets in the recruitment of circulating EPCs. In particular, using *in vitro* aggregation and flow-based adhesion assays, the adhesion molecule P-selectin was shown to play a significant role in this recruitment mechanism. In conclusion, this study has demonstrated that EPC transplantation has abundant potential for development into a viable and efficacious therapeutic angiogenic treatment.

CONTENTS

CHAPTER 1: INTRODUCTION

1.1 The mammalian vasculature	1
1.1.1 The structure of blood vessels.....	4
1.1.2 Arteries, capillaries and veins	6
1.1.3 Functions of the vascular endothelium	7
1.1.4 Interactions with the endothelium	
1.1.4.1 Fluid shear stress	10
1.1.4.2 Inflammatory cells and cytokines	13
1.1.4.3 Platelets and coagulation factors	14
1.2 The development of blood vessels	15
1.2.1 Vasculogenesis vs. angiogenesis.....	16
1.2.2 Mechanisms of angiogenesis	16
1.2.3 Assessing vessel growth.....	22
1.2.2.1 <i>In vitro</i> angiogenesis assays	22
1.2.2.2 <i>In vivo</i> angiogenesis assays	24
1.2.2.3 A gold standard angiogenesis assay?.....	25
1.3 Embryonic EPCs in the adult circulation?	27
1.3.1 EPCs in cardiovascular disease	28
1.3.2 A therapeutic potential for EPCs?.....	29
1.3.3 Defining the EPC	31
1.4 The potential of pluripotency	
1.4.1 Embryonic stem cells.....	33
1.4.2 Regaining potential with induced pluripotency.....	35
1.5 Hypothesis and objectives	38

CHAPTER 2: MATERIALS & METHODS

2.1 Cell culture	40
2.1.1 Cell lines	
2.1.1.1 Endothelial cells (ECs)	41
2.1.1.2 Endothelial progenitor cells (EPCs)	41

2.1.2	Subculture of cells.....	41
2.1.3	Cell counting.....	42
2.1.4	Assessment of cell viability using Trypan blue	42
2.1.5	Stem cell culture	
2.1.5.1	Murine embryonic fibroblast (MEF) feeder cells.....	45
2.1.5.2	Murine embryonic stem cells (ESCs) and induced pluripotent stem cells (iPSCs).....	46
2.1.5.3	Directed differentiation of ESCs and iPSCs.....	46
2.1.6	Quantum dot labelling of EPCs.....	48
2.1.7	Culture of cells on acid-washed coverslips for immunocytochemistry	49
2.1.8	Uptake of acetylated low-density lipoprotein (ac-LDL)	50
2.1.9	<i>In vitro</i> scratch wound assay.....	50
2.1.10	Cryopreservation of cultured cells	51
2.2	Gene expression analysis	
2.2.1	Nucleic acid isolation	
2.2.1.1	Extraction of RNA from cultured cells.....	52
2.2.1.2	Extraction of RNA from ECMatrix tubule formation gels	53
2.2.1.3	Removal of contaminating DNA by DNase I treatment.....	54
2.2.1.4	Spectrophotometry of nucleic acids.....	54
2.2.1.5	Denaturing RNA agarose gel electrophoresis.....	55
2.2.2	Reverse transcription (RT).....	56
2.2.3	Reverse transcription polymerase chain reaction (RT-PCR)	
2.2.3.1	Oligonucleotide primer design	56
2.2.3.2	Reaction conditions for RT-PCR	58
2.2.3.3	cDNA separation by agarose gel electrophoresis	60
2.2.3.4	Purification of cDNA from agarose gels.....	60
2.2.4	DNA sequencing	
2.2.4.1	Sequencing of RT-PCR products from purified agarose gels	61
2.2.4.2	DNA cloning by plasmid vector	62
2.2.4.3	Transformation of competent <i>E. coli</i> cells	62
2.2.4.4	Purification of plasmid DNA for sequencing.....	64
2.2.5	Quantitative real-time PCR (qPCR)	
2.2.5.1	Detection of DNA using SYBR Green dye	65
2.2.5.2	Preparation of DNA standards for qPCR	68
2.2.5.3	Reaction conditions for qPCR.....	68
2.2.5.4	Relative quantification of DNA.....	69
2.3	Immunocytochemistry (ICC)	
2.3.1	Preparation of coverslip-cultured cells for ICC.....	70
2.3.2	ICC protocol	

2.3.2.1	Lectin staining.....	71
2.3.2.2	Primary antibodies	71
2.3.2.3	Secondary antibodies	71
2.3.3	Preparation of ICC slides for imaging.....	74
2.4	Microscopy and imaging	
2.4.1	Fluorescent microscopy.....	74
2.4.2	Confocal microscopy.....	75
2.5	<i>In vitro</i> tubule formation assay	75
2.5.1	Preparation of ECMatrix assay gels	76
2.5.2	Assay protocol.....	76
2.5.3	Quantification of angiogenic potential	
2.5.3.1	Image processing.....	76
2.5.3.2	Quantification by node counting.....	78
2.5.3.3	Quantification by branch length measurement	78
2.5.4	<i>In vitro</i> EPC transplantation	79
2.5.5	Isolation of assayed cells for gene expression analysis	79
2.6	Preparation of washed murine platelets	
2.6.1	Exsanguination <i>via</i> inferior vena cava (IVC)	80
2.6.2	Isolation of platelets from whole blood.....	80
2.6.3	Counting washed murine platelets.....	82
2.7	<i>In vitro</i> cell aggregation assay	
2.7.1	Inhibition of adhesion by antibody and biochemical blockade	84
2.7.2	Aggregation assay protocol.....	85
2.7.3	Quantification of aggregation using Coulter size distribution	87
2.8	<i>In vitro</i> flow adhesion assay	
2.8.1	Preparation of glass microslides.....	87
2.8.2	Immobilisation of washed murine platelets on glass microslides.....	89
2.8.3	Inhibition of adhesion by antibody and biochemical blockade	89
2.8.4	<i>In vitro</i> flow adhesion assay protocol.....	89
2.8.5	Adherent cell spreading assay.....	91
2.9	<i>In vivo</i> experiments	
2.9.1	<i>Animal (Scientific Procedures) Act 1986</i>	94
2.9.1.1	Schedule 1 methods of termination	94
2.9.2	Anaesthesia and preparation for surgery	94
2.9.2.1	Cannulation of right common carotid artery (CCA).....	95
2.9.3	<i>In vivo</i> EPC transplantation	
2.9.3.1	Platelet depletion by administration of α -GPIIb α antibody	97

2.9.3.2 Acute hindlimb ischaemia by femoral artery (FA) ligation.....	98
2.9.3.3 Percutaneous sciatic nerve stimulation	98
2.9.3.4 Chronic hindlimb ischaemia by FA ligation.....	98
2.9.3.5 Overload of synergistic hindlimb muscles by extirpation of <i>m. tibialis anterior</i>	100
2.9.3.6 Intravascular injection of fluorescent EPCs	102
2.9.3.7 Tissue harvesting.....	102
2.10 Flow cytometry	
2.10.1 Tissue digestion.....	102
2.10.2 Flow cytometric analysis of tissue digests	103
2.11 Statistical analysis	103
 CHAPTER 3: CHARACTERISATION OF ENDOTHELIAL PROGENITOR CELLS	
3.1 Introduction	104
3.2 Hypothesis & objectives	108
3.3 Methods	
3.3.1 Optimisation of reaction conditions for RT-PCR and qPCR analysis.....	109
3.3.2 Optimisation of <i>in vitro</i> tubule formation assay.....	109
3.3.3 ICC of ECMatrix gel coverslips.....	113
3.4 Results	
3.4.1 Expression of lineage-specific markers in EPCs and ECs	
3.4.1.1 qPCR analysis of mRNA transcripts	115
3.4.1.2 ICC analysis of protein expression	116
3.4.1.3 Lectin staining and ac-LDL uptake.....	122
3.4.2 Assessment of angiogenic potential of EPCs and ECs	
3.4.2.1 Quantification of <i>in vitro</i> tubule formation using node counting.....	125
3.4.2.2 Quantification of <i>in vitro</i> tubule formation using branch length measurement.....	127
3.4.2.3 qPCR analysis of endothelial mRNA expression during <i>in vitro</i> tubule formation.....	127
3.5 Discussion	134
 CHAPTER 4: DERIVATION OF EPCs BY PLURIPOTENT STEM CELL DIFFERENTIATION	
4.1 Introduction	142
4.2 Hypothesis & objectives	144
4.3 Methods	
4.3.1 Optimisation of stem cell culture conditions.....	145
4.4 Results	
4.4.1 Expression of lineage-specific markers in differentiating ESCs and iPSCs	
4.4.1.1 qPCR analysis of mRNA transcripts	148

4.4.1.2 ICC analysis of protein expression	156
4.4.2 Assessment of angiogenic potential of ESCs and iPSCs	
4.4.2.1 Quantification of <i>in vitro</i> tubule formation using node counting.....	162
4.4.2.2 Quantification of <i>in vitro</i> tubule formation using branch length measurement.....	164
4.4.2.3 qPCR analysis of endothelial mRNA expression during <i>in vitro</i> tubule formation.....	164
4.5 Discussion	170
CHAPTER 5: <i>IN VITRO</i> TRANSPLANTATION OF ENDOTHELIAL PROGENITOR CELLS	
5.1 Introduction	180
5.2 Hypothesis & objectives	182
5.3 Methods	
5.3.1 Optimisation of Qdot labelling of EPCs	183
5.3.2 <i>In vitro</i> scratch wound assay of labelled EPCs.....	183
5.4 Results	
5.4.1 Node count quantification of tubule formation following transplantation	187
5.4.2 Branch length quantification of tubule formation following transplantation	188
5.4.3 Localisation of transplanted EPCs	188
5.4.4 qPCR analysis of mRNA expression following EPC transplantation	193
5.5 Discussion	198
CHAPTER 6: PLATELETS IN ENDOTHELIAL PROGENITOR CELL RECRUITMENT	
6.1 Introduction	203
6.2 Hypothesis & objectives	211
6.3 Methods	
6.3.1 Cell dissociation treatment	212
6.4 Results	
6.4.1 <i>In vitro</i> cell aggregation assay	
6.4.1.1 Blockade of selectin-mediated adhesion.....	215
6.4.1.2 Inhibition of α IIb β 3 integrin or platelet activation	217
6.4.2 <i>In vitro</i> flow adhesion assay.....	221
6.4.2.1 Blockade of selectin-mediated adhesion.....	224
6.4.2.2 Inhibition of GPVI binding	227
6.4.2.3 Inhibition of platelet activation.....	230
6.4.3 Adherent cell spreading assay.....	230
6.5 Discussion	237

CHAPTER 7: <i>IN VIVO</i> TRANSPLANTATION OF ENDOTHELIAL PROGENITOR CELLS	
7.1 Introduction	245
7.2 Hypothesis & objectives	252
7.3 Methods	
7.3.1 Optimisation of percutaneous sciatic nerve stimulation.	253
7.3.2 Route of administration of anti-GPIIb α platelet depletion antibody	255
7.4 Results	
7.4.1 EPC recruitment in abdominal viscera	258
7.4.2 Acute ischaemia	260
7.4.3 Chronic ischaemia.....	262
7.4.4 Overload of synergistic muscles by unilateral extirpation	264
7.5 Discussion	266
CHAPTER 8: FINAL CONCLUSIONS	277
REFERENCES	286
APPENDIX I: CULTURE MEDIA, REAGENTS & STOCK SOLUTIONS	314
APPENDIX II: MULTIPLE mRNA SEQUENCE ALIGNMENTS	317
APPENDIX III: PUBLICATIONS	319

FIGURES

Figure 1.1. The mammalian cardiovascular system	2
Figure 1.2. The structure of blood vessels.....	5
Figure 1.3. Comparison of arteries, capillaries and veins	8
Figure 1.4. Vasculogenesis.....	17
Figure 1.5. Sprouting angiogenesis.....	18
Figure 1.6. Splitting angiogenesis	21
Figure 1.7. Derivation of ESCs.....	34
Figure 1.8. Cellular reprogramming	36
Figure 2.1. Trypan blue exclusion assay.....	44
Figure 2.2. Hanging droplet method for directed differentiation	47
Figure 2.3. Denaturing RNA agarose gel electrophoresis.....	57
Figure 2.4. pCR 4-TOPO plasmid vector.....	63
Figure 2.5. Real-time DNA quantification using SYBR Green chemistry	66
Figure 2.6. Immunocytochemistry by antibody labelling.....	73
Figure 2.7. Image processing of <i>in vitro</i> tubule formation assays.....	77
Figure 2.8. Exsanguination <i>via</i> the inferior vena cava	81
Figure 2.9. Counting platelets using Coulter electrical impedance	83
Figure 2.10. <i>In vitro</i> cell-based aggregation assay.....	86
Figure 2.11. Quantification of aggregation using Coulter size distribution.....	88
Figure 2.12. <i>In vitro</i> flow adhesion assay.....	90
Figure 2.13. Quantification of <i>in vitro</i> captured cell spreading assays	93
Figure 2.14. Cannulation of the right common carotid artery	96

Figure 2.15. Acute hindlimb ischaemia by femoral artery ligation	99
Figure 2.16. Overload of synergistic hindlimb muscles by unilateral extirpation	101
Figure 3.1. Optimisation of RT-PCR reaction conditions	110
Figure 3.2. qPCR dissociation curve analysis.....	111
Figure 3.3. Optimisation of <i>in vitro</i> tubule formation assay	112
Figure 3.4. ICC of cells cultured on ECMatrix gel-coated coverslips	114
Figure 3.5. Relative expression of <i>VEGFR2</i> in EPCs and ECs.....	117
Figure 3.6. Relative expression of <i>VE-cadherin</i> in EPCs and ECs	118
Figure 3.7. Relative expression of <i>CD31</i> in EPCs and ECs	119
Figure 3.8. Detection of VEGFR2, CD133 and CD34 proteins in EPCs	120
Figure 3.9. Detection of VEGFR2, CD133 and CD34 proteins in ECs	121
Figure 3.10. Lectin staining and uptake of ac-LDL by EPCs and ECs.....	124
Figure 3.11. Assessment of angiogenic activity of EPCs and ECs by node counting	126
Figure 3.12. Assessment of angiogenic activity of EPCs and ECs by branch length	128
Figure 3.13. Relative expression of <i>VEGFR2</i> in tubule-forming EPCs and ECs.....	130
Figure 3.14. Relative expression of <i>VE-cadherin</i> in tubule-forming EPCs and ECs	131
Figure 3.15. Relative expression of <i>CD31</i> in tubule-forming EPCs and ECs	132
Figure 4.1. Optimisation of stem cell culture conditions	146
Figure 4.2. Relative expression of <i>VEGFR2</i> in differentiating ESCs	149
Figure 4.3. Relative expression of <i>VEGFR2</i> in differentiating iPSCs.....	151
Figure 4.4. Relative expression of <i>VE-cadherin</i> in differentiating ESCs	152
Figure 4.5. Relative expression of <i>VE-cadherin</i> in differentiating iPSCs	153
Figure 4.6. Relative expression of <i>CD31</i> in differentiating ESCs.....	154
Figure 4.7. Relative expression of <i>CD31</i> in differentiating iPSCs	155
Figure 4.8. Detection of VEGFR2 protein in differentiating ESCs and iPSCs	157
Figure 4.9. Detection of CD133 protein in differentiating ESCs and iPSCs.....	158
Figure 4.10. Detection of CD34 protein in differentiating ESCs and iPSCs.....	159

Figure 4.11. Assessment of angiogenic activity of d7 ESCs and iPSCs by node counting.....	163
Figure 4.12. Assessment of angiogenic activity of d7 ESCs and iPSCs by branch length.....	165
Figure 4.13. Relative expression of <i>VEGFR2</i> in tubule-forming d7 ESCs and iPSCs	166
Figure 4.14. Relative expression of <i>VE-cadherin</i> in tubule-forming d7 ESCs and iPSCs	167
Figure 4.15. Relative expression of <i>CD31</i> in tubule-forming d7 ESCs and iPSCs.....	169
Figure 4.16. Timeline of <i>VEGFR2</i> and <i>CD31</i> expression in differentiated ESCs.....	172
Figure 5.1. Optimisation of Qdot labelling of EPCs	184
Figure 5.2. <i>In vitro</i> scratch wound assay of Qdot-labelled EPCs	185
Figure 5.3. Effect of Qdot labelling on EPC migration rate.....	186
Figure 5.4. Tubule formation following EPC transplantation, quantified by node counting ..	189
Figure 5.5. Tubule formation following EPC transplantation, quantified by branch length ...	190
Figure 5.6. <i>In vitro</i> localisation of Qdot-labelled EPCs following 10% transplantation.....	191
Figure 5.7. <i>In vitro</i> localisation of Qdot-labelled EPCs following 50% transplantation.....	192
Figure 5.8. Relative expression of <i>VEGFR2</i> in EPC transplantation assays	194
Figure 5.9. Relative expression of <i>VE-cadherin</i> in EPC transplantation assays	195
Figure 5.10. Relative expression of <i>CD31</i> in EPC transplantation assays.....	197
Figure 6.1. Potential mediators of platelet-endothelial binding.....	207
Figure 6.2. The effect of cell dissociation solution on cell adhesion from flow	213
Figure 6.3. <i>In vitro</i> aggregation of EPCs, ECs and MEFs	216
Figure 6.4. <i>In vitro</i> aggregation of EPCs and ECs following non-specific selectin blockade ..	218
Figure 6.5. The effect of P-selectin blockade on <i>in vitro</i> aggregation of EPCs and ECs	219
Figure 6.6. <i>In vitro</i> aggregation following blockade of α IIb β 3 integrin	220
Figure 6.7. <i>In vitro</i> aggregation following clopidogrel/aspirin treatment	222
Figure 6.8. <i>In vitro</i> adhesion of EPCs, EC and MEFs to platelets from flow	223
Figure 6.9. <i>In vitro</i> flow adhesion of EPCs and ECs with increasing shear stress.....	225
Figure 6.10. <i>In vitro</i> flow adhesion of EPCs and ECs following selectin blockade	226
Figure 6.11. The effect of P-selectin blockade on <i>in vitro</i> flow adhesion of EPCs and ECs ...	228

Figure 6.12. <i>In vitro</i> flow adhesion of EPCs and ECs following platelet GPVI shedding.....	229
Figure. 6.13. The effect of abciximab on <i>in vitro</i> flow adhesion of EPCs and ECs	231
Figure 6.14. The effect of clopidogrel/aspirin on <i>in vitro</i> flow adhesion of EPCs and ECs.....	232
Figure 6.15. <i>In vitro</i> flow adhesion of EPCs prior to adherent cell spreading assays	233
Figure 6.16. Spreading of adherent EPCs following <i>in vitro</i> flow adhesion assays	234
Figure 6.17. EPC migration during adherent cell spreading assays.....	236
Figure 7.1. Optimisation of percutaneous sciatic nerve stimulation	254
Figure 7.2. Systemic platelet depletion by anti-GPIIb/IIIa antibody	256
Figure 7.3. Recruitment of EPCs in viscera following <i>in vivo</i> transplantation	259
Figure 7.4. <i>In vivo</i> recruitment of EPCs following acute hindlimb and platelet depletion.....	261
Figure 7.5. <i>In vivo</i> recruitment of EPCs following chronic hindlimb ischaemia.....	263
Figure 7.6. <i>In vivo</i> recruitment of EPCs following synergistic hindlimb muscle overload ...	265
Figure 7.7. Fibre type composition of murine hindlimb muscles	271
Figure 7.8. Proportional recruitment of EPCs following <i>in vivo</i> transplantation	275
Figure 8.1. <i>In vivo</i> fluorescence microscopy following EPC transplantation.....	280
Figure 8.2. Intravital microscopy following EPC transplantation	282
Figure 8.3. RT-PCR analysis of <i>PRH</i> expression in ESCs, EPCs and ECs	284

TABLES

Table 2.1. Primer sequences for RT-PCR	59
Table 2.2. Antibodies used for immunocytochemistry	72
Table 3.1. Quantification of protein expression in EPCs and ECs.....	123
Table 4.1. Optimisation of stem cell culture conditions	147
Table 4.1. Quantification of protein expression in differentiating ESCs.....	160
Table 4.2. Quantification of protein expression in differentiating iPSCs.....	161
Table 7.1. Comparison of <i>in vivo</i> cell transplantation regimes.....	248

ABBREVIATIONS

AF	Alexa Fluor
ANOVA	Analysis of variance
APES	3-aminopropyltriethoxysilane
bFGF	Basic fibroblast growth factor
BM	Bone marrow
BMMNCs	Bone marrow mononuclear cells
bp	Base pairs
cAMP	Cyclic adenosine monophosphate
CCA	Common carotid artery
CD31 / PECAM	Platelet-endothelial cell adhesion molecule
cDNA	Complementary deoxyribonucleic acid
CO ₂	Carbon dioxide
Ct	Threshold cycle
d	Day of differentiation
DAPI	4',6-diamidino-2-phenylindole
ddH ₂ O	Double-distilled water
DMEM	Dulbecco's modified Eagle's medium
DMSO	Dimethyl sulfoxide
DNA	Deoxyribonucleic acid
DNase	Deoxyribonuclease
dNTP	Deoxyribonucleic triphosphate
D-PBS	Dulbecco's phosphate buffered saline
dsDNA	Double-stranded deoxyribonucleic acid
EB	Embryoid body
EC	Endothelial cell
ECCM	Endothelial cell-conditioned medium
EDL	<i>m. extensor digitorum longus</i>

EDTA	Ethylenediaminetetraacetic acid
EGF	Epidermal growth factor
EHP	<i>m. extensor hallucis proprius</i>
EPC	Endothelial progenitor cell
EPO	Erythropoietin
ESC	Embryonic stem cell
FACS	Fluorescence-activated cell sorting
FBS	Foetal bovine serum
Flk-1	Foetal liver kinase 1 (murine VEGFR2)
G-CSF	Granulocyte colony-stimulating factor
GM-CSF	Granulocyte-macrophage colony-stimulating factor
HUVEC	Human umbilical vein endothelial cell
ICC	Immunocytochemistry
IGF	Insulin-like growth factor
IgG	Immunoglobulin G
IL	Interleukin
i.p.	Intraperitoneal
iPSC	Induced pluripotent stem cell
i.v.	Intravenous
LIF	Leukaemia inhibitory factor
LN ₂	Liquid nitrogen
MEF	Murine embryonic fibroblast
Mg ²⁺	Magnesium ion
MgCl ₂	Magnesium chloride
MMLV	Moloney murine leukaemia virus
MMP	Matrix metalloproteinase
mRNA	Messenger ribonucleic acid
MSC	Mesenchymal stem cell
NEAA	Non essential amino acids
NEC	No enzyme control
NO	Nitric oxide
NOS	Nitric oxide synthase
n.s.	Not significant

NTC	No template control
PBS	Phosphate buffered saline
PBSA	Phosphate buffered saline with albumin
PCR	Polymerase chain reaction
PDGF	Platelet-derived growth factor
PECAM / CD31	Platelet-endothelial cell adhesion molecule
PGI ₂	Prostacyclin
PI3K	Phosphatidylinositide 3-kinase
Qdot	Quantum dot
qPCR	Quantitative real-time polymerase chain reaction
RNA	Ribonucleic acid
RNase	Ribonuclease
RT	Reverse transcription
RTase	Reverse transcriptase
RT-PCR	Reverse transcription polymerase chain reaction
s.c.	Subcutaneous
SCF	Stem cell factor
SDF-1	Stromal cell-derived factor-1
SEM	Standard error of mean
SMC	Smooth muscle cell
Sol	<i>m. soleus</i>
ssDNA	Single-stranded deoxyribonucleic acid
T _a	Annealing temperature
TA	<i>m. tibialis anterior</i>
TAE	Tris-acetate-ethylenediaminetetraacetic acid
TGF-β	Transforming growth factor beta
T _m	Melting temperature
v/v	Volume/volume
VEGF	Vascular endothelial growth factor
VEGFR	Vascular endothelial growth factor receptor
w/v	Weight/volume

CHAPTER 1:

INTRODUCTION

1.1 The mammalian vasculature

The mammalian body is a complex network of interacting biological systems, all of which are both involved in and highly dependent upon homeostatic mechanisms that strive to maintain relative constancy within the internal environment (Kahn & Westerhoff, 1993). Furthermore, owing to the interconnected nature of the body's many biological systems, regulation by homeostasis is as much dependent on the connections between these individual systems as it is on the functions of the systems themselves. Accordingly, the mammalian circulatory system, in fact that of all higher vertebrates, has evolved into a highly efficient closed system for blood distribution and organ interaction. In contrast, invertebrates such as arthropods and molluscs, have a much less efficient open circulatory system and organisms of even more primitive phyla, such as Nematoda, lack a circulatory system altogether.

The cardiovascular system comprises the vasculature, a highly branched network of blood-containing vessels lined by endothelial cells (ECs), and the heart, an efficient pump that provides the force necessary to circulate blood around the body. Although the cardiovascular system forms a continuous loop, it consists of distinct regions, each with a specific purpose (**Fig. 1.1**). The systemic circulation is the longest portion of the system, carrying oxygenated blood away from the heart and around the body, before returning it to the heart. The pulmonary circulation then transports this oxygen-depleted blood to the lungs

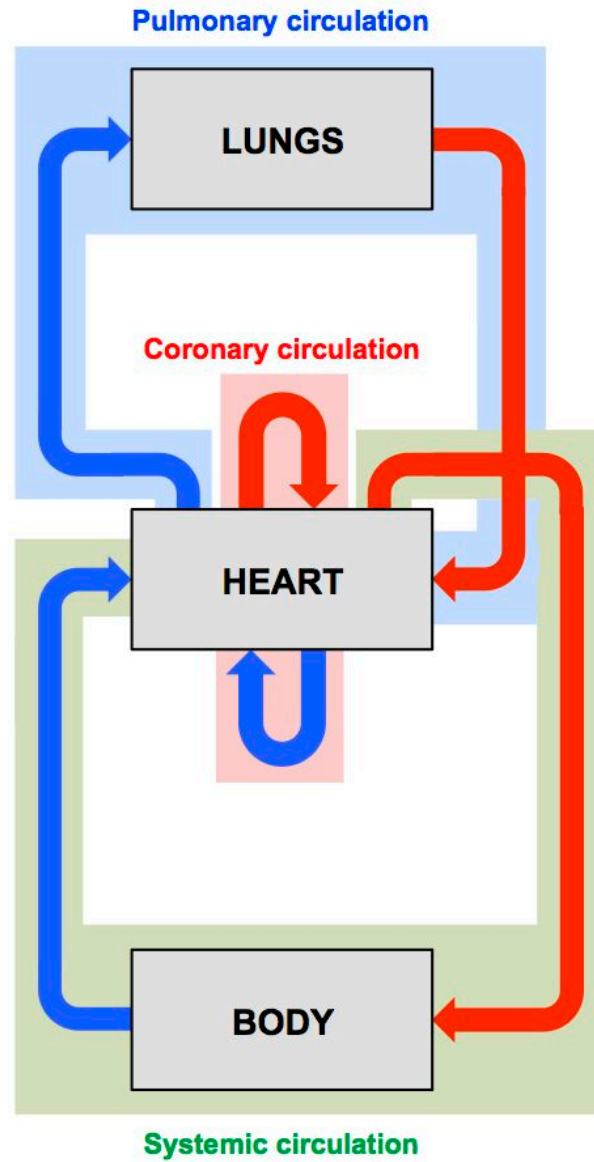


Figure 1.1. The mammalian cardiovascular system. The systemic circulation provides oxygenated blood (red) and nutrients to the tissues of the body, with deoxygenated blood (blue) being replenished by the lungs via the pulmonary circulation. The myocardium is supplied by the coronary circulation, an adjunct of the systemic circulation.

for replenishment. The heart itself, positioned at the centre of the cardiovascular system, is supplied by the coronary circulation, a small loop of the systemic circulation which provides the myocardium with necessary oxygen and nutrients from blood leaving the pulmonary circulation. As the sole supply for the myocardium, the coronary circulation is vital to the continued performance of the heart and, in health, provides a blood supply sufficient for the requirements of the cardiac muscles. However, the relatively narrow coronary vessels are particularly susceptible to blockage, such as that which occurs during the development of atherosclerosis, leading to an increased risk of myocardial infarction (MI) as cardiac demand outmatches the supply provided by the coronary circulation (Hansson, 2005). Furthermore, owing to the limited redundancy of blood supply within the heart, conditions affecting coronary blood vessels, such as coronary artery disease (CAD), are associated with particularly high morbidity and mortality (Okrainec *et al.*, 2004).

The main functions of blood are to facilitate aerobic respiration (by carrying oxygen [O₂] to and carbon dioxide [CO₂] away from sites of active respiration), to transport the absorbed products of digestion and to remove metabolic waste to the kidneys for excretion (Taylor & Weibel, 1981). Additionally, blood contributes to the maintenance of the internal environment by carrying secreted hormones between distant tissues, by the regulation of body temperature (through the redistribution of blood within the body) and pH and by transport of immune cells and clotting factors which protect against infection and injury (Hilaire & Duron, 1999).

Such is the importance of the circulation in the regulation of internal constancy that dysfunction of the blood vessel network has been identified as a contributory factor in many pathophysiological conditions. For example, tissue ischaemia, caused by an insufficient

delivery of oxygen and substrates by blood vessels, and cancer, in which deranged vessel growth provides nutrient supply for tumour cells with abnormal replication rates, are both exacerbated by dysregulation of vascular growth control (Adams & Alitalo, 2007).

1.1.1 The structure of blood vessels

The vasculature consists of a variety of vessels, from large arteries and veins of the main circulatory system, through progressively smaller arterioles and venules down to the finest capillaries of the microcirculation. Although there are significant differences in their functions and structure, arteries and veins are both composed of ECs, smooth muscle cells (SMCs), collagen and elastin arranged in three basic layers (**Fig. 1.2**). The innermost layer (the *tunica intima*) is the thinnest layer of the blood vessel, proximal to the vessel lumen through which blood flows, and consists of the endothelium, a single layer of squamous ECs. The endothelium is supported by a thin glycoprotein layer, called the basement membrane, as well as a layer of connective tissues. A dense ring of elastic collagen fibres, called the internal elastic lamina, surrounds the *tunica intima* and provides added flexibility to the vessel. The *tunica media* is the thickest middle layer of the vessel and is comprised of a mixture of SMCs, elastic fibres and connective tissue. The *tunica media* is controlled by the sympathetic nervous system, with smooth muscle providing tone and regulating changes in vessel diameter, whilst elastic tissues counteract the forces generated by sudden changes in blood pressure. Similarly to the *tunica intima*, the *tunica media* is further surrounded by the external elastic lamina containing collagen and elastic fibres. The outermost layer of the vessel, the *tunica adventitia*, is composed of dense connective tissue and functions to protect and support the relatively delicate blood vessel within. In larger vessels the *tunica adventitia* is surrounded by the network of autonomic nerves (the *nervi vasorum*) that are responsible for innervating the contractile functions of the vessel. Furthermore, whilst the *tunica intima* and

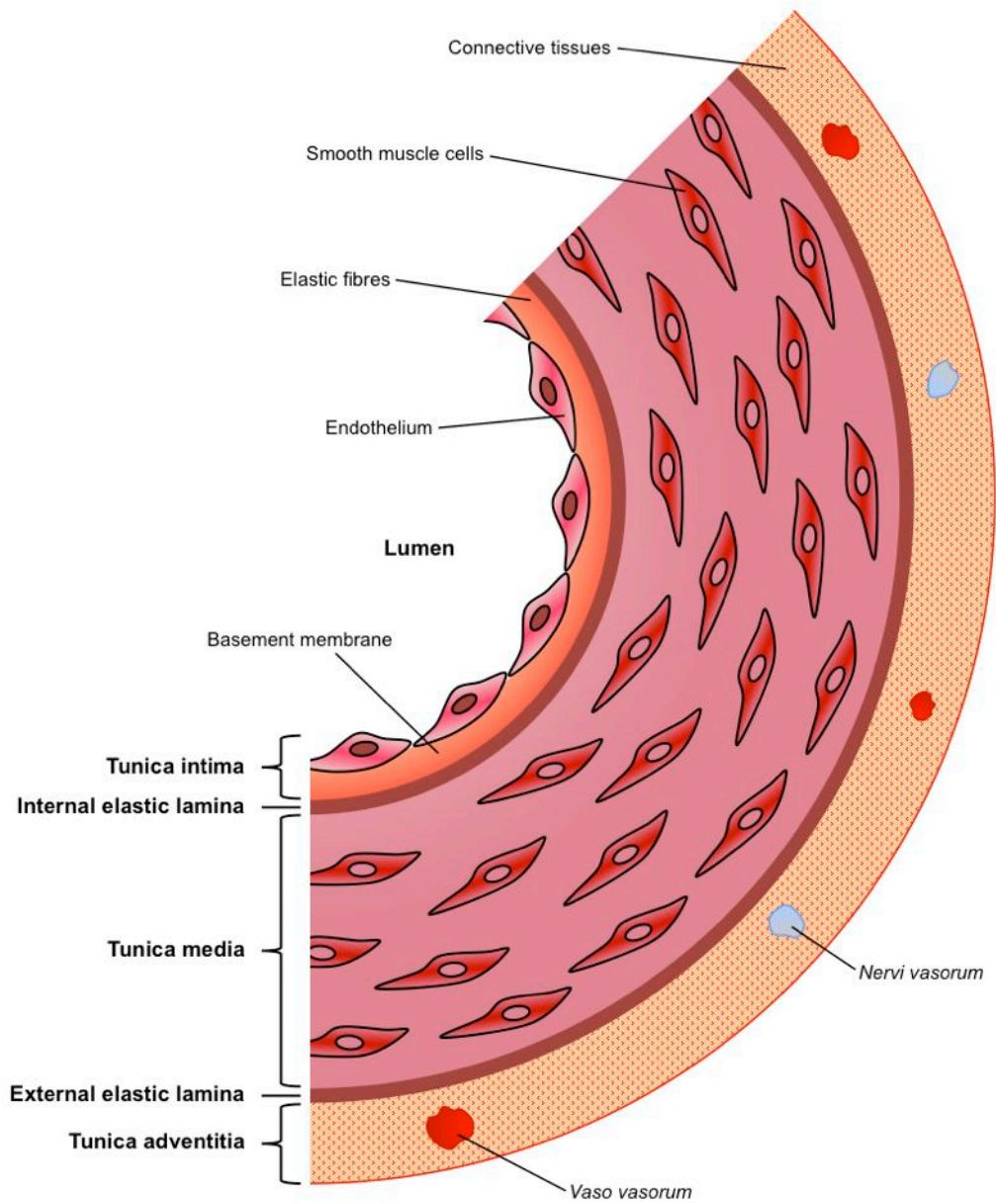


Figure 1.2. The structure of blood vessels. The basic anatomy of arteries and veins consists of the same three layers, the tunica intima, the tunica media and the tunica adventitia, separated by the internal and external elastic laminae.

and the innermost regions of the *tunica media* are supplied with nutrients and oxygen from the vessel lumen, the *tunica adventitia* is nourished by the *vaso vasorum*, a network of nutrient capillaries surrounding the vessel.

1.1.2 Arteries, capillaries and veins

Although similar in their basic anatomy, several differences exist in the exact composition and functions of arteries, capillaries and veins (**Fig. 1.3**). In general, the walls of arterial vessels are much thicker than that of veins and in general, as artery diameter decreases, the thickness of the wall also decreases. However, in smaller arterioles the ratio of wall thickness to lumen diameter actually increases, such that the size of the lumen, relative to the overall vessel diameter, decreases substantially. In large arteries, such as the aorta and pulmonary arteries, the *tunica media* contains a larger proportion of elastic fibres, having adapted to tolerate pulsatile flow and the greater blood pressures generated by blood leaving the heart at relatively high velocity. In smaller arteries, like those of the coronary circulation, an abundance of smooth muscle allows a greater extent of vasodilatation and vasoconstriction, helping to control the diameter of the smaller lumen, hence regulating convective delivery of blood around the body. The smallest arterioles contain the greatest relative amount of SMCs of the arterial vessels. In these small vessels, contraction of the *tunica media* causes significant changes in lumen size which allow fine modulation of the regional flow of blood into the tissue capillary bed, thus regulating systemic blood pressure.

Capillaries are comprised of only a single layer of endothelium, atop a basement membrane, which surrounds the lumen. Capillary diameter is much less than that of arteries or veins. Blood flows from arterioles into networks of capillaries that pass through tissues and organs and, owing to the larger surface area of the capillary bed, capillary blood flow is relatively

slow. This provides efficient oxygen delivery and the exchange of nutrients and metabolites by diffusion. Capillaries are also the main site of vascular development, through the process of angiogenesis, by which existing vessels are augmented and expanded to form new networks in response to increased regional metabolic demand.

Small venules connect with capillaries to remove deoxygenated blood from tissues, to be returned through increasingly large veins to the pulmonary circulation and, eventually, to be pumped back around the body. In comparison to arteries, veins have much larger vessel (and lumen) diameters but much thinner walls. The larger lumen allows a greater capacity for pooling of blood than arterial or capillary vessels, and a hence large proportion (around two thirds) of the total circulating blood volume is contained within the venular vessels. Although veins possess a *tunica intima* and *tunica adventitia* similar in structure and composition to arteries, the *tunica media* contains substantially less smooth muscle and elastic fibres. As a result, veins show reduced elasticity and a limited ability to vasoconstrict. Instead, blood is pushed forward by blood pressure gradients generated by the systemic circulation and the action of muscles surrounding the vessel. Valves within the vessel prevent the backflow of circulating blood and help maintain regional blood pressure. The lack of elastic tissue makes the walls of veins prone to compression by external forces, and to distention by intravascular pressures can cause venous aneurysms (Gillespie *et al.*, 1997). In addition, the thinner venous wall makes them susceptible to invasive tumours, particularly hepatocellular carcinoma (Chung *et al.*, 1995; Poon *et al.*, 2001).

1.1.3 Functions of the vascular endothelium

Although a simple squamous cell layer, the vascular endothelium is not an inert barrier but rather a dynamic organ with a wide range of systemic housekeeping and regulatory functions

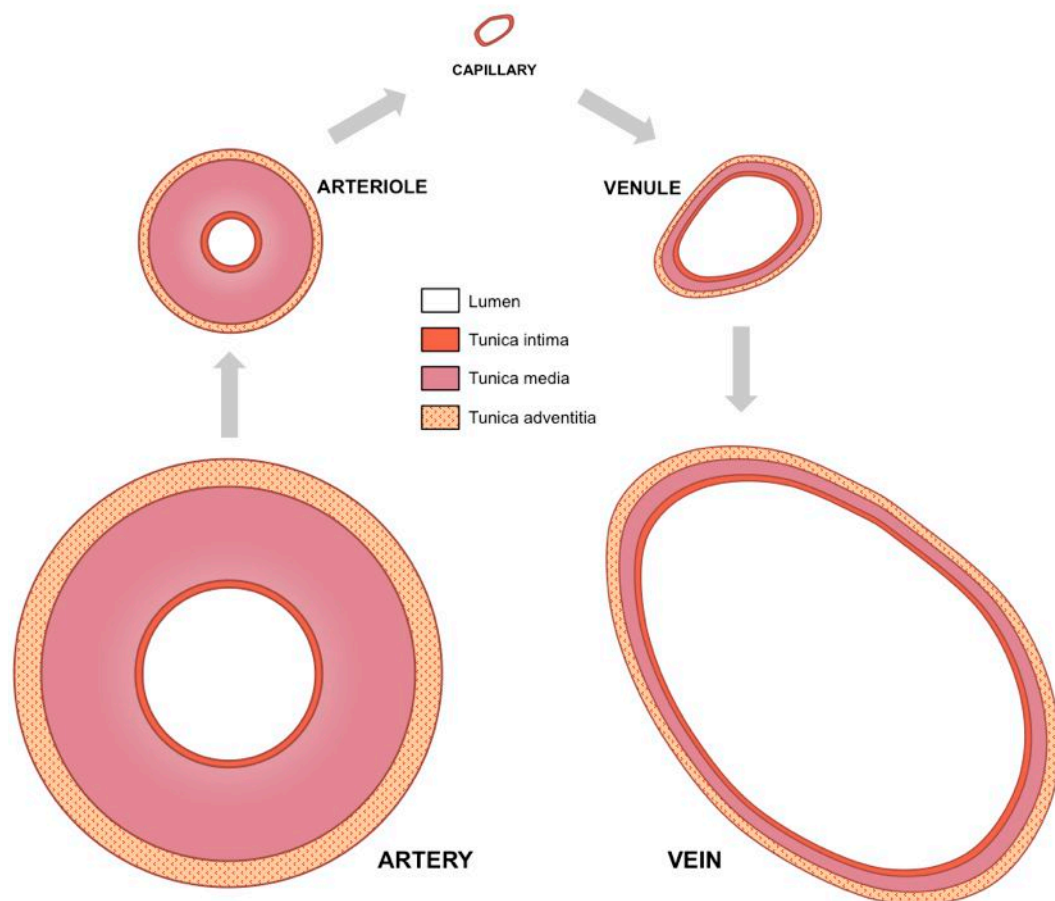


Figure 1.3. Comparison of wall composition in arteries, capillaries and veins. Arteries and arterioles have much thicker walls than veins and venules, with a relatively large tunica media containing many more elastic fibres and an abundance of smooth muscle. Veins have greater vessel and lumen diameters but do not have the elasticity or contractibility of arteries. Capillaries lack the tunica media and tunica externa of larger vessels and have a smaller lumen, but a far greater ratio of surface area to blood volume.

that ensure blood fluidity and vascular integrity. Its regulatory functions are particularly important in the microcirculation (i.e. the venules, arterioles and capillaries). This is because, compared to large vessels like the aorta, the total vessel cross-sectional area of the microcirculation is far higher and the ratio of endothelial surface to blood volume (where many potential interactions may occur) is at its greatest. The dynamic nature of the endothelium is also facilitated by its interaction with additional cell types, such as pericytes, fibroblasts and SMCs that are collectively known as the mural cells (Risau, 1997). These cells provide physical and biochemical stimuli necessary for the organised function of the endothelium, and are particularly important in subsequent vessel remodelling (Carmeliet, 2000).

The simplest function of the resting endothelium, owing to the the relatively smooth nature of the EC monolayer, is to decrease blood flow resistance and, hence, minimise the effort required by the heart to pump blood around the body efficiently (Schaper *et al.*, 1976). Furthermore, the endothelium ensures a consistent flow of blood by tightly-regulated anti-thrombotic mechanisms. The endothelium is a naturally non-thrombogenic substrate, expressing many factors that act as anti-platelet agents as well as actively degrading many of the circulating components of the coagulation cascade (Wu & Thiagarajan, 1996).

Aside from regulating haemostasis, the endothelium is also involved in the maintenance of basal vascular tone and the regulation of vessel contractility. The smooth musculature contained in the underlying *tunica media* is highly responsive to the coordinated release by ECs of specific vasoconstrictors and vasodilators. For example, nitric oxide (NO) is a primary mediator of basal tone, causing vascular smooth muscle relaxation upon secretion from the endothelium (Pique *et al.*, 1989), while endothelin-1 (ET-1) regulates vascular tone through

vasoconstriction and its production by both ECs and SMCs is downregulated in response to increased shear stress within the vessel lumen (Malek, A & Izumo, 1992). Approximately two-thirds of EC-produced ET-1 is secreted from the abluminal side of the endothelium, acting on SMCs in a paracrine manner to induce vessel constriction under low shear conditions (Wagner *et al.*, 1992). Furthermore, whilst ET-1 can act directly on SMCs to cause vasoconstriction, it also contributes to the regulation of vascular tone by stimulating NO activity, further illustrating the dynamic balance of functionality within the endothelium (Cardillo *et al.*, 2000).

1.1.4 Interactions with the endothelium

1.1.4.1 Fluid shear stress

The pulsatile flow of blood generates haemodynamic forces, such as hydrostatic pressure, vessel stretch and strain, and both laminar and non-laminar fluid shear stresses, that act upon the endothelium, influencing its activity and modulating its function. Fluid shear stress is defined as the force per unit area ($\text{dyn}\cdot\text{cm}^{-2}$) generated between two parallel surfaces, the SI derived unit of pressure being Pascals (Pa), defined as $1\text{ N}\cdot\text{m}^{-2}$ ($1\text{ dyn}\cdot\text{cm}^{-2} = 0.1\text{ Pa}$). In the cardiovascular system, fluid shear stress specifically refers to the forces applied between the blood contained within the lumen of a vessel and the endothelial monolayer that lines it (Nesbitt *et al.*, 2006). As blood moves across the boundary of the endothelium it generates a frictional drag. However, the 'no-slip condition' of fluid dynamics states that the velocity of blood at this boundary layer is zero, relative to the endothelium (Papaioannou & Stefanadis, 2005). A velocity gradient is therefore established, rising from the endothelium towards the lumen of the vessel, which generates a shear stress on the endothelial boundary layer, parallel to the flow of blood and proportional its viscosity (Braddock *et al.*, 1998).

The mean shear stress throughout the vasculature of healthy humans has been calculated to be approximately 1.5 Pa, although this only represents the average shear stresses applied to the endothelium in the major arteries that experience steady laminar (i.e. non-turbulent) flow (Cheng, C *et al.*, 2007). In reality, shear stresses vary greatly throughout the vasculature. For example, whilst a mean shear stress (similar to the systemic mean) of 1.15 ± 0.21 Pa is observed in the common carotid artery, a much lower shear stress of 0.48 ± 0.15 Pa is seen in the brachial artery (Dammers *et al.*, 2003). Furthermore, in addition to regional differences, vascular shear stresses can be significantly different over time, such as during embryonic development. In the foetal descending aorta, for instance, mean shear stress can increase to as much as 2.2 Pa during the second half of pregnancy (Struijk *et al.*, 2005).

The endothelium is able to sense changes in fluid shear stress and pressure *via* mechanoreceptors on the EC surface, which subsequently relay signals within the cell to the nucleus (Patrick & McIntire, 1995). The exact nature of this signal transduction is unclear and the mechanisms by which ECs sense force and initiate the subsequently observed biochemical responses remain unknown. However, mechanically inducible shear stress response elements (SSREs) have been identified in several genes, such as platelet-derived growth factor B (PDGFB), whose promoters are seen to respond to alterations in shear stress (Zhang, W & Chen, 2001; Miyakawa *et al.*, 2004). In addition, molecules on the cell surface, such as tyrosine kinase receptors and integrins which are sensitive to activation by conformational changes that may result from haemodynamic forces, are possible candidates for shear stress receptors (Davies *et al.*, 2005).

An immediate (i.e. seconds to minutes) response of ECs to elevated shear stress is the rapid release of vasodilatory factors, such as NO and prostacyclin (PGI₂), which relax the vessel,

increasing its luminal diameter and reducing shear stress back to normal levels (Vita *et al.*, 1989; Li *et al.*, 2003). These are important acute feedback mechanisms that coordinate the vessel's response to changes in blood pressure. This feedback mechanism has been prevented in rats treated with N^ω-nitro-L-arginine methyl ester (L-NAME), an inhibitor of NO synthase (NOS), which inhibited iliac arterial enlargement and, subsequently led to prolonged and elevated blood pressure (Guzman *et al.*, 1997).

Expression of other molecules that are important in the endothelium's maintenance of tone and contractility, such as ET-1, is also significantly affected by shear stress, however these transcriptional effects occur in the minutes to hours following changes in shear stress (Malek, AM *et al.*, 1999). In the medium-term, shear stress also differentially affects EC turnover by modulation of (i) the basal rate of cell proliferation through the ERK1/2 pathway (Kadohama *et al.*, 2007) and (ii) the rate of cell apoptosis by alterations in the expression of Bcl-2 (Dimmeler *et al.*, 1996; Gotoh *et al.*, 2000).

In the long-term, shear stress causes changes in cell phenotype and growth kinetics. Shear stress plays a role in reducing flow resistance by stimulating the reorientation of ECs parallel to the axis of flow, which streamlines the endothelium and, subsequently, reduces shear stress (Barbee *et al.*, 1995). This shear-responsive alignment has been repeatedly demonstrated *in vitro*, in both mono-cultures and co-cultures with SMCs (Dewey *et al.*, 1981; Malek, AM & Izumo, 1996), and is due to the reorganisation of cytoskeletal actin filaments in response to mechanotransduction from the cell surface (van der Meer *et al.*, 2010) and the recruitment of focal adhesion kinase (FAK) to focal adhesions, stimulated by flow (Petzold *et al.*, 2009).

Shear stress also influences endothelial permeability (Jo *et al.*, 1991). For example, increasing shear stress downregulates vascular cell adhesion molecule (VCAM)-1 but upregulates intracellular cell adhesion molecule (ICAM)-1 in the activated endothelium, suggesting a differential regulation of vascular permeability (Chiu *et al.*, 2004). The effect of shear stress on endothelial permeability is a major factor in conditions such as atherosclerosis, where accumulation of low density lipoprotein (LDL) on the vessel wall restricts vasculat perfusion (Ogunrinade *et al.*, 2002). Furthermore, owing to its modulation of leukocyte migration and transport of macromolecules across the endothelium, shear-mediated vascular permeability is also important during the initiation and resolution of inflammation.

1.1.4.2 Inflammatory cells and cytokines

Inflammation describes the protective response of the vasculature to physical or biochemical trauma and pathogens. This response primarily alters the luminal endothelial environment in order to promote enhanced recruitment and activation of circulating leukocytes. Following contact with inflammatory-activated ECs, leukocytes roll along the endothelium supported by weak selectin-mediated bonds (Langer, HF & Chavakis, 2009). The selectins (or selected lectins) are a family of cell adhesion molecules containing three closely-related subtypes that are differentially expressed by leukocytes (L-selectin), platelets (P-selectin) and the endothelium (E- and P-selectin) (Vestweber, 1992). Whilst all three are involved in leukocyte-endothelial interactions, P-selectin (and its ligand, P-selectin glycoprotein ligand [PSGL]-1) is particularly important in the rolling adhesion of leukocytes (Lim *et al.*, 1998; Klintman *et al.*, 2004). For example, it has been shown that P-selectin-deficient mice exhibit defective leukocyte behaviour during inflammation, including delayed recruitment to the endothelium, large numbers of circulating (i.e. non-recruited) leukocytes and an absence of rolling adhesion (Mayadas *et al.*, 1993). Following selectin-mediated recruitment, integrin molecules

on the surface of rolling leukocytes, such as lymphocyte function-associated antigen (LFA)-1 and macrophage (Mac)-1 antigen, are activated by chemokines, small chemotactic cytokines released from ECs such as interleukin (IL)-8, which subsequently stabilises the weak selectin bonds (Arfors *et al.*, 1987; Welt *et al.*, 2003). With the binding of leukocyte integrins to ICAM-1 and ICAM-2 (Hogg *et al.*, 2002) leukocytes arrest on the endothelium and transmigration occurs. Leukocytes either undergo paracellular migration, moving between the junctions of adjacent ECs, or transcellular migration, by travelling directing through the EC membrane (Wittchen, 2009). Paracellular leukocyte migration is dependent on the regulation of junctional proteins such as vascular endothelial (VE)-cadherin. A decrease in VE-cadherin causes a reduction in intercellular contacts, which in turn increases vascular permeability and allows the passage of recruited leukocytes to the abluminal side of the endothelium (Hordijk, 2003). In contrast, transcellular leukocyte migration relies of engulfment on the leukocyte by the luminal EC membrane and transport through the cell to the abluminal side (Mamdouh *et al.*, 2009).

1.1.4.3 Platelets and coagulation factors

The endothelium also interacts with platelets in the blood, thus playing an important role in haemostasis and regulation of the coagulation cascade. Initially, thrombin is formed by the cleavage of prothrombin by coagulation Factor X, and induces platelet activation by interaction with protease-activated receptors (PARs) on the platelet surface (Di Cera *et al.*, 1997). Thrombin is also the major target of the anti-thrombotic mechanisms of the endothelium, which usually prevent its formation and the subsequent initiation of the coagulation cascade. For example, ECs express the proteoglycan heparan sulphate which stimulates antithrombin-III (AT-III), a serine protease inhibitor which prevents the cleavage of prothrombin by Factor X (Carlson *et al.*, 1995; Tanaka *et al.*, 1998). The endothelium also

expresses tissue factor pathway inhibitor (TFPI) which, like AT-III, prevents additional thrombin formation through the inhibition of tissue factor (TF) and Factor VIIa (van 't Veer *et al.*, 1994). Furthermore, thrombomodulin (which interacts with thrombin to activate protein C, an important regulator of the anticoagulant pathway) and is also produced (in addition to its cofactor protein S) by the endothelium (Dahlbäck & Villoutreix, 2005). It is evident that the balance of the healthy endothelium is towards anti-thrombotic factors. However once activated, for example as the result of vascular injury, the endothelium rapidly promotes vascular constriction, platelet activation, and the formation of haemostatic plugs to prevent excessive or prolonged blood loss. Tissue factor is normally undetectable in the endothelium but is highly expressed following damage, as well as in response to inflammatory cytokines (such as tumour necrosis factor [TNF]), hypoxia, increased shear stress, and bacterial endotoxin (Krishnaswamy *et al.*, 1999). Tissue factor initiates coagulation pathways that ultimately result in fibrin formation, arresting blood loss from the damaged vessel (Balasubramanian *et al.*, 2002). Vessel damage also exposes collagen, contained within the subendothelial connective tissue, to which von Willebrand Factor (vWF) can bind, an important initial step in the adhesion and aggregation of platelets (Reininger *et al.*, 2006).

1.2 The development of blood vessels

The first blood vessels are seen to develop in the human embryo around 21 days post fertilisation (Demir *et al.*, 1989). Following the growth and development of this primitive vascular network, the vasculature continues to develop and remodel in the adult in response to increasing, and often unmet, metabolic demand. This need for additional oxygen and nutrients can result from increased exercise, wound healing or, detrimentally, as a consequence of certain pathological conditions.

1.2.1 Vasculogenesis vs. angiogenesis

The primitive embryonic vasculature forms *via* vasculogenesis (**Fig 1.4**). In the early embryo, mesenchymal stem cells (MSCs) in the bone marrow (BM) differentiate to form haemangioblasts, the common precursor of haematopoietic stem cells and endothelial-lineage angioblasts (Adams & Alitalo, 2007; Sirker *et al.*, 2009). During vasculogenesis these immature but lineage-committed angioblasts, termed endothelial progenitor cells (EPCs), migrate and congregate into clusters, called blood islands, forming the primary vascular plexus from which a complex microcirculation arises (Risau, 1997; Paleolog, 2005). In contrast, adult vascular growth occurs primarily through angiogenesis, whereby new capillaries develop endogenously from fully-differentiated endothelial cells (ECs) within existing vessels rather than the *de novo* formation of vessels seen in early embryogenesis (Hudlicka *et al.*, 1992; Asahara *et al.*, 1997). Progressive remodelling of the embryonic vasculature (by both sprouting and non-sprouting forms of angiogenesis) gives rise to the functional and complex adult circulation (Akeson *et al.*, 2001; Egginton, 2002).

1.2.2 Mechanisms of angiogenesis

Angiogenesis has been shown to occur in at least three distinct ways: (i) capillary sprouting, (ii) capillary splitting, and (iii) intussusception. Sprouting angiogenesis, often considered the classical model of vessel growth, involves the outward budding of an existing vessel to form a sprout which grows and fuses with another vessels to form a functional anastomosis. The process has several sequential stages (**Fig. 1.5**). First, angiogenic growth factors and cytokines induce pericellular protease activity which degrades the extracellular matrix (van Hinsbergh *et al.*, 2006). The matrix metalloproteinases (MMPs) are a family of secreted endopeptidases that degrade specific components of the basement membrane and are particularly important in the initial stages of sprouting angiogenesis. Several MMP types are produced by ECs,

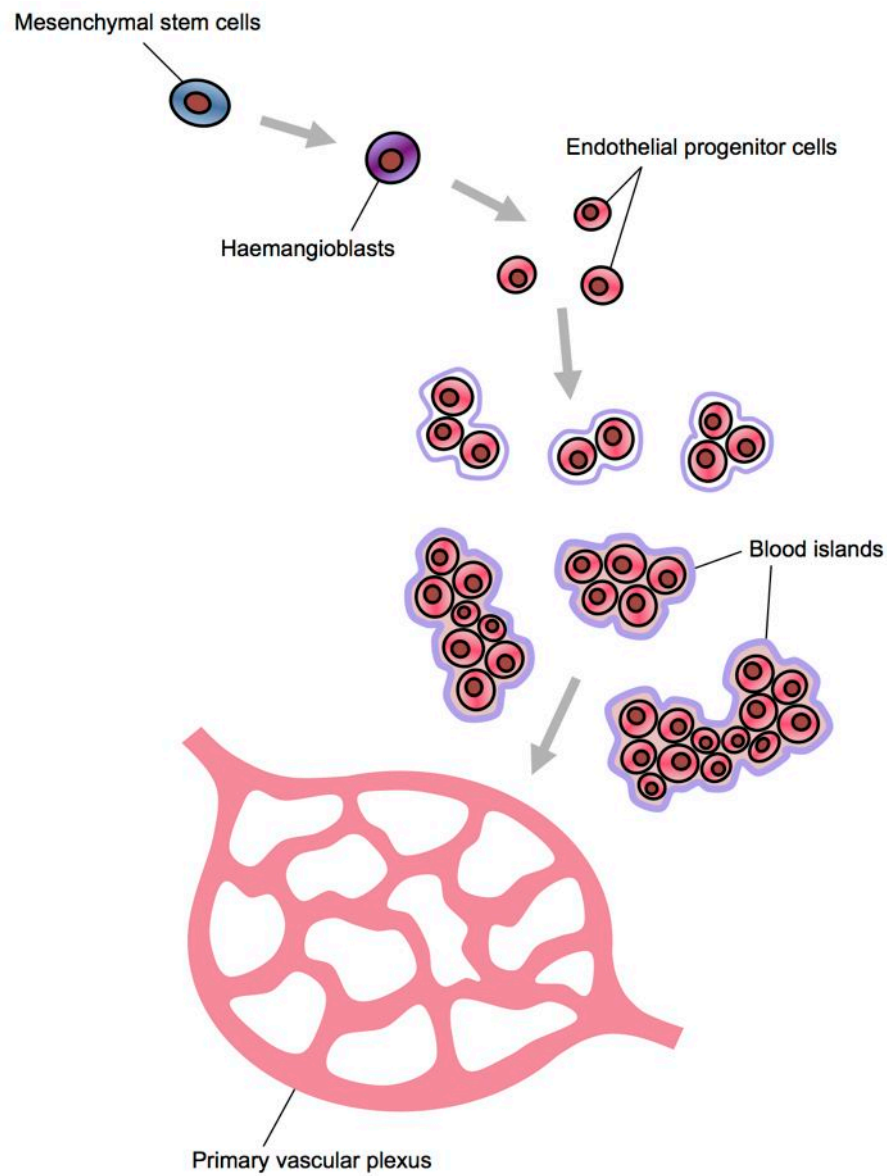


Figure 1.4. Vasculogenesis. Mesenchymal stem cells from the embryonic bone marrow give rise to haemangioblasts, the common precursor of haematopoietic stem cells and endothelial progenitor cells. During vasculogenesis these endothelial progenitor cells migrate and congregate to form blood islands and, upon expansion, the primary vascular plexus.

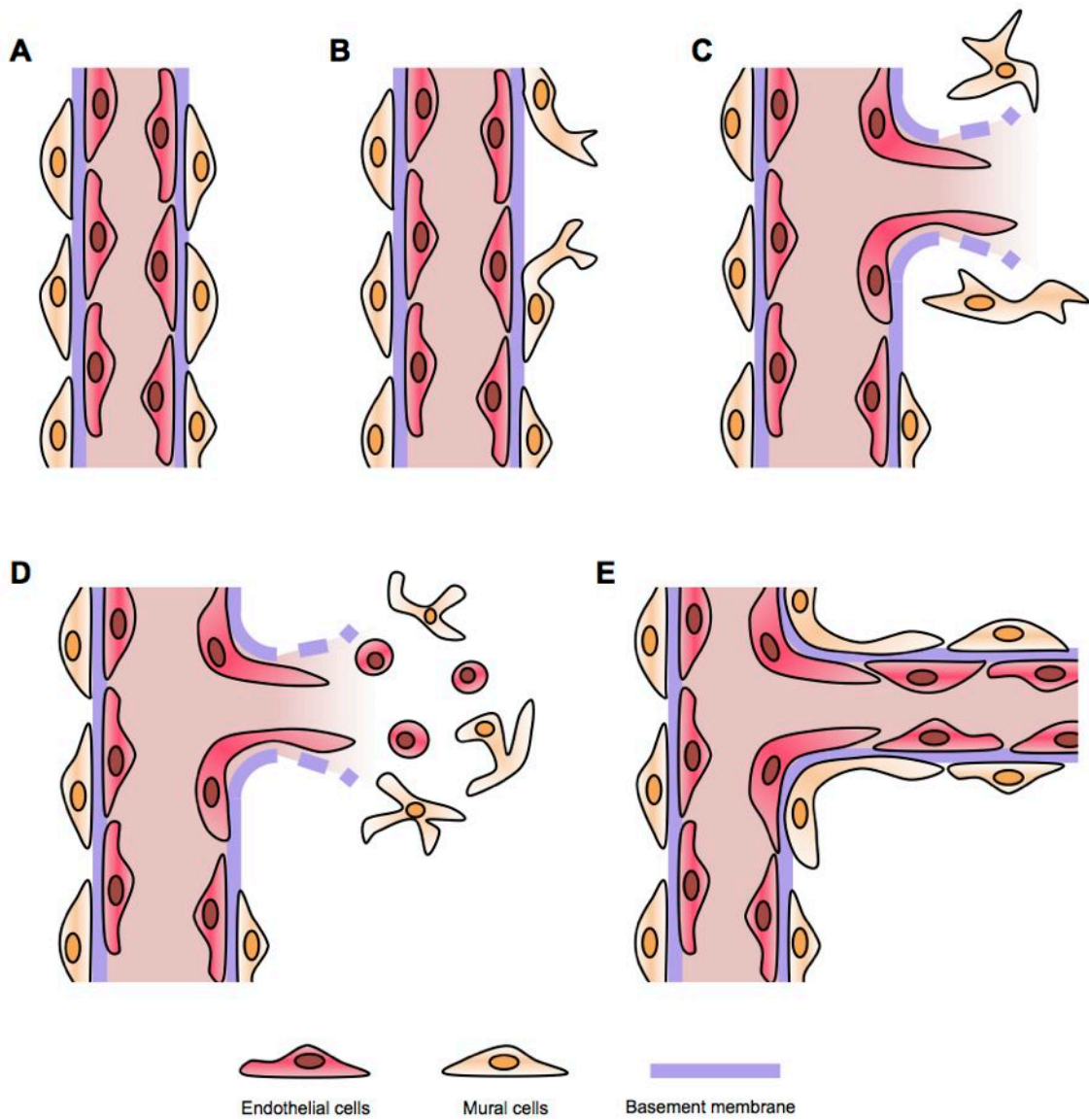


Figure 1.5. Sprouting angiogenesis. (A-C) Angiogenic growth factors and cytokines induce pericellular protease activity which degrades the extracellular matrix. (D) ECs migrate outwards into the surrounding matrix, proliferating and recruiting mural cells. (E) These cells then reorganise to form a luminal space, and the immature vessel is stabilised by the generation of a new basement membrane and recruitment of perivascular cells

including the zymogens MMP-1, MMP-2 and MMP-9, and the cell surface-bound MT1-MMP. In studies using MMP-2-deficient mice, reduced retinal angiogenesis was observed compared to both wildtype and MMP-9-deficient mice, highlighting the importance of MMPs (and particularly MMP-2) in vascular growth by sprouting, but suggesting differential roles for the MMP types in the dissolution of the extracellular matrix (Ohno-Matsui *et al.*, 2003). MMP-9 has in fact been implicated in angiogenesis in ischaemic muscle, suggesting a moderator effect through more indirect mechanisms than, for example, MMP-2 (Bendeck, 2004).

Following dissolution of the basement membrane, ECs migrate outwards through the vessel wall into the surrounding matrix (Arroyo & Winn, 2008). During the early stages of the angiogenic response some migrating ECs are selected for sprouting, becoming 'tip cells' which form the leading edge of the vessel outgrowth. Tip cells are highly migratory, with an abundance of filipodia, and work to direct the angiogenic sprout by sensing changes in specific factors, such as vascular cell growth factor (VEGF), in the interstitial environment (Gerhardt *et al.*, 2003). The development of the tip cell population is highly dependent on the interaction of Notch receptors with the Delta-like-4 (DLL4) ligand (Adams & Alitalo, 2007). DLL4 negatively regulates sprout formation and ensures that the early angiogenic outgrowth is organised and well-regulated (Suchting *et al.*, 2007). In a murine model of tumour angiogenesis, blockade of the Notch signaling pathway (by conditional inactivation of the Notch-mediated recombination signal-binding protein Jκ) has been shown to disrupt angiogenic regulation, although the subsequent effect on tumour vascular growth was highly dependent on tumour cell type (Hu, X-B *et al.*, 2009). Led by the migrating wave of tip cells, ECs then begin to proliferate, providing adequate numbers of cells for the formation of the new vessel. This population of ECs ('stalk cells') also reorganise to form a luminal space, and

the immature vessel is stabilised by the generation of a new basement membrane and recruitment of perivascular cells (Jain, 2003).

In addition to ECs, mural support cells (i.e. fibroblasts and pericytes) are important for angiogenic growth. The high level release of PDGFB from tip cells promotes the recruitment of pericytes, which express the complementary PDGF receptor β (PDGFR β), helping to stabilise the new vessel (Gerhardt *et al.*, 2003). Furthermore, the presence of monocyte chemotactic protein (MCP)-1 (which is produced by angiogenically active ECs), induced by treatment of rat aortic rings with angiopoietin (Ang)-1 *in vitro*, has been shown to enhance the recruitment of co-cultured mural cells (Aplin *et al.*, 2010).

In contrast to sprouting angiogenesis, rather than forming an adjunctive vessel, intussusceptive angiogenesis (a form of splitting angiogenesis) causes vascular development by dividing an existing capillary into two separate vessels (**Fig. 1.6**). First, the opposite walls of the vessel move inwards and the endothelium protrudes into the lumen, contacting with its opposite on the other side to form a transluminal pillar. The endothelial bilayer located at this 'kissing contact' is then perforated by the reorganisation of interendothelial junctions, resulting in the creation of a thin channel linking the interstitium on either side of the vessel (Burri, P H & Tarek, 1990; Djonov *et al.*, 2003). Cytoplasmic processes from interstitial pericytes and fibroblasts then invade into this channel (the inside of which will form the external wall of the new vessel) and support the newly reorganised interendothelial junctions by laying down collagen fibrils (Hall, 2006). The interstitial pillar then expands in diameter, through the enlargement and morphological remodelling of ECs, to form two separate vessels. Intussusception is a relatively quick process because, unlike sprouting angiogenesis, large-scale EC proliferation is not required (Rossi-Schneider *et al.*, 2010).

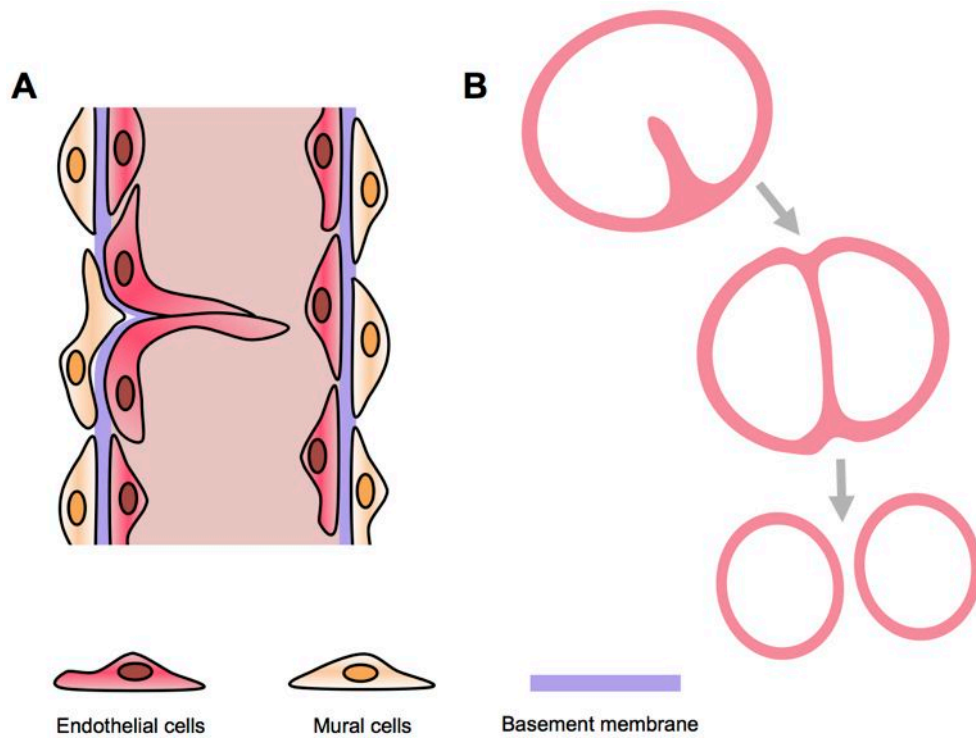


Figure 1.6. Intussusception. The endothelium protrudes into the lumen, contacting with its opposite on the other side to form a transluminal pillar. The interstitial pillar then expands in diameter, through the enlargement and morphological remodelling of ECs, to form two separate vessels. (A) Longitudinal and (B) cross-sectional aspects.

1.2.3 Assessing vessel growth

To achieve a better understanding of the processes involved in angiogenic growth, and the molecular mechanisms underpinning them, it is important to be able to study angiogenesis using a wide variety of *in vitro* and *in vivo* assays. These can be used to assess the angiogenic activity of tumour and other cell types, to study the effects of pro- and anti-angiogenic stimuli on those cells, and to explore the mechanisms by which those effects may be reproduced *in vivo*. Furthermore, assay models are important in the search for effective angiogenic modulators and, ultimately, potential therapeutic agents.

1.2.2.1 *In vitro* angiogenesis assays

As stated, specific processes (such as basement membrane disruption, cell migration, proliferation and reorganisation) must take place during angiogenesis and their coordination is vital for the appropriate angiogenic response to occur *in vivo*. However, using *in vitro* assays, the individual elements involved in angiogenesis can be demonstrated separately, providing the ability to study each isolated process in detail.

Protease-mediated disruption of the basement membrane is essential to allow migrating ECs access to the interstitial matrix. In particular, MMP-1, MMP-2 and MMP-9 are released by ECs as zymogens that must be activated in the extracellular compartment. These zymogens can be obtained from *in vitro* cultures grown on a physiological matrix and easily quantified using electrophoretic zymography (Zhang, H *et al.*, 2002). Following EC culture on a matrix protein substrate, MMP-containing medium is electrophoresed through a polyacrylamide gel containing gelatin, which is subsequently degraded by the secreted proteases. Staining with a protein dye allows the proteolytic activity of the secreted MMPs (visible as clear bands of proteolysis against a blue protein-rich background) to be quantified using densitometry.

Following basement membrane dissolution, ECs migrate outwards into the interstitial matrix and rapidly proliferate. The migratory response can be illustrated using a modified Boyden chamber system (Suchting *et al.*, 2005). A transwell insert containing a porous membrane forms two compartments in a tissue culture plate. The upper compartment is seeded with ECs and the lower compartment filled with a chemoattractant, such as a single recombinant chemokine or a range of factors derived from mural cell-conditioned medium (Carlevaro *et al.*, 1997; Bagheri-Yarmand *et al.*, 2000). Cells migrate across the membrane in response to the chemoattractant, the extent of which is analysed by phase contrast microscopy of the excised transwell filters. The rapid proliferation of migrating ECs can be also be demonstrated using a thymidine incorporation assay. Radioactively-labelled [³H]thymine is incorporated into a cell during mitosis in a manner proportional to the turnover of the cell cycle, giving an indication of the rate of EC proliferation (Lee, PC *et al.*, 1999; Hayashi *et al.*, 2007).

The potential of ECs to form blood vessels can also be demonstrated by highlighting the changes in individual cell morphology and overall cellular reorganisation that occur during the formation of EC tubules *in vitro* (Mukai *et al.*, 2008). Regardless of their origin, all ECs appear to form organised tubule networks when cultured in the appropriate environment. The most common *in vitro* tubule formation assay involves seeding cells on to a glycoprotein-rich (i.e. basement membrane-like) gel matrix which contains pro-angiogenic growth factors (Arnaoutova *et al.*, 2009). Subsequent tubule formation can then be quantified to give a definable measure of angiogenic potential. Unlike assays of other angiogenesis-related processes such as cell migration or proliferation, which can occur as a result of a variety of cellular stimuli other than those leading to angiogenesis, tubule formation assays are considered to be one of the most endothelial- and angiogenesis-specific *in vitro* tests (Madri *et al.*, 1988). However, although lumen-like structures have been observed when ECs

are cultured on Matrigel (Lawley & Kubota, 1989) they are often absent (Nicosia, RF *et al.*, 1984), meaning *in vitro* tubule formation does not exactly parallel the *in vivo* situation. Furthermore, it must be noted that certain non-endothelial cell types, such as primary human fibroblasts and metastatic breast and prostate carcinoma cells, have been observed to form tubule-like structures when cultured on a gel matrix, so care must be taken when interpreting results of tubule formation assays (Martin *et al.*, 1999; Donovan *et al.*, 2001).

1.2.2.2 *In vivo* angiogenesis assays

The earliest *in vivo* angiogenesis assays relied on visual observation of the increased vascular growth surrounding implanted tumours using chamber techniques (Conway *et al.*, 1951; Algire & Merwin, 1955). Additionally, histological assessment has always been important for understanding of the processes surrounding angiogenesis (Fox *et al.*, 2008). First described in 1913, the chorioallantoic membrane (CAM) assay involves placing tissue grafts on to the exposed CAM of week-old chick embryos, by making a resealable window in the shell of the egg (Murphy, 1913). Radial angiogenic outgrowth from the graft was then assessed by scoring vascularisation using a scale of 0 to 4. Whilst initially simplistic and limited by its semi-quantitative assessment of neovascularisation, the CAM assay has since been modified (by employing more quantitative scoring criteria) and is commonly used to study tumour cell invasion and the chemosensitivity of angiogenic cells to angiogenic stimuli (Ribatti, 2004).

Modern *in vivo* assays benefit from the use of advanced fluorescence microscopy and digital imaging processing to provide much more accurate and reproducible quantification of vessel growth. Similar to the modified CAM assay, the corneal angiogenesis assay involves the insertion of test cells or tissue into a pocket made in the cornea to stimulate the ingrowth of vessels from the peripheral limbal vasculature. This growth can be monitored by direct

observation throughout the assay, through histological or fluorescent staining, and quantified digitally by measuring the area of vessel invasion and the morphological parameters (i.e. length, diameter and tortuosity) of the developing vessels toward the angiogenic stimulus over time (Muthukkaruppan *et al.*, 1982; Auerbach *et al.*, 2003).

1.2.2.3 A gold standard angiogenesis assay?

A gold standard assay is one that gives the best (i.e. most specific and sensitive) readout possible under given conditions, and defines a benchmark against which all other assays can be judged. In terms of assessing angiogenesis, no such assay exists. Instead, a compromise must be made between the varying benefits and limitations of the available assays, based on the specific requirements and conditions of the proposed investigation.

In general terms, whilst *in vitro* angiogenesis assays are quicker, cheaper, easier to perform and (it can be argued) more ethical than *in vivo* alternatives, they are often considered inadequate when trying to replicate the complex *in vivo* environment. For example, whilst *in vitro* tubule formation assays have been shown to produce vessel-like structures containing a luminal space, formed by apoptotic degeneration of the centrally placed cells (Egginton & Gerritsen, 2003), EC structures grown on gel matrix proteins commonly contain no lumen and often resemble solid cords or cytoplasmic processes rather than true tubules (Kubota *et al.*, 1988; Goodwin, 2007).

It is a recognised limitation of static *in vitro* assays that important features of the internal environment, such as the influence of blood flow and shear stress, are not replicated as they might be in an integrative *in vivo* animal model (Nash, G & Egginton, 2007; Staton *et al.*, 2009). As previously discussed, the interactions of different cell types are important for a

well-regulated angiogenic response. The vessels formed in a culture dish during an *in vitro* tubule assay do so without the usual intracellular signals from pericytes, fibroblasts and other support cells. Co-culture assays have been described which uncover additional properties of established growth factors and highlight the important roles of extracellular matrix components and mural cells in effective vessel maturation that may not be evident from assays of a single cell type (Friis *et al.*, 2003; Beilmann *et al.*, 2004).

Modified *in vitro* organ culture systems, such as the rat aortic ring assay (Nicosia, R, 2009) and the excised chick aortic arch model (Wang *et al.*, 2009) are thought to better simulate the *in vivo* environment, but often use tissues that would not ordinarily give rise to angiogenic outgrowths *in vivo*. For example, as a naturally avascular environment, angiogenic growth must be forced in the cornea and it is perhaps, therefore, not a valid representative tissue in which to study angiogenesis. Interestingly, precisely for its avascularity the corneal angiogenesis assay is considered one of the best *in vivo* angiogenesis assays. This is because any vessel seen in the (normally) avascular cornea after angiogenic stimulation is unarguably evidence of new vascular growth, and can be easily identified and studied (Auerbach *et al.*, 2003). However, although desirable, the corneal assay is technically demanding, both in terms of the surgical procedures involved and the limited corneal space available in which to perform the assay. In contrast, the Matrigel plug assay is far less difficult to perform. Furthermore, this assay uses similar principles to *in vitro* tests (i.e. the gel matrix tubule formation assay) but applied to a whole organism, allowing comparative study between *in vitro* and *in vivo* models of angiogenesis (Passaniti *et al.*, 1992).

Ultimately it is clear that there is no single ideal system for demonstrating or quantifying vessel growth *in vitro* or *in vivo*. Consequently, the widely held opinion is that angiogenic

studies are best undertaken, as in this investigation, using a combination of established *in vitro* and *in vivo* techniques.

1.3 Embryonic EPCs in the adult circulation?

EPCs play an important role in the early stages of vasculogenesis, forming the basis for the developing (i.e. embryonic) circulatory system. However, it has become increasingly evident in recent years that EPC-mediated angiogenesis also occurs frequently in the mature (i.e. adult) vasculature (Shi *et al.*, 1998; Burri, Peter H & Djonov, 2002; Erdbruegger *et al.*, 2006).

The persistence of EPCs in the adult circulation, and perhaps more importantly their ability to form endothelial structures within the vasculature, has been understood since the early 1960s (Stump *et al.*, 1963; Bouvier *et al.*, 1970). However, it was not until the late 1990s when BM-derived cells, positive for both CD34 and vascular endothelial growth factor receptor (VEGFR)2, were shown to be present in the new vessels growing around the site of vascular injury that the potential contribution of EPCs to adult angiogenesis was made clear (Asahara *et al.*, 1997). It has since been shown that circulating EPCs can readily differentiate into endothelial-lineage cells and, in animal model of ischaemia, will incorporate into sites of neovascularisation (Iwami *et al.*, 2004). Accumulated evidence also shows that circulating EPCs are derived from the same BM niche as embryonic haemangioblastic EPCs, and share similar phenotypic and growth kinetic characteristics (Hristov & Weber, 2004). Furthermore, it is known that EPCs secrete a wide range of angiogenic factors, including VEGF, granulocyte colony-stimulating factor (G-CSF) and granulocyte-macrophage colony-stimulating factor (GM-CSF), and many proinflammatory cytokines such as monocyte MCP-1 and TF (Rehman *et al.*, 2003; Zhang, Y *et al.*, 2009).

There are many reported stimuli for EPC activity in both health and disease. An important example is NO which, when produced by osteoblasts in the BM microenvironment in response to hypoxia, mediates the release of EPCs into the circulation, an effect that is abrogated by L-NAME inhibition of NOS (Goldstein *et al.*, 2006). Hence, modulators of NO bioavailability, such as insulin growth factor (IGF)-1, also dramatically influence the number of EPCs in the peripheral blood (Thum *et al.*, 2007). Another potent stimulus for EPC BM release is erythropoietin (EPO), a glycoprotein hormone essential for erythrocyte production in the BM, which has been shown, in EPO-treated mice, to significantly increase the number of CD34⁺ VEGFR2⁺ cells in the spleen and peripheral blood (Heeschen *et al.*, 2003). Other natural mediators of EPC number include exercise, which has been shown to increase EPC mobilisation into the circulation (Laufs *et al.*, 2004; Steiner *et al.*, 2005) and ageing, which appears to have a negative effect on EPC mobilisation and functionality (Henrich *et al.*, 2004; Thum *et al.*, 2007), acting through differential changes in plasma VEGF and NO bioavailability.

1.3.1 EPCs in cardiovascular disease

In addition to their normal physiological role in vascular development, there is increasing evidence highlighting the pathophysiological stimulation of EPCs and implicating them in the recapitulation of vasculogenesis under certain pathological conditions. It has been demonstrated that the number of EPCs present in the circulation inversely correlates with the level of cardiovascular risk, as defined by a number of factors including smoking, hypertension, diabetes, a positive family history of CAD and hypercholesterolaemia (Vasa *et al.*, 2001; Hill *et al.*, 2003). Hence, circulating EPCs are a useful indicator of cardiovascular health and well as exerting positive benefits as a result of pathophysiological stimuli. For example, the re-endothelialisation of atherosclerotic lesions by EPCs introduced into

vessels *via* cell-seeded intravascular stents has been demonstrated (Shirota *et al.*, 2003), illustrating that mobilisation of EPCs from the BM, although only small in quantities when stimulated naturally, can occur during the response to cardiovascular disease (Roberts, N *et al.*, 2005). Increased mobilisation of EPCs has also been shown to be an underlying factor in several systemic responses to rheumatoid arthritis, including the increased supply of nutrients and oxygen to the synovial tissue (due to EPC-induced vessel growth) as well as the increased vascularisation brought about by aspects of the angiogenic response not involving EPCs (Paleolog, 2005). Other conditions, such as diabetes, coronary artery disease, and cerebral and cardiac ischaemia, have also been demonstrated to exhibit a natural involvement of EPCs (Ding *et al.*, 2007; Kawamoto, Atsuhiko & Asahara, 2007).

The large body of evidence for the positive angiogenic reaction of EPCs in a wide range of cardiovascular conditions (and the implication of their effective contribution to vascular regeneration) illustrates the important natural role for EPCs in the angiogenic response of the body to cardiovascular disease.

1.3.2 A therapeutic potential for EPCs?

The notion of exploiting EPCs as a tool for angiogenic therapy is an intriguing one and, based on their suggested angiogenic functions, may have great potential. In the main, two types of angiogenic therapy have so far been investigated, involving either endogenous or exogenous approaches. Broadly, endogenous therapies seek to initiate the body's natural angiogenic response by the addition of an externally applied stimulus, often the direct delivery of a pro-angiogenic substance, that results in increased mobilisation of existing BM-resident EPCs to the required site. For example, 3-hydroxy-3-methyl-glutaryl-Coenzyme A (HMG-CoA) reductase inhibitors, called statins, have been shown to stimulate endothelial bioreactivity

in vitro and enhance angiogenesis *in vivo*, through the VEGF-modulating PI3K/Akt signalling pathway (Dimmeler, 2010). Another strategy involves treatment with G-CSF, sometimes combined with stem cell factor (SCF), to vastly increase mobilisation of cells from the BM niche including MSCs, haematopoietic stem cells (HSCs) and, most importantly, EPCs (Wolfram *et al.*, 2007; Zhang, J-J *et al.*, 2007). Whilst data from these studies are promising, such treatments are often problematic because the delivery of a single drug is often insufficient to elicit the complete and prolonged response necessary for effective angiogenesis (Milkiewicz *et al.*, 2006; Williams, JL *et al.*, 2006).

Conversely, instead of attempting to mobilise host EPCs, exogenous treatments have also been investigated that involve donor EPCs being expanded *in vitro* before a much higher quantity than normally recruited is injected into the body, where they circulate in the blood until sequestered at the site of neovascularisation (Perry & Linch, 1996). Such transplantation therapies have shown merit in recent studies, including the improvement of hindlimb ischaemia in murine models following intramuscular EPC injection (Cho, S-W *et al.*, 2007) and increased atrial wall perfusion and left ventricular ejection fraction in human MI patients after intracardial infusion (Manginas *et al.*, 2007).

Significant problems still exist with EPC transplantation, such as poor HLA matching leading to increased immune rejection resulting in reduced transplantation efficiency (Garmy-Susini & Varner, 2005; Shantsila *et al.*, 2007), but it still shows the greatest potential for development into a viable treatment for cardiovascular conditions in which revascularisation is vital for disease resolution.

1.3.3 Defining the EPC

Though many studies illustrate the role of EPCs in angiogenesis and their potential for therapeutic transplantation, there is a remarkable lack of agreement on a clear definition for the EPC population. Several suggestions have been put forward as to what constitutes the definitive EPC, based upon gene expression profiles, and the observation of morphology and functional properties both *in vivo* and *in vitro*, but they tend to vary considerably (Hristov & Weber, 2004; Urbich & Dimmeler, 2004). Currently, the most commonly accepted definition is the presence of the surface markers VEGFR2, CD34 and CD133, with additional cited markers depending on the method of isolation or cellular application (Pearson, 2010).

Several techniques have been utilised to obtain EPCs but the most commonly used involves plating out CD34⁺, CD133⁺, or c-Kit⁺ mononuclear cells, themselves isolated from peripheral blood using magnetic beads (Zheng *et al.*, 2010). Two identifiable populations of progenitor cells originate from this method, called early- and late-outgrowth EPCs, named for their differing morphologies over time when cultured *in vitro* (Ingram *et al.*, 2005). However, whilst they are both termed EPCs, these two cell types demonstrate significant differences in their gene and protein expression profiles and apparent developmental origins. Early-outgrowth EPCs are narrow, spindle-shaped cells obtained after 4-7 days of culturing isolated mononuclear cells and share many characteristics with mature ECs, such as the expression of VEGFR2, VE-cadherin, platelet-endothelial cell adhesion molecule (PECAM, also known as CD31) and vWF, the uptake of acetylated low density lipoprotein (ac-LDL) and binding to *Ulex europaeus* agglutinin (Asahara *et al.*, 1997). However, unlike mature ECs, they have also been shown to highly express the leukocytic marker CD45 and the monocytic marker CD14, making a haematopoietic lineage origin likely (Gulati *et al.*, 2003; Rehman *et al.*, 2003). In contrast, late-outgrowth EPCs lose the expression of these markers and only

express CD34 and the endothelial markers like VEGFR2 and VE-cadherin (Brown *et al.*, 2009; Jodon de Villeroché *et al.*, 2010). Late-outgrowth EPCs proliferate from mononuclear cell cultures only after several weeks of culture and are relatively rare, compared to early-outgrowth EPCs. They have a much more flattened, squamous appearance and, perhaps as a result of their more endothelial-specific phenotype, give rise to much more EC-like progeny *in vitro*. Unlike early-outgrowth EPCs, which demonstrate a limited proliferative capacity, late-outgrowth EPCs have been shown to have a much greater propensity to form vascular tubule networks *in vitro* (Sieveking *et al.*, 2008).

Many important aspects of the EPC phenotype and origin remain unclear and this hinders clarification of their definition. For example, the differences observed between cell populations as reported in the literature are likely attributable to the choice of expression criteria used to select circulating cells from the blood. Changing the parameters for cell separation will clearly result in an isolated population with a different expression profile (and, very likely, a wholly different origin and angiogenic activity) whilst still being termed 'EPCs'.

Using these different (albeit all 'EPC') populations to perform additional characterisation further compounds the differences between reported EPC populations. Consequently, results are likely to show substantial variation, thus making consensus on an EPC definition even harder to achieve. Indeed, such contrary findings are evident in the literature: in contrast to the findings of the majority of EPC studies, as discussed previously, there are investigations that have made different, and sometimes contradictory, conclusions about the EPCs as indicators of cardiovascular health and disease. For example, a large population-based study focussed on the correlations between circulating EPC numbers, cardiovascular risk factors and disease found, unlike several other similar studies, that the level of circulating EPCs was

strongly associated with an increased cardiovascular risk score (Xiao *et al.*, 2007). Although difficult, establishing a definition for the exact EPC phenotype would go a long way towards transferring their potentially beneficial effects to a clinical setting, defining not just the cell type but a viable and reproducible method for their isolation and application.

1.4 The potential of pluripotency

1.4.1 Embryonic stem cells

Although there is debate as to the precise definition of pluripotency, it is accepted to refer to the potential of a cell to give rise to all cell types found in both the embryonic and adult organism (Baker, 2007). Embryonic stem cells (ESCs) have the broadest developmental potential of all the cell types in the body and are additionally characterised by an ability to continually renew themselves (Heng, Boon Chin *et al.*, 2006; Hombach-Klonisch *et al.*, 2008). Consequently, ESCs are of interest in many diverse fields of scientific research.

ESCs are derived from the developing mammalian embryo (**Fig. 1.9**). Embryogenesis begins with fertilisation, the fusion of the haploid gametes to form the diploid zygote. The zygote then rapidly divides into blastomere cells in a process known as embryonic cleavage. This forms a dense ball, called the *morula*, which is contained within a glycoprotein membrane (*zona pellucida*). Fluid secreted by the blastomeres creates a cavity within the morula, forming a hollow ball of cells called the blastocyst. The cells on the surface of the blastocyst differentiate to become the trophoctoderm, the embryonic epithelium, whilst the cells contained within the blastocyst form the inner cell mass (ICM) from which all the cells of the foetus will ultimately develop. ESCs are obtained by disruption of the ICM at this stage and subsequent *in vitro* culture of the disaggregated cells.

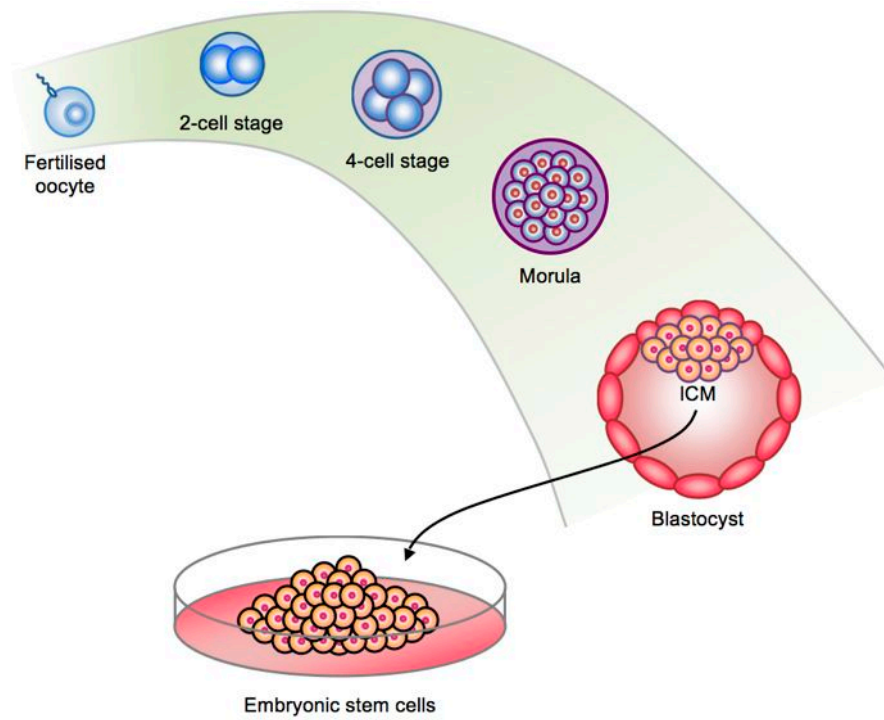


Figure 1.7. Derivation of ESCs. The fertilised oocyte rapidly divides into blastomere cells through embryonic cleavage, forming the morula. Fluid secreted by the blastomeres creates a cavity within the morula, forming a hollow ball of cells called the blastocyst. Cells contained within the blastocyst form the inner cell mass (ICM) from which ESCs are obtained.

The first ESCs were derived from the ICM of 129/Sv mice, and established *in vitro* using serum-supplemented medium and irradiated STO murine fibroblasts (Evans & Kaufman, 1981). A key factor secreted by these feeder cells, leukaemia inhibitory factor (LIF), has since been identified as an important regulator of the pluripotency phenotype *in vitro*, and maintains the naïve ESC state by signalling through the Stat3 pathway (Ying *et al.*, 2008). A range of genes expressed by ESCs, namely *Oct4*, *Nanog* and *Sox2*, are vital to their pluripotent phenotype and are expressed variously throughout embryogenesis and within *in vitro* cultures (Boyer *et al.*, 2005; Chen, X *et al.*, 2008).

1.4.2 Regaining potential with induced pluripotency

In addition to the study of naturally pluripotent ESCs, the development of cellular reprogramming methods has led to interest in the production of induced pluripotent stem cells (iPSCs) from unipotent somatic cells. As the terminally differentiated cells that make up every part of the body (aside from gametes and the gametocytes from which they are made) somatic cells do not exhibit the pluripotent potential of ESCs. However, through reprogramming, pluripotency can be induced within lineage-committed somatic cells. There are currently three approaches to cellular reprogramming: (i) nuclear transfer, (ii) cell fusion and (iii) transcription factor transduction (**Fig. 1.10**).

Somatic cell nuclear transfer (SCNT) involves transplanting a diploid somatic cell nucleus into an enucleated oocyte, such that the generated cell becomes a genetically identical clone of the original somatic cell. A well-publicised result of nuclear transfer, Dolly the sheep, proved that SCNT was a viable method of cloning (Wilmut *et al.*, 1997). Further investigations into SCNT-mediated reprogramming using the mouse oocyte have

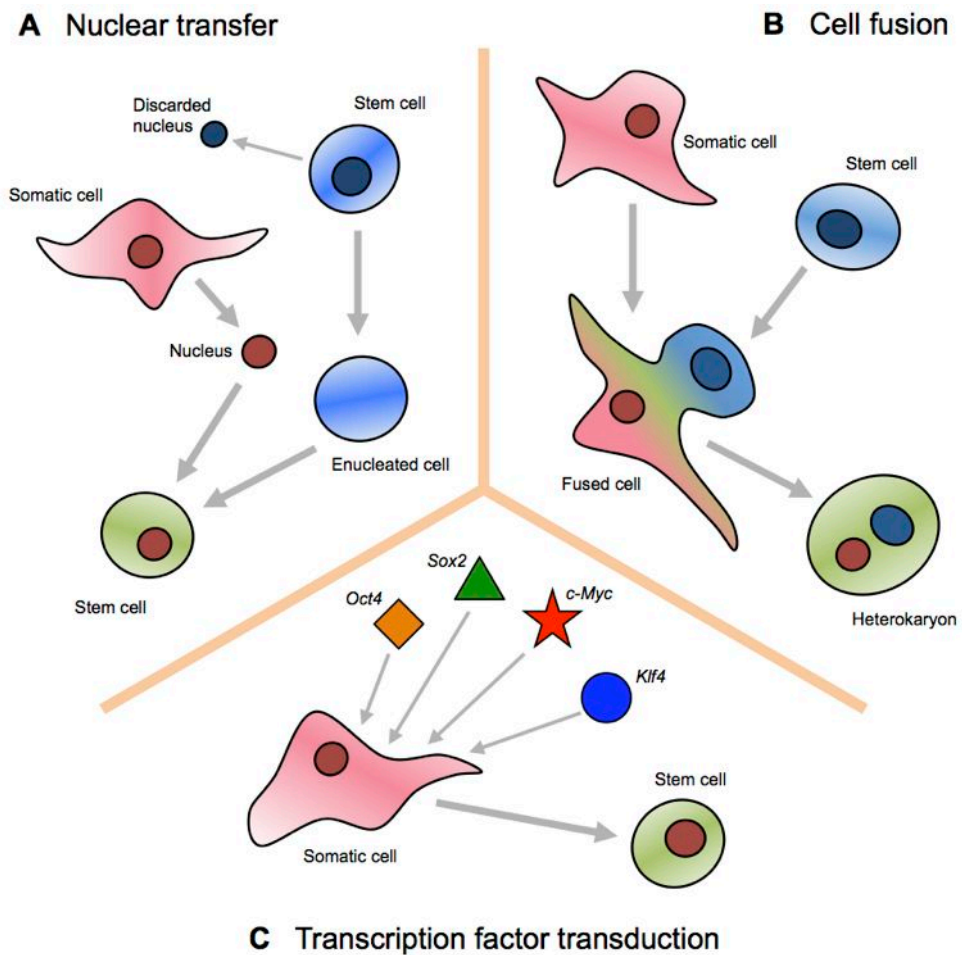


Fig 1.8. Cellular reprogramming. Approaches to cellular reprogramming include: **(A)** nuclear transfer, in which a diploid somatic cell nucleus is transplanted into an enucleated oocyte to generate an identical clone of the original somatic cell; **(B)** cell fusion, whereby an entire somatic cell is fused with a stem cell to create a single reprogrammed cell, a heterokaryon, which contains both somatic and pluripotent genetic material; and **(C)** transcription factor transduction, in which the particular genes associated with pluripotency are overexpressed to generate a pluripotent cell.

demonstrated that ESCs can be obtained with relatively high efficiency and are functionally indistinguishable from those derived from wildtype blastocysts (Yang, E *et al.*, 2007).

Similarly to nuclear transfer, cell fusion also involves the combining of cellular material. However, in this case, an entire somatic cell is fused with a stem cell to create a single reprogrammed cell, a heterokaryon, which contains both somatic and pluripotent genetic material. Cell fusion provided the means to demonstrate that the differentiated state of somatic cells was not fixed but that it could be reversed to regain a pluripotent phenotype (Blau *et al.*, 1985).

Arguably, the best examples of somatic 'plasticity' have been achieved using transcription factor transduction, in which the forced overexpression of particular genes disrupts the balance of regulators that maintain the somatic differentiated phenotype. iPSCs were first produced in this manner by the retroviral transduction of murine fibroblasts with a combination of transcription factors, namely *Oct4*, *Sox2*, *c-Myc* and *Klf4*, that were identified to be particularly associated with the pluripotency of ESCs (Takahashi, K & Yamanaka, 2006). Additional factors, such as *Nanog*, *Lin28* and *ESRRB*, have also been identified to induce pluripotency in somatic cells (Yu *et al.*, 2007; Ichida *et al.*, 2009). Direct cell reprogramming by transcription factor transduction has been successful in producing truly pluripotent cells which have been demonstrated to be capable of being differentiated to produce a full range of specific cell types, including ECs (Durcova-Hills *et al.*, 2008; Gai *et al.*, 2009; Osakada *et al.*, 2009; Song *et al.*, 2009).

1.5 Hypothesis and objectives

The natural angiogenic response of the vasculature to a wide range of cardiovascular diseases has been shown, at least in part, to involve circulating EPCs. Additionally, EPCs have been demonstrated to have a beneficial effect on blood vessel growth both *in vitro* and *in vivo* using a variety of angiogenesis assay models. However, the native EPC response to cardiovascular disease is often insufficient to resolve the condition without additional treatment. Furthermore, even with existing angiogenic treatments (which vary widely in effectiveness, cost and ease of application) some pathophysiologies remain difficult to treat. It is therefore important to explore the potential of EPCs as a tool for therapeutic angiogenic transplantation. We hypothesise that two relatively new and potentially advantageous sources of patient-specific cells, the use of differentiated ESCs and iPSCs, may be a viable alternative to EPCs for transplantation.

The aim of this investigation was to illustrate the highly angiogenic nature suggested of EPCs using an *in vitro* tubule formation model of angiogenesis. By quantifying tubule growth and assessing changes in messenger RNA (mRNA) expression and protein content, using quantitative real-time PCR (qPCR) and immunocytochemistry (ICC) respectively, it was hoped that a clearer understanding of the angiogenic potential of EPCs would be achieved. The use of EPCs as a tool for angiogenic therapy was also investigated, by assessing the effect of EPC transplantation on tubule growth, mRNA and protein expression in an established network of endothelial tubules. By the establishment of a robust *in vitro* model for the demonstration of angiogenic potential, as well as the accumulation of evidence to support the idea of EPCs as a therapeutic tool, it was intended that progression to a murine *in vivo* model would be possible. Ultimately, the comparisons made between *in vitro* and *in vivo* models may prove vital to the further development of angiogenic therapies involving EPCs. In addition to the

study of EPCs, this investigation proposed the potential of pluripotent stem cells as a viable alternative to EPCs for angiogenic transplantation and evaluated the efficiency of deriving endothelial-like cells (with, it is theorised, EPC-equivalent angiogenic potential) from ESCs and iPSCs using spontaneous and directed differentiation methods.

Hypothesis:

The highly angiogenic nature of EPCs can be exploited as a transplantable therapeutic tool for revascularisation of ischaemic tissues following cardiovascular disease, establishing a beneficial role for EPCs beyond low-level maintenance of adult vascular integrity. A population of similarly angiogenic cells can also be derived by in vitro differentiation of pluripotent stem cells to provide a rapidly-expandable and characterised alternative to natural EPCs for transplantation therapy.

The experiments described herein aimed to:

1. Characterise the phenotype and angiogenic behaviour of EPCs by endothelial-specific gene expression using qPCR, protein expression by ICC, cellular uptake of ac-LDL, lectin staining and *in vitro* tubule formation using a gel-based assay;
2. Derive EPC-like cells by *in vitro* differentiation of pluripotent ESCs and iPSCs using conditioned culture medium, and confirm their endothelial phenotype in comparison to natural EPCs using qPCR, ICC and *in vitro* tubule formation;
3. Demonstrate the beneficial effect of EPCs on angiogenesis, and the subsequent changes in endothelial-specific expression, following *in vitro* transplantation of EPCs into existing EC tubules;
4. Define a specific binding mechanism between circulating EPCs and blood platelets to illustrate the role of the 'platelet bridge' in angiogenic EPC recruitment, using *in vitro* aggregation and flow-based assays;
5. Demonstrate the targeted recruitment of EPCs to sites of angiogenesis *in vivo*, and the mediating role of platelets in EPC localisation, following transplantation of EPCs into murine models of hindlimb angiogenesis.

CHAPTER 2:

MATERIALS & METHODS

All reagents were purchased from Sigma-Aldrich (Dorset, UK) and all laboratory plastics were purchased from Greiner Bio-One (Gloucestershire, UK) unless otherwise stated.

2.1 Cell culture

All cell culture procedures were performed under sterile conditions in a Walker Class II Microbiological Safety Cabinet. Preparations of culture media were filter-sterilised using Minisart 0.2 μm single-use filter units (Sartorius Stedim Biotech, Surrey, UK). Culture media and reagents were pre-warmed to 37°C in a SUB Aqua water bath (Grant Instruments, Cambridgeshire, UK) for at least 30 min prior to use.

Cells were grown in tissue culture flasks (CellStar, Dorset, UK) pre-coated for 30 min with 0.1% gelatin, unless otherwise stated, and were maintained in a Heraeus HERAcCell 150 incubator (Thermo Fisher Scientific, Leicestershire, UK) with environmental conditions of 37°C and 5% CO₂. The size of culture flask varied according to the progress of each particular culture: initial cell cultures from cryopreserved stocks were grown in 25 cm² culture flasks; routine maintenance cultures in 75 cm² flasks; and cultures to be rapidly expanded in 175 cm² flasks. Regular observation of cell cultures was performed by brightfield microscopy at $\times 10$ objective magnification using an Eclipse TS100 inverted light microscope (Nikon, Surrey, UK) to monitor cell growth.

2.1.1 Cell lines

2.1.1.1 Endothelial cells (ECs)

Murine cardiac ECs (MCEC-1; Lidington *et al.*, 2002) were kindly provided by Professor Gerard Nash (University of Birmingham, UK). MCEC-1 cells were maintained in culture medium consisting of Dulbecco's modified Eagle medium (DMEM) supplemented with 10% foetal bovine serum (FBS), 1% penicillin-streptomycin solution, 2 mM L-glutamine, 10 U·ml⁻¹ heparin and 0.1 µg·ml⁻¹ recombinant murine epidermal growth factor (EGF). ECs were observed daily by brightfield microscopy and the culture medium changed every 48 h.

2.1.1.2 Endothelial progenitor cells (EPCs)

Murine foetal lung mesenchyme (MFLM)-4 EPCs (Akeson *et al.*, 2000) were obtained from Seven Hills Bioreagents (Ohio, USA). MFLM-4 cells were maintained in culture medium consisting of DMEM supplemented with 10% FBS, 1% penicillin-streptomycin solution, 2 mM L-glutamine, 25 mg·ml⁻¹ amphotericin B and 10 ng·ml⁻¹ basic fibroblast growth factor. EPCs were observed daily by brightfield microscopy and the culture medium changed every 48 h. To maintain their oligopotent phenotype, EPCs were routinely passaged before exceeding 70% confluence.

2.1.2 Subculture of cells

Cells maintained in 75 cm² culture flasks were passaged when 70-80% confluent. Culture medium was removed by vacuum aspiration and the cells washed with 5 ml Dulbecco's phosphate-buffered saline (D-PBS) before addition of 2 ml of 0.25% trypsin-ethylenediaminetetraacetic acid (EDTA) solution. Cells were then incubated at 37°C until they began to detach. The remaining attached cells were removed by washing the growing surface with 4 ml culture medium. The resulting cell suspension was transferred to a

15 ml conical tube, centrifuged at $600 \times g$ for 3 min and the pellet resuspended in fresh culture medium. The cells were distributed evenly between three 75 cm² flasks, culture medium added to a total volume of 12 ml and then returned to the incubator.

2.1.3 Cell counting

Trypsinised cells in suspension were quantified by using a haemocytometer. A 15 µl aliquot of the cell suspension was applied to the haemocytometer and the number of cells within the counting chamber counted using an inverted light microscope at $\times 10$ magnification. The volume of the haemocytometer counting chamber was 0.1 mm³ (equivalent to 1×10^{-4} ml) and hence the concentration of the cell suspension was calculated using the following formula:

$$\text{number of cells per ml} = \text{number of cells in } 0.1 \text{ mm}^3 \times (1 \times 10^4)$$

Two separate cell counts of a minimum of 200 cells were performed and the mean was calculated. If 200 cells could not be counted, the original cell suspension was centrifuged and resuspended in a smaller volume of medium.

2.1.4 Assessment of cell viability using Trypan blue

In order to assess the viability of subcultured cells, which can be detrimentally affected by passaging and freezing, a Trypan blue dye exclusion method was performed. Cell membrane integrity becomes impaired if a cell is dead or dying and as membrane potential collapses and the membrane becomes increasingly permeable, Trypan blue dye can penetrate the membrane and diffuses inwards to stain the cytoplasm (Tolnai, 1975). Conversely, the membrane of a healthy cell is able to exclude Trypan blue dye and therefore remains

unstained. This allows estimation of cell viability based upon the proportion of stained and unstained cells (**Fig. 2.1**).

Trypsinised cells were resuspended in D-PBS to a concentration of $2-4 \times 10^5$ cells·ml⁻¹. 500 µl of this cell suspension was transferred to a clean 1.5 ml microcentrifuge tube, to which 500 µl Trypan blue solution (4% w/v) was added. Cells were incubated in Trypan blue solution for 5 min before 15 µl was transferred to a haemocytometer and a cell count performed. A minimum of 500 cells was counted in total, with a separate count of blue-stained cells being made. Relative viability was calculated based upon the total number of cells counted and the number of those cells that had excluded the dye, thus:

$$\text{viability (\%)} = \frac{(\text{total number of cells} - \text{unstained cells})}{\text{total number of cells}} \times 100$$

It should be noted that Trypan blue staining was used only as a guide to cell viability. Trypan blue dye will readily bind to serum proteins present in culture medium, reducing contrast between viable and non-viable cells, and may lead to false-positive results (Altman *et al.*, 1993). Additionally, false-negative results may occur if the membrane integrity of a cell is sufficiently impaired to detrimentally affect viability but not to the extent that dye penetration occurs within the dye incubation or cell counting period. Furthermore, exclusion of the dye does not preclude the inability of a cell to successfully attach or proliferate in culture.

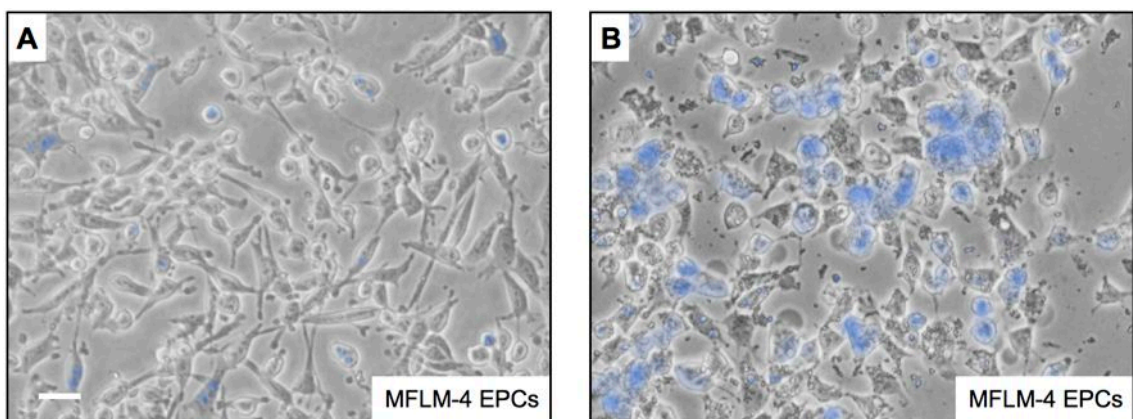


Figure 2.1. Trypan blue exclusion assay for the assessment of cell viability. Cultured cells were treated with 4% w/v Trypan blue dye for 5 min to identify (A) healthy and (B) impaired cells and thus estimate percentage cell viability. Scale bar = 20 μ m.

2.1.5 Stem cell culture

2.1.5.1 Murine embryonic fibroblast (MEF) feeder cells

Mitotically-inactivated feeder cells are required to maintain stem cells in an undifferentiated state. MEFs provide a physical support for embryonic stem cells (ESCs), which adhere as they would to the extracellular matrix *in vivo*, and secrete soluble factors that promote ESC growth (Xu *et al.*, 2001). Mitotic inactivation produces metabolically active, but non-proliferative, MEFs that continue to express specific cytokines and ligands necessary for ESC expansion (Roy *et al.*, 2001).

MEFs from Carworth Farm (CF-1) mouse embryos were obtained from American Type Culture Collection (ATCC; LGC Standards, Middlesex, UK) and cultured in DMEM with 10% FBS, 1% penicillin-streptomycin solution, 2 mM L-glutamine and 1% non-essential amino acids (NEAA). MEFs were observed daily under the microscope and the culture medium changed every 48 h. Mitomycin C treatment was used to produce mitotically inactive CF-1 MEFs. When 80-90% confluent, CF-1 MEFs were inactivated by incubation at 37°C / 5% CO₂ with medium containing 10 µg·ml⁻¹ mitomycin C for 2 h. After washing three times with 10 ml D-PBS, MEFs were incubated with 0.25% trypsin-EDTA solution. When beginning to detach, cells were washed with 6 ml medium and the cell suspension transferred to a 15 ml conical tube. MEFs were centrifuged at 600 × g for 3 min and the resulting pellet resuspended in fresh culture medium. Inactivated MEFs were counted using a haemocytometer (SEE 2.1.3) and cryopreserved in liquid nitrogen (LN₂) until required (SEE 2.1.10). To produce a confluent feeder layer of MEFs for stem cell culture, approximately 5×10⁵ cells were seeded into each well of a 6-well Corning Costar culture plate (VWR International, Leicestershire, UK).

2.1.5.2 Murine embryonic stem cells (ESCs) and induced pluripotent stem cells (iPSCs)

Stem cells were maintained in an undifferentiated state by the use of LIF (Chemicon, Livingston, UK). D3 ESCs derived from blastocysts of 129S2/SvPas mice were obtained from ATCC (LGC Standards) and QS/R27 iPSCs were kindly provided by Dr Huseyin Sumer (Monash Institute of Medical Research, Melbourne, Australia). ESCs and iPSCs were cultured at 37°C / 5% CO₂ on mitotically-inactivated fibroblast feeder layers. The culture medium for both cell lines comprised Knockout DMEM (Invitrogen, Paisley, UK) containing 15% ESC-screened HyClone FBS (Thermo Fisher Scientific), 1% penicillin-streptomycin solution, 2 mM L-glutamine, 0.1 mM β-mercaptoethanol and 10 ng·μl⁻¹ recombinant murine LIF. ESCs and iPSCs were observed daily by brightfield microscopy and culture medium changed every 24 h.

2.1.5.3 Directed differentiation of ESCs and iPSCs

The hanging droplet method was used for the directed differentiation of D3 ESCs and QS/R27 iPSCs down the endothelial lineage (**Fig. 2.2**). Undifferentiated stem cells maintained on MEF feeder layers were trypsinised and resuspended in 3 ml of differentiation medium (stem cell culture medium without LIF supplementation). The cell suspension was added to one well of a 6-well culture plate and incubated for approximately 45 min before removing and retaining the culture medium. Owing to their greater size and density the MEFs attach to the growing surface much quicker than the smaller stem cells which only attach after several hours. By removing the medium after 45 min this 'differential plating' of the two cell types can be exploited to produce a relatively pure population of stem cells, isolated from MEF feeders. The purity of the isolated stem cell population was estimated by visual assessment based upon the different sizes of the stem cells (4-6 μm diameter) and MEFs (10-12 μm). The concentration of stem cells was then measured using a haemocytometer (SEE **2.1.3**) and

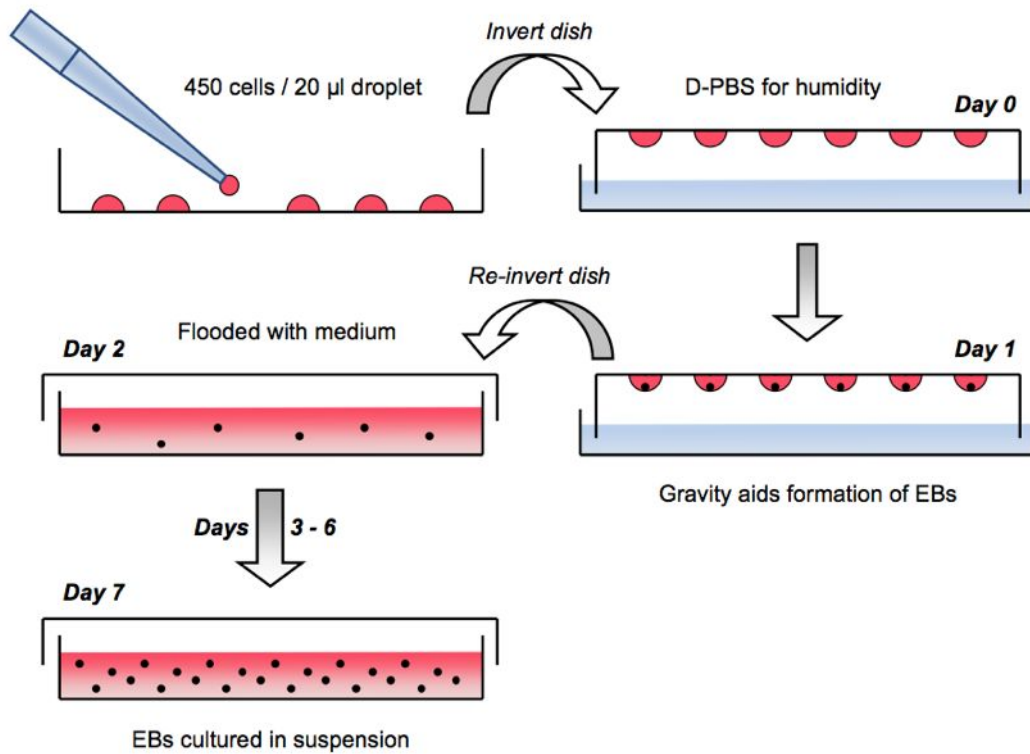


Figure 2.2. The hanging droplet method for directed differentiation of stem cells. Approximately 50 x 20 µl droplets (450 cells per droplet) of undifferentiated ESCs or iPSCs were cultured on humidified inverted Petri dishes to produce EBs. EBs were cultured at 37°C / 5% CO₂ for 48 h (d0-d1) before the dish was re-inverted and flooded with fresh differentiation medium. EBs were then cultured in suspension for d3-d7.

diluted with additional medium to 2×10^4 cells·ml⁻¹, resulting in approximately 400 cells per 20 µl of cell suspension.

For spontaneous differentiation, ESCs and iPSCs were resuspended in standard differentiation medium whilst for directed differentiation cells were resuspended in endothelial cell-conditioned medium (ECCM). ECCM was produced by incubating MCEC-1 culture medium on a monolayer of MCEC-1 cells at 37°C / 5% CO₂ for 24 h.

To produce hanging droplets, 20 µl drops were pipetted on to the base of a 100 mm Petri dish (Sarstedt, Leicestershire, UK) and the base inverted over a Petri dish lid containing 4 ml D-PBS. D-PBS was added to maintain humidity within the Petri dish and prevent the hanging droplets from drying out. The inverted dish was then incubated at 37°C / 5% CO₂ for 48 h, namely day of differentiation (d)0 and d1, to induce formation of embryoid bodies (EBs). After 48 h (d2) the D-PBS was removed from the lid and the dish re-inverted to its original orientation. The dish was flooded with 10 ml of differentiation media (stem cell medium minus LIF) and the newly-formed EBs cultured in suspension for a further 5 days (d3-d7). Nutrients were replenished every 24 h by careful replacement of 5 ml differentiation medium, avoiding removal of EBs.

2.1.6 Quantum dot labelling of EPCs

Non-specific labelling of MFLM-4 EPCs was performed using the Qtracker 655 Quantum dot kit (Invitrogen). Quantum dots (Qdots) are photostable, fluorescent nanocrystals composed of a cadmium semiconductor core surrounded by an additional zinc sulphide semiconductor shell and a polymer coating. The semiconductor material of the Qdot absorbs photons upon excitation with ultraviolet light and, like standard antibody-conjugated fluorophores, re-emits

them at a longer wavelength to produce a fluorescent signal. Qdots can be combined with a protein bioconjugate for targeted labelling or if unconjugated, as in this method, they can be used to non-specifically label an entire population of cells. Whilst the exact mechanism of non-specific cellular uptake of Qdots is unknown, it is thought to involve engulfing of the nanocrystal particles by the cell membrane (phagocytosis) and to be dependent on the size, coating and charge of the nanocrystal (Zhang, LW & Monteiro-Riviere, 2009). For non-specific labelling, EPCs were cultured in 25 cm² culture flasks, the existing culture medium removed and 6 nM Qdot labelling solution added, prepared using 3.6 µl Qtracker Component A, 4.8 µl Qtracker Component B and 1.2 ml MFLM-4 culture medium. Following incubation at 37°C / 5% CO₂ for 1 h, excess Qdot labelling solution was removed by washing twice with fresh culture medium. Labelled cells were visualised using fluorescence microscopy (SEE 2.4.1) by excitation of the Qdots between 405–615 nm and detection at 655 nm.

2.1.7 Culture of cells on acid-washed coverslips for immunocytochemistry

Cultured cells were grown on acid-washed coverslips for protein expression analysis using immunocytochemistry (SEE 2.3). 18 mm × 18 mm glass coverslips were soaked in 1M hydrochloric acid overnight in a fume hood. After soaking, coverslips were rinsed with double-distilled water (ddH₂O) and washed with 100% ethanol for 20 min, before being placed on Whatman[®] blotting paper (Whatman plc., Kent, UK) and dried in a 60°C oven for 1 h. Cultured cells were trypsinised, centrifuged and resuspended in appropriate culture medium as previously stated (SEE 2.1.2). Differentiating EBs were transferred into 1.5 ml tubes (Sarstedt) and centrifuged at 600 × g for 4 min. The supernatant was discarded and the EB pellet incubated with 500 µl of pre-warmed 0.25% trypsin-EDTA solution at 37°C / 5% CO₂ for 90 s. To further dissociate the EBs the cell suspension was gently pipetted

and 500 μ l differentiation medium added. After further centrifugation at $600 \times g$ for 4 min, the supernatant was discarded and the dissociated cells resuspended in fresh differentiation medium. Prior to dissociation of cells, glass coverslips were placed in a 6-well plate and 200 μ l of 0.1% gelatin added to the centre of the coverslip. After 15 min the excess gelatin was aspirated, the cells added to the coverslips and the 6-well plate incubated overnight at $37^{\circ}\text{C} / 5\% \text{CO}_2$.

2.1.8 Uptake of acetylated low-density lipoprotein (ac-LDL)

The endothelial phenotype of ECs, EPCs and the cells derived from ESCs and iPSCs was confirmed by uptake of 1,1'-dioctadecyl-3,3,3',3'-tetramethylindocarbocyanine perchlorate (Dil)-labelled ac-LDL (Biomedical Technologies, Inc., Massachusetts, USA). Cells grown on glass coverslips were incubated with $10 \mu\text{g}\cdot\text{ml}^{-1}$ Dil-ac-LDL in culture medium for 4 h at $37^{\circ}\text{C} / 5\% \text{CO}_2$. Following uptake of Dil-ac-LDL, cells were washed with D-PBS to remove excess Dil-ac-LDL before fixation and imaging (SEE 2.3).

2.1.9 *In vitro* scratch wound assay

The scratch wound assay involves the creation of an artificial gap in a monolayer of cultured cells, causing the cells on either side to migrate towards the centre in order to close the gap. By measuring the width of the gap at regular intervals throughout the assay the rate of migration can be established (Liang *et al.*, 2007).

After labelling cultured EPCs with Qdots, the cell monolayer was scraped once with a sterile 200 μ l pipette tip to create the scratch wound; scraped cells and debris were removed by washing with culture medium. Care was taken to create gaps of similar width in both labelled and unlabelled (control) assays, to reduce variations that might result from differences in

scratch wound width. Cells were then returned to the incubator and imaged at 0 h, 5 h and 10 h using fluorescent microscopy. To quantification migration, the distance moved by the leading edge of cells was measured at four loci along the length of the scratch wound and the following formula used:

$$\text{migration rate } (\mu\text{m}\cdot\text{min}^{-1}) = \frac{\text{distance migrated } (\mu\text{m})}{\text{time (min)}}$$

2.1.10 Cryopreservation of cultured cells

In order to maintain long-term viability of liquid nitrogen (LN₂) stored cell stocks, cryopreservation was performed. The rate of cooling during cryopreservation is important: it controls the rate at which water changes from its liquid to solid glassified phase and has a significant effect on the viability of cells after subsequent thawing. The rate of conversion of water to ice affects the rate at which the concentration of the cryopreservation medium surrounding the cells changes, directly altering its osmolality and the movement of water across the cell membrane. At an optimal rate of cooling, water leaves the cell rapidly and uniformly, maintaining thermodynamic equilibrium across the membrane and resulting in very little ice formation inside the cell itself which could result in deformation and rupture of the cell membrane (Mazur, 1970). Cell viability was also maintained by the use of dimethyl sulfoxide (DMSO) as a cryoprotectant. DMSO penetrates the cell membrane, preventing the formation of large ice crystals. In this way, if intracellular ice formation does occur during cryopreservation, the resulting ice crystals are small and have a reduced potential to damage the cell membrane (Whittingham *et al.*, 1972). Cells were cryopreserved immediately following passage (SEE 2.1.2). After trypsinisation the centrifuged cell pellet was resuspended

in 500 μ l fresh culture medium (appropriate to cell type) and transferred to a 2 ml cryovial containing 500 μ l cell freezing medium (consisting of 60% DMEM, 20% FBS and 20% DMSO; SEE **Appendix I**). Cryovials were placed in a Nalgene 'Mr. Frosty' freezing container (VWR) filled with 200 ml isopropanol and stored at -80°C for 3 h before being transferred to LN_2 storage. The surrounding isopropanol has a constant rate of cooling (approximately 1°C per min) which is optimum for maximum cell viability (McGann, 1979).

2.2 Gene expression analysis

2.2.1 Nucleic acid isolation

2.2.1.1 Extraction of RNA from cultured cells

Total RNA was extracted from cells using the RNAqueous-4PCR kit (Ambion, Cheshire, UK). Cultured cells were centrifuged and collected as a cell pellet at the time of passage (SEE **2.1.2**). The cells were washed in 500 μ l D-PBS, centrifuged at $16000 \times g$ for 1 min and the supernatant discarded. 500 μ l of Lysis/Binding solution (containing guanidinium thiocyanate) was then added to the cell pellet and thoroughly mixed by pipetting for 3 min. Vortex-mixing of the cell lysate was avoided to prevent shearing of RNA. Guanidinium thiocyanate is a strong denaturant which lyses cell membranes and rapidly inactivates cellular ribonucleases (Chomczynski & Sacchi, 1987). 500 μ l of 64% ethanol was then added, the lysate transferred to a silica filter cartridge inserted into a sterile 1.5 ml microcentrifuge tube and the mixture drawn through the filter by centrifugation at $16000 \times g$ for 1 min in a Heraeus Biofuge Fresco benchtop centrifuge (Thermo Fisher Scientific). The maximum size of the filter cartridge reservoir (800 μ l) required the lysate-ethanol to be filtered in two separate aliquots of 500 μ l, with the flow-through discarded after each centrifugation. The filter-bound RNA was washed with 600 μ l Wash Solution 1, centrifuged at $16000 \times g$ for 1 min and the flow-through discarded. The RNA was then washed with two subsequent additions of 400 μ l Wash

Solution 2/3, each followed by centrifugation at $16000 \times g$ for 1 min with the flow-through discarded. The filter cartridge was transferred to a clean microcentrifuge tube and centrifuged once more to remove the last traces of ethanol from the wash solutions before being placed into a sterile 1.5 ml RNase-free collection tube. RNA was eluted from the silica filter using 20 μ l Elution Solution, pre-warmed to 75°C , followed by centrifugation at $16000 \times g$ for 1 min. A second application of 20 μ l Elution Solution and a final centrifugation at $16000 \times g$ for 2 min ensured maximum RNA yield. RNA was transferred to a sterile 1.5 ml microcentrifuge tube and stored at -80°C .

2.2.1.2 Extraction of RNA from ECMatrix tubule formation gels

In vitro tubule formation assays were performed using ECMatrix gel to assess the angiogenic potential of ECs and EPCs (SEE 2.5). Total RNA was extracted from ECMatrix gels using the RNAqueous-Micro kit (Ambion). Similar in principle to the RNAqueous-4PCR kit, this kit has a smaller diameter silica filter and is designed for RNA isolation from small-scale ($\leq 5 \times 10^5$) cell samples.

Assayed cells were isolated from ECMatrix gel and collected as a cell pellet (SEE 2.5.5). The cells were then washed in 500 μ l D-PBS, centrifuged at $16000 \times g$ for 1 min and the supernatant discarded. 500 μ l Lysis/Binding solution (containing guanidinium thiocyanate) was then added to the cell pellet and thoroughly mixed by pipetting for 3 min, followed by the addition of 500 μ l of 64% ethanol. Vortex-mixing of the cell lysate was avoided to prevent shearing of RNA. The lysate-ethanol mixture was transferred to a filter cartridge inserted into a sterile 1.5 ml microcentrifuge tube and drawn through the filter by centrifugation at $16000 \times g$ for 1 min in a Heraeus Biofuge Fresco benchtop centrifuge (Thermo Fisher Scientific). The maximum size of the filter cartridge reservoir (800 μ l) required

the lysate-ethanol be filtered in two separate aliquots of 500 μl , with the flow-through discarded after each centrifugation. The filter-bound RNA was washed with 600 μl Wash Solution 1, centrifuged at $16000 \times g$ for 1 min and the flow-through discarded. The RNA was then washed with two subsequent additions of 400 μl Wash Solution 2/3, each followed by centrifugation at $16000 \times g$ for 1 min with the flow-through discarded. The filter cartridge was transferred to a clean microcentrifuge tube and centrifuged once more to remove the last traces of ethanol from the wash solutions before being placed into a sterile 1.5 ml RNase-free collection tube. RNA was eluted from the filter using 20 μl Elution Solution, pre-warmed to 75°C , followed by centrifugation at $16000 \times g$ for 1 min. A second application of 20 μl Elution Solution and a final centrifugation at $16000 \times g$ for 2 min ensured maximum RNA yield. RNA was transferred to a sterile 1.5 ml microcentrifuge tube and stored at -80°C .

2.2.1.3 Removal of contaminating DNA by DNase I treatment

Contaminating DNA was removed from eluted RNA by treatment with DNase I. The eluted solution was mixed with 4 μl (0.1 volume) of 10x DNase Buffer (100 mM Tris, 25 mM MgCl_2 , 1 mM CaCl_2) and 1 μl DNase I ($2 \text{ U}\cdot\mu\text{l}^{-1}$) and incubated at 37°C for 30 min. The DNase reaction was inactivated by addition of 4 μl (0.1 volume) of DNase I Inactivation Reagent and incubation at room temperature for 2 min. The solution was then centrifuged at $16000 \times g$ for 2 min to pellet the DNase I and any remaining DNA. After centrifugation the RNA-containing supernatant was transferred to a sterile 1.5 ml microcentrifuge tube and stored at -80°C .

2.2.1.4 Spectrophotometry of nucleic acids

The concentrations of RNA samples were measured using a ND-1000 NanoDrop spectrophotometer (Thermo Fisher Scientific). The sample pedestal was first cleaned with 2 μl polymerase chain reaction (PCR)-grade H_2O . The spectrophotometer was then calibrated

to zero ('blanked') using 1 μl Elution Solution to provide a reference measurement of background light absorbance against which sample light absorbance could be compared. To measure RNA concentration a 1 μl sample was pipetted on to the sample pedestal and its light absorbance measured at 260 nm. The ND-1000 Spectrophotometer v3.2 software (Thermo Fisher Scientific) then calculated the RNA concentration ($\text{ng}\cdot\mu\text{l}^{-1}$) using a modified form of the Beer-Lambert equation and the wavelength-dependent molar absorptivity (or extinction) coefficient to correlate measured light absorbance with sample concentration:

$$c = \frac{(A \times e)}{b}$$

where: c = nucleic acid concentration ($\text{ng}\cdot\mu\text{l}^{-1}$);
 A = absorbance (absorbance units, AU);
 e = extinction coefficient ($\text{ng}\cdot\text{cm}\cdot\mu\text{l}^{-1}$);
 b = light path length (cm).

2.2.1.5 Denaturing RNA agarose gel electrophoresis

The integrity of extracted RNA was assessed using a denaturing RNA agarose gel electrophoresis method. A 1.2% agarose gel was prepared by dissolving 1.8 g Molecular Grade Agarose (Bioline, London, UK) in 150 ml 1 \times Tris-acetate-EDTA (TAE) buffer (SEE **Appendix I**). The agarose-TAE solution was heated in a microwave, with regular mixing every 30 s, until the agarose was complete dissolved (approximately 2 min). The solution was poured into a 14 cm \times 12 cm gel casting tray with a 24 well comb and left to solidify to produce an agarose gel of 8 mm thickness. 10 μl of RNA was combined with 6 μl formamide, 1 μl of 1 $\text{mg}\cdot\text{ml}^{-1}$ ethidium bromide and 2 μl 6 \times Loading Buffer (SEE **Appendix I**) and incubated at 65°C for 5 min before being cooled on ice for 5 min. The RNA sample was then loaded on to the gel, which was submerged in TAE buffer, and a potential of 70 V was applied for 1 h.

An RNA marker containing bands corresponding to 28S and 18S ribosomal RNA was used to aid assessment of RNA integrity by comparing the clarity and relative intensity of the same bands in the RNA sample (**Fig. 2.3**). For visualisation of the gel the ChemiGenius² Bio Imaging gel documentation system (SynGene, Cambridgeshire, UK) was used and images recorded using GeneSnap v6.08 image acquisition software (SynGene).

2.2.2 Reverse transcription (RT)

RNA from cultured cells was reverse transcribed using the BioScript reverse transcription (RT) system (Bioline) to produce complementary DNA (cDNA). 1 µg of RNA was pre-incubated with 2 µl Oligo d(T)₁₈ (50 µM) primer at 70°C for 5 min, in a reaction volume made up to 20 µl with PCR-grade H₂O. To this pre-incubation mixture was added 6 µl 5x Reaction Buffer, 2.5 mM of each deoxyribonucleotide (dNTP), 1 µl RNase Inhibitor (40 U·µl⁻¹), 1 µl Moloney murine leukaemia virus (MMLV) reverse transcriptase (RTase) enzyme (200 U·µl⁻¹) and PCR-grade H₂O up to 30 µl. Reactions were incubated in a PTC-200 DNA Engine Thermal Cycler (Bio-Rad, Hertfordshire, UK) at 42°C for 1 h, followed by denaturation of the RTase by incubation at 70°C for 10 min. No enzyme control (NEC) reactions (minus RTase) and non template control (NTC) reactions (minus RNA) were performed alongside each RNA sample to confirm that contaminating DNA had been completely removed and that all RT reagents used were DNA- and RNA-free, respectively.

2.2.3 Reverse transcription polymerase chain reaction (RT-PCR)

2.2.3.1 Oligonucleotide primer design

Oligonucleotide primers for RT-PCR were designed using previously published genomic and mRNA transcript sequences available from the NCBI GenBank database (<http://www.ncbi.nlm.nih.gov/Genbank>). The following formula was used to calculate the

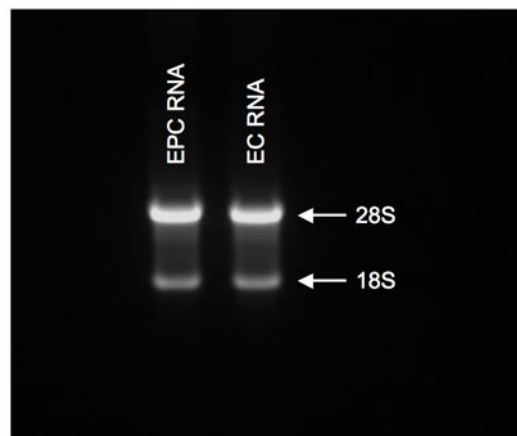


Figure 2.3. Denaturing RNA agarose gel electrophoresis. The quality of RNA used for gene expression analysis was confirmed by the relative intensity (2:1) of the 28S and 18S ribosomal RNA bands.

melting temperature (T_m) of designed primers and is considered an appropriate indication of primer-DNA annealing temperature (T_a) (Sambrook *et al.*, 1989):

$$T_m = \%GC \times 0.41 + 64.9 - \left(\frac{600}{n} \right)$$

where: T_m = melting temperature of primer;
 %GC = percentage of G and C bases in primer;
 n = total number of bases in primer.

Primers sets (forward and reverse) for use in the same reaction were designed to have similar GC content and total numbers of base pairs (bp) to produce complementary primers with similar annealing temperatures (**Table 2.1**). During primer design, the specificity and homology of each primer set to the intended gene of interest were confirmed using the NCBI Mouse BLAST facility (<http://blast.ncbi.nlm.nih.gov/Blast.cgi>). After oligonucleotide primer synthesis (by Invitrogen) the optimum reaction conditions for each primer set were determined by performing several RT-PCRs using the calculated T_m , $T_m + 1^\circ\text{C}$ or $T_m - 1^\circ\text{C}$ as the reaction annealing temperature and a range of MgCl_2 concentrations.

2.2.3.2 Reaction conditions for RT-PCR

RT-PCR was used to determine expression of particular genes of interest. Each reaction contained 2 μl of cDNA template, 5 μl of 10 \times NH_4 Reaction Buffer (Bioline), 1.5-2.5 mM MgCl_2 (Bioline; see **Table 2.1** for concentration), 25 mM of each dNTP (Bioline), 0.5 μM of each forward and reverse primer (Invitrogen), 2.5 U *Thermus aquaticus* (Taq) DNA polymerase (Bioline) and PCR-grade H_2O up to 50 μl . RT-PCR was performed in a PTC-200 DNA Engine Thermal Cycler (Bio-Rad) according to pre-inputted programmes. Each RT-PCR

Primer	Nucleotide Sequence	Product	T _a	Ext	MgCl ₂
VEGFR2_F	5'-TCTGTGGTTCTGCGTGGAGA-3'	270 bp	56°C	45 s	1.5 mM
VEGFR2_R	5'-GTATCATTTCCAACCACCCT-3'				
VE-cad_F	5'-TCCTCTGCATCCTCACCATCACA-3'	122 bp	58°C	30 s	2.0 mM
VE-cad_R	5'-GTAAGTGACCAACTGCTCGTGAAT-3'				
CD31_F	5'-CGCACCTTGATCTTCCTTTC-3'	244 bp	58°C	30 s	2.5 mM
CD31_R	5'-AAGGCGAGGAGGGTTAGGTA-3'				
β-actin_F	5'-CACCACACCTCCTACAATGAGC-3'	242 bp	60°C	30 s	1.0 mM
β-actin_R	5'-TCGTAGATGGGCACAGTGTGGG-3'				

Table 2.1. Primer sequences for RT-PCR.

_F, forward; *_R*, reverse; *T_a*, annealing temperature; *Ext*, extension time.

programme consisted of an initial denaturation stage, multiple cycles of denaturation, annealing and extension, and a final extension stage. Initial denaturation (95°C for 5 min) was used to completely melt the DNA template before commencement of the reaction. The cycling stage (repeated 25 to 35 times) included: denaturation at 95°C for 30 s, to separate the double-stranded (ds)DNA template; annealing at T_m for 30 s, to bind primers to the complementary region of the single-stranded (ss)DNA; and extension at 72°C for 30-45 s, when the polymerase enzyme replicates DNA between the primer-bound regions of the template. The extension time used for each reaction (**Table 2.1**) was based on the processivity of the Taq polymerase, i.e. the average number of nucleotide base pairs added by the enzyme per second of the reaction, calculated by the manufacturer to be $10 \text{ bp}\cdot\text{s}^{-1}$. Final extension (72°C for 5 min) was performed to extend any remaining single-stranded DNA (ssDNA) in the reaction.

2.2.3.3 cDNA separation by agarose gel electrophoresis

RT-PCR products were resolved on a 2% agarose gel, prepared by heating 3 g of Molecular Grade Agarose (Bioline) in 150 ml 1× TAE buffer (SEE **Appendix I**) and adding 15 µl of $1 \text{ mg}\cdot\text{ml}^{-1}$ ethidium bromide before cooling. 20 µl of each RT-PCR product, combined with 4 µl 6× Loading Buffer (SEE **Appendix I**) was loaded on to the gel, which was submerged in TAE buffer, and a potential of 100 V applied across the gel for 1 h. 7 µl of a 100-1000 bp DNA marker (Hyperladder VI, Bioline) was also loaded on to the gel to allow estimation of the size of the RT-PCR product.

2.2.3.4 Purification of cDNA from agarose gels

cDNA was isolated from agarose gels and purified with the QIAquick Gel Extraction Kit (QIAGEN). Each DNA band (approximately 100 mg of gel) was excised from the gel using a

sterile scalpel with the aid of a NucleoVISION UV Transilluminator (NucleoTech, California, USA) and placed in a sterile 1.5 ml microcentrifuge tube. 300 µl QG Buffer (3 µl per mg of gel) was added and the tube incubated at 50°C to dissolve the agarose gel. The tube was mixed by inversion every 5 min until completely solubilised (approximately 15 min). 100 µl isopropanol (1 µl per mg of gel) was then added and the tube inverted several times to precipitate the DNA. The solution was transferred into a QIAquick Spin Column placed in a clean microcentrifuge tube and drawn through the column by centrifugation at 16000 × g for 1 min to bind the DNA to the filter. The flow-through was discarded. The filter was washed by the addition of 500 µl QG Buffer and centrifugation at 16000 × g for 1 min to remove any traces of agarose and by the addition of 750 µl PE Buffer and centrifugation at 16000 × g for 1 min to remove salts and ethidium bromide. After each wash stage the flow-through was discarded. The filter column was again centrifuged at 16000 × g for 1 min to remove any remaining PE buffer before being transferred into a sterile 1.5 ml microcentrifuge tube. 30 µl of PCR-grade H₂O was added to the centre of the filter and the column centrifuged at 16000 × g for 1 min to elute the DNA. The concentration of DNA was measured using a NanoDrop spectrophotometer (SEE 2.2.1.4) before storage at -20°C.

2.2.4 DNA sequencing

2.2.4.1 Sequencing of RT-PCR products from purified agarose gels

RT-PCR products were sequenced to confirm that the intended genes of interest had been amplified and was performed by the Molecular Biology Service (Department of Biological Sciences, University of Warwick, UK). For sequencing 10 ng of purified RT-PCR product (SEE 2.7), 5.5 pmol forward primer and PCR-grade H₂O up to 10 µl was supplied to the Molecular Biology Service. 4Peaks v1.7.2 software (Mek&Tosj.com, Amsterdam, The Netherlands) was used to view the returned chromatograms and the EMBL-EBI ClustalW facility

(<http://www.ebi.ac.uk/Tools/clustalw/>) was used to align sequencing results to published sequences to confirm homology.

2.2.4.2 DNA cloning by plasmid vector

RT-PCR products of relatively short DNA sequences (e.g. 122 bp amplicon of *VE-cadherin* gene) were inserted into a plasmid vector (*pCR 4-TOPO*, **Fig. 2.4**) before sequencing using the TOPO TA Cloning Kit for Sequencing (Invitrogen). Taq polymerase has a terminal transferase activity which results in a single deoxyadenosine (A) residue being added to the 3' end of the amplified RT-PCR product. Conversely the *PCR 4-TOPO* vector is linearised with single 3' deoxythymidine (T) overhangs. The complementarity of the additional 3' residues allows RT-PCR products to ligate efficiently into the *pCR 4-TOPO* vector. Each 6 µl cloning reaction comprised 4 µl RT-PCR product (SEE **2.2.3.4**), 1 µl Salt Solution and 1 µl *pCR 4-TOPO* vector. The reaction mix was incubated for 30 min at room temperature before being placed on ice and used to transform competent *Escherichia coli* (*E. coli*) cells.

2.2.4.3 Transformation of competent *E. coli* cells

After cloning the *pCR 4-TOPO* construct was transformed into Subcloning Efficiency Chemically Competent DH5α *E. coli* Cells (Invitrogen). Competence is the ability of a cell to take up extracellular DNA from its surrounding environment and can be chemically induced to improve uptake of the vector-PCR product construct. The *pCR 4-TOPO* vector contains genes encoding for ampicillin and kanamycin resistance to enable selection of successfully transformed cells using selective agar plates.

Prior to transformation, one vial of DH5α competent cells was thawed on ice. 2 µl of the TOPO cloning reaction was added to the cell vial, gently mixed by inversion and incubated

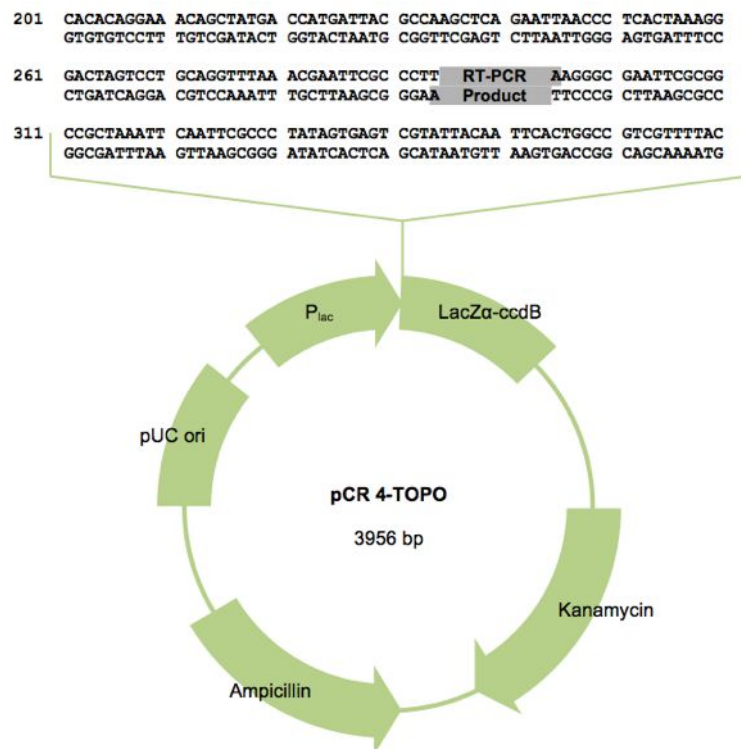


Figure 2.4. pCR 4-TOPO plasmid vector. Single 3' deoxythymidine (T) overhangs allow ligation of vector to RT-PCR products possessing Taq-resulting deoxyadenine (A) residues. Regions encoding resistance to ampicillin and kanamycin allow selection of successfully transformed cells. Adapted from manufacturer's documentation.

on ice for 30 min. The cells were heat shocked in a 42°C water bath for 30 s and immediately returned to ice for 2 min. 950 µl of room temperature Super Optimal broth with Catabolite repression medium was then added and the vial incubated at 37°C for 1 h on a horizontal shaker at 200 rpm. After shaking, 50 µl of the transformed cells were spread on to a pre-warmed selective agar plate containing 100 µg·ml⁻¹ kanamycin and incubated at 37°C overnight. The following morning five separate colonies were picked from the agar plate using sterile pipette tips. Each tip was placed in a sterile 15 ml conical tube and 10 ml lysogeny broth medium containing 100 µg·ml⁻¹ kanamycin was added. The conical tubes were incubated at 37°C overnight on a horizontal shaker at 200 rpm to produce an expanded quantity of transformed cells.

2.2.4.4 Purification of plasmid DNA for sequencing

Plasmid DNA was isolated from transformed cells using the QIAprep Miniprep kit (QIAGEN). The procedure involves lysis of bacterial cells by alkaline lysis buffer, adsorption of plasmid DNA on to a silica filter in the presence of a high salt buffer, and washing and elution of plasmid DNA from the filter. Bacterial cells in suspension in 15 ml microcentrifuge tubes were harvested by centrifugation at 5400 × g for 10 min at 4°C and removal of the supernatant. The bacterial pellet was suspended in 250 µl Buffer P1 and transferred to a clean 1.5 ml microcentrifuge tube. The bacteria were resuspended completely by aspiration until no clumps remained to ensure complete lysis of the cells. 250 µl Buffer P2 was added to the tube and mixed gently but thoroughly by inverting the tube 5 times. 350 µl Buffer N3 was then added to the tube and mixed by inverting the tube a further 5 times. The bacterial lysate was centrifuged at 16000 × g for 10 min to form a compact white pellet. The supernatant was transferred to a QIAprep spin column, centrifuged at 16000 × g for 1 min and the flow-through discarded. The spin column was washed by the addition of 500 µl Buffer PB and

centrifugation at $16000 \times g$ for 1 min, and then the addition of 750 μl Buffer PE and further centrifugation at $16000 \times g$ for 1 min. The flow-through was discarded and the spin column centrifuged for an additional min to removal residual wash buffer. The spin column was then transferred to a clean 1.5 ml microcentrifuge and the DNA eluted by addition of 50 μl Buffer EB and centrifugation at $16000 \times g$ at 1 min. Eluted plasmid DNA was prepared for sequencing as previously described (SEE 2.2.4.1).

2.2.5 Quantitative real-time PCR (qPCR)

2.2.5.1 Detection of DNA using SYBR Green dye

Assay of DNA and cDNA was performed by qPCR using SYBR Green chemistry. SYBR Green I is an asymmetrical cyanine dye which intercalates into the minor groove of double-stranded DNA (dsDNA) and produces a complex that emits a green fluorescent signal (524 nm) upon excitation with blue light (485 nm) (Zipper, 2004). The intensity of the fluorescent signal is proportional to the amount of SYBR-bound DNA present and so measurement of the fluorescent signal can be used to quantify DNA (Fig. 2.5). During the qPCR reaction the fluorescent signal is measured at every cycle during and immediately following the product extension phase. During the reaction the number of copies of the gene of interest increases exponentially as described by the following equation (Livak, 2001):

$$X_n = X_0 \times (1 + E_x)^n$$

where: X_n = number of molecules of gene of interest at cycle n ;

X_0 = initial number of molecules of gene of interest;

E_x = efficiency of amplification of gene of interest;

n = number of completed cycles.

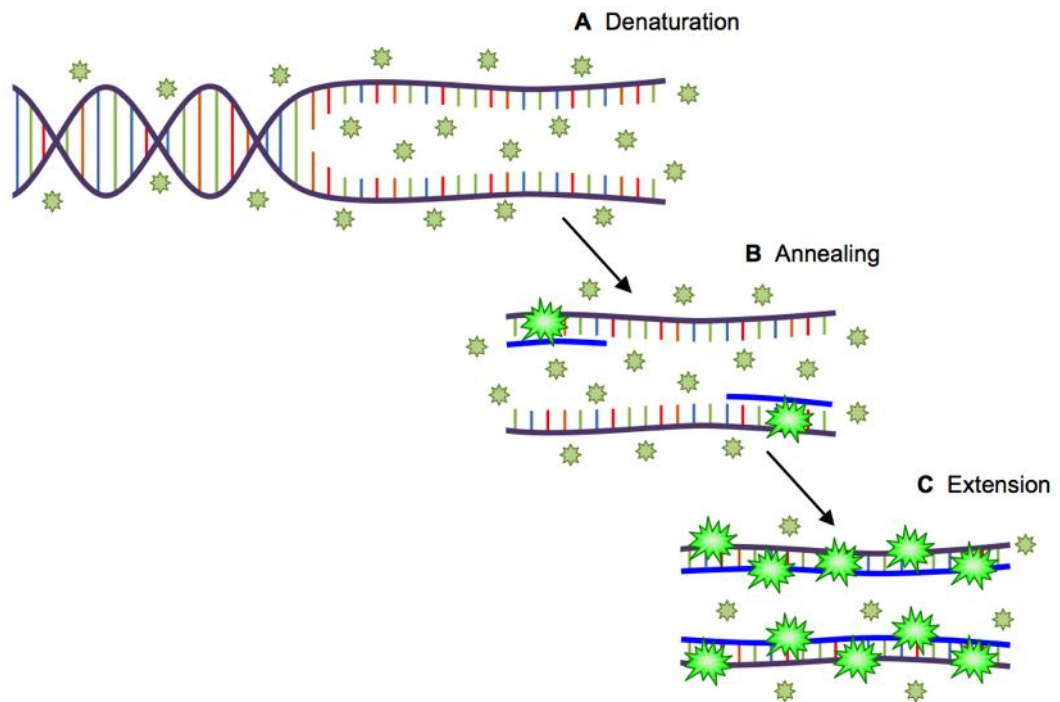


Figure 2.5. Real-time DNA quantification using SYBR Green chemistry. Double-stranded DNA is denatured (A) in the presence of SYBR Green. The dye is incorporated during annealing (B) and extension (C) and emits a fluorescent signal proportional to the number of new copies of the gene.

As the reaction progresses the number of copies of the gene of interest, and hence the fluorescent intensity, increases after every cycle until the fluorescent signal crosses the threshold level. At this threshold cycle (C_t) the signal intensity increases exponentially, rising significantly above the background fluorescence detected within the reaction. For that reason a sample containing a high concentration of DNA will cross the C_t and reach the exponential phase sooner than a sample containing a low concentration and thus the C_t can be directly correlated to the number of copies of the gene of interest in the reaction (Bustin, 2000). By using a series of standards diluted to a known concentration of specific product, a standard curve can be generated, represented by the following equation:

$$y = mx + c$$

where: $y = C_t$ value;

$m =$ gradient of the curve;

$x =$ initial concentration of the standard;

$c =$ constant determined by Rotor-Gene software.

The standard curve equation can be used to quantify DNA by comparing the C_t values of unknown samples to the standard curve and extrapolating their concentration. The coefficient of correlation (r^2) describes how the C_t values of the DNA standards compare to their initial concentrations and how straight a standard curve is generated (Pfaffl, 2001). Linearity of the standard curve (where r^2 is close or equal to 1) ensures greater accuracy of DNA quantification when extrapolating concentrations of unknown samples based on the defined standards. Reaction efficiency (E) describes how well the target product is amplified and therefore, as ideally the number of target products should double at each cycle, E should be close to 100% (Bustin, 2000; Marino *et al.*, 2003).

2.2.5.2 Preparation of DNA standards for qPCR

Standards of known DNA concentration are required for qPCR and were prepared by dilution of purified RT-PCR products. RT-PCR was performed to amplify a gene of interest from cDNA, before being electrophoresed and purified from agarose gel (SEE 2.2.3). The concentration of the eluted cDNA was measured using the NanoDrop spectrophotometer (SEE 2.2.1.4) and diluted to $2 \text{ ng}\cdot\mu\text{l}^{-1}$ (Standard 1) using PCR-grade H_2O . Nine subsequent serial dilutions were performed to produce Standards 2 to 9 (2×10^{-1} to $2\times 10^{-9} \text{ ng}\cdot\mu\text{l}^{-1}$). Diluted DNA standards were stored at -20°C until needed.

2.2.5.3 Reaction conditions for qPCR

Each qPCR reaction (25 μl total volume) contained 1 μl cDNA template, 12.5 μl SensiMix, 0.5 μl 50x SYBR Green I Solution, 0.2 μM each of forward and reverse primers and PCR-grade H_2O . Primers designed for RT-PCR were also used for qPCR (Table 2.1). qPCR was performed in a Rotor-Gene 3000 rotary real-time cycler (QIAGEN). Initial denaturation was performed at 95°C for 15 min, followed by 50 cycles of: denaturation at 95°C for 10 s; annealing at 55°C (for *VEGFR2* and *CD31*) or 57°C (for *VE-cadherin* and *β -actin*) for 15 s; and extension at 72°C for 15 s. Data were acquired in the FAM/SYBR fluorescent channel during this final extension phase. An additional acquisition step was included to eliminate primer dimerisation from the subsequent analysis, the reaction temperature of which was based on the temperature at which the specific product started to melt. This was determined using dissociation curve analysis, performed by ramping the reaction temperature from 62 - 99°C in 1°C increments every 5 s to determine the melting point of each product in the reaction.

2.2.5.4 Relative quantification of DNA

Relative quantification of cDNA was performed in triplicate in two separate reactions to produce six results per gene of interest. The two extreme values were excluded in order to negate variation caused by pipetting error and the four remaining values were used to calculate mean gene expression \pm standard error of mean (SEM). The method of relative DNA quantification involves comparing expression of mRNA transcripts of the gene of interest in experimental samples to a reference sample. The comparison of experimental samples with an unknown or changing number of cells was possible using a separate qPCR reaction providing quantification of a housekeeping gene. Relative DNA quantification is performed using the following formula (Pfaffl, 2001):

$$\text{Ratio} = \frac{(E_{\text{target}})^{\Delta \text{target Ct}}}{(E_{\beta\text{-actin}})^{\Delta \beta\text{-actin Ct}}}$$

where: E_{target} = efficiency of qPCR for the gene of interest;

$E_{\beta\text{-actin}}$ = efficiency of qPCR for β -actin gene;

$\Delta \text{target Ct}$ = difference in Ct values (control Ct – sample Ct) for gene of interest;

$\Delta \beta\text{-actin Ct}$ = difference in Ct values (control Ct – sample Ct) for β -actin gene.

Results of relative quantification were expressed as a ratio of the levels of mRNA transcripts of the gene of interest (i.e. *VEGFR2*, *CD31* or *VE-cadherin*) in an experimental sample in comparison to a defined control sample. The data obtained for the genes of interest were referenced to the housekeeping gene β -actin as an internal control, to account for differences in cell number and initial RNA load (Schmittgen & Zakrajsek, 2000).

2.3 Immunocytochemistry (ICC)

ICC was used to detect the presence and location of specific proteins expressed by cells by the use of antibodies specific to those proteins. After being grown on glass coverslips (SEE 2.1.7) cells were prepared by fixation, permeabilisation and blocking before antibody incubation. Fixation preserves the structure of the cell and maintains cellular proteins in a form that can be recognised by the chosen antibody. Permeabilisation of the cell membrane allows antibodies to diffuse into the cell and is necessary when intracellular proteins are being localised. Blocking minimises non-specific labelling by reducing the affinity of antibodies to bind to proteins other than those of interest. After blocking, cells were incubated with a primary antibody which bound to the protein of interest, washed to remove unbound primary antibody, incubated with a fluorescently-labelled secondary antibody targeted to the primary antibody and finally washed to remove any unbound secondary antibody. Imaging was performed using fluorescent or confocal microscopy (SEE 2.4).

2.3.1 Preparation of coverslip-cultured cells for ICC

Cells grown on glass coverslips were transferred to 6-well plates and fixed by addition of 1 ml of 4% paraformaldehyde (SEE **Appendix I**) for 30 min at room temperature. If intracellular proteins were being labelled permeabilisation was performed using 1 ml of 1% Triton X-100 (SEE **Appendix I**) for 15 min at room temperature; if cell-surface proteins were being labelled the permeabilisation stage was omitted. Following permeabilisation cells were washed three times with 2 ml PBS for 5 min and then blocked with antibody blocking solution (SEE **Appendix I**) for 30 min at room temperature. Cells were either stained immediately or the coverslips stored in 3 ml blocking solution at 4°C until required.

2.3.2 ICC protocol

2.3.2.1 Lectin staining

Prior to antibody staining, cells were labelled with lectin, a sugar-binding glycoprotein that is highly specific for carbohydrate moieties found on cell membranes. Cells were incubated with $0.5 \text{ mg}\cdot\text{ml}^{-1}$ fluorescein-conjugated *Griffonia (Bandeiraea) simplicifolia* lectin I (Vector Laboratories Inc., California, USA) in PBS for 1 h at 37°C . Excess lectin was removed by washing three times with blocking buffer for 5 min each before primary antibody incubation.

2.3.2.2 Primary antibodies

Antibodies raised against the stem cell adhesion factor CD34 (AbD Serotec, Oxfordshire, UK), endothelial-specific proteins VEGFR2 and CD133 (Abcam, Cambridgeshire, UK), and the component of the mitochondrial electron transport chain COXI (Molecular Probes, Invitrogen) were used to analyse expression of those proteins (**Table 2.2A**). Coverslips were inverted over $50 \mu\text{l}$ of primary antibody diluted in blocking solution, atop a square of flexible plastic film (Parafilm[®]; Pechiney Plastic Packaging, Illinois, USA) inside a 10 cm Petri dish (**Fig. 2.6**). Tissue paper, moistened with distilled water, was placed inside the dish and the dish sealed with Parafilm to maintain humidity. Primary antibody incubation was performed overnight at 4°C . Following primary antibody incubation, cells were washed three times with blocking solution for 5 min each before labelling with secondary antibody.

2.3.2.3 Secondary antibodies

Secondary antibodies were prepared in a total of $50 \mu\text{l}$ blocking solution and applied to coverslips as with primary antibodies. Secondary antibodies were conjugated with fluorescent labels to enable localisation using fluorescent and confocal microscopy (**Table 2.2B**). Following secondary antibody incubation, cells were washed three times with

A	Target Protein	Clonality	Isotype	Host	Final Concentration
	Mouse VEGFR2	Polyclonal	IgG	Goat	4 $\mu\text{g}\cdot\text{ml}^{-1}$
	Mouse CD133	Polyclonal	IgG	Rabbit	2 $\mu\text{g}\cdot\text{ml}^{-1}$
	Mouse CD34	Monoclonal	IgG	Rat	5 $\mu\text{g}\cdot\text{ml}^{-1}$
	Mouse COX I	Monoclonal	IgG	Mouse	3 $\mu\text{g}\cdot\text{ml}^{-1}$

B	Reactivity	Host	Conjugate	Dilution
	Goat IgG	Rabbit	AF 488	5 $\mu\text{g}\cdot\text{ml}^{-1}$
	Rabbit IgG	Donkey	AF 594	4 $\mu\text{g}\cdot\text{ml}^{-1}$
	Rat IgG	Chicken	AF 594	5 $\mu\text{g}\cdot\text{ml}^{-1}$
	Mouse IgG	Donkey	AF 488	6 $\mu\text{g}\cdot\text{ml}^{-1}$

Table 2.2. (A) Primary and (B) secondary antibodies used for immunocytochemistry.

AF, Alexa Fluor.

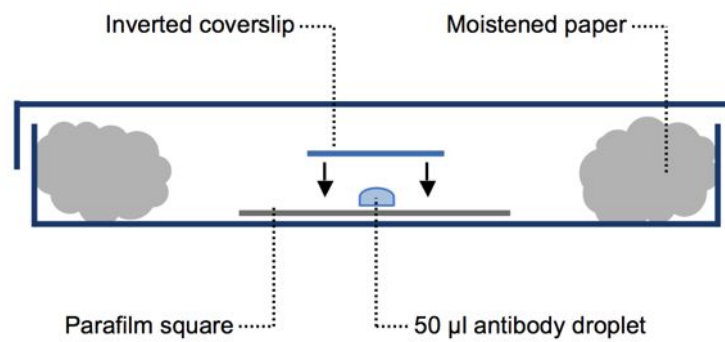


Figure 2.6. Immunocytochemistry by antibody labelling. Cells cultured on gelatin-coated coverslips were inverted over 50 µl primary or secondary antibody atop Parafilm within a humidified Petri dish.

blocking solution for 5 min each. Negative controls were included in each experiment, comprising incubation with blocking solution without primary antibody followed by normal incubation with the secondary antibody. These were used to identify non-specific binding of the secondary antibody and thus prevent false identification of positive results.

2.3.3 Preparation of ICC slides for imaging

Antibody-labelled coverslips were inverted and mounted on a glass microscope slide using 10 μ l Vectashield Mounting Medium with 4',6-diamino-2-phenylindole (DAPI) (Vector Laboratories Inc.). DAPI is a cell-membrane-permeable counterstain that binds to DNA, producing a blue fluorescent signal (460 nm) upon excitation with ultraviolet light and enabling identification of cell nuclei. Coverslips were sealed around the edge using clear nail varnish to prevent mounting medium from drying out. Coverslips were either imaged immediately or stored at -20°C.

2.4 Microscopy and imaging

2.4.1 Fluorescent microscopy

Fluorescent microscopy was performed using an Eclipse TE-2000 fluorescent microscope (Nikon). Cells were visualised using $\times 10$ and $\times 20$ magnification objectives and images were acquired with a Digital Sight DS-L1 Camera Control Unit (Nikon). For fluorescent microscopy, DAPI was excited at 360 nm and detected at 460 nm, Alexa Fluor (AF) 488 was excited at 488 nm and detected at 519 nm, and AF 594 was excited at 594 nm and detected at 617 nm.

2.4.2 Confocal microscopy

Confocal microscopy of tissue sections and cells was performed using a Zeiss 510 META confocal microscope (Carl Zeiss Ltd., Hertfordshire, UK) with $\times 40$ and $\times 63$ oil differential interference contrast objectives with numerical aperture (NA) of 1.3 and 1.4, respectively. The diameter of the microscope detection pinhole was set to 1 Airy unit. At this diameter the pinhole aperture matches the Airy disc, the inner circle of the light diffraction pattern being produced by the excitation light as it passes through the pinhole. Adjustment of the pinhole diameter to 1 Airy unit was performed automatically by the microscope control software, based upon the magnifying factor and NA of the objective in use and the wavelength of the excitation source. Matching the pinhole diameter to the Airy disc reduces interference by light from outside the focal plane, increasing the signal:noise ratio and allowing optimal acquisition of minimally thin optical sections. Data were captured in 512×512 pixel format and confocal z-stacks were rendered from $1 \mu\text{m}$ optical sections to aid localisation of fluorescent signals on the z axis.

2.5 *In vitro* tubule formation assay

Assessment of the angiogenic activity of cultured cells was performed using the *In Vitro* Angiogenesis Assay Kit (Chemicon) with adaptations made to the manufacturer's original protocol. When cultured on ECMatrix gel (a semi-solid substance composed of basement membrane proteins) endothelial cells align and cluster to form tube-like networks. Growth factors, such as tumour necrosis factor β and basic fibroblast growth factor (bFGF), and proteolytic enzymes, such as plasminogen and MMPs, are included in the ECMatrix gel to stimulate endothelial cells and optimise tubule formation. The angiogenic potential of cells cultured on ECMatrix gel was then determined by quantification of tubule formation by tubule node counting and measurement of tubule branch length.

2.5.1 Preparation of ECMatrix assay gels

ECMatrix assay gels were prepared in a 5°C cold room using pre-cooled pipette tips and microcentrifuge tubes to prevent premature solidification of the gel matrix. The ECMatrix Gel Solution and Diluent Buffer components, stored at -20°C, were thawed overnight on ice at 4°C. For each assay gel 3 µl (1 volume) Diluent Buffer was added to 27 µl (9 volumes) ECMatrix Gel Solution in a sterile microcentrifuge tube and slowly mixed by pipetting, avoiding incorporation of bubbles. 30 µl of the diluted ECMatrix solution was then transferred to a sterile 18 mm × 18 mm glass coverslip and spread evenly across the surface using the pipette tip. Gel-coated coverslips were incubated at 37°C for 30 min prior to addition of cells to allow the ECMatrix to polymerise. ECMatrix gels were prepared in duplicate to allow RNA analysis and ICC to be performed in parallel.

2.5.2 Assay protocol

Once solidified, each assay gel was placed in the bottom of a well of a 6-well culture plate (Thermo Fisher Scientific). Cells to be assayed (ECs, EPCs and cells derived from ESCs and iPSCs) were removed from culture by trypsinisation and resuspended in culture medium. Cells were seeded on to the assay gels in 300 µl medium at a density of 8×10^4 cells per well and the 6-well plate returned to the 37°C / 5% CO₂ incubator. Tubule formation was then inspected every hour under an Eclipse TS100 inverted light microscope (Nikon).

2.5.3 Quantification of angiogenic potential

2.5.3.1 Image processing

Digital images of each *in vitro* tubule formation assay were processed using ImageJ v10.2 software (Research Services Branch, National Institutes of Health, Maryland, USA) before quantification of tubule formation (**Fig. 2.7**). Images were initially manipulated using two

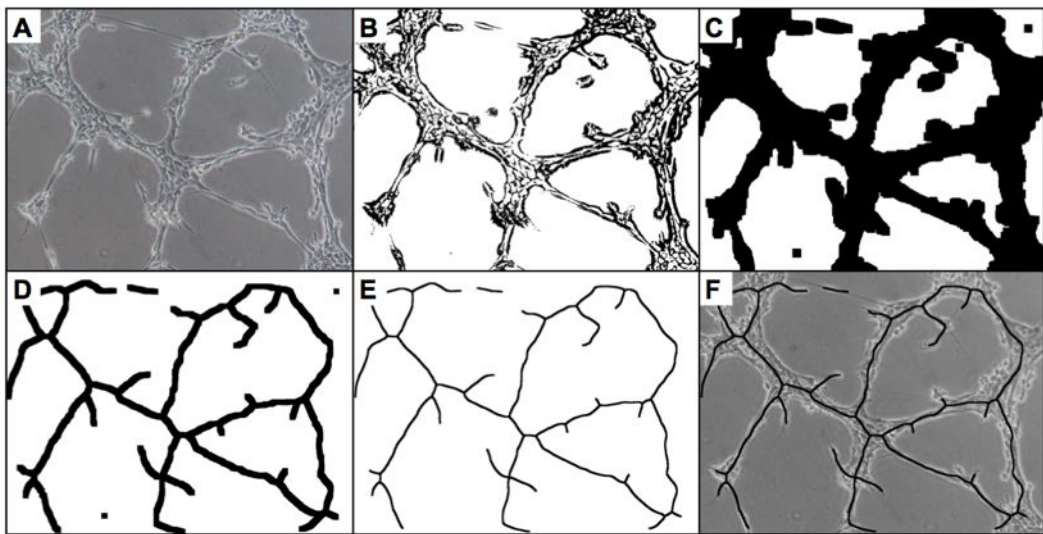


Figure 2.7. Image processing of in vitro tubule formation assays. The original image (A) is binary encoded and high-pass filtered (B), then simplified by repeated cycles of 'skeletonisation' and 'dilation' (C, D) to produce a network schematic (E) to be overlaid on the original image (F).

sequential colour and threshold filters to produce first greyscale and then binary-encoded (i.e. black and white) images. High-pass filtering was also applied to remove out-of-focus structures and background image artefacts. This was followed by repeated cycles of 'erosion' and 'dilation' processing operations to isolate the longitudinal centre of each branch and produce a simplified schematic of the tubule network.

2.5.3.2 Quantification by node counting

Tubule formation was quantified by counting nodes, a node being defined as a point at which tubules intersected or formed a junction. Each type of node was graded based on its structure: branch end-points were graded as 1; branch-branch intersections as 2; junctions of three and four branches as 3 and 4 respectively; and nodes formed of 5 or more branches as 5+. At 2 h intervals the average number of each type of node in each assay (based on five random fields of view) was calculated as mean node number \pm SEM.

2.5.3.3 Quantification by branch length measurement

Quantification of tubule formation was also performed by measuring tubule branch length using AQuaL: Angiogenesis Quantification software (Boettcher *et al.*, 2009). Using the software, each simplified tubule schematic image was tagged with points and connecting lines. Single points were then defined as either end points or branch junctions and a connecting line network generated automatically. The branch network was automatically measured by the software and the overall length of branches recorded. Distance calibration, based upon the resolution and magnification factor of the image, enabled the relative length (in pixels) of connecting lines to be converted to accurate absolute lengths (in microns) enabling comparison of replicate assays. Measurements were made at 2 h intervals (using five random fields of view) and the mean branch length per mm^2 of assay \pm SEM calculated.

2.5.4 *In vitro* EPC transplantation

To investigate the effect of *in vitro* EPC transplantation a quantity of EPCs were introduced into an *in vitro* tubule formation assay gel containing a pre-formed EC tubule network. In order to avoid a large difference in cell density between standard tubule assays and those transplanted with additional cells (which could produce ambiguous data) it was decided that the quantity of EPCs used for transplantation would be 10% of the original EC seeding density. This allowed EPCs to be introduced into the EC tubule network whilst minimising the change in cell density as a result of transplantation. Furthermore it was decided that the initial EC seeding density of assay gels intended for transplantation would be 90% of the original EC seeding density to equalise the final cell density in standard and transplanted assays. An ECMatrix gel coverslip was prepared (SEE 2.5.1) and seeded with 7.2×10^4 ECs in 300 μ l EC culture medium. At 5 h a suspension of 8×10^3 EPCs in 50 μ l D-PBS was pipetted evenly over the gel surface and the gel returned to the 37°C / 5% CO₂ incubator. Tubule formation was inspected every hour after transplantation at x10 magnification using an Eclipse TS100 inverted light microscope (Nikon).

2.5.5 Isolation of assayed cells for gene expression analysis

Cells from within *in vitro* tubule formation assay gels were isolated in order to extract RNA for the analysis of gene expression. This was performed using Cell Recovery Solution (BD Biosciences, Oxfordshire, UK), a proprietary preparation which depolymerises ECMatrix gel without enzymatic digestion or the need for incubation at high temperatures. This results in cells being released from the gel with minimal biochemical changes, heat damage or the digestion of extracellular receptors and adhesion molecules. To isolate cells, ECMatrix gel coverslips were transferred to a clean well of a 6-well culture plate and washed with 1 ml D-PBS to remove culture medium. 2 ml Cell Recovery Solution was added to the well

and the plate left on ice for 1 h to depolymerise the ECMatrix gel. The gel solution was then transferred to a 15 ml conical tube and centrifuged at $300 \times g$ for 5 min to pellet the assayed cells. The cell pellet was washed by removal of the supernatant, addition of 1 ml D-PBS and centrifugation at $300 \times g$ for 5 min. The supernatant was discarded and the cell pellet processed for nucleic acid extraction (SEE 2.2.1.2) or snap-frozen in LN₂ and stored at -80°C.

2.6 Preparation of washed murine platelets

2.6.1 Exsanguination *via* inferior vena cava (IVC)

Whole blood was collected *via* the IVC of C57BL/6 mice for the isolation of murine platelets (Fig. 2.8). Exsanguination was carried out under inhalant anaesthesia induced using 5% v/v isoflurane (Merial Animal Health Ltd., Essex, UK) with 1 L·min⁻¹ oxygen (O₂). For further information regarding *in vivo* procedures, SEE 2.9. To access the body cavity a 4 cm transverse midline incision was made in the skin, starting from a point just above the genitals, followed by a similar-sized incision into the peritoneum. The abdominal viscera were then moved aside using blunt forceps and the inferior vena cava (IVC) identified. 700-800 µl blood was taken from the IVC using a 26G Microlance™ 3 needle (BD Biosciences) attached to a 1 ml sterile plastic syringe containing 100 µl acid-citrate-dextrose (ACD) anticoagulant (SEE Appendix I) and gently mixed by inversion. Following exsanguination, the mouse was terminated by cervical dislocation (SEE 2.9.1.1) and blood processed for the isolation of washed murine platelets.

2.6.2 Isolation of platelets from whole blood

Prior to platelet isolation, modified Tyrode's buffer (SEE Appendix I) was supplemented with 0.9 mg·ml⁻¹ glucose and warmed to room temperature. 800 µl whole blood was transferred to a 1.5 ml microcentrifuge tube containing 200 µl modified Tyrode's buffer (with glucose) and

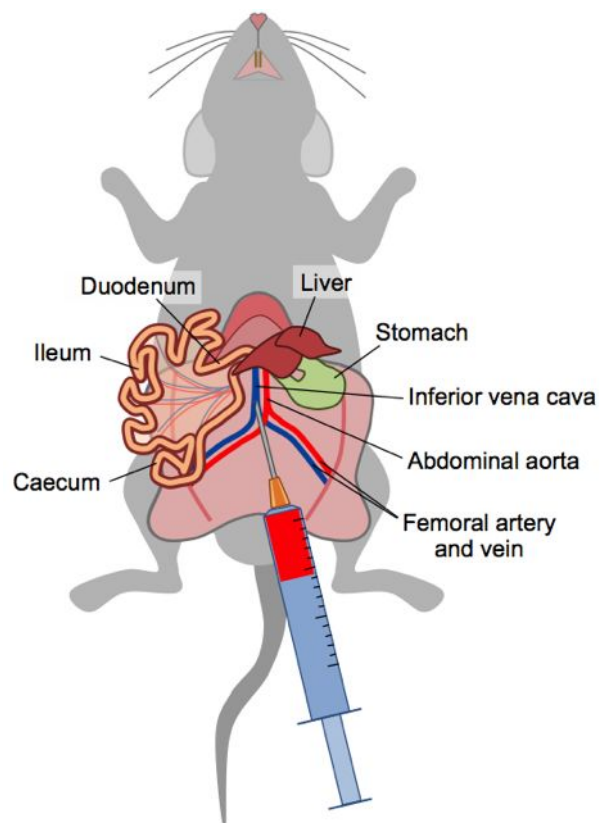


Figure 2.8. Exsanguination via the inferior vena cava. Following incision into the skin and peritoneum and displacement of the abdominal viscera, blood from the inferior vena cava was taken into a syringe containing acid-citrate-dextrose anticoagulant.

centrifuged at $500 \times g$ for 5 min to generate platelet-rich plasma (PRP). The PRP supernatant was then transferred to a clean 1.5 ml microcentrifuge tube and centrifuged at $120 \times g$ for 6 min to remove any remaining erythrocytes and leukocytes. PRP was finally transferred to a fresh 1.5 ml microcentrifuge tube containing $1 \mu\text{l}$ of $10 \mu\text{g}\cdot\text{ml}^{-1}$ prostacyclin (PGI_2) to prevent platelet aggregation and centrifuged at $1000 \times g$ for 6 min. The supernatant was discarded and the remaining platelet pellet retained for fluorescent labelling.

2.6.3 Counting washed murine platelets

Washed murine platelets were counted using the Coulter Multisizer II analyser (Beckman Coulter, Buckinghamshire, UK), employing the Coulter electrical impedance method to provide size distribution analysis of particulate suspensions drawn through a glass aperture (**Fig. 2.9**). Platelets resuspended in $500 \mu\text{l}$ modified Tyrode's buffer were diluted 1:1000 by the addition of $10 \mu\text{l}$ platelet suspension to 10 ml ISOTON II Diluent (Beckman Coulter) in a 20 ml Coulter sample cup (Sarstedt). The sample cup was capped and gently inverted twice to ensure equal distribution of platelets throughout the diluent before being loaded on to the Coulter sampling stand. With the mercury manometer, responsible for sample aspiration by volume displacement, set to $500 \mu\text{l}$ and voltage channel limits set to measure particles between $1\text{-}4 \mu\text{m}$ (i.e. platelets) the diluted platelet suspension was analysed. To calculate platelet concentration, the dilution factor (DF) of the analysed platelet sample was first calculated using the following equation:

$$\text{dilution factor} = \frac{\text{sample volume (ml)} + \text{diluent volume (ml)}}{\text{manometer volume (ml)} \times \text{sample volume (ml)}}$$

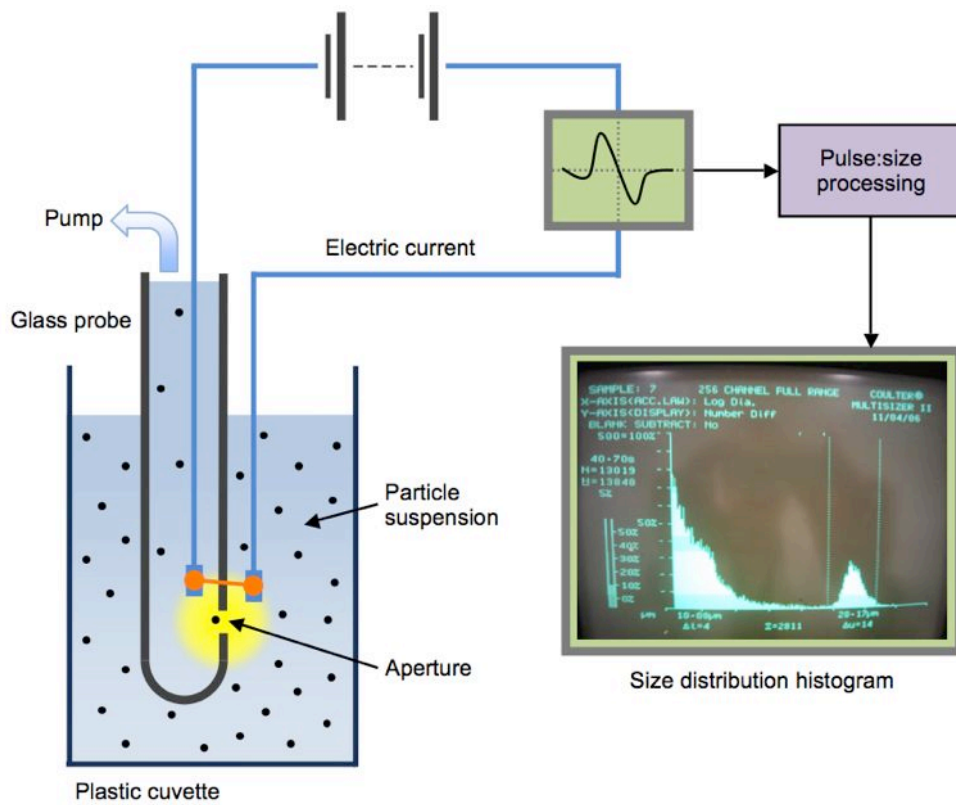


Figure 2.9. Counting washed murine platelets using Coulter electrical impedance. Fluctuations in electrical current as particles pass between electrodes positioned on either side of the glass probe aperture are processed to count platelets.

The DF, along with the returned channelised particle count, was then used to calculate total platelet concentration in the undiluted suspension:

$$\text{platelet concentration (platelets}\cdot\text{ml}^{-1}\text{)} = \text{DF} \times \text{particle count}$$

2.7 *In vitro* cell aggregation assay

Platelet-EPC interactions were investigated using a simple cell-based aggregometry assay. A mixed preparation of washed murine platelets and cultured cells was gently agitated and the resultant aggregates analysed by Coulter size distribution to determine the extent of platelet-mediated cell-cell binding.

2.7.1 Inhibition of adhesion by antibody and biochemical blockade

Prior to *in vitro* aggregation assays, cultured cells and/or washed platelets were treated to inhibit certain adhesion molecules and mechanisms. Non-specific selectin-mediated adhesion was inhibited by treatment of cells with 0.4, 0.8 or 1.2 $\mu\text{g}\cdot\text{ml}^{-1}$ dextran sulphate (DxSO_4) for 1 h at 37°C. The sulphate group of the DxSO_4 molecule has been shown to block heparan binding, a major component of selectin interactions, and hence it can interfere with selectin-mediated adhesion (Yanaka *et al.*, 1996; Nash, GB *et al.*, 2001; Zhang, XW *et al.*, 2001). In parallel with DxSO_4 assays, control experiments were performed using cells incubated with dextran only. A biologically inert branched polysaccharide, dextran is simply the microcarrier used to transport sulphate into the cell, and theoretically should have no significant effect on selectin-mediated adhesion (Buttrum *et al.*, 1993).

Specific blockade of P-selectin was performed using 5 or 10 $\mu\text{g}\cdot\text{ml}^{-1}$ rat anti-mouse CD62P blocking antibody (BD Pharmingen, Oxfordshire, UK) for 1 h at 37°C. To further elucidate the roles of cell- and platelet-bound selectins in the proposed adhesion mechanism, parallel experiments were carried out in which either: (i) cultured cells only or (ii) cultured cells *and* washed platelets were treated.

Blockade of platelet $\alpha\text{IIb}\beta\text{3}$ integrin (GPIIb/IIIa) was performed by incubation of washed platelets with 10, 25 or 50 $\mu\text{g}\cdot\text{ml}^{-1}$ abciximab (ReoPro™; Centocor Ortho Biotec, Inc., Pennsylvania, USA) for 45 min at 37°C.

Platelet activation was inhibited by incubation of washed platelets with 10 or 20 $\mu\text{g}\cdot\text{ml}^{-1}$ each combined clopidogrel and aspirin (M&A Pharmachem, Lancashire, UK) in Tyrode's buffer for 45 min at 37°C.

2.7.2 Aggregation assay protocol

Cultured cells (EPCs, ECs or MEFs) were isolated from culture flasks using 0.25% trypsin-EDTA solution and centrifuged at $600 \times g$ for 3 min to form a cell pellet. Cells were resuspended in modified Tyrode's buffer (with 0.9 $\text{mg}\cdot\text{ml}^{-1}$ glucose) to a density of 1×10^6 cells·ml⁻¹. Platelets were isolated from mouse whole blood and counted (SEE 2.6) and resuspended in Tyrode's buffer to a density of 2×10^7 platelets·ml⁻¹. 1 ml of cell suspension and 500 μl of platelet suspension were added to a 7 ml plastic bijou bottle (Scientific Laboratory Supplies Ltd., Nottinghamshire, UK), a magnetic flea added and the bottle placed on a magnetic stirrer inside a heated 37°C Perspex box (**Fig. 2.10**). The cell-platelet suspension was gently agitated for 15 min, with 10 μl aliquots of the suspension removed at 0, 1, 2, 3, 5, 10 and 15 min for analysis.

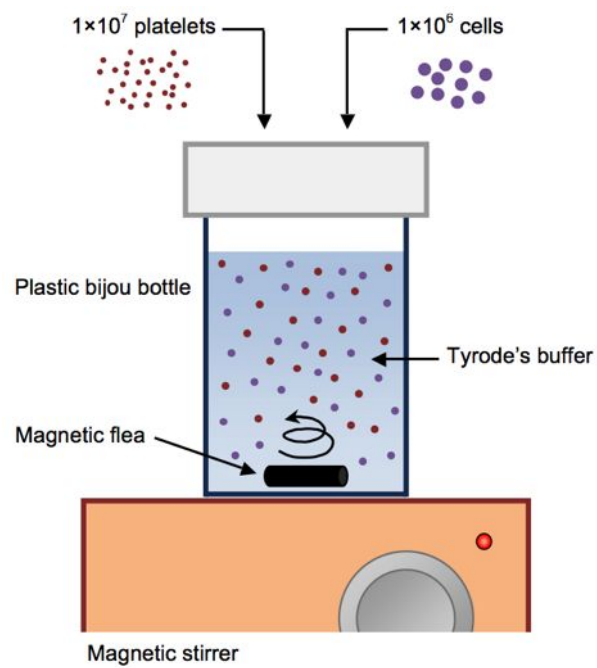


Figure 2.10. *In vitro cell-based aggregation assay.* A suspension of 1×10^7 washed platelets and 1×10^6 cells in Tyrode's buffer was gently agitated at 37°C using a magnetic stirrer. Resultant aggregates were analysed by Coulter size distribution.

2.7.3 Quantification of aggregation using Coulter size distribution

10 μ l samples taken from aggregation assays were diluted 1:1000 by the addition of 10 ml ISOTON II Diluent (Beckman Coulter) in a 20 ml Coulter sample cup (Sarstedt) and analysed using the Coulter Multisizer II (Beckman Coulter) as previously described (SEE **Chapter 2.6.3**). Size channel gating (**Fig. 2.11**) was used to distinguish between and separately count platelets, single cells and differently-sized aggregates at each time-point.

2.8 *In vitro* flow adhesion assay

2.8.1 Preparation of glass microslides

Microslides are 50 mm open-ended glass capillary tubes (CamLab, Cambridgeshire, UK) with a rectangular cross-sectional area of 0.9 mm² (0.3 × 3 mm) and a total culture surface area of 150 mm². Microslides were coated with 3-aminopropyltriethoxysilane (APES) to create a positively charged surface on which to immobilise isolated murine platelets. Microslides were placed in 70% nitric acid (in ddH₂O) for 24 h, washed ten times with ddH₂O, transferred to 50 ml conical tubes and washed a further three times with ddH₂O. After washing, conical tubes were inverted over tissue paper to remove excess water and filled twice with 30 ml acetone and twice with 30 ml of 4% APES (SEE **Appendix I**), inverting the tubes three times between each wash. Microslides were then covered with 30 ml of 4% APES, conical tubes inverted three times and incubated at room temperature overnight. Following incubation, microslides were washed twice with 30 ml acetone and twice with 30 ml ddH₂O, inverting three times between each wash. The microslides were then placed on Whatman[®] blotting paper (Whatman plc.) in a 37°C oven to dry for 1 h before autoclaving.

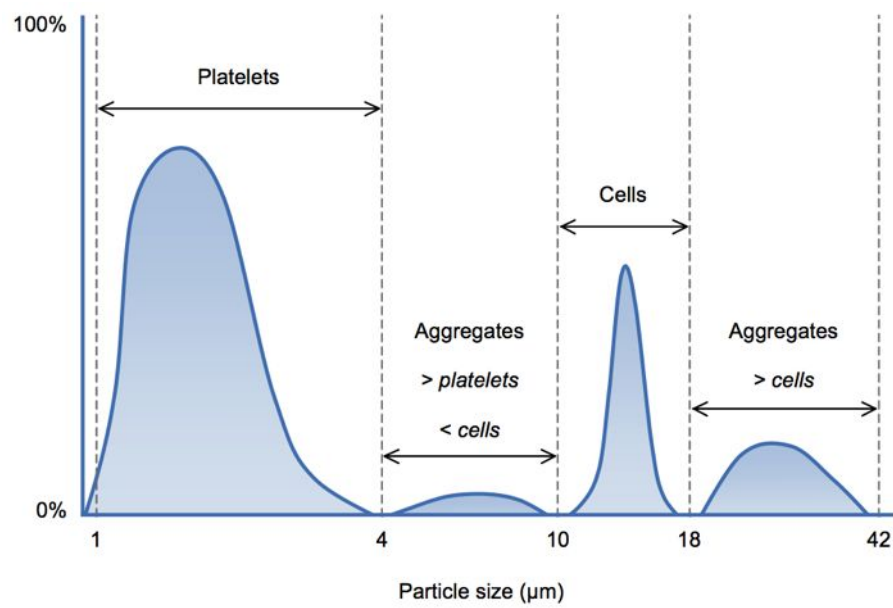


Figure 2.11. Quantification of cell-platelet aggregation using Coulter size distribution. Channel gating was used to identify unbound platelets (1-4 μm), platelet aggregates (4-10 μm), single cells (10-18 μm) and cellular aggregates (18-42 μm) at each time-point.

2.8.2 Immobilisation of washed murine platelets on glass microslides

Washed murine platelets were isolated and counted (SEE 2.6). Using PBS with 0.15% albumin (PBSA), platelets were diluted to a density of 2×10^8 platelets·ml⁻¹. 50 µl of this suspension was gently pipetted into an APES-coated glass microslide. Filled microslides were incubated at room temperature for 1 h to bind platelets to the inner surface. After incubation, excess unbound platelets were removed by gently flushing the microslide with 500 µl PBSA.

2.8.3 Inhibition of adhesion by antibody and biochemical blockade

Similarly to *in vitro* aggregation assays, prior to *in vitro* flow adhesion assays cultured cells and/or washed platelets were treated to inhibit particular adhesion mechanisms (SEE 2.7.1). Furthermore, shedding of platelet surface GPVI prior to platelet isolation was performed by Dr. Ian Packham (University of Birmingham). C57BL/6 mice were treated with 2 µg·g⁻¹ anti-GPVI antibody (Emfret Analytics, Würzburg, Germany), administered by intraperitoneal (i.p.) injection. Prior to injection, sodium azide preservative was removed from the antibody by microdialysis over 18 h using high retention cellulose dialysis tubing (flat width = 23 mm; Sigma-Aldrich). A 70% reduction in platelet surface GPVI expression was induced over 7 days, confirmed by flow cytometric analysis of isolated platelets (SEE 6.4.2.2).

2.8.4 *In vitro* flow adhesion assay protocol

The *in vitro* flow adhesion assay comprised a glass microslide mounted on the stage of a phase-contrast video-microscope with recording equipment, through which a cell suspension was perfused at a constant flow rate (Fig. 2.12). One end of a platelet-seeded microslide was connected, *via* silicon tubing sealed with double-sided adhesive tape, to an electronic switching valve (Lee Products, Buckinghamshire, UK). Two reservoirs, containing the cell suspension or 0.15% PBSA wash buffer, were connected to the microslide through this

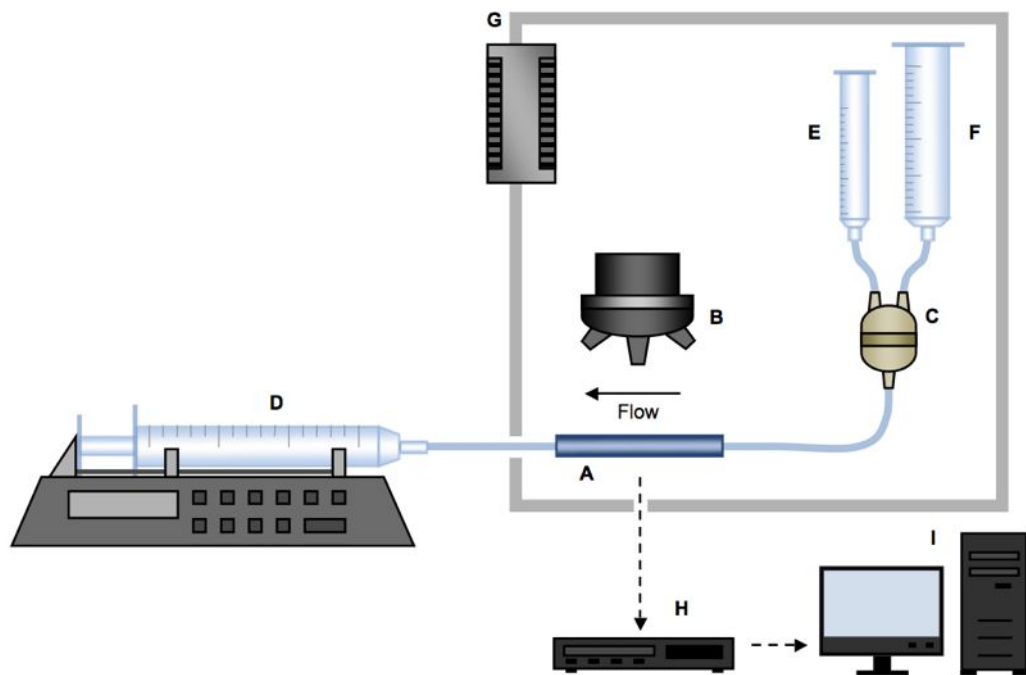


Figure 2.12. In vitro flow adhesion assay. Glass microslide (A) mounted on a phase-contrast video microscope (B), attached via silicon tubing to an electronic switching valve (C) and a 50 ml glass syringe (D) held in an electronic pump producing a wall shear stress of 0.025 Pa. Reservoirs contained cells to be perfused (E) or PBSA wash buffer (F). Assays were performed within a 37°C heated Perspex box (G). Video recordings were made (H) and analysed using Image-Pro Plus software (I).

switching valve. An electronic syringe pump (Harvard Apparatus, Kent, UK), similarly attached and sealed to the other end of the microslide, maintained flow through the microslide. Adhesion assays were performed using a flow rate generating a wall shear stress of 0.025 Pa, calculated using the following equation:

$$Q = \frac{w \times h^2 \times T}{6\eta}$$

where: Q = flow rate of the fluid ($\mu\text{l}\cdot\text{s}^{-1}$);
 w = width of the microslide (mm);
 h = height of the microslide (mm);
 T = wall shear stress (Pa);
 η = viscosity of the fluid (7×10^{-3} Pa for aqueous buffers).

The entire system was contained within a heated 37°C Perspex box to maintain a constant temperature throughout the assay. Platelet-seeded microslides were washed with PBSA buffer for 3 min to remove remaining unbound platelets, followed by perfusion of a cell suspension at a density of 2×10^6 cells·ml⁻¹ for 5 min. After cell perfusion microslides were washed again with PBSA buffer for 6 min to remove non-adhered cells. Fourteen randomly selected fields of view along the centre of the microslide were recorded for quantification of cell adhesion using Image-Pro Plus v7 software (Media Cybernetics Inc., Maryland, USA). Adherent cell counts were normalised per unit area over time (i.e. cells per mm² of microslide per min of perfusion).

2.8.5 Adherent cell spreading assay

The effect of platelets on cell spreading immediately following capture from flow was also investigated using the *in vitro* flow adhesion assay system. Adhesion assays were performed

using EPCs as previously described, then adherent cells recorded continuously for 3 h to quantify cell spreading and migration (**Fig. 2.13**). In addition to cell spreading assays using untreated EPCs and platelets, assays were performed in the presence of $1 \text{ U}\cdot\text{ml}^{-1}$ thrombin (to evoke maximal platelet activation) or $10 \text{ }\mu\text{g}\cdot\text{ml}^{-1}$ PGI_2 (to silence cell and platelet receptor expression). Spreading assays were also carried out using microslides pre-coated with murine P-selectin instead of immobilised platelets. P-selectin microslides were prepared using APES-coated glass microslides (SEE **2.8.1**) treated with $10 \text{ }\mu\text{g}\cdot\text{ml}^{-1}$ recombinant murine P-selectin/Fc Chimera (R&D Systems, Minneapolis, USA) for 1 h at 37°C and blocked with 1% PBSA for 30 min at room temperature.

Following cell spreading assays, image capture was performed every 10 min on each cell within the recorded field of view using Image Pro Plus v7.0 software (Media Cybernetics, Inc., Maryland, USA) to produce a time-lapse sequence. Using ImageJ software (NIH Research Services Branch) threshold and binary filters were applied to each time-lapse image to identify cell borders and automatically calculate cell area based on microscope magnification and image resolution. Cell migration was tracked by following each cell's calculated centre of mass to determine its absolute and relative position within the field of view. Cell migration data were used to produce polar plots and angle histograms using MATLAB v7.6 software (Mathworks, Inc., Massachusetts, USA).

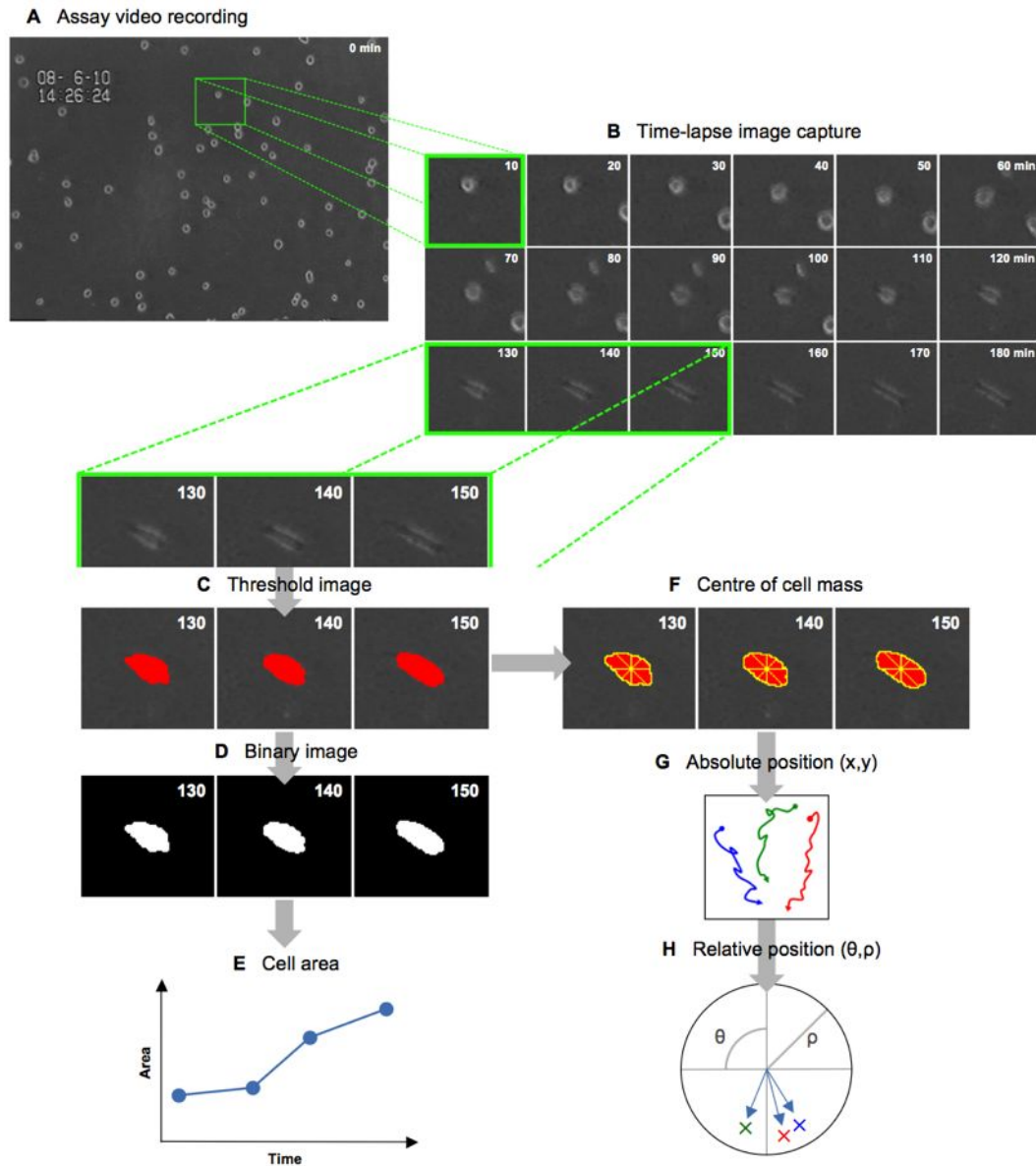


Figure 2.13. Quantification of in vitro captured cell spreading assays. Image capture was performed on assay video recordings (A) to produce a time-lapse sequence (B). Digital filters were applied to identify cell borders (C, D) and cell area automatically calculated (E). Centre of cell mass was calculated (F) to give each cell's absolute position as Cartesian (x,y) coordinates (G). These were converted to polar (θ, ρ) coordinates to calculate each cell's position (its angle and distance) relative to its origin (H).

2.9 *In vivo* experiments

2.9.1 *Animal (Scientific Procedures) Act 1986*

All *in vivo* experiments described in the following methods were conducted with the ethical approval of the University of Birmingham, under Project License 40/2872 and Personal License 40/9104 granted by the Home Office in accordance with the *Animal (Scientific Procedures) Act 1986*. Animals were obtained from Charles River Laboratories International Inc. (Kent, UK) and housed at 21°C on a 12 h light:dark cycle. Six-week-old C57BL/6 male mice were used, to avoid effects on angiogenesis that may be caused by hormonal changes during menstrual cycling. All animals were kept with littermates in an enriched environment and given standard laboratory mouse chow and water *ad libidum*.

2.9.1.1 Schedule 1 methods of termination

At the conclusion of each experimental procedure animals were terminated by dislocation of the neck, a humane method deemed appropriate under Schedule 1 of the *Animals (Scientific Procedures) Act 1986*.

2.9.2 Anaesthesia and preparation for surgery

Prior to surgery, anaesthesia was induced by administration of 5% v/v inhalant isoflurane (Merial Animal Health Ltd.) with 1 L·min⁻¹ O₂ and maintained throughout the surgical procedure using 3% v/v isoflurane with 1 L·min⁻¹ O₂. Alternatively, anaesthesia was induced by combined i.p. injection of 1 mg·g⁻¹ ketamine (Pfizer, Kent, UK) and 0.2 mg·g⁻¹ xylazine (Animal Care Ltd., North Yorkshire, UK) (SEE **Appendix I**). To ensure a sufficient depth of anaesthesia the toe of one hindlimb was pinched firmly between the experimenter's fingernails. If the limb was withdrawn the mouse was considered to be inadequately anaesthetised whilst no reflex indicated medium to deep anaesthesia had been attained. This

pedal reflex test was used regularly throughout each surgical procedure to monitor depth of anaesthesia.

Once fully anaesthetised the mouse was placed on its back to expose the ventral surface of the abdomen and the areas appropriate to the procedure being performed were shaved with an electric hair clipper: the neck for cannulation of the carotid artery and the hindlimb for arterial ligation, sciatic nerve stimulation or hindlimb muscle extirpation. The mouse was positioned on a heat pad to maintain 37°C body temperature and the limbs extended and secured in place using surgical tape. To avoid compromising respiratory function care was taken not to over-extend the forelimbs. The head was also secured by placing a loop of silk surgical suture behind the front upper incisors, pulling it taut and securing it to the work area.

2.9.2.1 Cannulation of right common carotid artery (CCA)

Cannulation of the right CCA was performed to allow administration of platelet-depleting antibody and intravascular transplantation of EPCs, and was carried out under ketamine-xylazine anaesthesia (**Fig. 2.14**). To expose the right CCA, a 2 cm transverse incision was made in the skin of the neck and the underlying muscles carefully separated using blunt forceps. The neurovascular bundle containing the right CCA was then identified and blunt dissection performed with cotton buds to clean away the surrounding subcutaneous fat and connective tissues. Fine forceps were used to pierce the membranous sheath surrounding the neurovascular bundle and the bundle gently dissected to separate the carotid artery from the vein and nerve. A length of 5-0 braided black silk suture (Surgical Specialties Corporation, Pennsylvania, USA) was passed underneath the dissected artery and the anterior end occluded by securely tying a surgeon's knot. A loose ligature was then placed around the posterior end of the vessel and gentle tension applied to temporarily occlude blood flow.

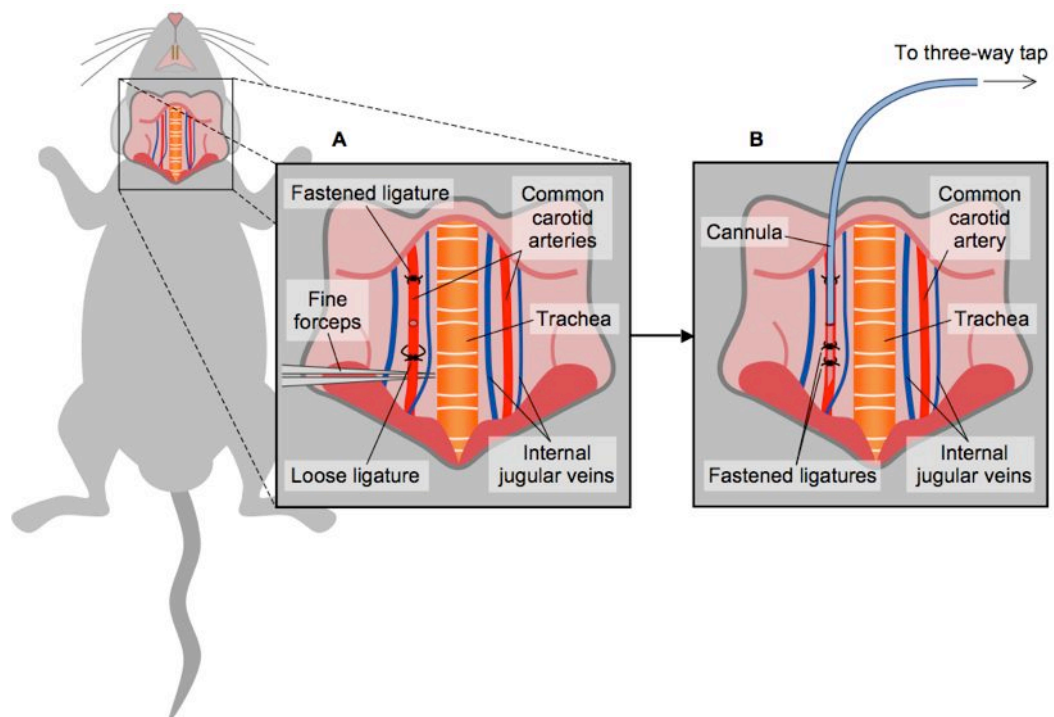


Figure 2.14. Cannulation of the right common carotid artery. (A) A secure ligature was placed at the anterior end of the vessel and blood flow temporarily occluded using fine forceps and a loose ligature whilst a small incision was made. **(B)** A length of polythene cannula attached to a three-way tap was then inserted into the vessel and secured by fastening two ligatures.

A small incision was made in the CCA using micro-dissecting scissors and a length of Portex[®] polythene tubing (0.61 mm external diameter, 0.28 mm internal diameter; PP10; Smiths Medical International, Hertfordshire, UK) was inserted and secured by fastening the loose ligature.

2.9.3 *In vivo* EPC transplantation

To investigate the homing and recruitment of EPCs during the angiogenic response, *in vivo* transplantation of fluorescently-labelled murine EPCs was carried out in C57BL/6 mice following either: (i) electrical stimulation of the acutely-ischaemic hindlimb, (ii) electrical stimulation of the acutely-ischaemic hindlimb following systemic platelet depletion, (iii) chronic ischaemia of the hindlimb, or (iv) overload of synergistic hindlimb muscles by extirpation of *m. tibialis anterior*. To account for variances in the limb dominance of experimental animals, ligation, stimulation and extirpation were performed on alternating hindlimbs between procedures. Following EPC transplantation, the muscles of both ipsilateral and contralateral hindlimbs and the internal organs were harvested, digested with collagenase and analysed using flow cytometry to localise transplanted EPCs. All surgical procedures involved in EPC transplantation were carried out under ketamine-xylazine anaesthesia, unless otherwise stated.

2.9.3.1 Platelet depletion by administration of α -GPIIb α antibody

To investigate the effect of platelet involvement in the recruitment of EPCs following transplantation, systemic platelet depletion (>95%) was performed over 1 h by administration of 2 $\mu\text{g}\cdot\text{g}^{-1}$ monoclonal rat anti-mouse GPIIb α antibody (Emfret Analytics) *via* CCA cannula (SEE 2.9.2.1). Following platelet depletion, acute hindlimb ischaemia was induced and percutaneous sciatic nerve stimulation performed.

2.9.3.2 Acute hindlimb ischaemia by femoral artery (FA) ligation

In both normal and platelet-depleted mice, FA ligation was performed to induce acute hindlimb ischaemia (**Fig. 2.15**). A 2 cm incision was made along the medial aspect of the extended hindlimb, exposing the femoral neurovascular bundle. The FA was carefully separated from the femoral vein and nerve using fine forceps and occluded using a microvascular clip. Care was taken to place the clip as high as possible to maximise limb ischaemia by occlusion of collateral blood vessels in the hindlimb. Ischaemia was maintained for 30 min whilst percutaneous sciatic nerve stimulation was performed.

2.9.3.3 Percutaneous sciatic nerve stimulation

Following induction of acute ischaemia in normal or platelet-depleted mice, the muscles of the ipsilateral hindlimb were vigorously exercised by percutaneous electrical stimulation of the left sciatic nerve. The dorsal muscles of the extended left hindlimb were exposed by carefully removing the skin and underlying connective fascia. Platinum electrodes connected to an S8 Stimulator through a Stimulus Isolation Unit (Grass Medical Instruments, Massachusetts, USA) were then used to apply an electrical current of 5-10 V (at a frequency of 10 Hz with a pulse duration of 0.3 ms) directly to the surface of the exposed muscle in order to innervate the sciatic nerve. Electrical stimulation was performed for 30 min, occasionally resting the ischaemic hindlimb to avoid muscle fatigue that might result in an attenuated exercise response. The FA-ligating vascular clip was then removed, the hindlimb reperfused for 15 min and intravascular transplantation of EPCs carried out (SEE **2.9.3.6**).

2.9.3.4 Chronic hindlimb ischaemia by FA ligation

Similarly to acute ischaemia, chronic hindlimb ischaemia was induced over 48 h by FA ligation, performed under isoflurane anaesthesia. For post-operative analgesia, 2.5 $\mu\text{l}\cdot\text{g}^{-1}$

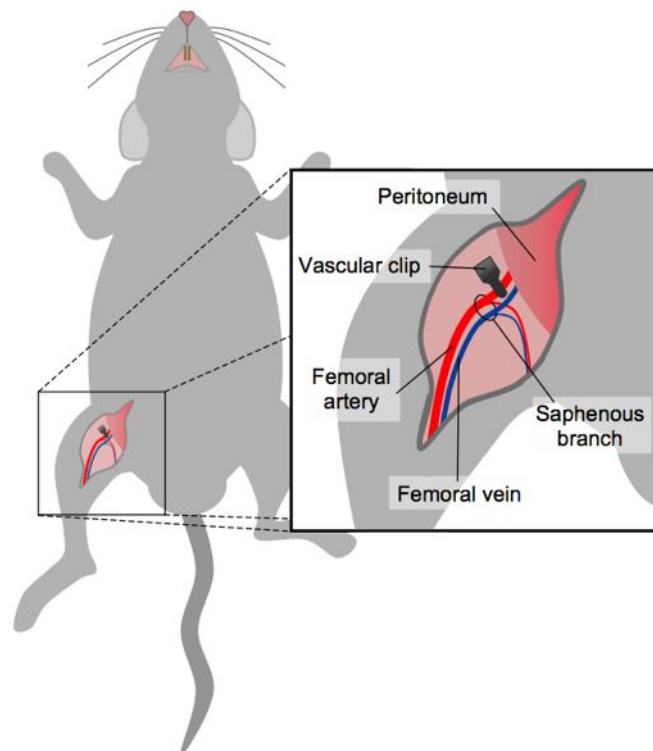


Figure 2.15. Acute hindlimb ischaemia by femoral artery ligation. After dissection of the femoral artery from the femoral vein and nerve, a micro vascular clip was applied for 30 min, taking care to position the clip above the saphenous branch to maximise limb ischaemia.

buprenorphine (Temgesic®; Merck Sharp & Dohme Ltd., Hertfordshire, UK) was administered by subcutaneous (s.c.) injection. A 2 cm incision was made along the medial aspect of the extended hindlimb, and the FA carefully separated from the femoral vein and nerve. A length of 10-0 non-absorbable polypropylene suture (Prolene™; Ethicon Ltd., North Yorkshire, UK) was passed underneath the proximal end of the dissected artery and blood flow occluded by securely tying a surgeon's knot. The incision in the skin of the hindlimb was then closed with simple interrupted sutures using 6-0 coated polyglactin 910 (Vicryl™; Ethicon Ltd., North Yorkshire, UK). The free ends of each stitch were trimmed to reduce irritation and prevent delayed wound healing caused by scratching or nibbling. Animals were transferred to a heated recovery cage with *ad libitum* access to food and water and monitored until fully alert. After 48 h, intravascular transplantation of EPCs was performed (SEE 2.6.3.6).

2.9.3.5 Overload of synergistic hindlimb muscles by extirpation of *m. tibialis anterior*

Unilateral extirpation of the *m. tibialis anterior* was carried out under isoflurane anaesthesia to cause overload of the synergistic hindlimb muscles *m. extensor digitorum longus* and *m. extensor hallucis proprius* (Fig. 2.16). Before surgery, for post-operative analgesia, 2.5 µl·g⁻¹ Temgesic® buprenorphine (Merck Sharp & Dohme Ltd.) was administered by s.c. injection. A 1.5 cm incision was then made in the lateral aspect of the extended hindlimb, parallel to the tibia, to expose the *m. tibialis anterior*. The muscle was lifted away from the underlying *m. extensor digitorum longus* and *m. extensor hallucis proprius* using fine forceps. A single clean cut was made in the proximal end of the *m. tibialis anterior*, at a point approximately one third along its length, and the muscle removed. Any local bleeding was staunches by replacing the extirpated muscle and applying gentle pressure to present necessary clotting factors. The hindlimb was then gently cleaned with sterile PBS to remove clotted blood, before topical administration of 40 µl of 150 mg·ml⁻¹ long-acting penicillin

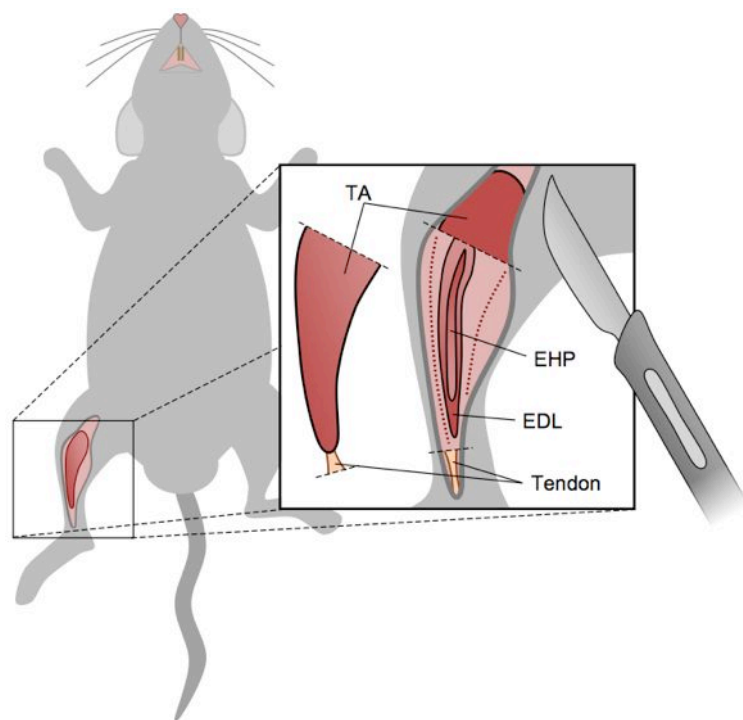


Figure 2.16. Overload of synergistic hindlimb muscles by unilateral extirpation. The m. tibialis anterior (TA) was separated from the underlying m. extensor digitorum longus (EDL) and m. extensor hallucis proprius (EHP) and two thirds of the muscle removed using a scalpel. Absorbable polyglactin suture was used to close the skin incision and animals recovered for 48 h before in vitro EPC transplantation.

(Betamox LA; Norbrook Pharmaceuticals, Cumbria, UK). This was allowed to absorb for 10-20 s before blotting away the excess with a sterile cotton swab. The hindlimb incision was then closed with using 6-0 coated Vicryl™ polyglactin 910 (Ethicon Ltd.). After 48 h, intravascular transplantation of EPCs was carried out.

2.9.3.6 Intravascular injection of fluorescent EPCs

Transplantation was performed by intravascular injection of EPCs (prior labelled with Qdots, SEE 2.1.6). A total of 2×10^6 fluorescent EPCs in 100 μ l PBS was slowly infused by CAA cannula (SEE 2.9.2.1) over a period of 1 min followed by an additional infusion of 100 μ l PBS over 1 min to ensure clearance of EPCs from the cannula dead space into the circulation. Transplanted EPCs were allowed to circulate for 15 min, after which the mouse was terminated by cervical dislocation and the hindlimb muscles and internal organs harvested.

2.9.3.7 Tissue harvesting

For the analysis of EPC homing following transplantation, the *m. tibialis anterior*, *m. extensor digitorum longus* and *m. soleus* muscles of both ipsilateral and contralateral hindlimbs, as well as the heart, lungs, liver, kidney, ileum and spleen, were removed, weighed and processed for flow cytometric analysis (SEE 2.10).

2.10 Flow cytometry

2.10.1 Tissue digestion

Following the *in vivo* transplantation of fluorescently-labelled EPCs into mice, harvested tissues were incubated in 500 μ l of 10 mg·ml⁻¹ collagenase Type II from *Clostridium histolyticum* (in PBS) for 37°C for 3 h to produce a homogenous cell suspension, which was then diluted 1:10 with additional PBS for flow cytometric analysis.

2.10.2 Flow cytometric analysis of tissue digests

To localise fluorescent EPCs in digested muscles and tissues of transplanted animals, flow cytometric analysis was performed using a FACSCaliber flow cytometer (BD Biosciences) running CellQuest v7.6.1 software (BD Biosciences). Prior to analysis, voltages of the forward scatter (FSC) and side scatter (SSC) diode detectors were adjusted to place homogenised cells from non-transplanted control tissue digests within the boundaries of the acquisition dot plot. Similarly, the photomultiplier tube (PMT) voltage of the fluorescence (FL) channel used for the detection of transplanted EPCs (655 nm wavelength) was adjusted to place the fluorescence peak of control tissues within the first log decade of the fluorescence histogram. Sample digests were then analysed, acquiring 5×10^4 events per sample, and data recorded using CellQuest Pro v7.0 software (BD Biosciences). Flow cytometry data were analysed using FlowJo v8.7 software (Tree Star, Inc., Oregon, USA) and the percentage of positive fluorescence events detected normalised to tissue mass using the following equations:

$$\text{positive events} = \frac{\text{total events} \times \% \text{ positive events}}{100}$$

$$\text{positive events per mg tissue} = \frac{\text{positive events}}{\text{tissue mass (mg)}}$$

2.11 Statistical analysis

Data transformation and statistical analysis was performed using Prism v5.0b software (Graphpad Software, Inc., California, USA). Statistical differences were calculated using two-way analysis of variance (ANOVA) and *post hoc* multiple comparisons performed using the Bonferroni test, unless otherwise stated.

CHAPTER 3:

CHARACTERISATION OF ENDOTHELIAL PROGENITOR CELLS

3.1 Introduction

EPCs are implicated in the angiogenic response to a variety of cardiovascular disorders. However, before investigating a therapeutic application for EPCs, it is important to fully characterise their phenotype and to understand their inherent potential for vascular repair.

As previously discussed, there is little consensus on a definitive EPC. Multiple expression profiles have arisen from the many investigations undertaken since their initial discovery. This discrepancy may be due to the heterogeneous nature of primary EPCs, including definitions that place them as subsets of peripheral blood mononuclear cells (PBMNCs), bone marrow mononuclear cells (BMMNCs) and mesenchymal stem cells (MSCs) (Barber & Iruela-Arispe, 2006), and the various procedures used to isolate them, including surface marker selection and *in vitro* culture of tissue outgrowths (Hirschi *et al.*, 2008). Furthermore, there is evidence to suggest that contamination of mononuclear cells with platelet protein-containing microparticles may be responsible, at least in part, for the misinterpretation of the subsequent EPC phenotype, highlighting the problem of artefactual findings when attempting to definitively characterise EPCs (Prokopi *et al.*, 2009). However, throughout a wide range of studies there are several common markers frequently cited as being integral to the endothelial precursor phenotype, namely VEGFR2, VE-cadherin, CD31, CD133 and CD34 (Iida *et al.*,

2005; Povsic *et al.*, 2009), and it is these that have been used in this study to characterise the chosen cell lines.

VEGFR2 is a receptor tyrosine kinase with a high affinity for VEGF. Binding of VEGF leads to autophosphorylation of the receptor complex and activation of multiple downstream targets involved in mitogenesis and endothelial proliferation (Zhu *et al.*, 1999). Playing a pivotal role in the initiation of vasculogenesis by angioblasts in the embryo, both the *VEGFR2* gene and its product (the receptor complex) are expressed in abundance at the earliest stages of endothelial development and remain expressed throughout all stages of development (Kabrun *et al.*, 1997).

VE-cadherin is a transmembrane protein found on all endothelial lineage cells. It influences the movement of growth factors and migrating cells to potential sites of angiogenesis by the control of adherens junctions in the vascular endothelium and, as a target for agents affecting vascular permeability, it is an important factor in vascular remodelling (Montero-Balaguer *et al.*, 2009). VE-cadherin is first expressed in the peripheral layer of vasculogenic blood islands in the developing embryo and is therefore a marker of late-stage maturation of EPCs into ECs (Vittet *et al.*, 1996).

CD31 is an adhesion molecule located at the cell-cell borders of the cell of the vascular endothelium. It has been shown to have homophilic adhesive functions (binding to identical CD31 molecules on neighbouring cells) whilst also mediating cellular adhesion through interactions with heterophilic CD31 ligands (Muller *et al.*, 1992; Prager *et al.*, 1996). Angiogenesis involves the movement of endothelial cells to sites of new growth and the involvement of CD31 in cell-cell adhesion accords it influence over cell migration through the

endothelium. CD31 is linked to both embryonic vasculogenesis and adult angiogenesis, and is considered indicative of early vascular development and angiogenic potential (Kanayasu-Toyoda *et al.*, 2003).

CD133 is a transmembrane glycoprotein which, although its biological function remains unknown, is recognised as a marker of endothelial (Peichev *et al.*, 2000), lymphangiogenic (Salven *et al.*, 2003) and myoangiogenic (Shmelkov *et al.*, 2005) progenitors.

CD34 is a cell-surface glycoprotein that, like CD31, functions as a cell-cell adhesion factor. It has been suggested to mediate cell proliferation, adhesion to the stromal cell bone marrow microenvironment and the trafficking of haematopoietic cells *via* extravasation between ECs [Nielsen & McNagny, 2008]. CD34 is found on subsets of mesenchymal stem cells, such as EPCs and haematopoietic cells of the umbilical cord, and is therefore used as a general marker of a pluripotent phenotype and very early endothelial precursors (Krause *et al.*, 1994).

In addition to determining their genomic and proteomic phenotype, to fully characterise the cell lines used in this study the angiogenic activity of each cell type was investigated. Each of the individual elements of the angiogenic response (basement membrane disruption, EC expansion and migration, and reorganisation to form tubules) can be demonstrated *in vitro*. Quantification of these elements can provide a definable measure of the angiogenic potential of the cell in question. For instance, the ability of ECs to form blood vessels by changing morphology and cellular organisation to form tubule structures has been widely demonstrated and this, as here, can be illustrated using an *in vitro* assay (Mukai *et al.*, 2008). Regardless of their exact origin, all ECs appear to form organised tubule networks when cultured in the appropriate environment; the most common tubule formation assay involves seeding cells into

glycoprotein-rich (i.e. basement membrane-like) gel matrixes containing angiogenesis-stimulating growth factors (Arnaoutova *et al.*, 2009). Unlike assays of other angiogenic processes, such as cell proliferation or migration (that can occur as a result of a variety of cellular stimuli other than angiogenesis), tubule formation assays are considered to be one of the most angiogenesis-specific *in vitro* tests. However it must be noted that in some circumstances non-endothelial cells, such as fibroblasts, can be seen to form tubule-like structures when cultured on a gel matrix, so care must be taken when interpreting results of *in vitro* tubule formation assays (Martin *et al.*, 1999).

3.2 Hypothesis & objectives

It was hypothesised that the observed pattern of endothelial expression is specific to the stage of maturation, and that those characteristics will change during development from naïve stem-like EPCs to fully differentiated mature ECs. In addition, owing to their documented involvement in both embryonic vasculogenesis and adult angiogenesis, it is believed that, by *in vitro* tubule formation, EPCs will be shown to possess significant angiogenic potential.

Using *in vitro* cell culture, the experiments described in this chapter aimed to:

1. generate lineage-specific characterisation profiles for EPCs and ECs, focussing on analysis of gene and protein expression by qPCR and ICC, respectively;
2. demonstrate and quantify the angiogenic potential of EPCs and ECs using an *in vitro* tubule formation assay;
3. determine changes in lineage-specific expression occurring endothelial cell tubule formation *in vitro*;
4. provide reference profiles for the subsequent characterisation of endothelial-like cells to be derived from the differentiation of pluripotent stem cells.

3.3 Methods

3.3.1 Optimisation of reaction conditions for RT-PCR and qPCR analysis

Prior to analysis of gene expression, reaction conditions for oligonucleotide primers were optimised by performing parallel RT-PCR reactions using a range of annealing temperatures based around the calculated T_m and $MgCl_2$ concentrations from 1.5-3.0 mM. After agarose gel electrophoresis of the reaction products, the conditions producing the most intense single band of the correct size were used for all subsequent reactions using that primer set (**Fig. 3.1**).

For qPCR, fluorescence data were acquired during the extension phase of the reaction, with an additional acquisition stage included to eliminate primer dimers from the analysis. This elimination method works because primer dimers melt at a lower temperature than the gene product of interest and SYBR Green only produces a fluorescent signal when bound to dsDNA (Ririe *et al.*, 1997). Using each reaction product's dissociation curve (**Fig. 3.2**) the final acquisition temperature was set at a temperature slightly below the melting temperature of the product of interest (at which point melted, single-stranded dimers will not fluoresce), providing a measurement of the fluorescent signal generated by the product of interest only.

3.3.2 Optimisation of *in vitro* tubule formation assay

Before investigating the angiogenesis potential of EPCs and ECs, the *in vitro* tubule formation assay was optimised by testing ECMatrix gel quantity and cell seeding density. The optimum amount of ECMatrix gel was first tested using different amounts of ECMatrix gel (10-50 μ l) to coat the glass coverslips. The ideal initial seeding density was also tested, over a range of 5×10^4 - 1×10^5 cells per assay gel. The combination of gel quantity and seeding density that produced the clearest and most reproducible images (**Fig. 3.3**) were then used for all subsequent analyses of angiogenic potential, to ensure comparable results between cell types.

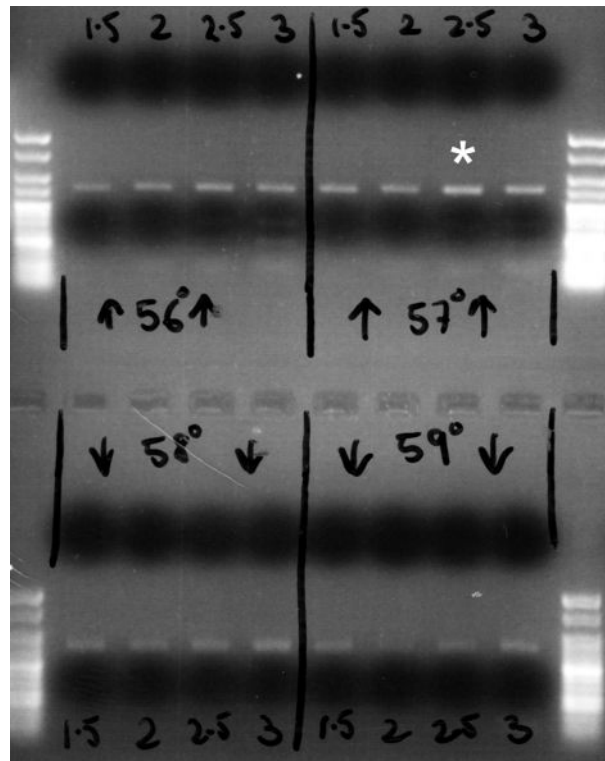


Figure 3.1. Optimisation of RT-PCR reaction conditions. Parallel reactions were performed for each primer set (CD31 shown) using a range of annealing temperatures and $MgCl_2$ concentrations. Conditions produced the most intense band (indicated $*$) were used for subsequent RT-PCR analysis and are detailed in Chapter 2.

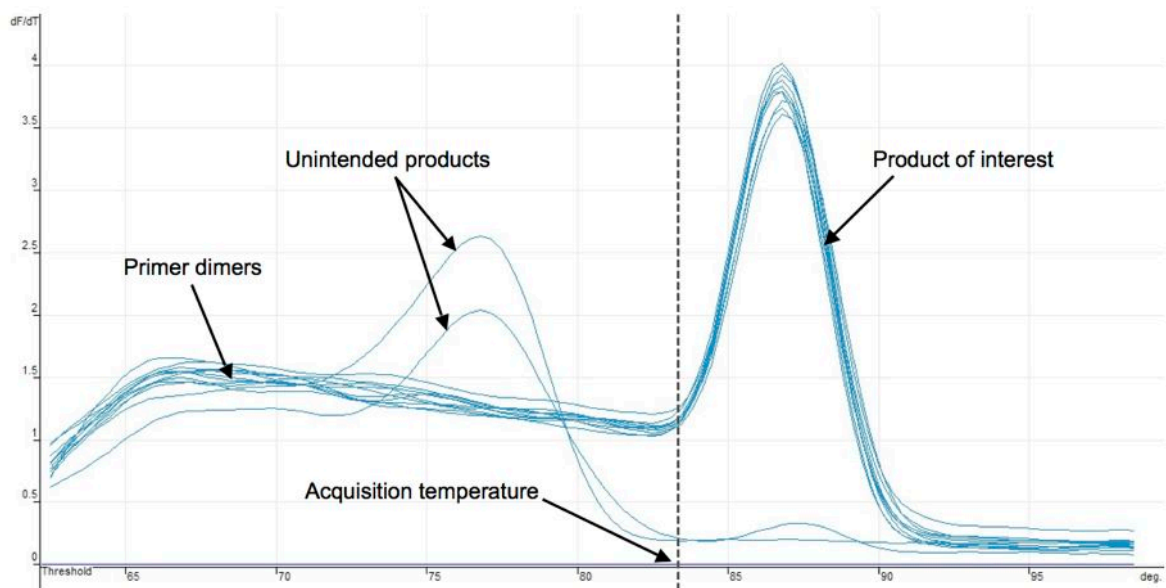


Figure 3.2. qPCR dissociation curve analysis. The final acquisition temperature was based upon the melting temperature of the product of interest (β -actin shown). As each differently-sized gene product has a specific melting temperature (depending on length and GC content), products could be easily distinguished from primer dimers or other unintended reaction products using dissociation curve analysis.

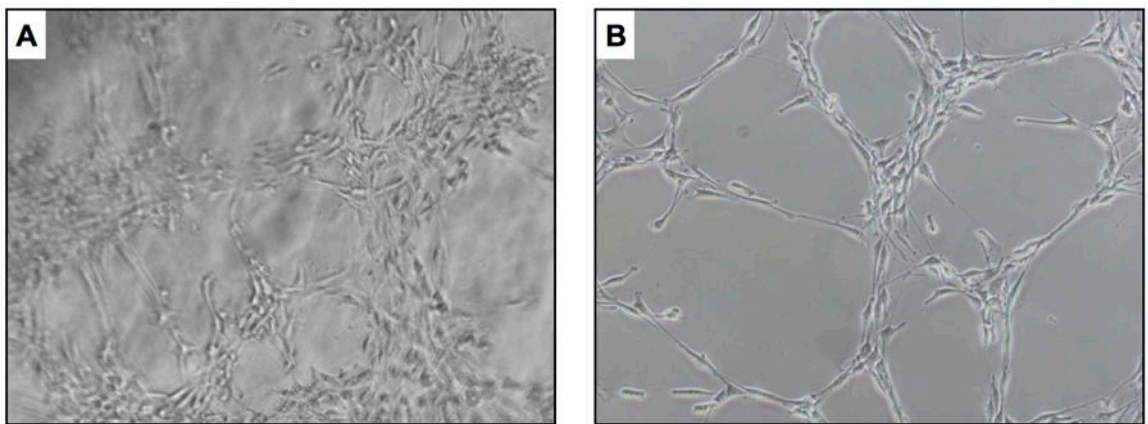


Figure 3.3. Optimisation of in vitro tubule formation assay. Preliminary assays were performed using (A) the manufacturer's default protocol before different ECMatrix gel quantities and cell seeding densities were tested to produce (B) optimum tubule formation and imaging conditions, which are detailed in Chapter 2.

3.3.3 ICC of ECMatrix gel coverslips

Protein expression analysis was performed on cultured EPCs and ECs as part of the characterisation study. In an effort to generate a complete characterisation of cells both in static culture and during *in vitro* tubule formation, ICC was intended to be carried out, as with qPCR, on cells isolated from the *in vitro* tubule formation assay. Trial staining was performed with the same anti-VEGFR2 antibody used for the analysis of cultured cells. Cells grown on ECMatrix gel were prepared for ICC by fixation and blocking before primary antibody incubation, washing and finally labelling with secondary antibody. A combination of primary and secondary antibody concentrations, blocking and washing durations and imaging methods (fluorescent and confocal microscopy) were tested. However, even the clearest results (**Fig. 3.4**) were considered inadequate for satisfactory characterisation (likely the result of antibody retention within the ECMatrix gel) and so ICC analysis of assayed cells was abandoned.

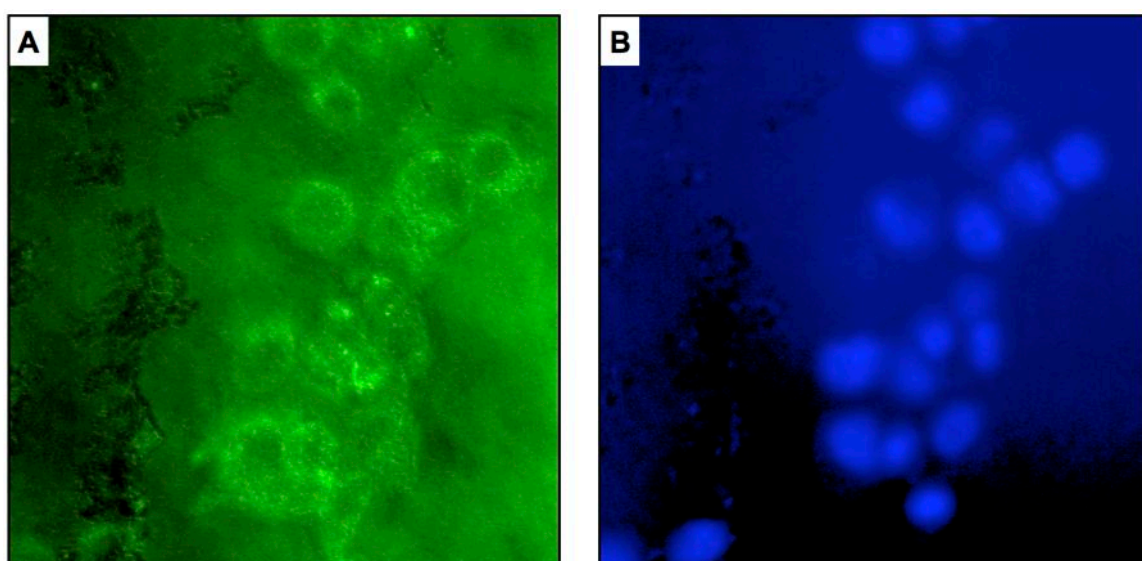


Figure 3.4. ICC of cells cultured on ECMatrix gel-coated coverslips. Detection of (A) VEGFR2 expression was tested on cells from in vitro tubule formation assays (EPCs shown above) with (B) nuclear staining using DAPI. Even with optimal staining conditions, resultant images were not considered clear enough for subsequent protein expression analysis of EPCs or ECs.

3.4 Results

The phenotype of EPCs and ECs were determined by endothelial-specific mRNA expression analysis using qPCR and the identification of cell surface protein expression using ICC. Additional characterisation was performed by staining with *Griffonia simplicifolia* lectin and the assessment of ac-LDL uptake in culture. The angiogenic potential of each cell line was then assessed by culturing on *in vitro* angiogenesis assay gel for 14 h, with quantification of subsequent tubule formation by node counting and branch length measurement. Changes in endothelial-specific mRNA expression over the 14 h assay period were also determined by qPCR.

An increase in cell culture confluency has been indicated to be a stimulus for EPC maturation and so may have an effect on mRNA or protein expression. In order to observe this effect, characterisation of endothelial-specific expression was performed using EPCs and ECs maintained at different levels of culture confluency (60%, 80% and 100%).

3.4.1 Expression of lineage-specific markers in EPCs and ECs

3.4.1.1 qPCR analysis of mRNA transcripts

Expression of *VEGFR2*, *VE-cadherin* and *CD31* mRNA transcripts was quantified using qPCR. Gene expression was normalised between cell types by calculating the relative ratio of the number of mRNA transcripts of each gene of interest to the number of transcripts of the housekeeping gene *β -actin*. Ideally, housekeeping genes are expressed at the same level in all samples under all conditions, allowing normalisation of qPCR data by accounting for variations in the tested samples which are not representative of true differences in the number of transcripts.

The relative expression of *VEGFR2* was significantly greater in EPCs than ECs, with the level of expression in EPCs increasing by 10% as culture confluency increased from 60% to 80% (**Fig. 3.5**). Fewer *VEGFR2* mRNA transcripts were detected in both 60% and 80% confluent ECs compared to EPCs, with no significant difference in expression as a result of culture confluency. *VEGFR2* expression decreased dramatically in both EPCs (by 89%) and ECs (by 90%) as the cells reached 100% confluency.

The relative expression of *VE-cadherin* in 60% confluent ECs was significantly higher than the other cells analysed (**Fig. 3.6**). The number of transcripts in 80% confluent ECs was observed to be 5% lower than in 60% confluent ECs, whilst *VE-cadherin* expression in EPCs was seen to increase by 18% between 60% and 80% confluency. The lowest expression of *VE-cadherin* in each cell line, as with *VEGFR2*, was observed in 100% confluent cells, with an 89% decrease in EPCs and a 96% decrease in ECs.

Expression of *CD31* was found to be greatest in 60% confluent EPCs, with a 9% reduction in the number of mRNA transcripts as EPCs became 80% confluent (**Fig. 3.7**). *CD31* expression was not significantly different between 60% and 80% confluent ECs. Once more, significant decreases in mRNA transcripts were observed in both cell lines (88% in EPCs; 82% in ECs) as culture confluency increased from 80% to 100%.

3.4.1.2 ICC analysis of protein expression

To further characterise EPCs and ECs, protein expression of the endothelial markers *VEGFR2* and *CD133* and the progenitor/pluripotency marker *CD34* was analysed in EPCs and ECs (at 60%, 80% and 100% confluency) using ICC. The presence of each of the three proteins was detected in ECs (**Fig. 3.8**) and EPCs (**Fig. 3.9**) at every level of confluency.

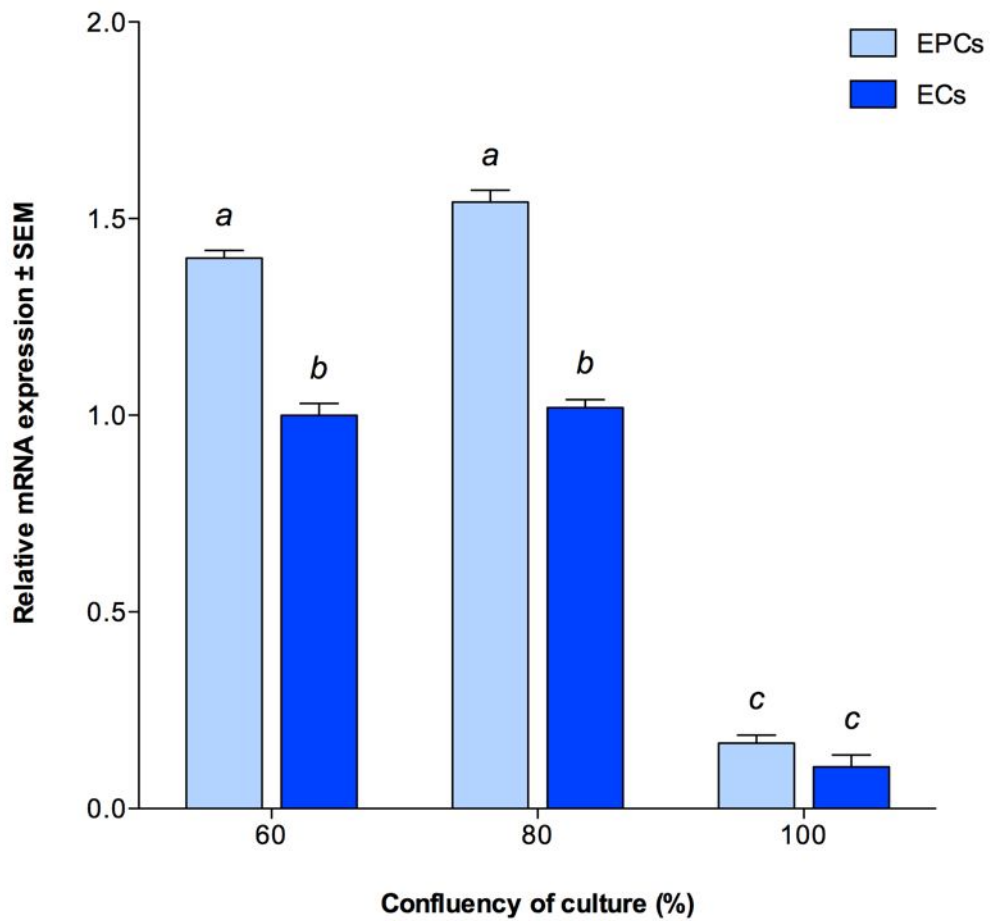


Figure 3.5. Relative expression of VEGFR2 in EPCs and ECs at increasing levels of culture confluency, determined by qPCR analysis of mRNA transcripts. Gene expression normalised to housekeeping gene β -actin, presented as mean expression \pm SEM ($n = 3$) relative to ECs at 60% confluency. Columns with different letters as superscripts are significantly different from each other ($P < 0.05$).

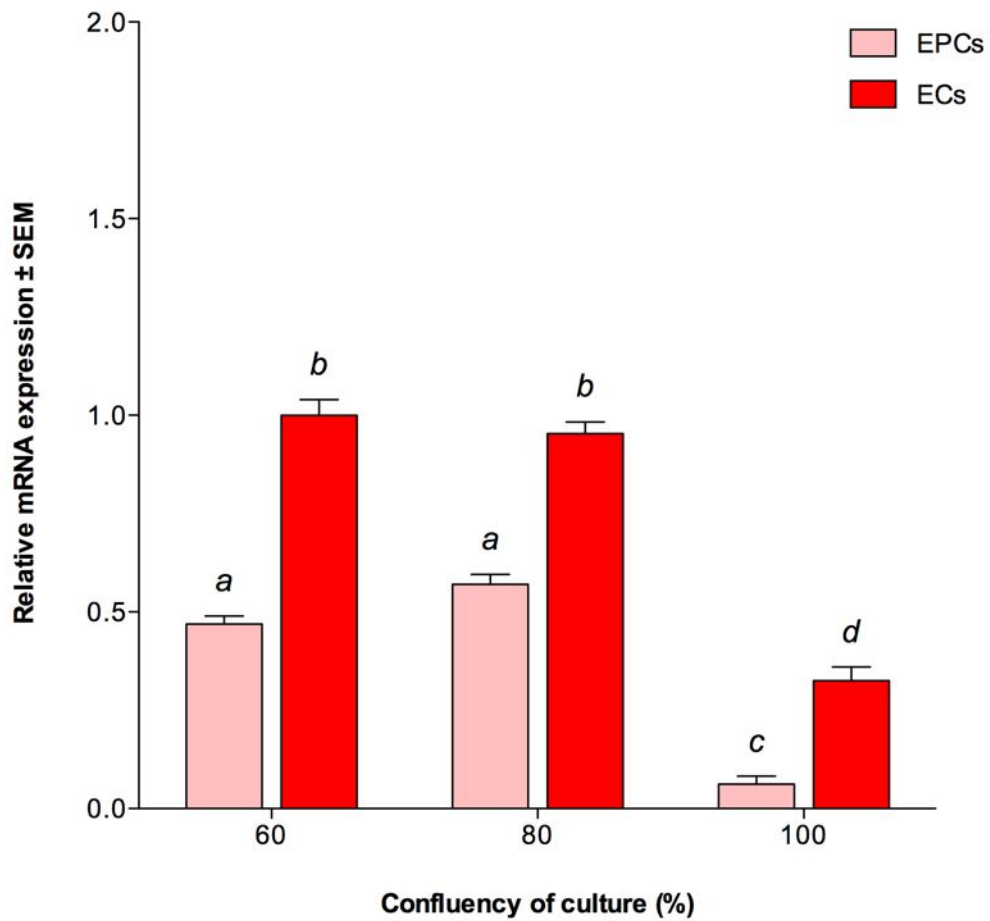


Figure 3.6. Relative expression of VE-cadherin in EPCs and ECs at increasing levels of culture confluency, determined by qPCR analysis of mRNA transcripts. Gene expression normalised to housekeeping gene β -actin, presented as mean expression \pm SEM ($n = 3$) relative to ECs at 60% confluency. Columns with different letters as superscripts are significantly different from each other ($P < 0.05$).

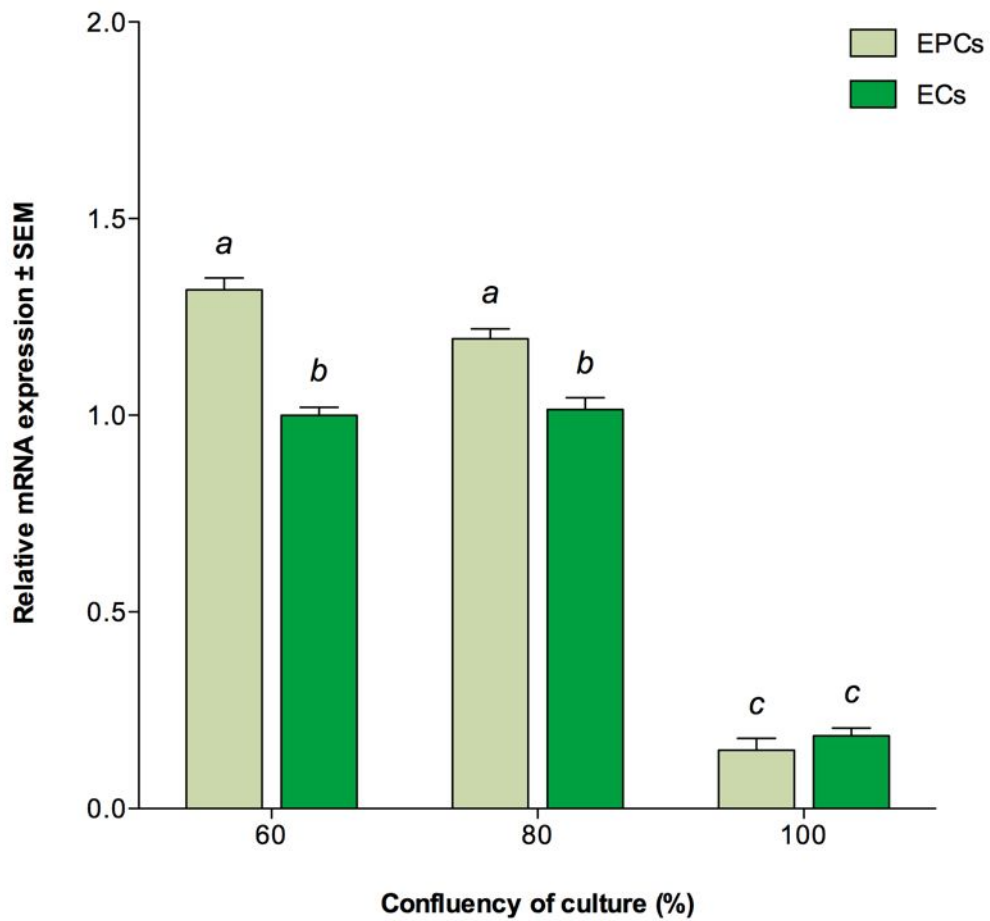


Figure 3.7. Relative expression of CD31 in EPCs and ECs at increasing levels of culture confluency, determined by qPCR analysis of mRNA transcripts. Gene expression normalised to housekeeping gene β -actin, presented as mean expression \pm SEM ($n = 3$) relative to ECs at 60% confluency. Columns with different letters as superscripts are significantly different from each other ($P < 0.05$).

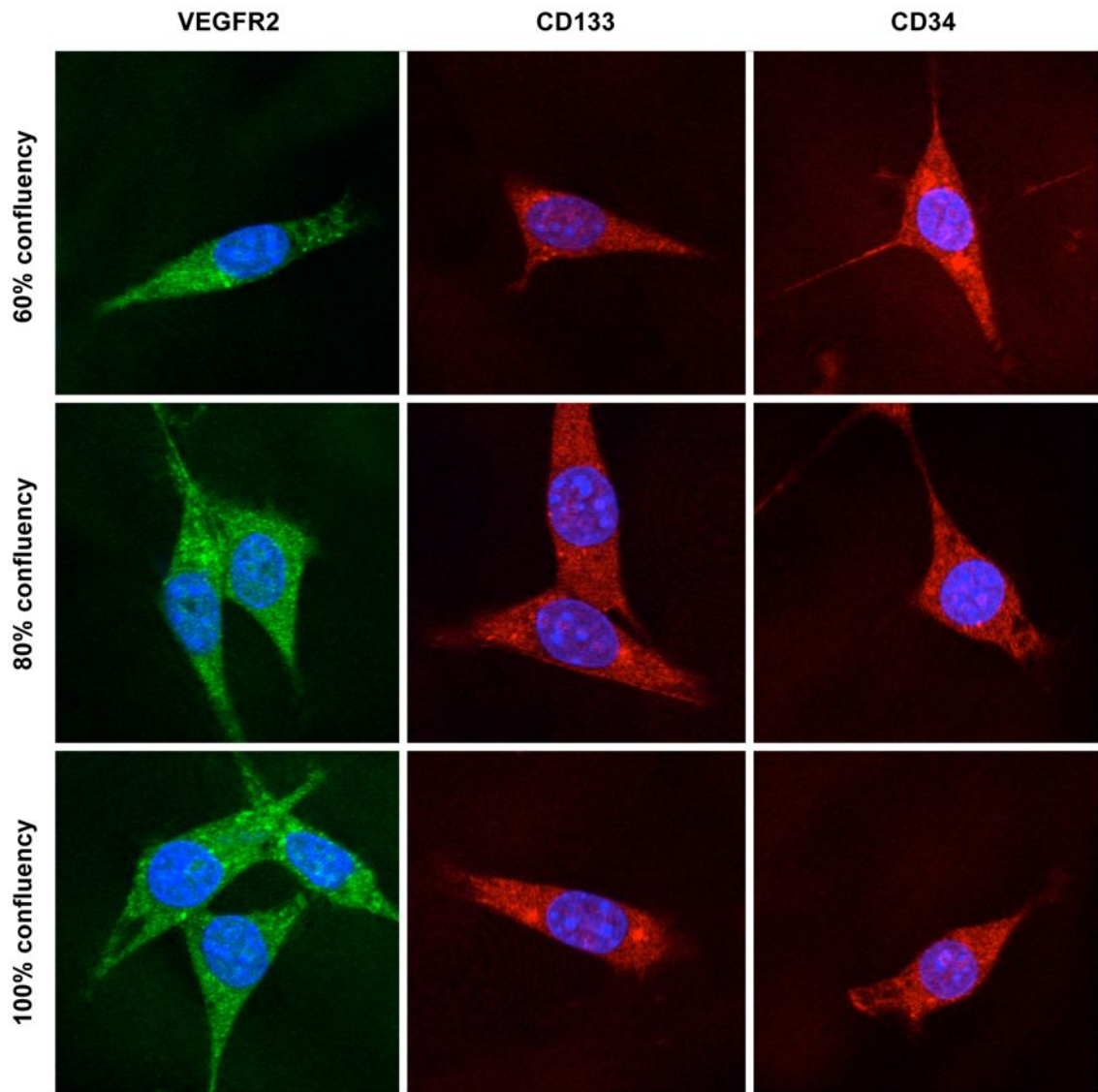


Figure 3.8. Detection of VEGFR2 (green), CD133 (red) and CD34 (red) proteins in EPCs at increasing levels of culture confluency, determined by ICC analysis. Nuclear staining (blue) was performed using DAPI-containing mounting medium.

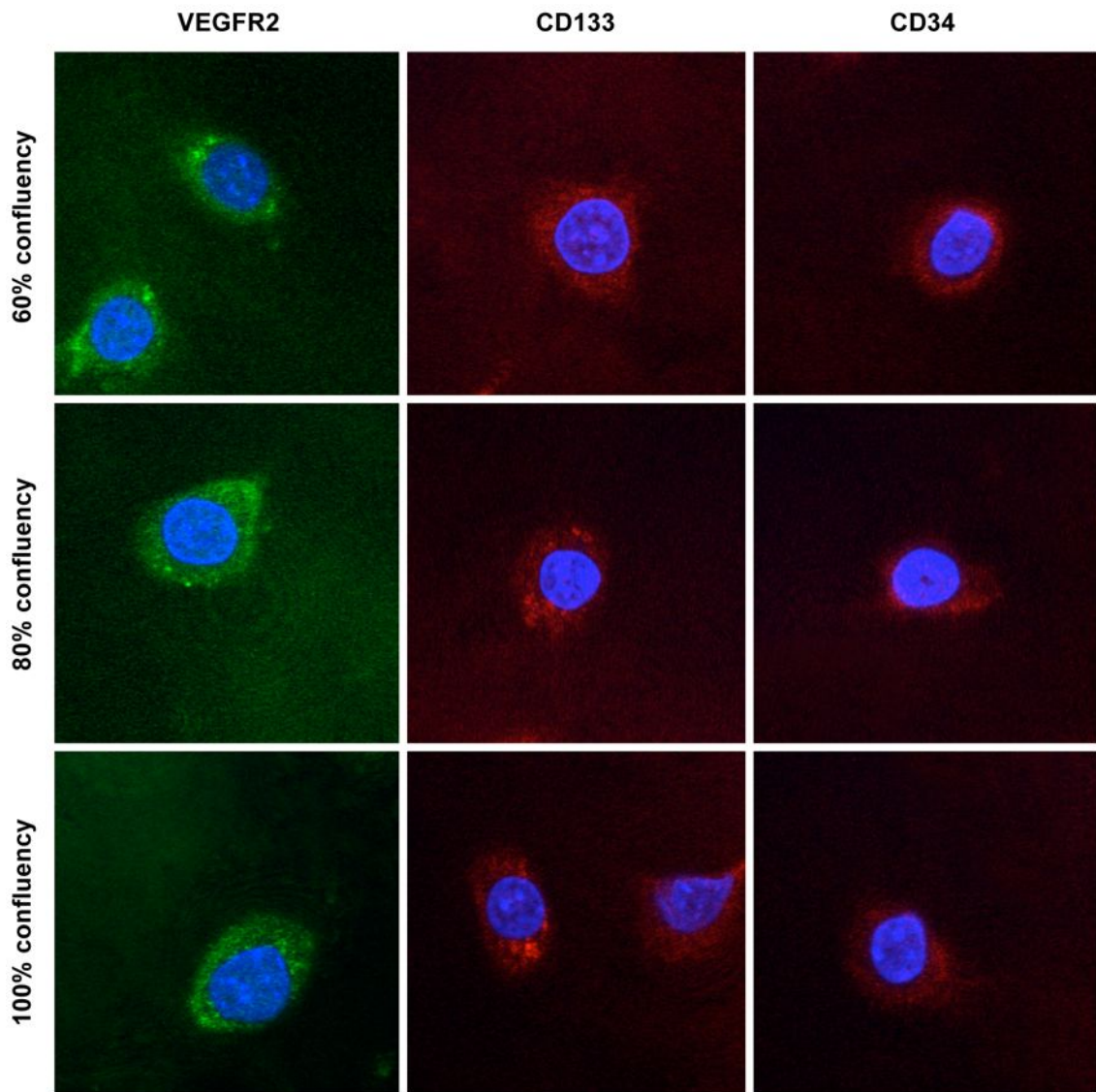


Figure 3.9. Detection of VEGFR2 (green), CD133 (red) and CD34 (red) proteins in ECs at increasing levels of culture confluency, determined by ICC analysis. Nuclear staining (blue) was performed using DAPI-containing mounting medium.

Quantification of protein expression based on mean fluorescence intensity (MFI; **Table 3.1**) demonstrated that neither the expression of VEGFR2, VE-cadherin or CD31 was significantly different between EPCs and ECs ($P>0.05$). Furthermore, unlike the expression of mRNA transcripts, expression of the three endothelial-specific proteins was not significantly affected by changes in culture confluency, in either cell line ($P>0.05$).

3.4.1.3 Lectin staining and ac-LDL uptake

Cells were further characterised using fluorescently-conjugated *Griffonia (Bandeiraea) simplicifolia* lectin I and DiI-labelled ac-LDL (**Fig. 3.10**). Positive labelling of lectin was observed in both EPCs and ECs, and both cell lines were seen to take up ac-LDL in culture. The labelling index for both lectin staining and ac-LDL uptake (calculated by the number of positively labelled cells across the range of cells [30 of each cell type] observed) was determined to be 1.

Cell	Protein	Confluency	MFI	% exp	# cells
EPC	VEGFR2	60%	0.46 ± 0.08	100	30
		80%	0.38 ± 0.09	83	34
		100%	0.46 ± 0.11	89	27
	VE-cadherin	60%	0.34 ± 0.07	87	19
		80%	0.39 ± 0.10	100	23
		100%	0.36 ± 0.09	92	28
	CD31	60%	0.42 ± 0.12	98	21
		80%	0.39 ± 0.13	91	26
		100%	0.37 ± 0.10	86	30
EC	VEGFR2	60%	0.36 ± 0.08	78	23
		80%	0.39 ± 0.09	85	29
		100%	0.32 ± 0.06	70	34
	VE-cadherin	60%	0.36 ± 0.10	92	31
		80%	0.38 ± 0.07	97	29
		100%	0.39 ± 0.09	100	17
	CD31	60%	0.43 ± 0.12	100	23
		80%	0.36 ± 0.05	84	19
		100%	0.33 ± 0.07	77	26

Table 3.1. Quantification of endothelial-specific protein expression in EPCs and ECs.
MFI, mean fluorescence intensity (arbitrary units); % exp, percentage expression relative to maximum observed in both cell types; # cells, number of cells analysed.

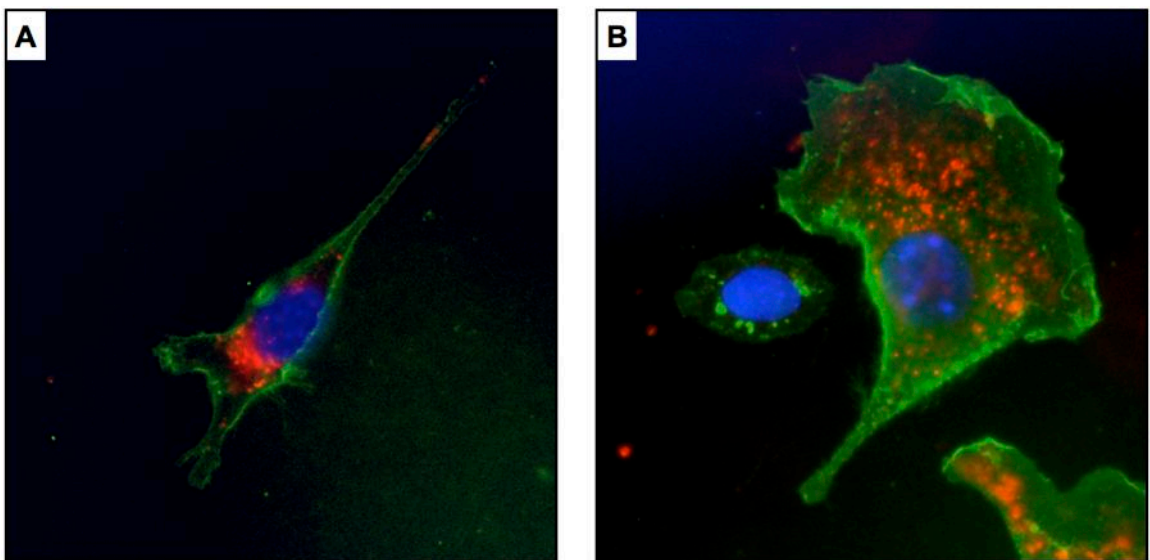


Figure 3.10. Lectin staining and uptake of ac-LDL. Additional characterisation of (A) EPCs and (B) ECs was performed using *Griffonia simplicifolia* lectin (green) and Dil-ac-LDL (red). Nuclear staining (blue) was performed using DAPI-containing mounting medium.

3.4.2 Assessment of angiogenic potential of EPCs and ECs

To determine whether EPCs or ECs possessed angiogenic potential, and were thus able to form endothelial tubules, cells were cultured on ECMatrix gel for 14 h. Tubule formation was then quantified by node counting and branch length measurement.

3.4.2.1 Quantification of *in vitro* tubule formation using node counting

Complexity of tubule formation was first quantified by counting nodes, a node being defined as a point at which formed tubules intersect or form a junction. At 2 h intervals, nodes were graded according to the type of structure: tubule end-points as N1; intersection between two tubules as N2; junctions of three or four branches as N3 or N4, respectively; and junctions comprising five or more branches as N5+. The average number of each type of node formed at each time-point throughout the assay was found to be similar for both EPCs and ECs (**Fig. 3.11**).

A large number of N1 nodes were observed at 2 h, decreasing as the assay progressed as multiple end-points joined together to form intersections and junctions. For both EPCs and ECs, the difference in N1 node number was significant between every time-point throughout the assay ($P < 0.05$). The number of N2 nodes was maximal at 4 h for both cell lines; after 6 h the number of N2 nodes decreased and were last evident at 10-12 h. For EPCs, the change in the number of N2 nodes was significant between 4 h and 8 h ($P < 0.01$) and 8 h and 10 h ($P < 0.05$) and, for ECs, between 4 h and 6 h, and 8 h and 10 h ($P < 0.05$). For both EPCs and ECs the number of N3 nodes was greatest at 6 h, after which time the number of nodes decreased, until 10-12 h when no N3 nodes were present. The change in the number of N3 nodes was statistically significant for EPCs between 2 h and 4 h ($P < 0.01$) and for both EPCs and ECs between 4 h and 6 h, and 6 h and 8 h ($P < 0.05$). N4 nodes were first observed at 4 h for both EPCs and ECs, with the maximum number at 6 h, after which they decreased in number and

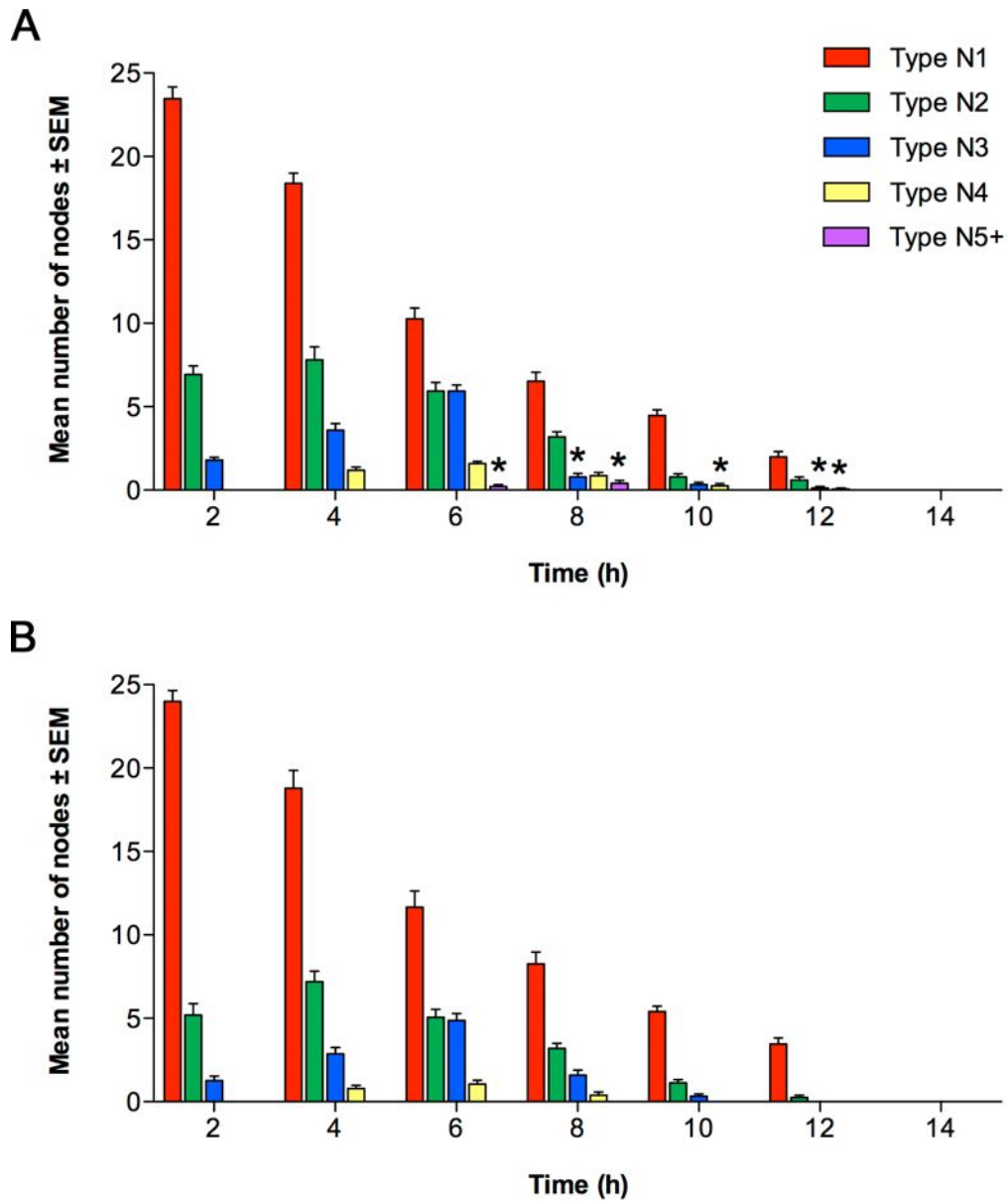


Figure 3.11. Assessment of angiogenic activity of (A) EPCs and (B) ECs cultured on in vitro tubule formation assay ECMatrix gel for 14 h, determined by node counting. Data presented as mean number of node type \pm SEM ($n = 3$) from five random fields of view at each time-point. Significant differences between cell types at each time-points are indicated (* $P < 0.05$).

were last observed at 8 h (ECs) and 10 h (EPCs). The difference in the number of N4 nodes was significant between 6 h and 8 h for both cell lines ($P < 0.05$) and between 8 h and 10 h for EPCs only ($P < 0.05$). N5+ nodes were only evident in assays containing EPCs, and were observed between 6-8 h; the difference between the number of N5+ nodes between 6 h and 8 h was not significant ($P > 0.05$). Towards the end of the assay, as tubules began to disintegrate and their nodal structures deteriorate, the total number of nodes (of all types) reduced until no tubule networks remained. No tubule end-points or junctions of any type were observed at 14 h for either EPCs and ECs.

3.4.2.2 Quantification of *in vitro* tubule formation using branch length measurement

Measurement of branch length was also used to quantify tubule formation at each time-point, performed using AQual: Angiogenesis Quantification software. The pattern of tubule growth indicated by branch length measurement, as with quantification by node counting, was similar for EPCs and ECs (**Fig. 3.12**). The mean branch length of EPC tubules at 6 h was significantly greater than ECs. Branch length had decreased by 8 h with significantly lower branch length observed for ECs. The mean branch lengths for both cell lines continued to decrease from 8 h to 14 h, until no branches were measured. Aside from 10-12 h, the difference in branch length was significant at every time-point for both EPCs and ECs ($P < 0.01$).

3.4.2.3 qPCR analysis of endothelial-specific mRNA expression during *in vitro* tubule formation

Expression of the endothelial-specific markers *VEGFR2*, *VE-cadherin* and *CD31* in EPCs and ECs cultured on *in vitro* angiogenesis assay gels was determined by qPCR. For analysis of each of the three markers, cells were recovered from ECMatrix gel with Cell Recovery Solution, at each time-point and relative expression determined by the ratio of the marker of interest to *β-actin* transcripts. In order to ensure cells at all time-points were treated in the same manner,

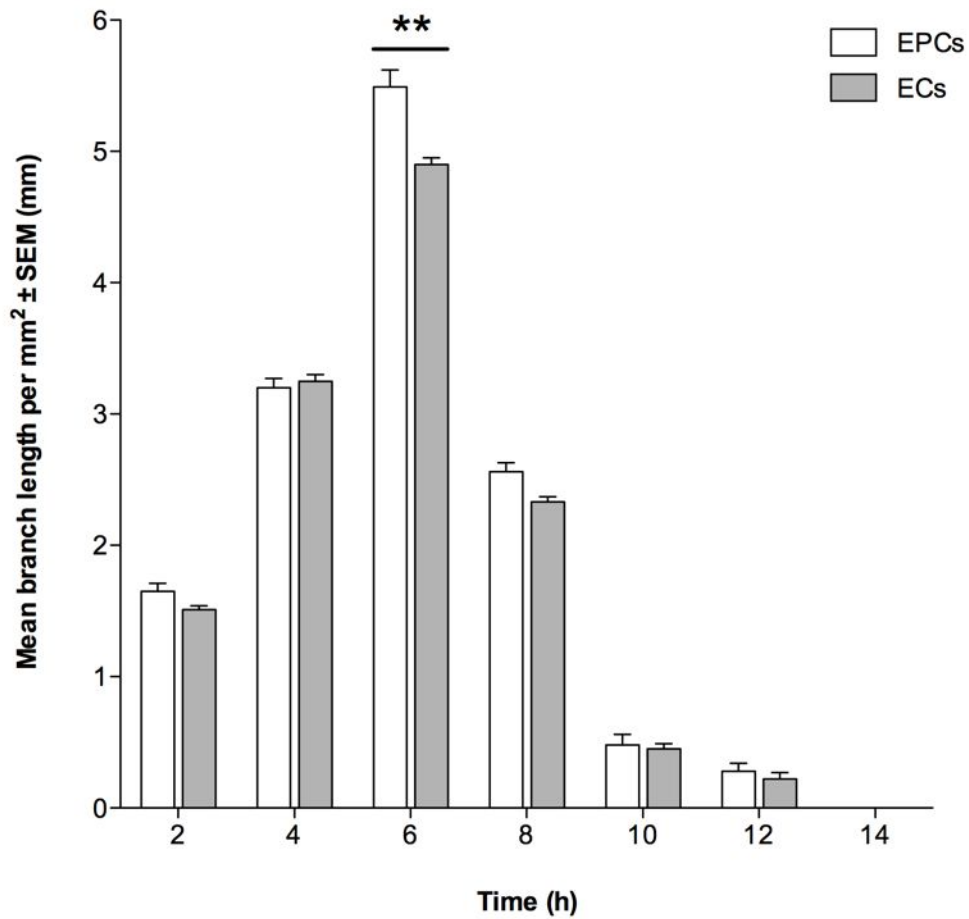


Figure 3.12. Assessment of angiogenic activity of EPCs and ECs cultured on in vitro tubule formation assay ECMatrix gel for 14 h, determined by branch length measurement. Data presented as mean branch length per mm² of assay ± SEM (n = 3) from five random fields of view at each time-point. Significant differences between cell types are indicated (P<0.01).**

EPCs and ECs for analysis of expression at 0 h were resuspended in appropriate growth media and added to ECMatrix gel, the gel then immediately depolymerised and the cells recovered by centrifugation. The relative ratio of *VEGFR2* mRNA transcripts in assayed cells recovered immediately was determined to be comparable to levels in 60% confluent EPCs and ECs, respectively, from static *in vitro* cultures (SEE 3.4.1.1). *VEGFR2* expression increased in both EPCs and ECs from 0 h to 2 h, with a significantly greater increase seen in EPCs (**Fig. 3.13**). Maximal expression of *VEGFR2* was observed at 2 h and 4 h for EPCs and EC, respectively, after which the number of *VEGFR2* transcripts decreased progressively until 14 h. The level of *VEGFR2* expression in EPCs and ECs between 6 h and 8 h showed no significant difference. Throughout the assay, for both cells lines, the change in the level of *VEGFR2* expression was significant at each time-point ($P < 0.05$), except for EPCs between 6 h and 8 h, and 12 h and 14 h ($P > 0.05$).

Expression of *VE-cadherin* in EPCs was initially observed to decrease between 0 h and 2 h before increasing again, reaching its maximum at 8 h, whilst expression in ECs increased from 0 h to its maximum at 4 h (**Fig. 3.14**). The number of *VE-cadherin* transcripts then decreased from 4 h and 6 h onwards in EPCs and ECs, respectively, and no significant difference in expression was observed between EPCs and ECs between 8 h and 14 h. Over the course of the assay, the change in the number of transcripts of *VE-cadherin* mRNA in EPCs was only significant between 6 h and 8 h, and 10 h and 12 h ($P < 0.05$). In ECs, the change in expression was only significant between 10 h and 12 h ($P < 0.05$).

Expression of *CD31* in EPCs initially increased from 0 h to 4 h followed by a slight reduction in the level of expression at 6 h (**Fig. 3.15**). Conversely, the number of *CD31* transcripts in ECs initially decreased from 0 h to 4 h before increasing to its maximum at 6 h. Maximal *CD31*

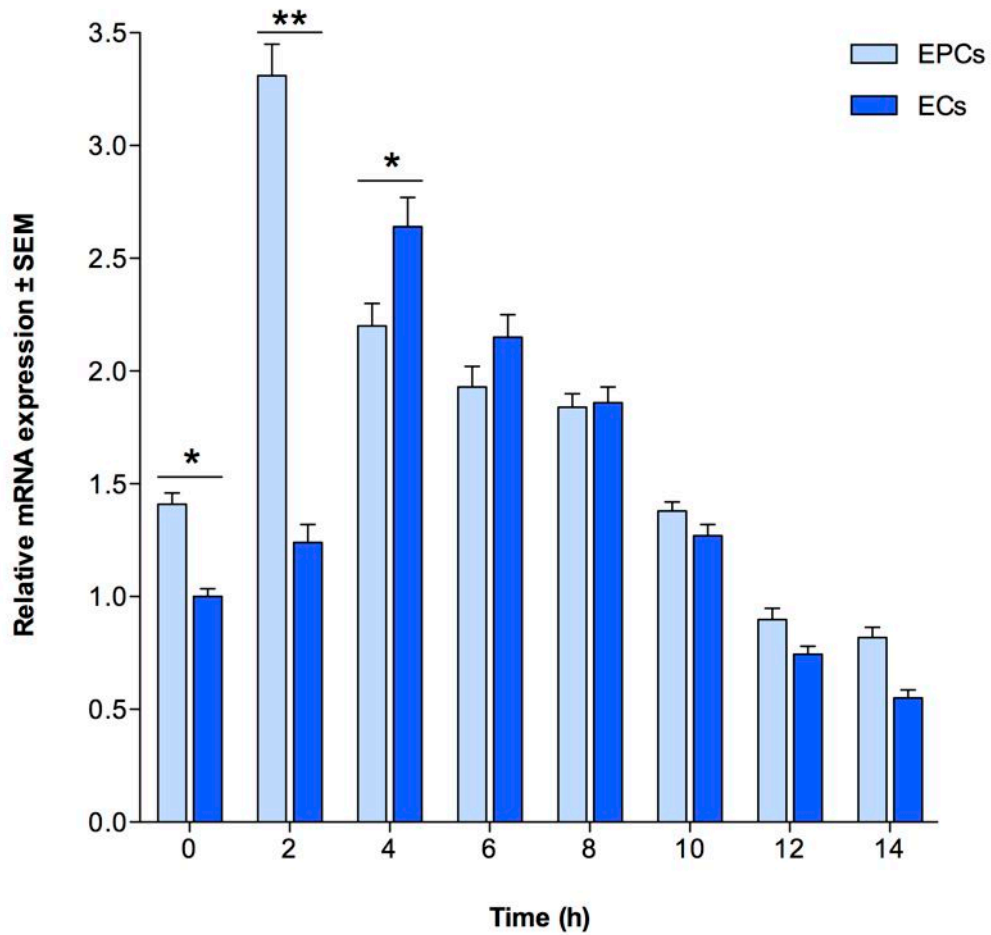


Figure 3.13. Relative expression of VEGFR2 in EPCs and ECs cultured on ECMatrix gel for 14 h, determined by qPCR analysis of mRNA transcripts. Gene expression at each time-point normalised to housekeeping gene β -actin, presented as mean expression \pm SEM ($n = 3$) relative to ECs at 0 h. Significant differences between cell types are indicated (* $P < 0.05$, ** $P < 0.01$).

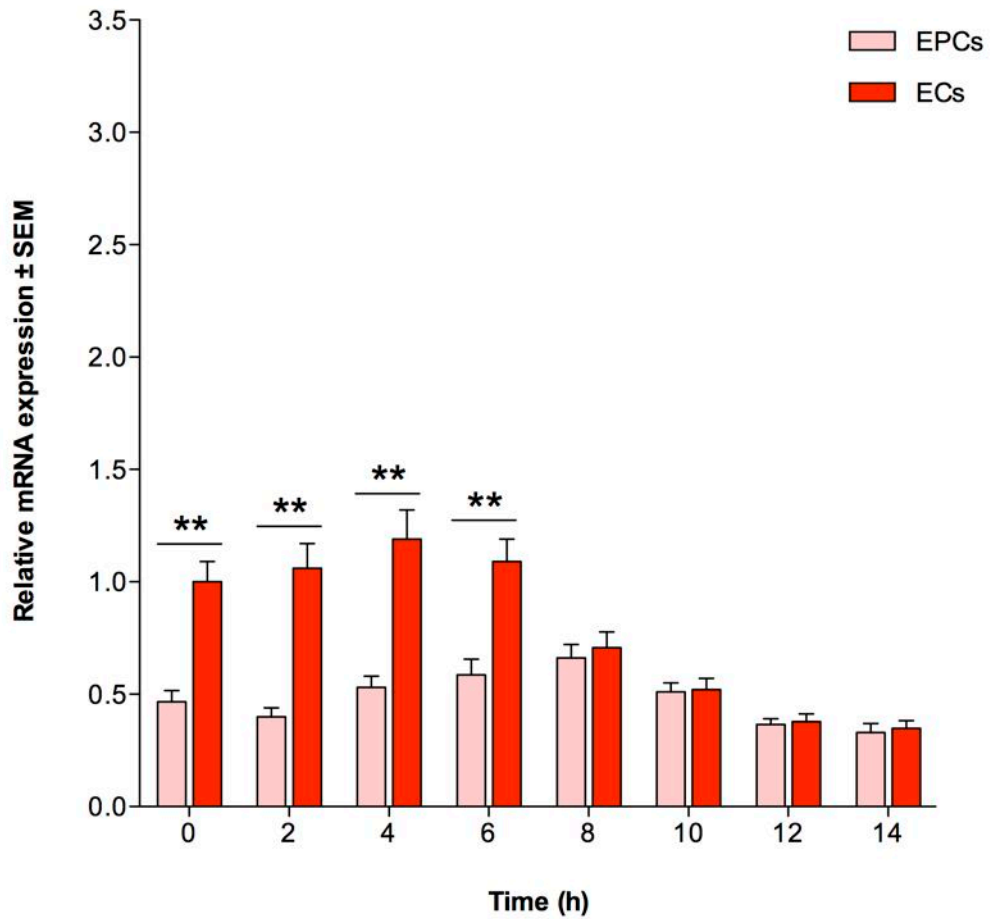


Figure 3.14. Relative expression of VE-cadherin in EPCs and ECs cultured on ECMatrix gel for 14 h, determined by qPCR analysis of mRNA transcripts. Expression at each time-point normalised to housekeeping gene β -actin, presented as mean expression \pm SEM ($n = 3$) relative to ECs at 0 h. Significant differences between cell types are indicated (** $P < 0.01$).

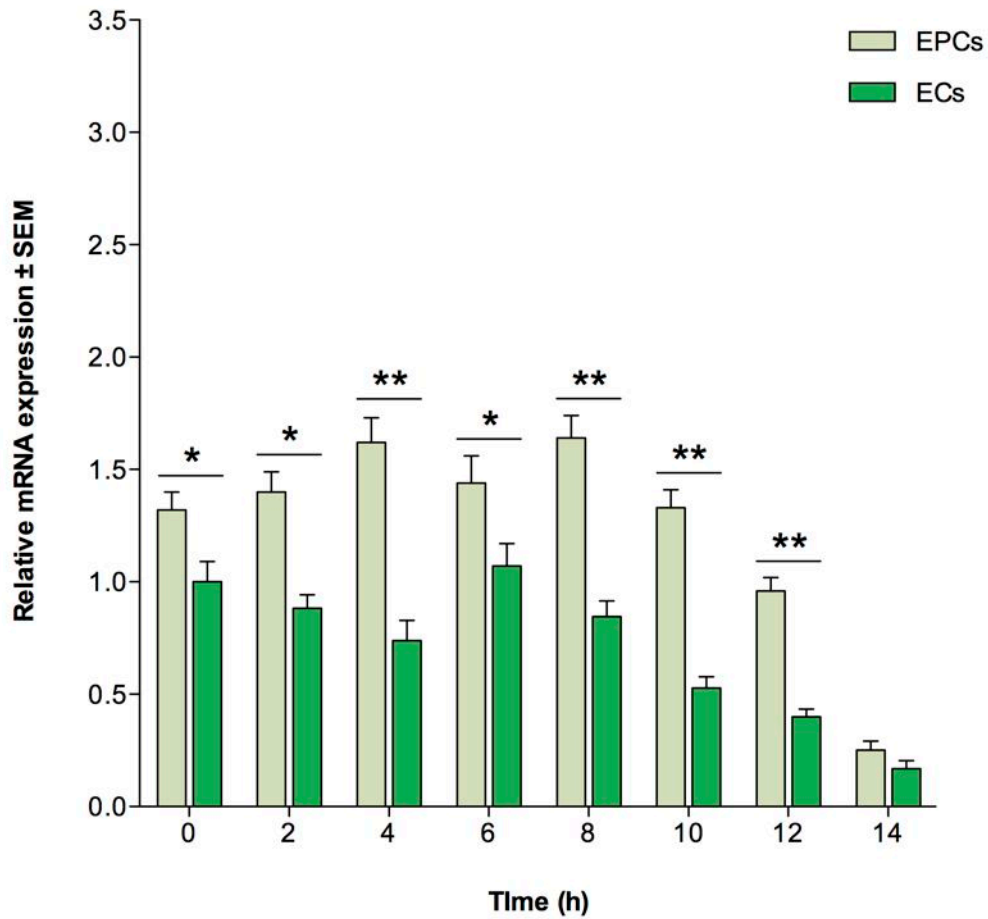


Figure 3.15. Relative expression of CD31 in EPCs and ECs cultured on ECMatrix gel for 14 h, determined by qPCR analysis of mRNA transcripts. Gene expression at each time-point normalised to housekeeping gene β -actin, presented as mean expression \pm SEM ($n = 3$) relative to ECs at 0 h. Significant differences between cell types are indicated (* $P < 0.05$, ** $P < 0.01$).

expression in EPCs was observed at 8 h after which time-point expression in both EPCs and ECs decreased progressively until 14 h. At each time-point between 8 h and 14 h, the change in *CD31* expression in EPCs was statistically significant ($P < 0.01$). In EPCs, expression changed significantly between 4 h and 6 h ($P < 0.01$) and each time-point between 6 h and 10 h ($P < 0.05$). Throughout the assay, for both cells lines, the change in the level of *VEGFR2* expression was significant at each time-point ($P < 0.05$), except for EPCs between 6 h and 8 h, and 12 h and 14 h ($P > 0.05$).

3.5 Discussion

EPCs are considered to be highly angiogenic, having been shown to have a natural role in neovascularisation, and as such it was decided that they warranted further investigation as a potential tool for therapeutic angiogenesis. However, before exploring this potential, or alternative sources of progenitor-like cells for transplantation, it was first necessary to characterise the murine EPC and EC cell lines chosen for use in this study.

Experiments of this nature are often performed using immortalised cell lines which, unlike primary cells isolated from animals, are easily obtainable (either from established stocks or commercial sources) and can be expanded without limit. Immortalised cell lines are often originally derived from tumour tissues, and can produce phenotypes that differ significantly from their natural *in vivo* counterparts; having adapted to *in vitro* culture, many cell lines lose intracellular interactions and tissue-specific secretions of growth factors and cytokines. However, in light of the many complexities involved in using primary cells (or the added complexity of animal models) the use of immortalised cell lines is considered to be an acceptable, and arguably preferable, alternative for the study of basic cellular mechanisms. Furthermore, there is evidence to suggest that certain functions relating to several intrinsic signalling pathways, such as ErbB and PI3K, are better conserved in immortalised cell lines than previously thought (Pan *et al.*, 2009).

The specific endothelial cell lines used in this study were carefully chosen to be accurate representations of their respective stages of endothelial development. The endothelial progenitor cell line MFLM-4 was derived from primary cultures of murine foetal lung harvested from dams of the inbred mouse strain FVB/N at embryonic day 14.5. Following disruption of harvested lungs, mouse lung mesenchyme cultures were transformed to express

SV40 large T antigen and neomycin resistance gene (Akeson *et al.*, 2000). Selection medium was then used to select and expand the immortalised MFLM-4 population, which was subsequently cloned and successfully maintained in continuous culture for more than three years. After its derivation, a wide range of characterisation experiments was performed on MFLM-4, intended to confirm the endothelial precursor nature of the cell line. Using flow cytometry it was determined that MFLM-4 expressed several proteins and receptor tyrosine kinases associated with the endothelial phenotype and function, namely CD34, CD31, angiotensin converting enzyme (ACE), vWF, VEGFR1 and 2, and Tie-2. Similarly to MFLM-4, the murine cardiac endothelial cell line MCEC-1 has been shown to compare favourable to other equivalent endothelial cell types. MCEC-1 was isolated from the hearts of H-2Kb-tsA58 transgenic mice and propagated in a similar manner to MFLM-4 EPCs to produce a stable, immortalised cell line (Lidington *et al.*, 2002). Characterisation performed prior to publication revealed an endothelial-specific phenotype (with expression of CD31, endoglin, ICAM-1, ICAM-2 and VCAM-1), a high level of responsiveness to endothelial growth factors, and the ability to facilitate the rolling and firm adhesion of human neutrophils and murine monocytes.

MFLM-4 EPCs and MCEC-1 ECs were selected as examples of two distinct points along the continuum of endothelial maturation, namely precursor and mature cells. In addition to demonstrating the endothelial nature and maturation stage of the two cell lines, characterisation also served two additional purposes. Firstly, the characterisation of EPCs and ECs in static culture provided a baseline reference against which the changes in expression associated with the cellular response to an angiogenic stimulus could be compared. When cultured on ECMatrix gel, endothelial cells are stimulated by growth factors and basement membrane proteins within the gel to begin the formation of tubule networks. By analysing lineage-specific expression in these assayed cells, and comparing this data to cells from static

cultures, changes in expression can be correlated with the progression of tubule formation. Secondly, the characterisation of EPCs and ECs allowed an estimation of the efficiency of the subsequent process of deriving cells appropriate for angiogenic therapy transplantation, by comparison of differentiating pluripotent cells, such as ESCs or iPSCs, with an 'ideal' precursor cell phenotype (as defined by the MFLM-4 cell line).

The relative gene expression of *VEGFR2*, *VE-cadherin* and *CD31* in EPCs and ECs was determined by qPCR. As has been previously demonstrated in the literature, differences in the expression of all three markers were observed between the stages of endothelial maturation represented by the two cell lines. Overall, transcripts of both *VEGFR2* and *CD31* mRNA were determined to be more abundant in EPCs than in ECs, whilst a greater number of *VE-cadherin* transcripts were observed in ECs.

When interpreting the differences observed in expression between the two cell lines it must be noted that although the EPC and EC cell lines are part of the same spectrum of endothelial lineage, they do originate from different sources: MFLM-4 EPCs were generated from primary cultures of lung mesenchyme from foetal FVB/N mice and MCEC-1 ECs were isolated from the hearts of transgenic adult C57BL/6 mice. The two cell lines are therefore independent populations and comparisons are made with the understanding that absolute differences in mRNA levels between the two may not be representative of expression at the same two stages of maturation within a single cell line. However, if relative changes and the overall pattern of the three endothelial markers in the two cell lines are considered instead, comparisons between the two independent populations have more validity. After consideration, it was decided that the benefits of using these two established and well-documented cell lines

(i.e. their ease of availability and culture as well as their reproducible and stable phenotype) outweighed the potential ambiguity that may arise from their comparison.

VEGFR2 plays an important role in the initiation of vasculogenesis by angioblasts in the developing embryo. The level of both the *VEGFR2* gene and its product (the VEGFR2 receptor complex) varies at different stages of endothelial maturation and correlates with vasculogenic and angiogenic activity; when the requirement for mitogenesis is high, as during neovascularisation when endothelial proliferation is upregulated, VEGFR2 expression is similarly increased (Dunk & Ahmed, 2001). Given this, the greater abundance of *VEGFR2* transcripts observed in EPCs compared to ECs suggests that MFLM-4 EPCs have a much greater migratory potential. Being at an earlier stage of endothelial development it was expected, as has been demonstrated in numerous past studies, that EPCs would show a significantly greater level of *VEGFR2* expression; the high level of expression observed in this study is evidence of their precursor nature. Furthermore, as VEGFR2 is the primary transducer of VEGF signals through pathways such as Raf-Mek-ERK that promotes cell proliferation (Takahashi, T *et al.*, 1999), the increase in expression seen in both EPCs and ECs as culture confluency increased from 60% to 80% confirms its role in endothelial proliferation. That a similar increase in *VEGFR2* expression was not observed in either EPCs or ECs as confluency reached 100% does not, as may be assumed, preclude this role. It may be argued that a reduction would not be seen if the VEGFR2 expression positively correlated with cell proliferation. However contact inhibition, whereby cell growth is arrested when close cell contact occurs, must be considered. It has been demonstrated to have a significant effect on a wide range of genes and gene products in many cell types (Zou *et al.*, 2006), as well as decreasing cell locomotion and altering the growth kinetics of ECs (Lee, Y *et al.*, 1994). With this in mind, low levels of

VEGFR2 transcripts in 100% confluent cultures, as well as the other genes analysed in this study, may simply be a demonstration of this effect.

VE-cadherin is an important component of vascular remodelling and is a marker of maturation of EPCs into a more mature phenotype. Unlike *VEGFR2*, the number of *VE-cadherin* transcripts was determined to be greater in ECs than in EPCs. This correlates with the understanding that *VE-cadherin* expression increases as endothelial cells develop from a precursor to mature phenotype (Kiran *et al.*, 2011). Furthermore, the increase in *VE-cadherin* expression seen in EPC between 60% and 80% confluency suggests that VE-cadherin is indeed upregulated as EPCs proliferate and mature towards an EC-like phenotype. Similarly to *VEGFR2*, the expression of *VE-cadherin* was observed to decrease significantly in both cell lines as culture confluency reached 100% and is also likely to indicate contact inhibition.

CD31 has been demonstrated to have influence over EC migration and is a marker of early vascular development and angiogenic potential. Expression of *CD31* was determined to be higher in EPCs than in ECs, further demonstrating the naïve phenotype of the EPCs indicated by the high level of *VEGFR2* transcripts. Interestingly, whilst *VEGFR2* and *VE-cadherin* expression in EPCs was seen to increase with culture confluency, expression of *CD31* was observed to decrease with increasing EPC confluency. Lower *CD31* expression was observed in ECs (at both 60% and 80% confluency) which are, in essence, EPCs further along the continuum of endothelial lineage. This suggests that the decrease in *CD31* expression may continue throughout the differentiation of EPCs to a level comparable to that seen in ECs, and is consistent with established findings that *CD31* is a marker of the early endothelial lineage (Kanayasu-Toyoda *et al.*, 2003). Again, as with *VEGFR2* and *VE-cadherin*, the number of *CD31* transcripts significantly declined in both cell lines at 100% culture confluency and, as

discussed, this likely demonstrates the reductive effect of contact inhibition of gene expression.

It should be noted that expression of mRNA transcripts may not always represent the current state of function of the cell in question because the functional gene products of those expressed transcripts (i.e. proteins and enzymes) may be produced to a greater or lesser extent (Pascal *et al.*, 2008). For example, VEGF activity has been shown to be regulated by post-translational modification and stabilisation of VEGF mRNA and so cause a difference in cell function not revealed by assessment of mRNA expression alone (Levy *et al.*, 1995; Stein *et al.*, 1995). For this reason determination of the expression of VEGFR2 protein in EPCs and ECs was carried out using ICC, to allow comparison with *VEGFR2* gene expression. Interestingly, although the number of *VEGFR2* mRNA transcripts showed a significant reduction as culture confluency increased, cell surface expression of VEGFR2 protein did not appear to be similarly affected. This may be due to a decreased demand for the surface protein to be produced (by gene transcription and translation), which results in a reduction in mRNA abundance, without a need for the existing surface protein to be actively removed or internalised. This finding highlights the relative independence of gene and protein expression and shows that one is not always representative of the other. Protein expression analysis of CD133 and CD34 (although not combined with gene analysis) was used for additional characterisation of EPCs and ECs and their surface expression (similarly expressed at equivalent levels regardless of confluency) further confirmed the endothelial nature of the EPCs and ECs.

Angiogenic potential is the ability of endothelial cells to respond to a pro-angiogenic stimulus. Here, the angiogenic potential of EPCs and ECs was determined using an *in vitro* tubule formation assay, by culture of the cells on a proprietary gel matrix, ECMatrix.

Tubule formation was then quantified by measurement of the total length of tubules and the type and number of junctions formed between them. Both EPCs and ECs were observed to form complex tubule networks over the 14 h assay course but only the networks formed by EPCs were seen to contain nodes consisting of five or more branches, suggesting a greater network complexity. In addition, although the branch length measurements taken at each time-point were similar for both cell lines, the maximum total tubule length measured for EPCs (at 6 h) was significantly greater. It should be noted that in certain circumstances, a level of complexity could be observed which is not indicative of the true nature of the tubule network. For instance, if two separate tubules were crossing each other but were not physically joined, this would be treated as a junction of 4 tubules (N4 node) during the subsequent image analysis, increasing the apparent complexity of the network without an actual increase in N4 nodes. This could perhaps be further elucidated using confocal microscopy to identify the position of each tubule in the z-plane (i.e. from the top to the bottom of the ECMatrix gel layer) in addition to the x and y planes visible using routine brightfield microscopy. Here, as the angiogenic potential of EPCs and ECs illustrated by node counting correlated with branch length data, we concluded that it is unlikely that the observed increased network complexity in EPCs is an artefact of our particular image analysis. Therefore if, as is suggested in the literature (Ponce, 2009; Staton *et al.*, 2009; Arnaoutova & Kleinman, 2010), tubule length and node complexity positively correlate with angiogenic potential then it can be suggested that EPCs, which form networks of greater total length and complexity, have a higher angiogenic potential than ECs.

Although quantification of *in vitro* tubule formation revealed similar growth kinetics in both cell lines, the expression of some endothelial-specific genes was shown to vary greatly between EPCs and ECs during tubule formation. For example, whilst expression of *VEGFR2*,

thought to be integral to the angiogenic response, was similar in both cell lines, the pattern of CD31 expression, considered an indicator of angiogenic potential, was different as tubule formation progressed. This discrepancy may highlight that, whilst both cell lines appear to behave similarly in terms of tubule formation, the mechanisms by which they act may be driven (at least *in vitro*) by different cellular signalling pathways, although comparable data from other studies are limited. It has previously been shown that cells of different origins, namely human umbilical vein endothelial cells (HUVECs) and placental trophoblast cells, demonstrate similar tubule formation on Matrigel but differential expression profiles across a wide range of genes (Fukushima *et al.*, 2008). However, without further study or additional data for comparison, it is difficult to interpret the variations in expression seen between EPCs and ECs, which are of the same lineage origin but represent different stages of endothelial maturation. Aside from the physiological transformation that must occur during cellular differentiation, it is conceivable that expression changes may represent an artefact of the assay system rather than the natural behaviour of the cells themselves.

The data obtained from the characterisation of MFLM-4 EPCs and MCEC-1 ECs correlate with the understanding that maturation of one cell type into another is accompanied by alterations in mRNA expression and the subsequent production of gene products necessary for the correct functioning of the intended cell type. The expression patterns observed indeed served to confirm the purported phenotypes of the two cell lines used and allowed comparison of the changes in expression that occur during angiogenic stimulation and *in vitro* tubule formation of EPCs and ECs. In addition, characterisation of the two representative cell types provided a reference for the subsequent derivation of progenitor-like cells from pluripotent stem cells.

CHAPTER 4:

DERIVATION OF ENDOTHELIAL PROGENITOR CELLS BY PLURIPOTENT STEM CELL DIFFERENTIATION

4.1 Introduction

ESCs and iPSCs are both potential alternative sources of cells to EPCs for therapeutic angiogenic transplantation. To produce endothelial-like cells, pluripotent stem cells must be allowed (or manipulated) to differentiate towards the endothelial lineage. The endothelial lineage, as with many cell types, is not a collection of separate, distinct stages of maturation between which cells abruptly transition. Instead, it is a continuum consisting of particular periods of cellular development that pass gradually from one to the next. Consequently, although particular stages of maturation can be defined and are individually recognised, differentiating cells exist as points on a continuous spectrum of lineage rather than as discrete cell phenotypes (Kim, S & von Recum, 2009). The expression patterns of specific surface markers during the maturation of EPCs into ECs have been widely investigated. By analysing changes in the expression of *VEGFR2*, *VE-cadherin* and *CD31* the point on the spectrum of endothelial lineage at which a differentiating cell lies can be determined. Determining the stage of stem cell maturation, and confirming commitment to the endothelial lineage, allows better characterisation of the stem cells' current phenotype and the development of their angiogenic potential.

Pluripotent cells can be maintained in an undifferentiated state *in vitro* by the addition of leukaemia inhibitory factor (LIF). Whilst LIF induces differentiation in murine myeloid leukaemia cells, it has been shown to suppress differentiation of cultured murine ESCs without reducing their ability to subsequently differentiate into diverse somatic cell types

(Williams, R *et al.*, 1988). Once the LIF blockade is removed, stem cells begin to differentiate spontaneously, potentially producing cells of all possible types and lineages. By guiding differentiation towards a specific lineage, for instance using EC-conditioned medium (ECCM) containing lineage-appropriate growth factors and stimulants, the yield of a particular cell type may be increased. Conditioned medium has been previously shown to increase the efficiency of directed differentiation of pluripotent ESCs, initially into a mixed population of endothelial progenitors and haematopoietic colony-forming cells, and ultimately into mature endothelial cells (Bordoni *et al.*, 2007; Sun *et al.*, 2009). The exact mechanism of the effect of ECCM on stem cell differentiation has been widely investigated, but remains unknown. However, it appears that the successful direction of differentiation is dependent on the specific cocktail of factors secreted by the cells used to condition the differentiation medium (Bentz *et al.*, 2006). The recipe for this cocktail is still unclear but it has been demonstrated that the effect of ECCM on differentiation can be enhanced by further supplementation of factors such as GM-CSF, SCF, EPO and IL-3 (Davis *et al.*, 1997; Zhao, H-P *et al.*, 2003). One aim of this investigation was to explore whether ECCM treatment during differentiation could be used to improve the process of producing highly angiogenic endothelial-like cells from ESCs and iPSCs.

4.2 Hypothesis & objectives

It was hypothesised that cells possessing a genomic and proteomic phenotype, as well as an angiogenic potential, comparable to natural EPCs could be derived by *in vitro* differentiation of pluripotent stem cells. Two stem cell populations were used: natural ESCs isolated from murine blastocysts and iPSCs generated by the retroviral reprogramming of somatic cells. Furthermore, it was postulated that the production of precursor-like cells from these sources could be positively influenced by the application of ECCM, culture medium containing growth factors and soluble cytokines released by mature ECs in culture.

Using *in vitro* cell culture, the experiments described in this chapter aimed to:

1. produce cells with an EPC-comparable phenotype by the *in vitro* differentiation of ESCs and iPSCs;
2. determine the effect of ECCM on the efficiency of stem cell differentiation;
3. demonstrate and quantify the angiogenic potential of those derived cells using an *in vitro* tubule formation assay;
4. compare and contrast ESCs and iPSCs as alternatives to natural EPCs in possible angiogenic therapies.

4.3 Methods

4.3.1 Optimisation of stem cell culture conditions

Prior to EPC derivation, a variety of MEF feeders and cell culture media were tested to determine optimal culture conditions for stem cells.

As previously discussed, CF-1 cells are primary MEFs (i.e. requiring passage and with a limited culture lifespan) which, once mitotically-inactivated with mitomycin C, are used to support stem cells in culture. In comparison, Sandoz inbred Swiss mice (SIM) embryo-derived, thioguanine- and ouabain-resistant (STO) cells are a continuous line of fibroblasts (Bernstein *et al.*, 1976). They have the advantage of being easily grown without requiring regular replenishment from primary sources or frozen cell stocks. Furthermore, STO-neomycin-LIF (SNL) 76/7 cells are STO cells which have been transfected with a vector construct to stably express human LIF cDNA (Nagy, 2003). This negates the need for LIF-supplemented culture medium in order to maintain pluripotency. In parallel, D3 ESCs were cultured on either CF-1, STO or SNL 76/7 fibroblasts for 72 h, with growth medium changed every 24 h, and observed for size and quantity (**Fig. 4.1**). Three modified formulations of culture medium were tested: 'Stem cell medium' containing Knockout DMEM (Invitrogen) and ES-screened FBS (Thermo Fisher Scientific) (Facucho-Oliveira *et al.*, 2007), 'Soriano medium' containing DMEM and ESC-optimised FBS (Invitrogen) (Chen, WV & Soriano, 2003), and 'EmbryoMax medium' containing ES FBS (Millipore, Hertfordshire, UK). Semi-quantitative assessment of stem cell colonies was performed based on visual observations (**Table 4.1**). Large, regularly-shaped colonies, showing a distinctive halo around their perimeter, were used to determine optimum culture conditions, namely CF-1 feeder cells and ESC medium.

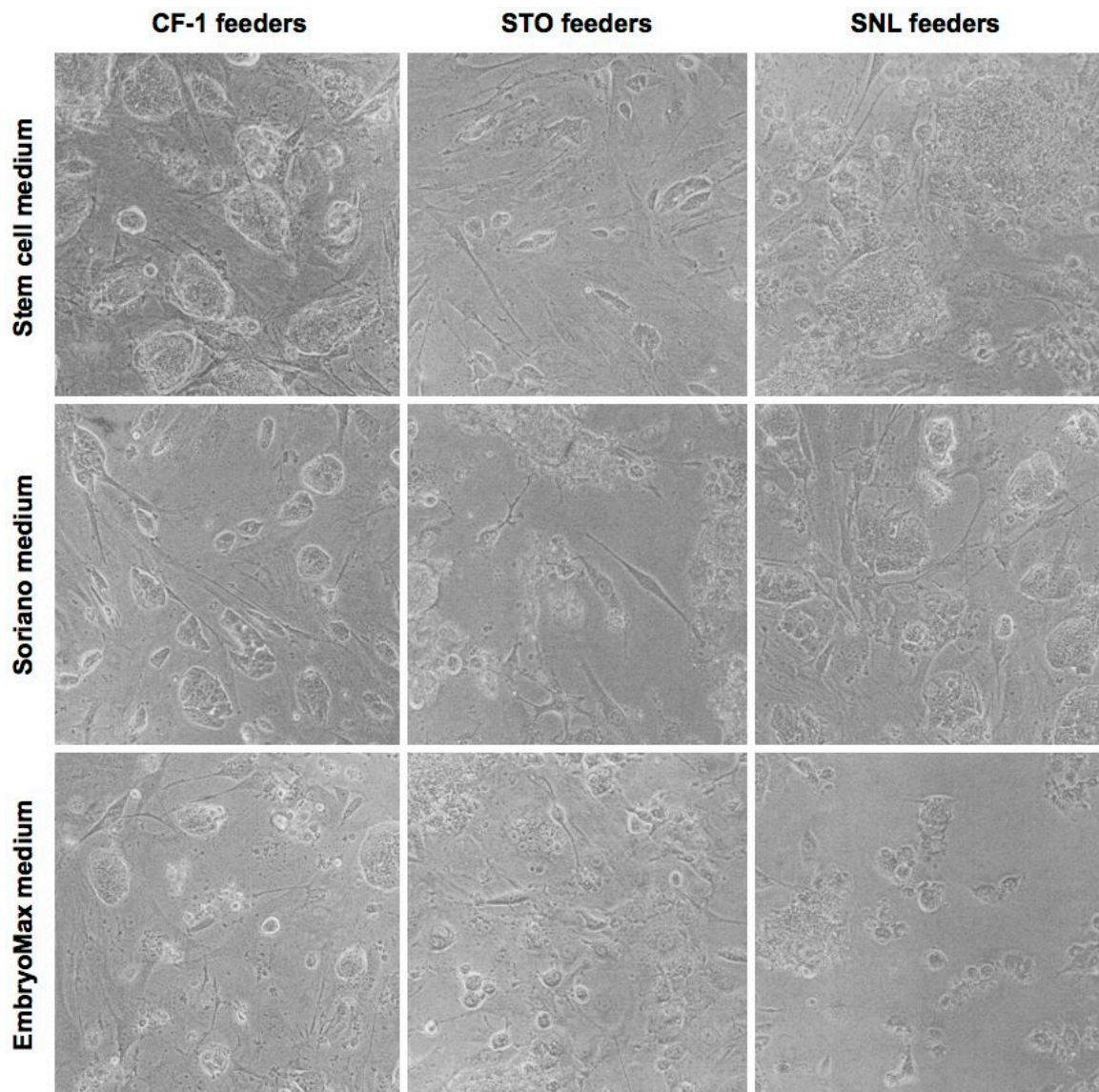


Figure 4.1. Optimisation of stem cell culture conditions. D3 ESCs were cultured on mitotically-inactivated CF-1, STO or SNL 76/7 feeders for 72 h at 37°C / 5% CO₂ with stem cell, Soriano or EmbryoMax medium changed every 24 h.

		<i>Feeder cells</i>		
		CF-1	STO	SNL
<i>Medium</i>	Stem cell	+++	+	-
	Soriano	++	-	++
	EmbryoMax	+	+	-

Table 4.1. Semi-quantitative assessment of stem cell culture conditions.

4.4 Results

D3 ESCs and QS/R27 iPSCs were differentiated for 28 days using the hanging droplet method in order to derive endothelial-like cells. Spontaneous differentiation was performed using stem cell culture medium without LIF supplementation. Directed differentiation was performed using ECCM, growth medium conditioned by 24 h exposure to ECs in culture. ECCM was used for the initial 48 h of hanging droplet culture after which the culture plates were flooded, as in spontaneous differentiation, with routine stem cell differentiation medium. Characterisation was performed throughout the course of differentiation using qPCR and ICC to determine endothelial-specific gene and protein expression, respectively.

4.4.1 Expression of lineage-specific markers in differentiating ESCs and iPSCs

4.4.1.1 qPCR analysis of mRNA transcripts

The expression of *VEGFR2*, *VE-cadherin* and *CD31* in differentiated stem cells was analysed. Data were normalised to the level of *β-actin* expression in each cell type and expressed relative to that observed in 60% confluent ECs.

Transcripts of *VEGFR2* mRNA were detected in both ESCs and iPSCs from d1 of differentiation using both spontaneous and directed methods. In ESCs, expression was significantly different between differentiation treatments from d1 to d6 (**Fig. 4.2**). Previously, the differing expression of *VEGFR2* mRNA transcripts in EPCs and ECs was demonstrated: a higher level of expression was detected in subconfluent EPCs compared to ECs (SEE **3.4.1.1**). In the two populations of differentiating ESCs, the level of *VEGFR2* expression was observed to exceed that of ECs at d2 (in directed differentiation) and at d4 (in spontaneous differentiation), reaching a level of expression comparable to EPCs at d7 (in directed differentiation) and at d14 (in spontaneous differentiation).

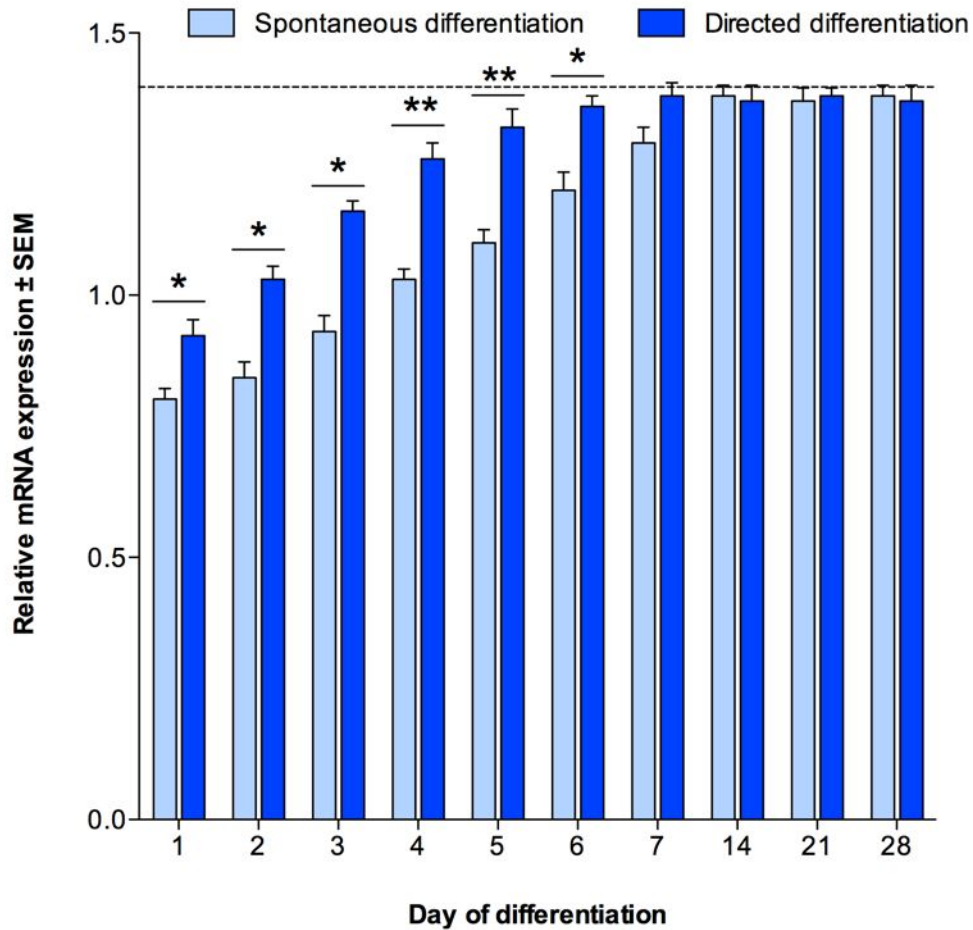


Figure 4.2. Relative expression of VEGFR2 in ESCs over 28 days of spontaneous and directed differentiation, determined by qPCR analysis of mRNA transcripts. Gene expression normalised to housekeeping gene β -actin, presented as mean expression \pm SEM ($n = 3$) relative to ECs at 60% confluency. Relative expression observed in 60% confluent EPCs indicated by dotted (---) line. Significant differences between differentiation treatments are indicated (* $P < 0.05$, ** $P < 0.01$).

Unlike ESCs, the expression of *VEGFR2* in differentiating iPSCs was not significantly different between treatments; expression was observed to exceed that seen in ECs at d5 but did not reach a level comparable to EPCs before d28 (**Fig. 4.3**).

Very low levels of *VE-cadherin* mRNA transcripts were detected in both ESCs and iPSCs (**Fig. 4.4** and **Fig. 4.5**). In neither differentiation treatment (of either cell type) was expression observed to reach that of EPCs or ECs before d28, and there was no significant difference between spontaneously- and directly-differentiated cells.

Transcripts of *CD31* mRNA were present in both ESCs and iPSCs from d1 onwards. Expression in directly- and spontaneously-differentiated ESCs was observed to exceed that seen in ECs at d5 and d7, respectively (**Fig. 4.6**).

From d2 to d14, the expression of *CD31* was significantly different between differentiation treatments, increasing to a level similar to that observed in ECs by d14 (in directed differentiation) and by d21 (in spontaneous differentiation). In iPSCs, in both differentiation treatments, transcripts of *CD31* mRNA were determined to increase from d1 to d28 but did not reach a level comparable to the expression observed in either ECs or EPCs during the course of differentiation (**Fig. 4.7**). There was no significant difference between the expression of *CD31* in spontaneously- and directly-differentiated iPSCs.

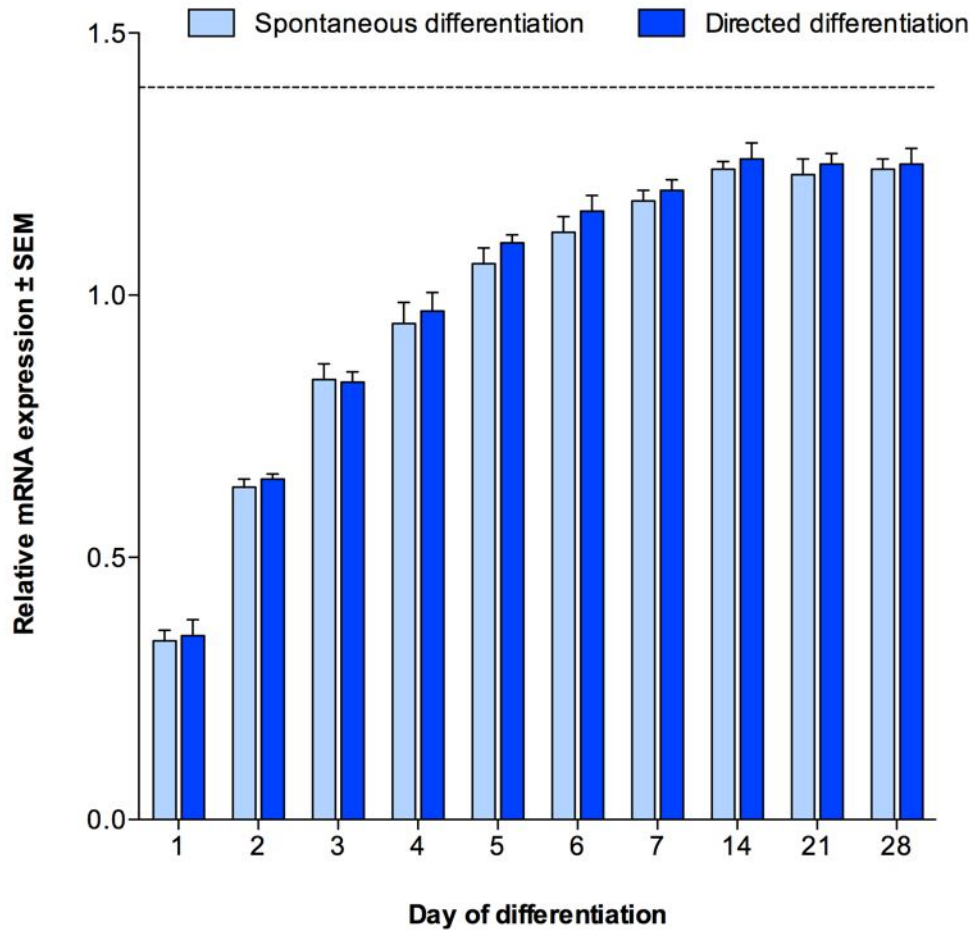


Figure 4.3. Relative expression of VEGFR2 in iPSCs over 28 days of spontaneous and directed differentiation, determined by qPCR analysis of mRNA transcripts. Gene expression normalised to housekeeping gene β -actin, presented as mean expression \pm SEM ($n = 3$) relative to ECs at 60% confluency. Relative expression observed in 60% confluent EPCs indicated by dotted (---) line. No significant difference was observed between differentiation treatments.

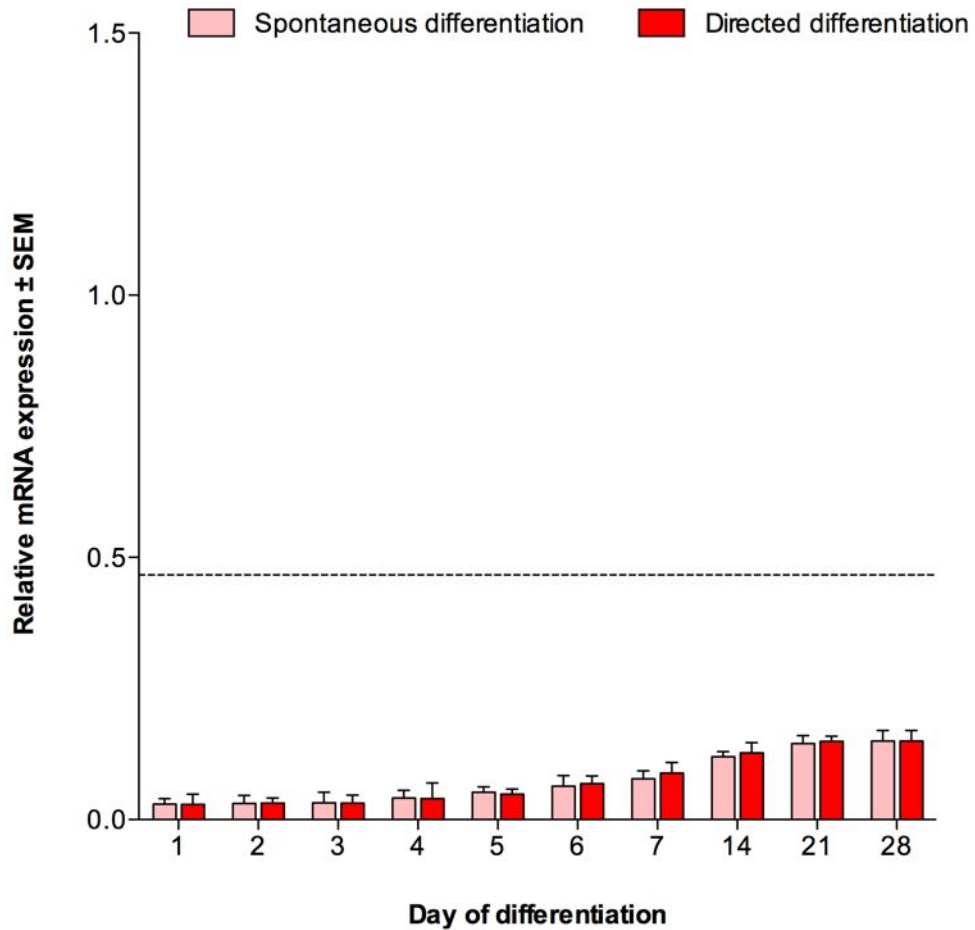


Figure 4.4. Relative expression of VE-cadherin in ESCs over 28 days of spontaneous and directed differentiation, determined by qPCR analysis of mRNA transcripts. Gene expression normalised to housekeeping gene β -actin, presented as mean expression \pm SEM ($n = 3$) relative to ECs at 60% confluency. Relative expression observed in 60% confluent EPCs indicated by dotted (---) line. No significant difference was observed between differentiation treatments.

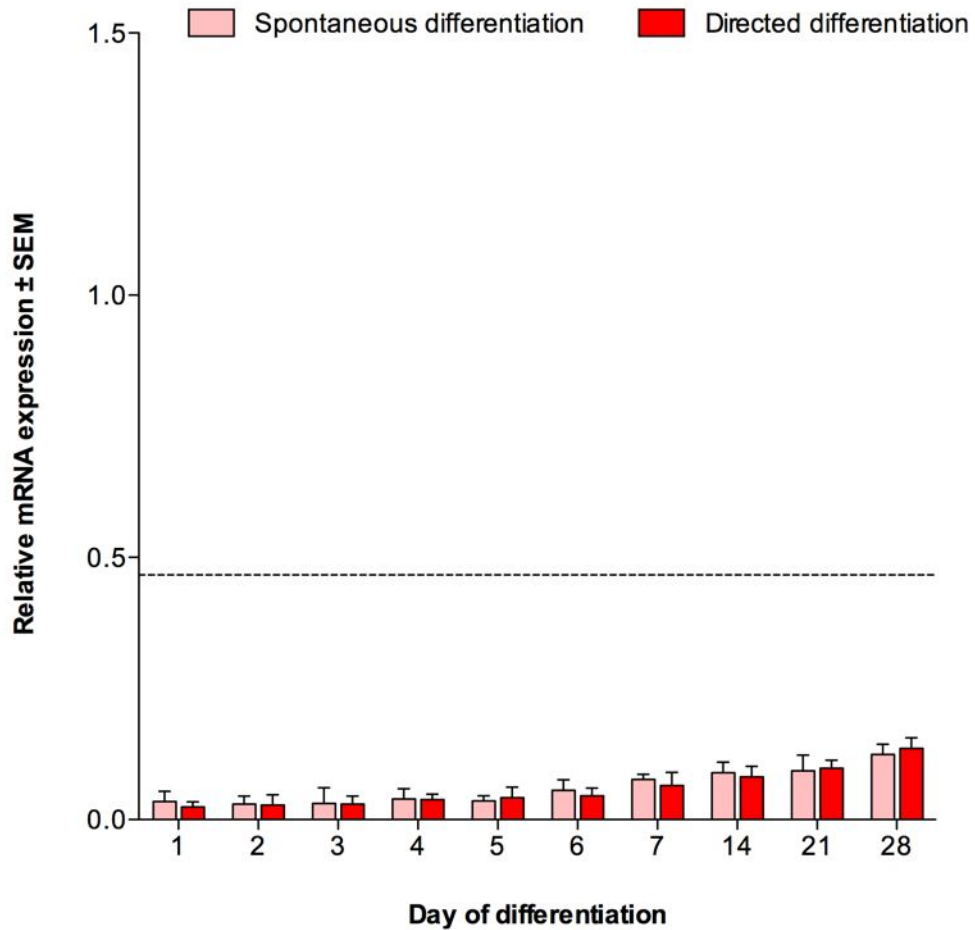


Figure 4.5. Relative expression of VE-cadherin in iPSCs over 28 days of spontaneous and directed differentiation, determined by qPCR analysis of mRNA transcripts. Gene expression normalised to housekeeping gene β -actin, presented as mean expression \pm SEM ($n = 3$) relative to ECs at 60% confluency. Relative expression observed in 60% confluent EPCs indicated by dotted (----) line. No significant difference was observed between differentiation treatments.

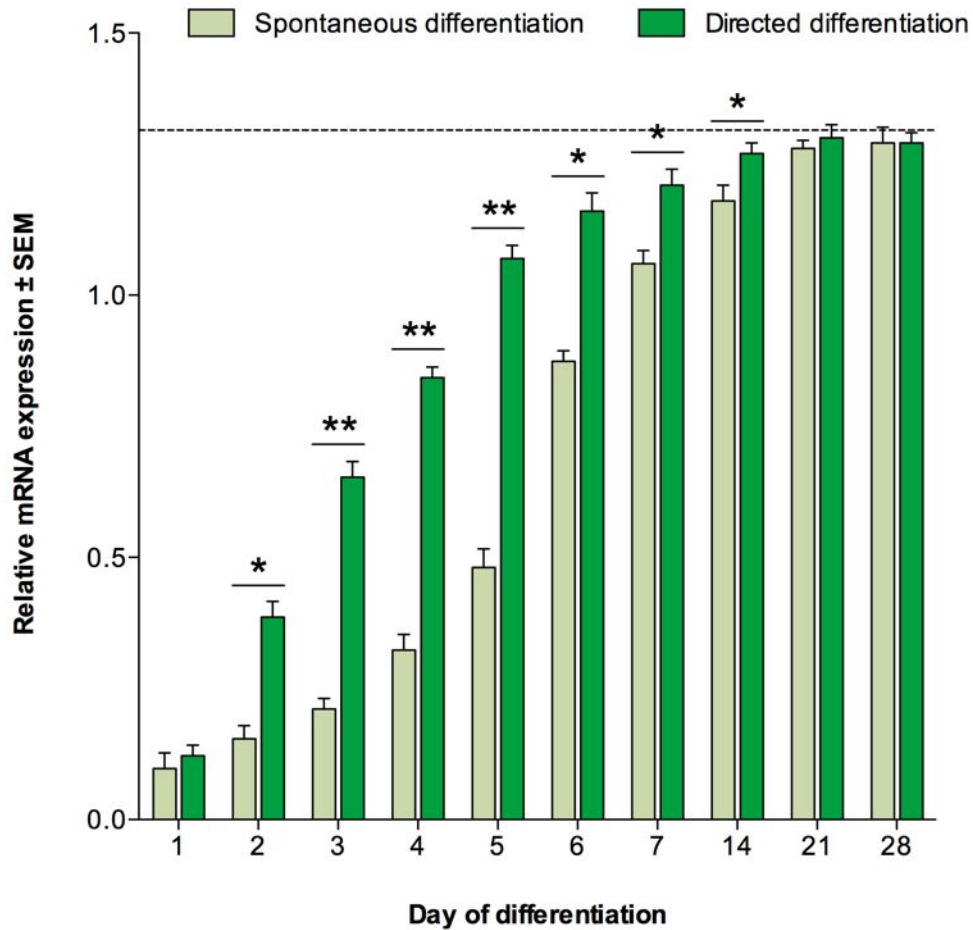


Figure 4.6. Relative expression of CD31 in ESCs over 28 days of spontaneous and directed differentiation, determined by qPCR analysis of mRNA transcripts. Gene expression normalised to housekeeping gene β -actin, presented as mean expression \pm SEM ($n = 3$) relative to ECs at 60% confluency. Relative expression observed in 60% confluent EPCs indicated by dotted (---) line. Significant differences between differentiation treatments are indicated (* $P < 0.05$, ** $P < 0.01$).

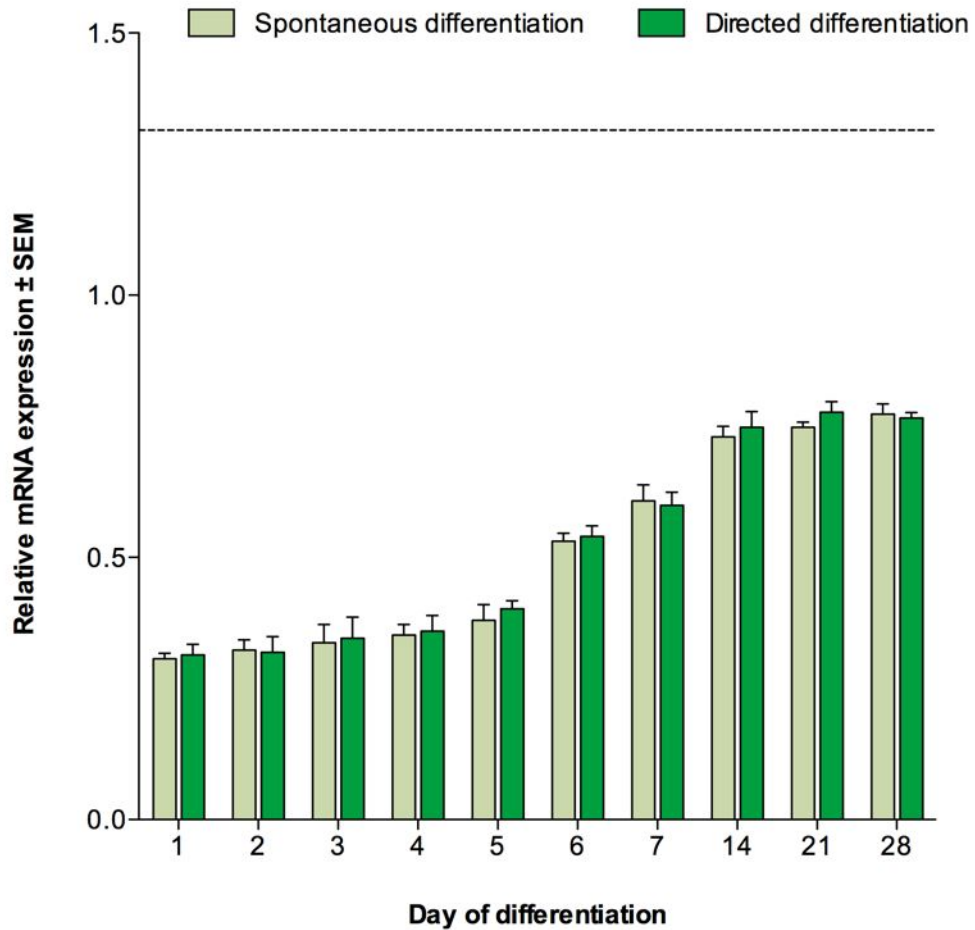


Figure 4.7. Relative expression of CD31 in iPSCs over 28 days of spontaneous and directed differentiation, determined by qPCR analysis of mRNA transcripts. Gene expression normalised to housekeeping gene β -actin, presented as mean expression \pm SEM ($n = 3$) relative to ECs at 60% confluency. Relative expression observed in 60% confluent EPCs indicated by dotted (---) line. No significant difference was observed between differentiation treatments.

4.4.1.2 ICC analysis of protein expression

To further compare the differentiation of ESCs and iPSCs into the endothelial-lineage cells, and to support observations made by qPCR, expression of the proteins VEGFR2 (**Fig. 4.8**), CD133 (**Fig. 4.9**) and CD34 (**Fig. 4.10**) were detected using ICC. Quantification (by mean fluorescence intensity) of the expression of each protein in ESCs (**Table 4.1**) and iPSCs (**Table 4.2**) demonstrated differences in the levels of expression between the two differentiating cell types.

VEGFR2 protein was detected in both spontaneously- and directly-differentiated ESCs on d1 of differentiation, whilst it was not observed in iPSCs differentiated using either method until d7 (**Fig. 4.8**). In both cell types, and using both spontaneous and directed differentiation treatments, the expression of VEGFR2 increased over the period of differentiation. The maximum VEGFR2 expression was detected in directly-differentiated ESCs at d28 (**Table 4.2**). Compared to this, comparable expression was observed in spontaneously-differentiated ESCs (95% of maximum) with less expression in iPSCs (79% and 84% for spontaneous and directed differentiation, respectively; n.s.) (**Table 4.3**). At d7, d14 and d21 the expression of VEGFR2 was significantly lower in iPSCs (using both differentiation treatments) compared to ESCs ($P < 0.05$).

Similarly to VEGFR2, CD133 expression was detected in d1 ESCs differentiated using both spontaneous and directed differentiation but not evident in either spontaneously- and directly-differentiated iPSCs until d7 (**Fig. 4.9**). Likewise, maximum VE-cadherin expression was observed in d28 directly-differentiated ESCs with less expression seen in spontaneously-differentiated d28 ESCs (98%), directly-differentiated iPSCs (88%) and spontaneously-differentiated iPSCs (85%; all n.s.) (**Fig 4.10**).

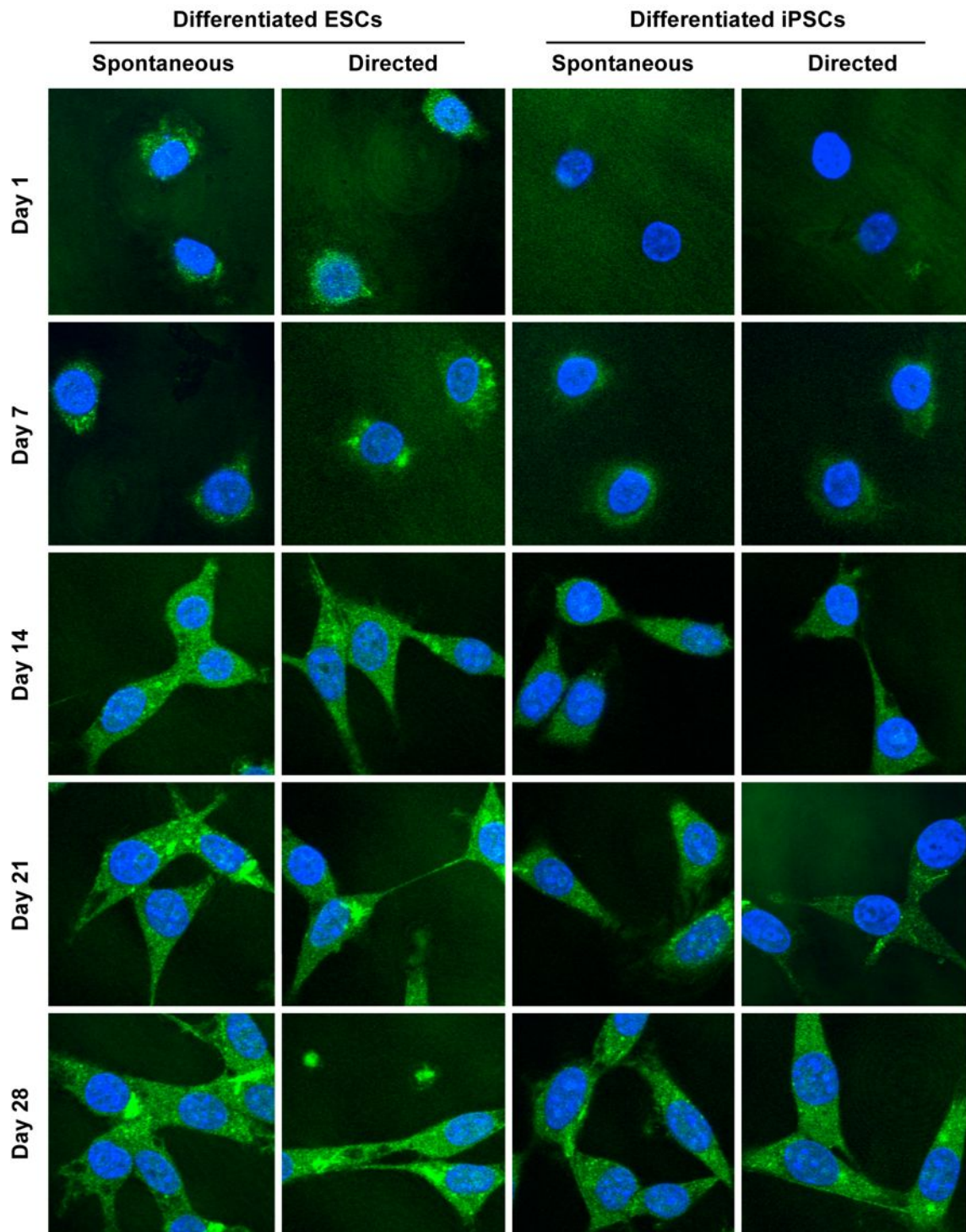


Figure 4.8. Detection of VEGFR2 protein (green) in differentiating ESCs and iPSCs, determined by ICC analysis. Nuclear staining (blue) was performed using DAPI-containing mounting medium.

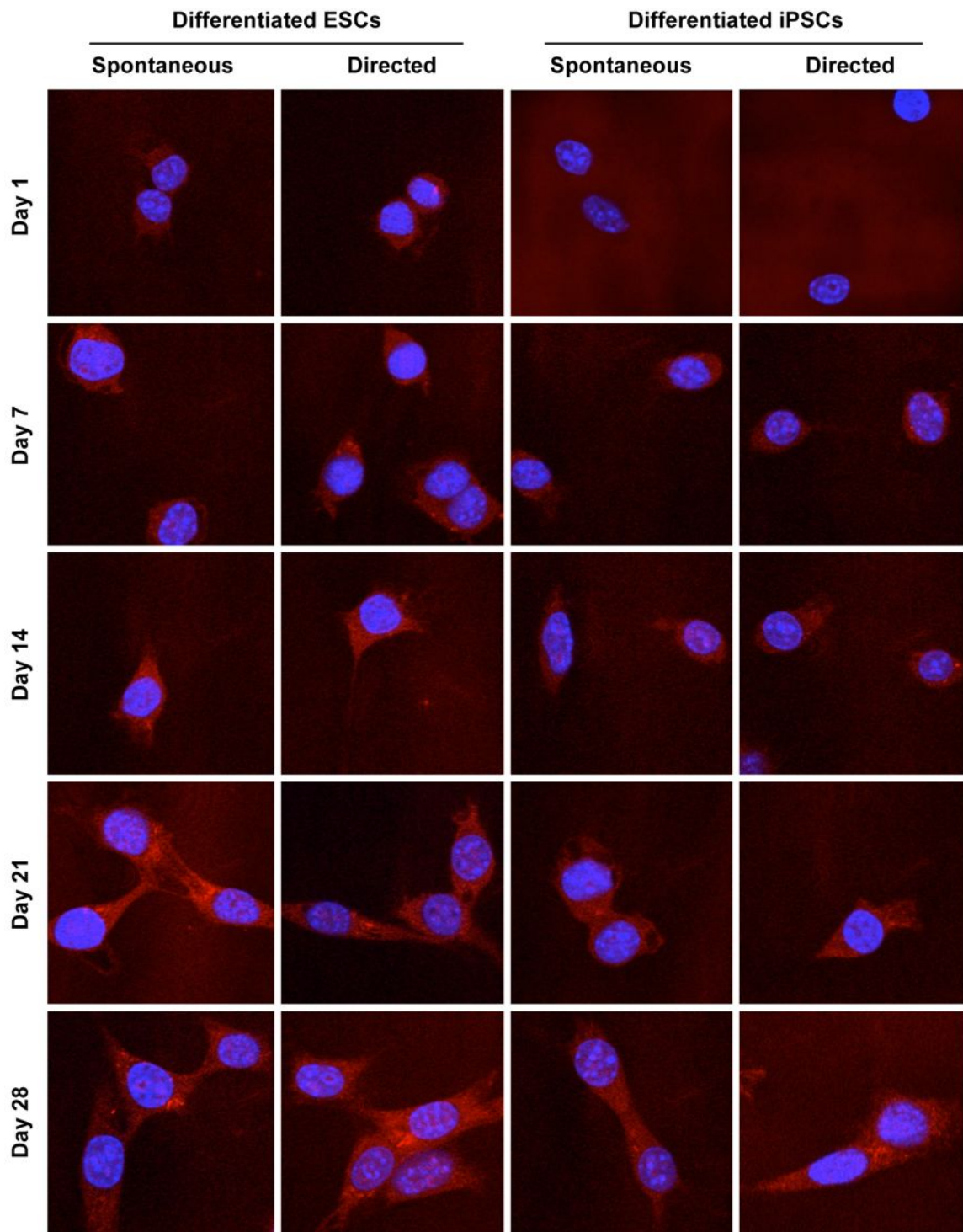


Figure 4.9. Detection of CD133 protein (red) in differentiating ESCs and iPSCs, determined by ICC analysis. Nuclear staining (blue) was performed using DAPI-containing mounting medium.

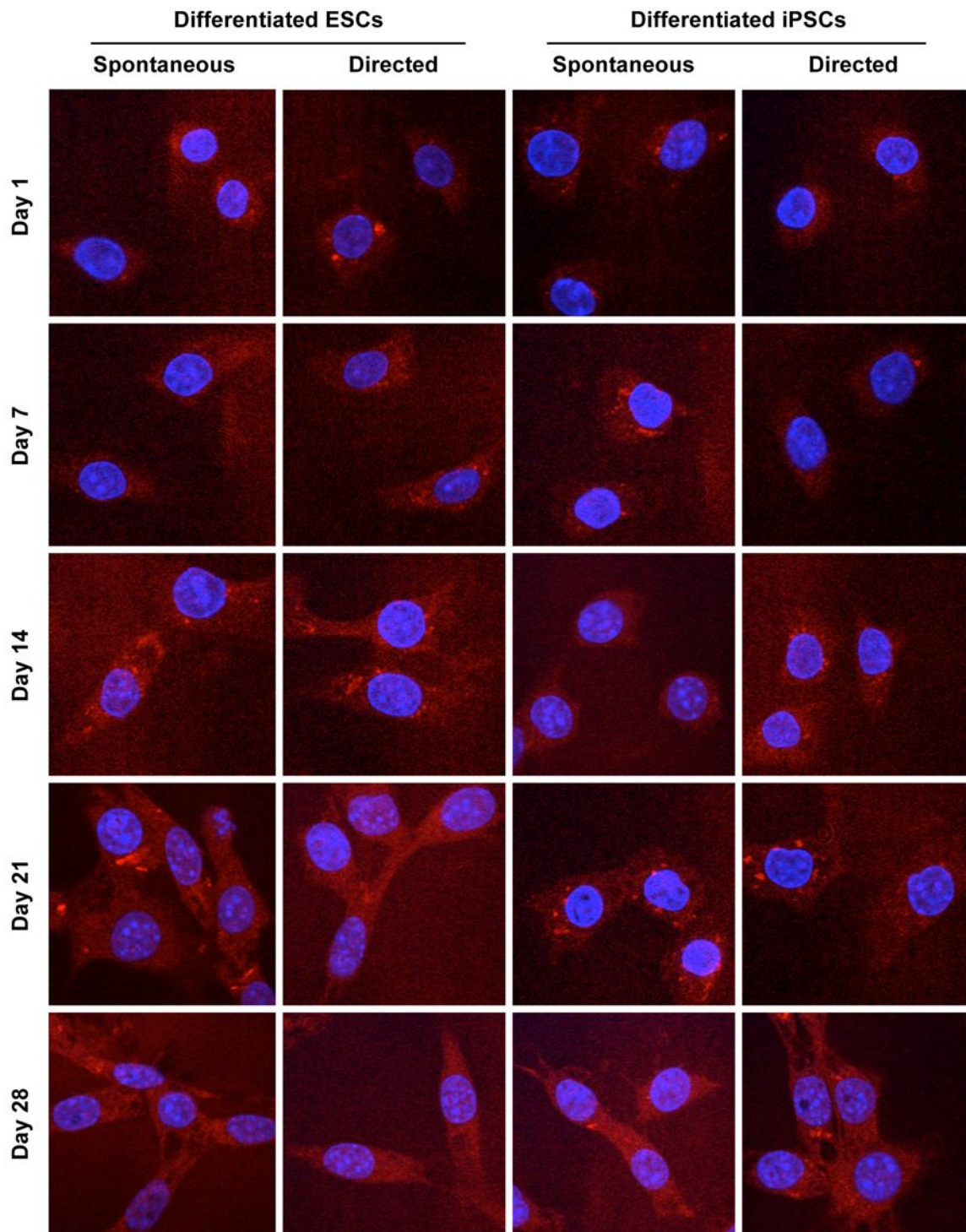


Figure 4.10. Detection of CD34 protein (red) in differentiating ESCs and iPSCs, determined by ICC analysis. Nuclear staining (blue) was performed using DAPI-containing mounting medium.

Treatment	Protein	Day	MFI	% exp	# cells
Spontaneous	VEGFR2	1	0.06 ± 0.04	14	33
		7	0.14 ± 0.06	33	33
		14	0.32 ± 0.10	74	23
		21	0.42 ± 0.09	98	19
		28	0.41 ± 0.12	95	21
	VE-cadherin	1	0.09 ± 0.03	23	25
		7	0.19 ± 0.07	48	29
		14	0.32 ± 0.13	80	34
		21	0.38 ± 0.10	95	31
		28	0.39 ± 0.13	98	30
	CD31	1	0.06 ± 0.03	15	29
		7	0.09 ± 0.04	22	18
		14	0.27 ± 0.11	66	20
		21	0.37 ± 0.09	90	23
		28	0.37 ± 0.10	90	17
Directed	VEGFR2	1	0.11 ± 0.05	26	20
		7	0.28 ± 0.08	65	21
		14	0.35 ± 0.14	81	32
		21	0.40 ± 0.10	93	21
		28	0.43 ± 0.12	100	19
	VE-cadherin	1	0.08 ± 0.05	20	17
		7	0.25 ± 0.09	63	21
		14	0.31 ± 0.10	78	26
		21	0.34 ± 0.14	85	25
		28	0.40 ± 0.12	100	19
	CD31	1	0.04 ± 0.02	10	34
		7	0.13 ± 0.05	32	19
		14	0.20 ± 0.06	49	23
		21	0.41 ± 0.09	100	27
		28	0.38 ± 0.10	93	18

Table 4.2. Quantification of endothelial-specific protein expression in differentiating ESCs.

MFI, mean fluorescence intensity (arbitrary units); % exp, percentage expression relative to maximum observed in both ESCs and iPSCs (Table 4.3); # cells, number of cells analysed.

Treatment	Protein	Day	MFI	% exp	# cells
Spontaneous	VEGFR2	1	0.00 ± 0.00	0	28
		7	0.04 ± 0.02	9	22
		14	0.13 ± 0.05	30	31
		21	0.19 ± 0.07	44	30
		28	0.34 ± 0.09	79	33
	VE-cadherin	1	0.00 ± 0.00	0	23
		7	0.14 ± 0.06	35	17
		14	0.27 ± 0.09	68	29
		21	0.35 ± 0.13	88	28
		28	0.34 ± 0.15	85	30
	CD31	1	0.03 ± 0.02	7	22
		7	0.12 ± 0.06	29	27
		14	0.21 ± 0.09	51	21
		21	0.28 ± 0.07	68	18
		28	0.39 ± 0.11	95	27
Directed	VEGFR2	1	0.00 ± 0.00	0	30
		7	0.03 ± 0.01	7	26
		14	0.15 ± 0.06	35	20
		21	0.12 ± 0.05	28	18
		28	0.36 ± 0.10	84	25
	VE-cadherin	1	0.00 ± 0.00	0	31
		7	0.17 ± 0.08	43	28
		14	0.26 ± 0.12	65	19
		21	0.36 ± 0.10	90	23
		28	0.35 ± 0.12	88	18
	CD31	1	0.04 ± 0.02	10	30
		7	0.06 ± 0.03	15	28
		14	0.25 ± 0.08	61	23
		21	0.21 ± 0.07	51	19
		28	0.38 ± 0.08	93	24

Table 4.3. Quantification of endothelial-specific protein expression in differentiating iPSCs

MFI, mean fluorescence intensity (arbitrary units); % exp, percentage expression relative to maximum observed in both ESCs (Table 4.2) and iPSCs; # cells, number of cells analysed.

Comparable expression of CD34 protein was detected in both ESCs and iPSCs (using both treatments) from d1 of differentiation (n.s.). Unlike VEGFR2 and VE-cadherin, the maximum expression of CD34 was observed in directly-differentiated ESCs at d21, although expression was equivalent to that seen in both cell types using both differentiation treatments at d28 (n.s.). Throughout the period of differentiation, no differences were observed in the expression of VEGFR2, VE-cadherin or CD31 between differentiation treatments in either cell type (Tables 4.2 & 4.3).

In addition to the increase in expression of all three markers in both ESCs and iPSCs throughout the differentiation period, the morphology of both cell types was observed to develop from a rounded shape (characteristic of stem cells) into a more elongated, spindle-shaped morphology (as demonstrated by MFLM-4 EPCs) as differentiation progressed.

4.4.2 Assessment of angiogenic potential of ESCs and iPSCs

ESCs and iPSCs from d7 of directed differentiation were selected for angiogenic potential assessment. Cells were cultured on ECMatrix gel to assess their angiogenic potential in comparison to EPCs and ECs, by quantification of tubule formation by node counting and branch length measurement.

4.4.2.1 Quantification of *in vitro* tubule formation using node counting

The pattern of nodes formed by d7 ESCs was found to be similar to that of both EPCs and ECs (Fig. 4.11A): the number of N1 nodes was maximal at 2 h and decreased throughout the assay; the number of N2, N3 and N4 nodes increased to their maximum towards the mid-point of the assay; and N5+ nodes were only evident at 8 h. Only N1 and N2 nodes were observed throughout the assay of d7 iPSCs (Fig. 4.11B). The number of N1 nodes was observed to be

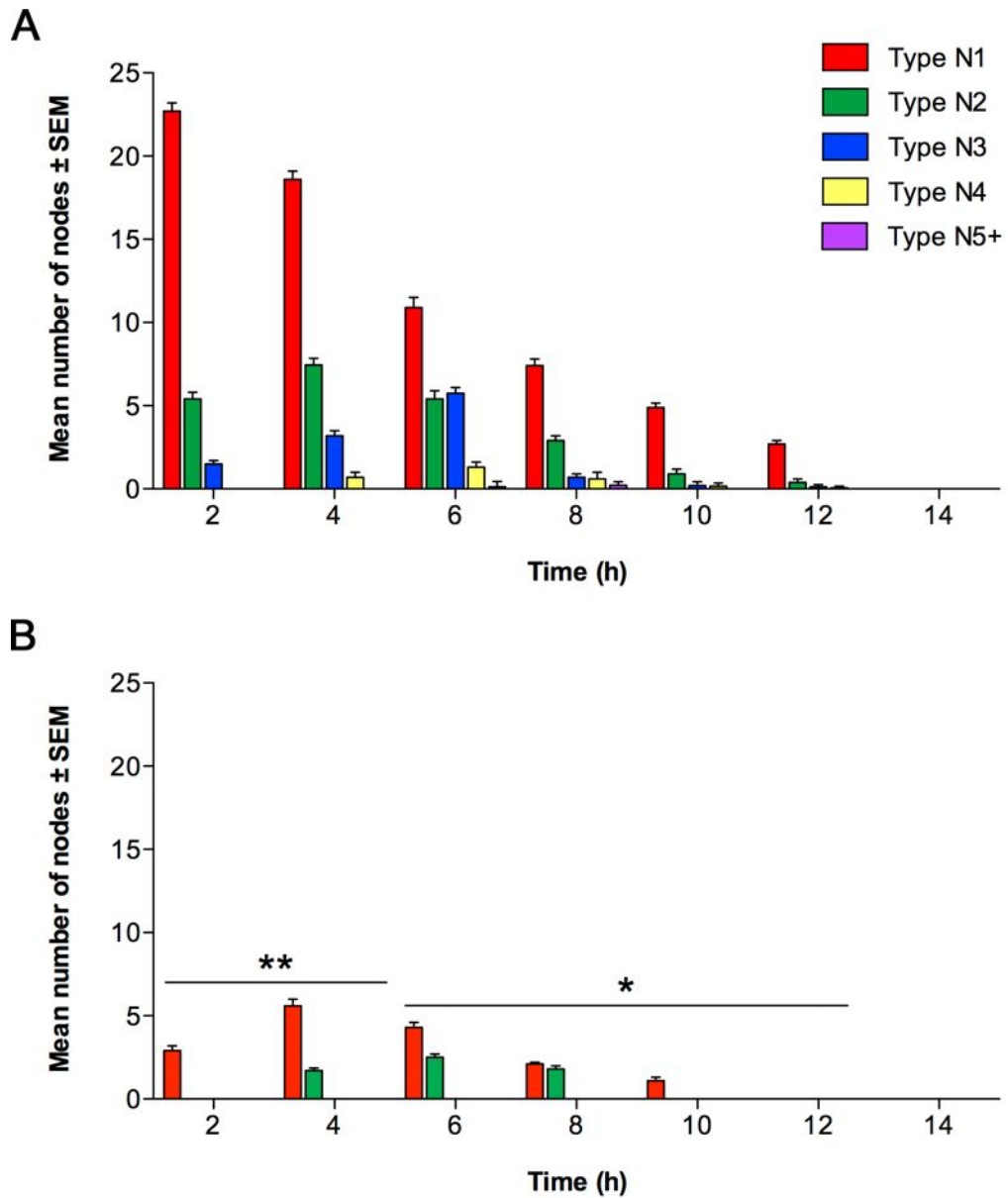


Figure 4.11. Assessment of angiogenic activity of (A) d7 ESCs and (B) d7 iPSCs cultured on ECMatrix gel for 14 h, determined by node counting. Data presented as mean number of node type \pm SEM ($n = 3$) from five random fields of view at each time-point. Significant differences between cell types at each time-point are indicated (* $P < 0.05$, ** $P < 0.01$).

greatest at 4 h and N2 nodes were maximal at 6 h. No N3, N4 or N5+ nodes were observed at any time. The patterns of nodes were significantly different between ESCs and iPSCs.

4.4.2.2 Quantification of *in vitro* tubule formation using branch length measurement

The pattern of tubule growth by d7 ESCs indicated by branch length measurement, as with quantification by node counting, was similar to EPCs (**Fig. 4.12**). Mean branch length increased from 0 h to 6 h, with maximal length observed at 6 h. Mean branch length measurements of d7 iPSCs were significantly lower than ESCs, however maximal length was also measured at 6 h. No branches were evident at 14 h for either cell line.

4.4.2.3 qPCR analysis of endothelial-specific mRNA expression during *in vitro* tubule formation

Endothelial-specific gene expression in d7 ESCs and iPSCs during *in vitro* tubule formation was analysed using qPCR. The number of *VEGFR2* mRNA transcripts detected in ESCs increased by 72% between 0 h and 2 h, and by a further 17% between 2 h and 4 h, at which time *VEGFR2* expression was maximal (**Fig. 4.13**). The number of transcripts then decreased progressively (by, on average, 22% at each time-point) between 4 h and 14 h. The relative expression of *VEGFR2* in d7 iPSCs was observed to increase by just under twofold between 0 h and 6 h (its maximum) then decrease by 72% between 6 h and 14 h.

Expression of *VE-cadherin* in differentiated ESCs was observed to be maximal at 4 h, having increased by 17% from 0 h (**Fig. 4.14**). The number of transcripts was not significantly different between 0 h and 2 h, or between 4 h and 6 h. The expression of *VE-cadherin* in ESCs then decreased by 60% between 6 h and 14 h. A greater than threefold increase was seen in *VE-cadherin* expression in iPSCs between 0 h and 6 h, followed by a decrease of 62% between 6 h and 14 h.

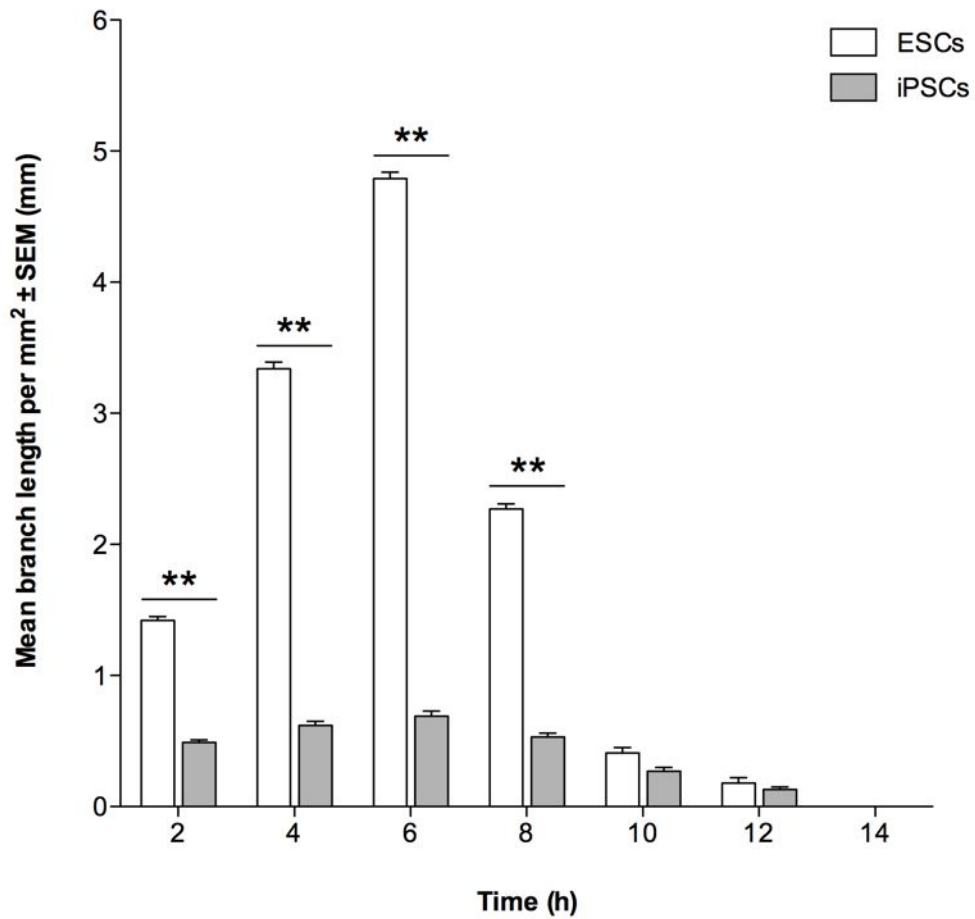


Figure 4.12. Assessment of angiogenic activity of ESCs and iPSCs cultured on ECMatrix gel for 14 h, determined by branch length measurement. Data presented as mean branch length per mm² of assay ± SEM (n = 3) from five random fields of view at each time-point. Significant differences between cell types are indicated (**P < 0.01).

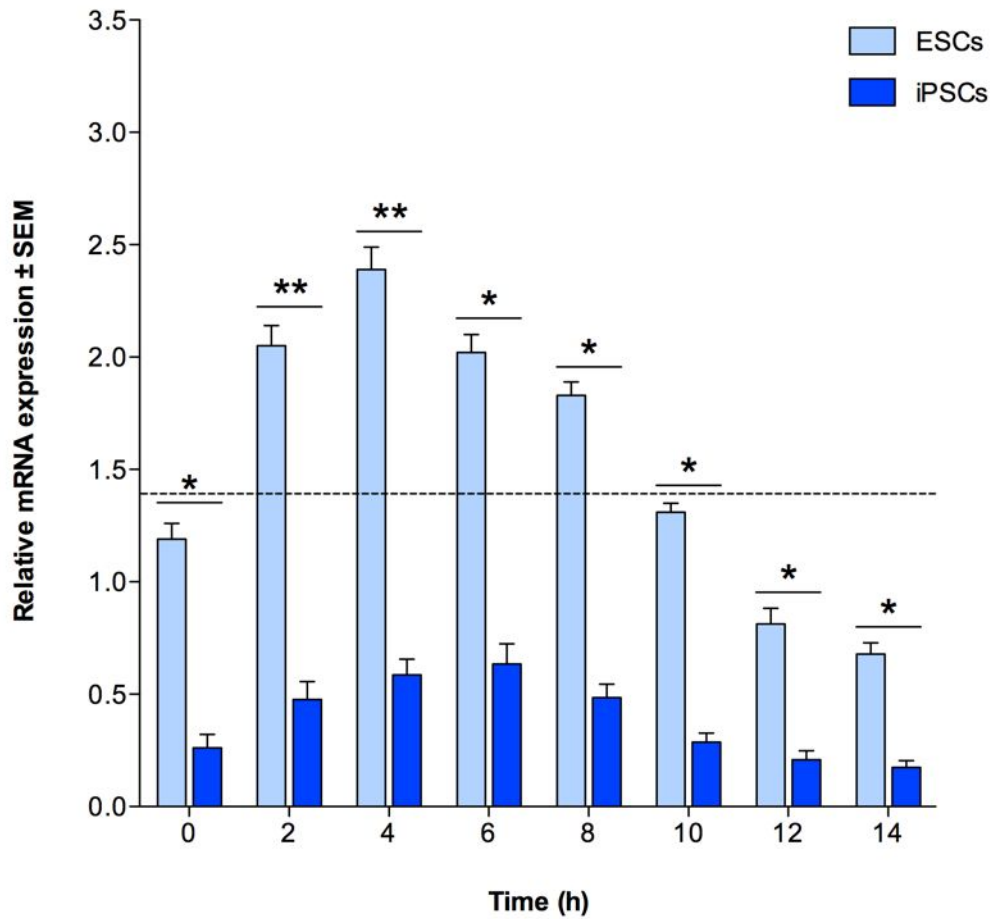


Figure 4.13. Relative expression of VEGFR2 in d7 ESCs and iPSCs cultured on ECMatrix gel for 14 h, determined by qPCR analysis. Gene expression normalised to housekeeping gene β -actin, presented as mean expression \pm SEM ($n = 3$) relative to ECs at 0 h. Relative expression observed in EPCs indicated by dotted (----) line. Significant differences between cell types are indicated (* $P < 0.05$, ** $P < 0.01$).

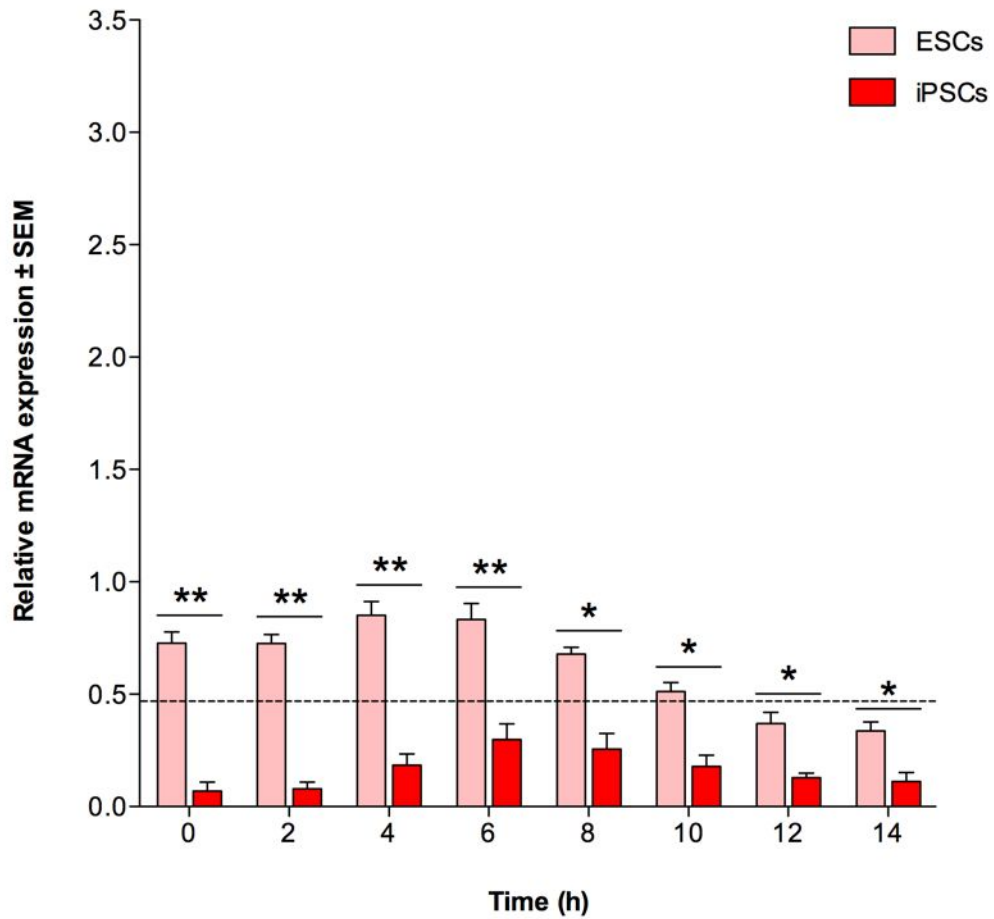


Figure 4.14. Relative expression of VE-cadherin in d7 ESCs and iPSCs cultured on ECMatrix gel for 14 h, determined by qPCR analysis. Gene expression normalised to housekeeping gene β -actin, presented as mean expression \pm SEM ($n = 3$) relative to ECs at 0 h. Relative expression observed in EPCs indicated by dotted (----) line. Significant differences between cell types are indicated (* $P < 0.05$, ** $P < 0.01$).

The number of *CD31* transcripts detected in differentiating ESCs was significantly different between 0 h and 6 h (**Fig. 4.15**). *CD31* expression decreased between 8 h and 12 h (by, on average, 26% at each time-point) and by a further 69% between 12 h and 14 h. The expression of *CD31* transcripts in iPSCs was observed to be maximal at 4 h, increasing by 75% from 0 h. The number of transcripts then decreased progressively, by an average of 25% at each time-point until 14 h.

The changes in expression of all three endothelial-specific markers in iPSCs during the *in vitro* tubule formation assay were shown to be much smaller than those observed in ESCs. In addition the maximum numbers of mRNA transcripts of each gene in iPSCs were determined to be far less than the maximum numbers detected in ESCs, and by similar amounts: *VEGFR2* expression in assayed iPSCs was observed to be maximal at 6 h and was over three times less than in ESCs; the expression of *VE-cadherin* was at its highest at 6 h and was just under three times less than in ESCs; and the greatest number of *CD31* transcripts were detected at 4 h, just over three times less than the number of transcripts observed in ESCs.

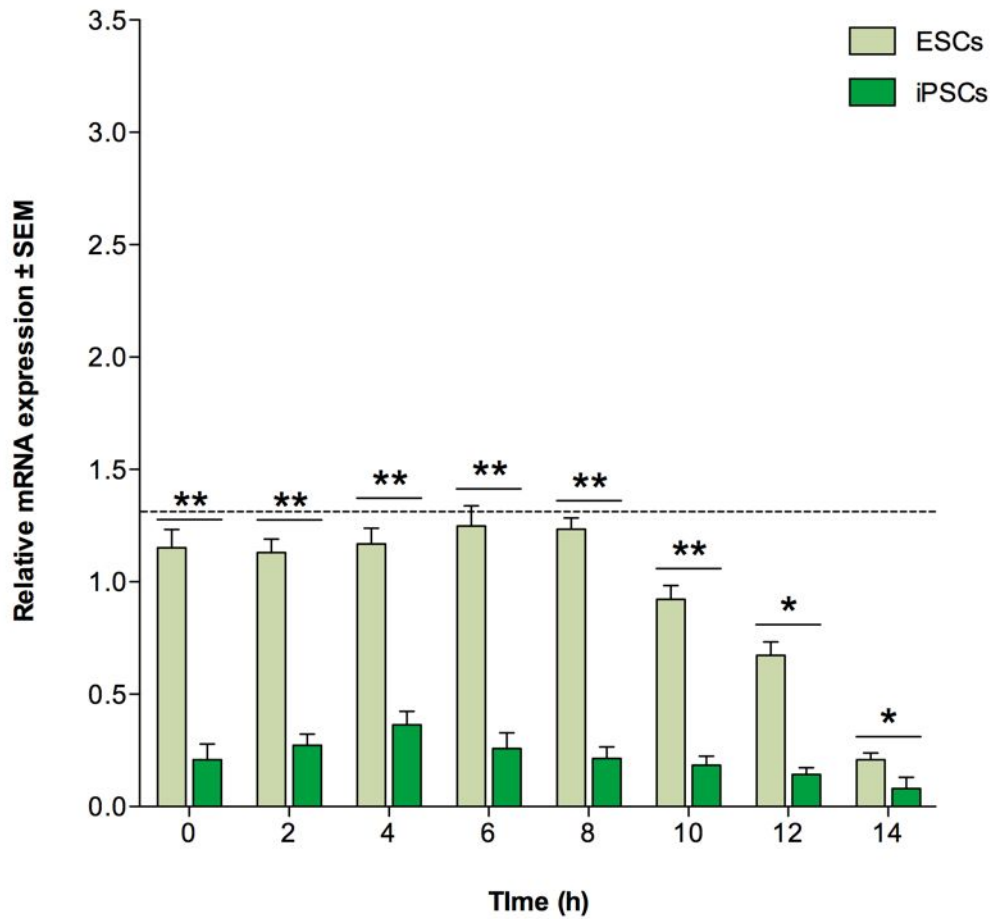


Figure 4.15. Relative expression of CD31 in d7 ESCs and iPSCs cultured on ECMatrix gel for 14 h, determined by qPCR analysis. Gene expression normalised to housekeeping gene β -actin, presented as mean expression \pm SEM ($n = 3$) relative to ECs at 0 h. Relative expression observed in EPCs indicated by dotted (----) line. Significant differences between cell types are indicated (* $P < 0.05$, ** $P < 0.01$).

4.5 Discussion

Hanging droplet differentiation was used to derive endothelial lineage cells from D3 ESCs and QS/R27 iPSCs. Such cells have been hypothesised to be a potential source of cells for therapeutic angiogenic transplantation and an alternative to using endogenous EPCs which can be difficult to expand sufficiently *in vitro* whilst maintaining their precursor phenotype. Both spontaneous and directed methods of differentiation were used, and the two methods compared to assess whether the differentiation of pluripotent cells could be positively influenced by the presence of EC-secreted cytokines and growth factors. The mRNA expression of the endothelial markers *VEGFR2*, *VE-cadherin* and *CD31* in differentiating ESCs and iPSCs was then analysed by qPCR, and the protein expression of VEGFR2, CD133 and CD34 assessed by ICC.

Very low mRNA levels of the three endothelial markers were detected in undifferentiated (d0) ESCs and iPSCs. However, even well-maintained stem cells cultured in an undifferentiated state using mitotically-inactivated MEF feeder layers and LIF supplementation can exhibit a small amount of spontaneous differentiation, roughly 5-10% of the cell population, both in response to variations in culture conditions and as part of the natural maintenance of the colony (Richards & Bongso, 2006). For this reason, low levels of endothelial-specific expression observed in ESCs and iPSCs at d0 were considered negligible and not to represent majority differentiation towards the endothelial lineage. In both populations significant expression of all three markers was observed at d1 using both differentiation treatments, representing initiation of the development towards an endothelial phenotype.

Both *VEGFR2* and *CD31* were previously shown to be expressed at a higher level in MFLM-4 EPCs compared to MCEC-1 ECs (SEE 3.4.1.1). A greater abundance of mRNA transcripts of

these two genes demonstrates a more naïve, precursor-like phenotype (Allen *et al.*, 2008). By the end of the differentiation period, expression of *VEGFR2* and *CD31* in ESCs had increased to a level equivalent to that seen in natural EPCs suggesting that, at least as defined by those two markers, an endothelial precursor phenotype had developed (**Fig. 4.16**). The effect of ECCM on the expression of *VEGFR2* and *CD31* throughout ESC differentiation was significant: patterns of expression were forward-shifted in directed differentiation, with ESCs attaining a precursor-like level of expression more rapidly in the presence of conditioned medium, compared to spontaneous differentiation using basic culture medium alone. Furthermore, the pattern-shifting effect of ECCM was seen to increase as differentiation continued. In the early stages of differentiation there was an apparent forward-shift of 2 days as a result of ECCM treatment, with the occurrence of EC-comparable expression shifting from d4 to d2 (for *VEGFR2*) and from d7 to d5 (for *CD31*). As differentiation progressed, and ESCs expressed higher levels of transcripts similar to EPCs, ECCM produced a forward-shift of 7 days, from d14 to d7 (for *VEGFR2* expression) and from d28 to d21 (for *CD31* expression).

Unlike *VEGFR2* and *CD31*, the number of *VE-cadherin* transcripts was determined to be greater in ECs than EPCs; *VE-cadherin* expression is indicative of later-stage development towards a mature EC-like state (Bagley *et al.*, 2008). During differentiation, although *VE-cadherin* expression in ESCs was observed to increase over the 28 day period, neither spontaneously- or directly-differentiated ESCs reached a level of expression similar to that seen in either EPCs or ECs. Additionally, there was no significant effect on *VE-cadherin* expression by the treatment of ESCs with ECCM. These findings may be explained by the fact that, unlike *VEGFR2* and *CD31* which are associated with early endothelial development, *VE-cadherin* expression has been shown to be much more dynamic in (and indicative of) the later stages of maturation. Hence, significant changes in the number of

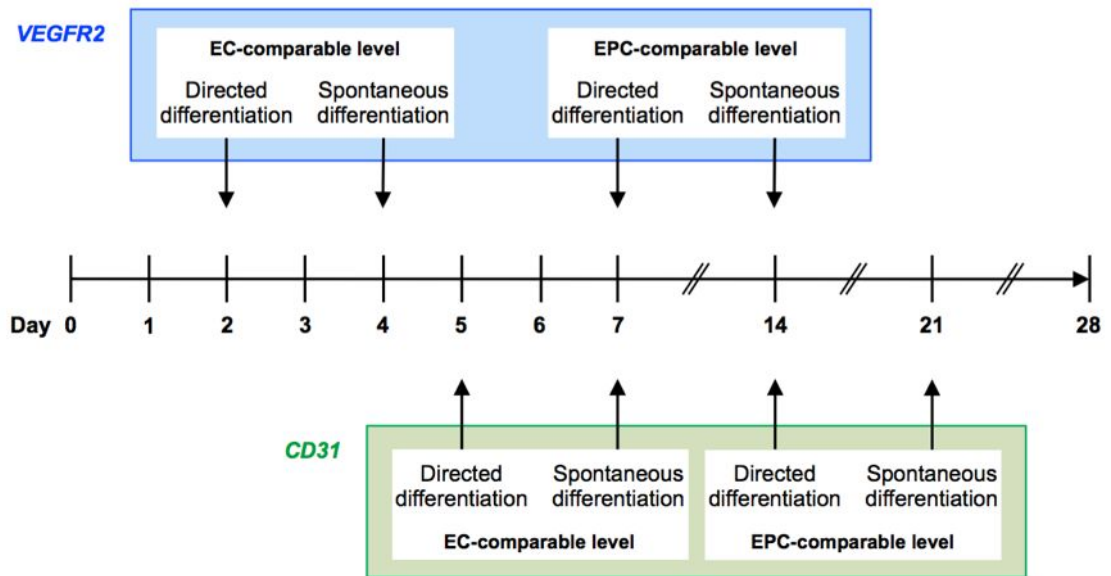


Figure 4.16. Timeline of VEGFR2 and CD31 expression in spontaneously- and directly-differentiated ESCs. Time-points indicated represent day at which expression of each protein was first observed to reach levels equivalent to either MFLM-4 EPCs or MCEC-1 ECs.

VE-cadherin transcripts may have become apparent if culture of the differentiating ESCs had been continued beyond 28 days.

Regardless of the day at which expression first reached EPC- or EC-equivalent levels, the number of endothelial-specific mRNA transcripts detected in both ESC differentiation treatments were determined to be similar by d28. Whilst the use of ECCM has been widely demonstrated to improve the rate of endothelial differentiation, resulting in earlier onset of endothelial-specific expression during the course of differentiation, the final expression patterns of ECCM-differentiated cells are comparable to naturally- and spontaneously-differentiated cells (Zhao, H-P *et al.*, 2003; Kubo *et al.*, 2005). It appears that directed differentiation has the effect of significantly increasing the rate of development from a pluripotent stem cell to a precursor-like cell of the endothelial lineage (as evident by earlier high-level expression of *VEGFR2* and *CD31*) but does not affect the final phenotype of the cell (based on the final number of *VEGFR2*, *VE-cadherin* and *CD31* mRNA transcripts present in each treatment at d28). In essence, it would seem that ECCM treatment does not make the resulting cells 'more' endothelial than their naturally-existing counterparts but rather it simply increases maturation from their initial pluripotent state.

Basic growth medium used for *in vitro* cell culture is intended to replicate the supply of nutrients and growth factors available in the *in vivo* compartment. ECCM further modifies this nutrient supply by adding factors specific to the endothelial environment which, it would appear, has a significant effect on endothelial development *in vitro*. Paracrine release from the endothelium at sites of angiogenesis could be thought of as the *in vivo* parallel of ECCM treatment; when naïve circulating BM-derived cells (which may be or potentially develop into EPCs) are localised at these sites, paracrine secretions from the activated endothelium

may have a similar effect of endothelial development, although whether the factors contained within the ECCM *in vitro* parallel those released at the site of EPC recruitment *in vivo* remains to be clarified. However, these releasates may signal a change from the bone marrow environment to the pro-endothelial environment at sites of neovascularisation, stimulating EPC maturation.

Through ICC analysis it was determined that, in addition to endothelial-specific gene expression, differentiated ESCs exhibited (to different degrees) protein expression determined to be present in natural EPCs and ECs. VEGFR2, CD133 and CD34 were detected to be present from the first days of differentiation and continued to be expressed throughout the 28 day period of observation. In contrast, the development patterns of the endothelial-specific proteins did not appear to be affected by ECCM in the same way as gene expression. However, the analysis of the MFI from fluorescent images may not be accurate enough to distinguish the changes in protein expression brought about by ECCM treatment. Techniques such as flow cytometry or Western blotting may be required to better elucidate the effect of ECCM on endothelial-specific protein. In addition, only surface proteins were quantified using the MFI method whereas using Western blotting the total (surface and intracellular fractions) of each each protein could be detected and quantified.

Regardless of its effect on protein expression, ECCM was observed to significantly alter levels of mRNA transcripts during differentiation. The action of ECCM is known to be related to the particular combination of paracrine factors released into the culture medium as it is conditioned, such as VEGF-C (Kono *et al.*, 2006). In addition, it has been demonstrated that the effect of ECCM can be augmented by the inclusion of additional factors, such as SCF and EPO, and by doing so the efficiency of directed differentiation can be further modified to

produce a larger population of homogeneous progenitor-like cells (Zhao, H-P *et al.*, 2003). However, the precise combination of factors necessary for efficient directed differentiation into particular cell types is not yet clear and certain potentially important factors, such as paracrine secretions and environmental influences arising from *in vitro* culture, remain unknown (Kado *et al.*, 2008). For this reason, aside from the understanding that soluble factors are involved and the demonstration of their effect in this investigation, the exact mechanism by which ECCM affects cellular expression in differentiating stem cells is not yet fully understood.

It has been broadly demonstrated that pluripotency can be induced in a lineage-committed somatic cell by retroviral transfection of the stem-associated genes *Oct4*, *Sox2* and *Klf4*. Insertion of these genes is intended to induce their expression within the cell with the aim of altering the cell's behaviour to regain differentiation potential. Indeed, iPSCs derived from reprogrammed somatic cells have been shown to give rise to cells of all three germ layers (Lee, G *et al.*, 2009). Evidence for the similarities between ESCs and iPSCs (i.e. in pluripotency-related expression, patterns of DNA methylation and the formation of teratomas and viable chimaeras) is abundant, and studies have previously shown successful production of ECs from iPS sources by directed differentiation (Narazaki *et al.*, 2008; Schenke-Layland *et al.*, 2008). However, the full extent of homology between induced and naturally pluripotent stem cells remains to be understood. Indeed, there is evidence to support the view that iPSCs and ESCs are not as closely related as some data suggests. For instance, whilst they appear outwardly indistinguishable from ESCs, it has been shown that iPSCs retain a unique gene expression signature even after extended culture and differentiation, which makes them quite different from cells derived from naturally pluripotent sources (Chin *et al.*, 2009). The functional implications of this difference, particularly in terms of a therapeutic angiogenic

application, is unclear because, to date, there are limited data describing the functional differences in either undifferentiated or differentiated iPSCs compared to ESCs. Whilst many groups have shown that iPSCs are identically pluripotent to ESCs, by EB and teratoma formation (Lowry *et al.*, 2008; Park *et al.*, 2008), some evidence suggests differences in their relative abilities to undergo directed differentiation (Choi *et al.*, 2009; Karumbayaram *et al.*, 2009).

Compared to ESCs, clear differences were observed in the expression patterns of the three endothelial-specific markers in differentiating iPSCs. For example, unlike differentiating ESCs, no significant differences in gene expression were seen as a result of ECCM treatment. The expression of *VEGFR2* in both spontaneously- and directly-differentiated iPSCs was determined to be at an EC-equivalent level by d5, between one and three days later than in ESCs, depending on ESC differentiation treatment. Furthermore, whilst the number of *VEGFR2* transcripts in iPSCs (both treatments) continued to increase after d5, expression appeared to plateau by d14 and did not reach a level similar to that in EPCs before the end of the differentiation period. The increase in iPSC expression of *VE-cadherin* and *CD31* was similarly gradual. However, unlike *VEGFR2*, expression of *VE-cadherin* and *CD31* was not observed at a level comparable to either EPCs or ECs before d28. The observations made of differentiating iPSCs not only suggest that treatment with ECCM has no significant effect of the development of endothelial-specific expression (owing to similar levels of transcripts in the two differentiation treatments) but also that iPSCs are less-readily differentiated into endothelial-like cells. This is indicated by their delayed and reduced endothelial-specific expression compared to the cells derived from ESCs. This seemingly contradicts data from previously published published studies that suggest that ESCs and iPSCs share identical

pluripotent properties and the capacity for endothelial lineage differentiation (Niwa *et al.*, 2009).

If, in this study, ESCs and iPSCs were identical in their potential for differentiation, one might expect a similar response to ECCM treatment in both cell lines. However, there are recent data which correlate with our findings of iPSC potential, showing that cells derived from human iPSCs, such as haemangioblasts, show limited growth rate, differentiation capacity, early senescence and a predisposition to apoptosis (Feng *et al.*, 2010). Further adding to the confusion, whilst iPSC lines have been produced from a range of somatic cell types, for example through the formation of EBs as used here (Lengerke *et al.*, 2009; Ye *et al.*, 2009) or by co-culture with stromal cells (Choi *et al.*, 2009), the proliferative potential and apoptotic behaviour of these cells is often unclear or unreported. There is evidence to indicate the involvement of p53/p21 apoptotic pathways in the reprogramming process (Hong *et al.*, 2009), perhaps explaining the slow growth kinetics and high level of senescence seen in iPSCs and iPSC-derived lines. Furthermore, although the viral insertion of transgene-encoded transcription factors intended for reprogramming are reported to be silenced in the final reprogrammed cell population, it is possible that reactivation could occur under certain differentiation conditions, significantly affecting the outcome of differentiation (and, with reference to this study, the subsequent effect of ECCM on EPC derivation).

To further investigate the efficiency of stem cell differentiation into endothelial-like cells, the angiogenic potential of differentiated ESCs and iPSCs was assessed using an *in vitro* tubule formation assay and compared to that of natural EPCs and ECs. Cells from d7 of directed differentiation were selected for culture on ECMatrix gel because endothelial-specific expression at this stage of differentiation was determined to be at least equivalent to the

minimum expression seen in natural endothelial cells. It was determined that d7 ESCs and iPSCs, although not identical to characterised EPCs or ECs, best represented a precursor-like endothelial phenotype; the same day of differentiation was used for both ESCs and iPSCs to enable comparisons between the angiogenic potential of the two cell types.

When cultured on ECMatrix gel, d7 ESCs demonstrated tubule growth analogous to that of EPCs and ECs, indicating a similar response to the angiogenic stimulus of the gel. In contrast, d7 iPSCs did not demonstrate an angiogenic potential equivalent to either EPCs or ECs, producing a pattern of tubule formation that was significantly different to ESCs. Some N1 and N2 nodes were observed during the assay of iPSCs, although the average number of nodes at each time-point was significantly less than the large numbers of tubule end-points and intersections seen in the previous EPC, EC or d7 ESC assays. No N3, N4 or N5+ nodes, which were relatively abundant in all other assays, were identified at any point during the assay period. Branch length measurements also revealed a difference in the angiogenic potential of ESCs and iPSCs. Although both assays produced a similar pattern of measurements (with maximum branch length recorded at 6 h) the mean lengths measured at each time-point were significantly different: iPSC branch lengths were very much smaller than those produced by ESCs which, as with node counts, were similar to EPC and ECs.

In terms of deriving angiogenic endothelial-like cells from iPSCs, it is interesting that differentiating ESCs and iPSCs demonstrate significantly different tubule formation growth patterns in our study. In addition to the phenotypic characterisation of endothelial cells produced from reprogrammed somatic cells (Choi *et al.*, 2009), the formation of tubule structures (as seen in this study with EPCs, ECs and ESCs) has been demonstrated by iPSC-derived MSCs cultured on Matrigel-coated plates (Lian *et al.*, 2010). As discussed previously,

this discrepancy may be due to reprogramming inefficiencies in the iPSCs or other as yet unknown factors involved in the spontaneously- and directly-differentiated generation of progenitor-like cells from iPSCs.

qPCR analysis identified the expression of *VEGFR2*, *VE-cadherin* and *CD31* in tubule-forming ESCs to be essentially identical to EPCs over the course of the assay. In contrast, d7 iPSCs showed much lower levels of all three markers than were observed in assayed EPCs. These findings indeed suggest that cells of an equivalent endothelial phenotype and angiogenic potential to natural EPCs can be derived from pluripotent ESCs, but that iPSCs treated in the same manner do not produce comparable cells. EPCs have been widely demonstrated in the available literature to be capable of exerting a beneficial effect when used therapeutically (Liew *et al.*, 2006). Whilst iPSCs appear to have limited potential, ESCs may be a viable source of cells for such therapy if, as the results here suggest, rapidly-expandable ESCs can be used to derive highly-angiogenic EPC substitutes.

CHAPTER 5:

IN VITRO TRANSPLANTATION OF ENDOTHELIAL PROGENITOR CELLS

5.1 Introduction

Having demonstrated the highly angiogenic nature of EPCs, the notion of exploiting them, or equivalent cells derived from ESCs, for angiogenic therapy becomes more realistic. With the proliferative capacity of their embryonic counterparts, which are responsible for forming the basis of the entire mammalian vasculature, and their propensity to form tubule structures *in vitro*, it is conceivable that adult EPCs could be used to revascularise ischaemic tissues or repair vascular damage. With this in mind, the investigation turned towards finding an effective method of utilising EPCs as a therapeutic tool.

Before considering *in vivo* transplantation it was important to establish a robust *in vitro* model of EPC transplantation, in order to provide sufficient justification for subsequent animal experiments. The tubule formation assay, previously used to demonstrate angiogenic potential, was adapted to investigate transplantation of EPCs by studying their effect on EC tubules grown *in vitro*. By applying the quantification techniques of node counting and branch length measurement, the physical effect of transplantation could be assessed. Considering the highly angiogenic behaviour demonstrated by EPCs *in vitro*, it was believed they were likely to produce significant effects when transplanted, which would be reflected in the subsequent growth patterns of the affected EC tubules and by changes in endothelial-specific gene expression, as determined by qPCR.

To extend the scope of the *in vitro* transplantation model beyond the functional readout of tubule growth patterns, the effect of transplanted cell density and the localisation of EPCs after transplantation were also considered. Just as EC seeding density has a significant effect on tubule formation *in vitro* (SEE 3.3.2), cell quantity may have a differential effect on the outcome of EPC transplantation. Evidence suggests that the number of EPCs in the adult circulation is dynamic, illustrated by low levels in healthy adults but dramatically increased numbers in certain conditions such as rheumatoid arthritis (Paleolog, 2005), cerebral and cardiac ischemia (Ding *et al.*, 2007), acute myocardial infarction (Shintani *et al.*, 2001) and following burns (Gill *et al.*, 2001). For this reason, it was decided that investigating multiple EPC quantities may aid understanding of the role of EPCs in different *in vivo* scenarios and, hence, varying transplantation therapies. Aside from the release of pro-angiogenic factors by EPCs localised at sites of neovascularisation, one potential mechanism by which EPCs are thought to improve vascular performance during angiogenesis is through fusion with the existing vessel wall, resulting in incorporation of EPCs with vascular and perivascular cells (Beeres *et al.*, 2008). By labelling EPCs with fluorescent Qdots prior to transplantation, physical localisation of the transplanted cells was made possible. This was performed to allow better understanding of the interaction between the transplanted EPCs and the existing EC tubules, and hence possible mechanisms of any observed effects, as well as to identify the consequences of altering cell transplantation quantity.

5.2 Hypothesis & objectives

It was hypothesised that transplanted EPCs would have a beneficial effect on the growth of EC tubules, which could be demonstrated using an *in vitro* transplantation model. It was also thought that significant changes in endothelial-specific gene expression brought about by the interaction of EPCs with existing tubules would be evident throughout the period of transplantation. Additionally, localisation and behaviour of transplanted EPCs was hypothesised to be differentially affected by relative transplantation density.

Using an *in vitro* tubule formation assay, the experiments described in this chapter aimed to:

1. investigate the effect of *in vitro* EPC transplantation on EC tubule formation;
2. analyse changes in endothelial gene expression resulting from transplantation;
3. ascertain the effect of relative cell density on EPC transplantation;
4. determine the pattern of localisation of transplanted EPCs in relation to EC tubules.

5.3 Methods

5.3.1 Optimisation of Qdot labelling of EPCs

Non-specific labelling of EPCs was performed using Qdots, fluorescent nanoparticles which are phagocytosed from a concentrated labelling solution. To determine the optimum concentration, EPCs were incubated with a range of Qdot labelling solutions, based on the manufacturer's suggested working range, at 2 nM, 6 nM and 20 nM. After washing to remove unbound Qdots, labelled EPCs were visualised by fluorescence microscopy (**Fig. 5.1**). The optimum labelling concentration (6 nM) was determined by a ubiquitous distribution of Qdots throughout the EPC culture, wherein all cells observed were labelled with between 1-5 Qdots. At 2 nM, many EPCs were observed to remain unlabelled following incubation and washing which was deemed unsatisfactory for subsequent localisation experiments. A further criterion for optimal labelling was a minimum of excess, unbound Qdots following incubation. At 20 nM, even after washing, a proportion of extracellular Qdots remained in the culture (localised to cellular fragments and culture debris) which could interfere with subsequent localisation experiments.

5.3.2 *In vitro* scratch wound assay of labelled EPCs

Prior to using Qdot-labelled EPCs for subsequent experiments, an *in vitro* scratch wound assay (SEE 2.1.9) was performed to determine the effect of Qdot labelling on EPC migration (and, by association, functional capacity). Fluorescent microscopy was used to visualise the scratch wound assay (**Fig. 5.2**) and the distance moved by the leading edge of cells measured. There was no significant difference between the rates of cell migration demonstrated by unlabelled EPCs and those incubated with Qdots (**Fig. 5.3**).

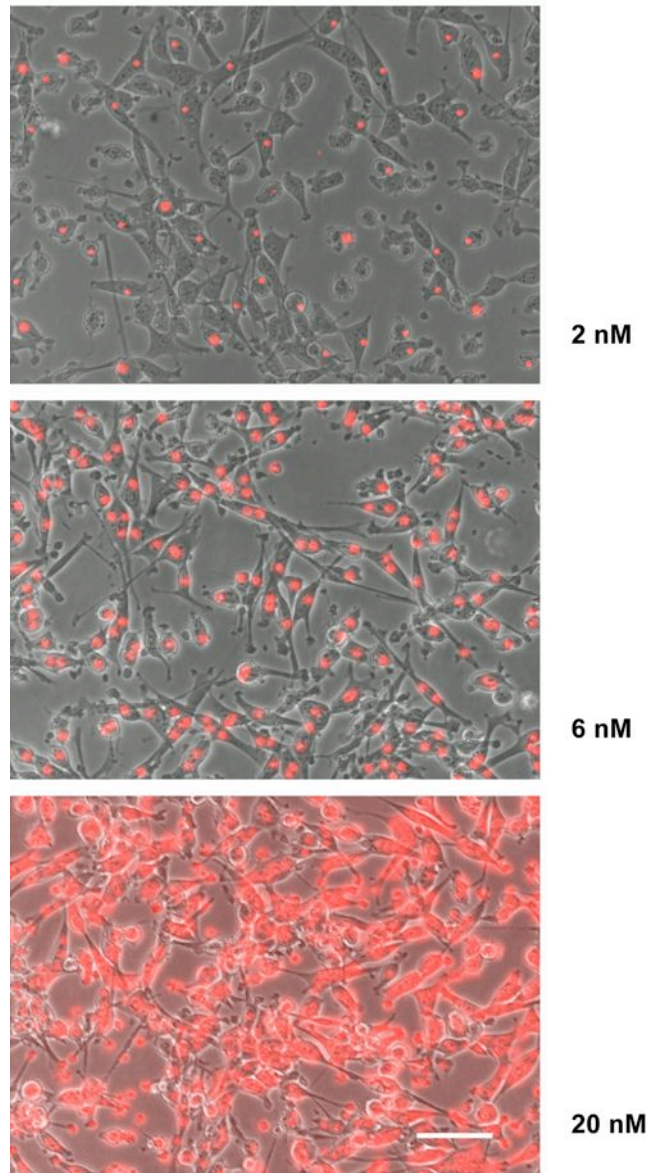


Figure 5.1. Optimisation of Qdot labelling of EPCs. Labelling solutions of 2 nM, 6 nM and 20 nM concentrations were tested by incubation for 1 h at 37°C / 5% CO₂. Scale bar = 50 µm.

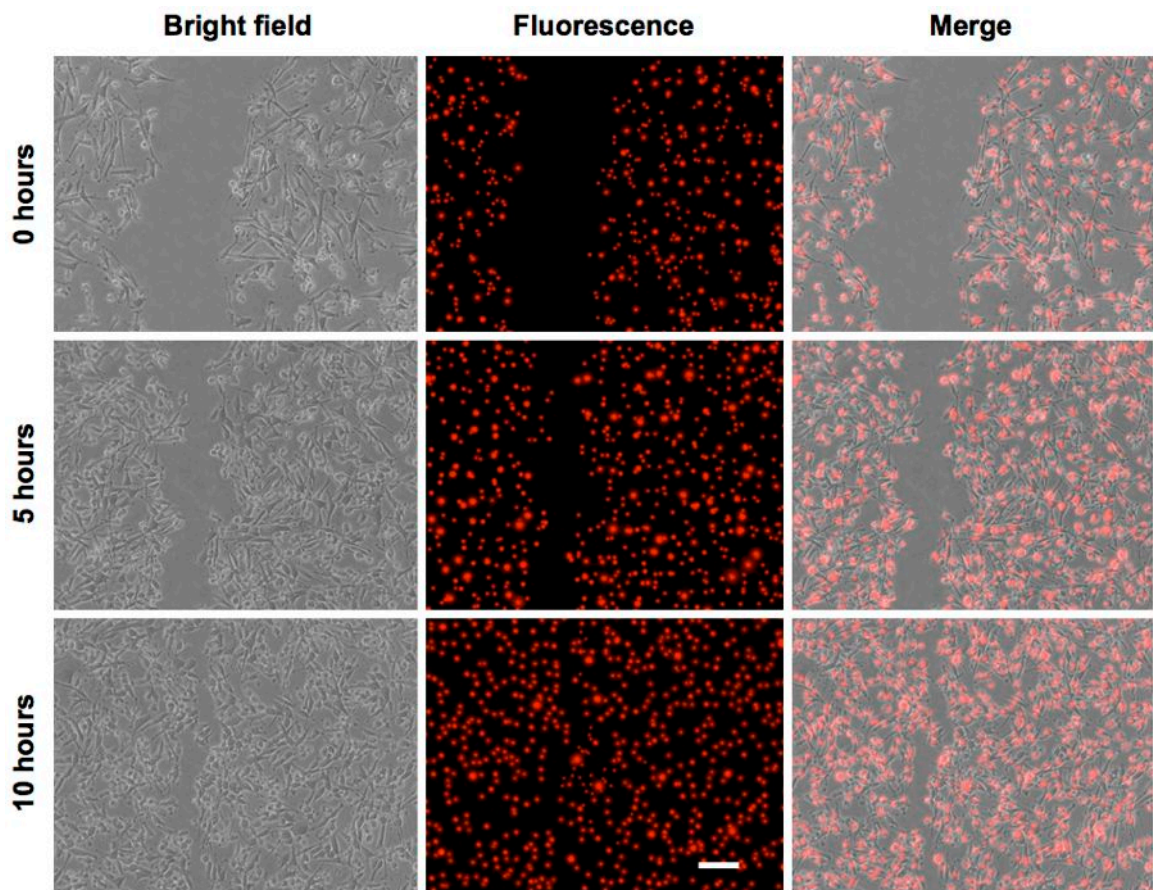


Figure 5.2. In vitro scratch wound assay of Qdot-labelled EPCs. Cells labelled with 6 nM Qdots were imaged using fluorescent microscopy to detect Qdots (red) at 655 nm. Unlabelled EPCs (not shown) were used as a control for comparison of migration rate. Scale bar = 50 μm .

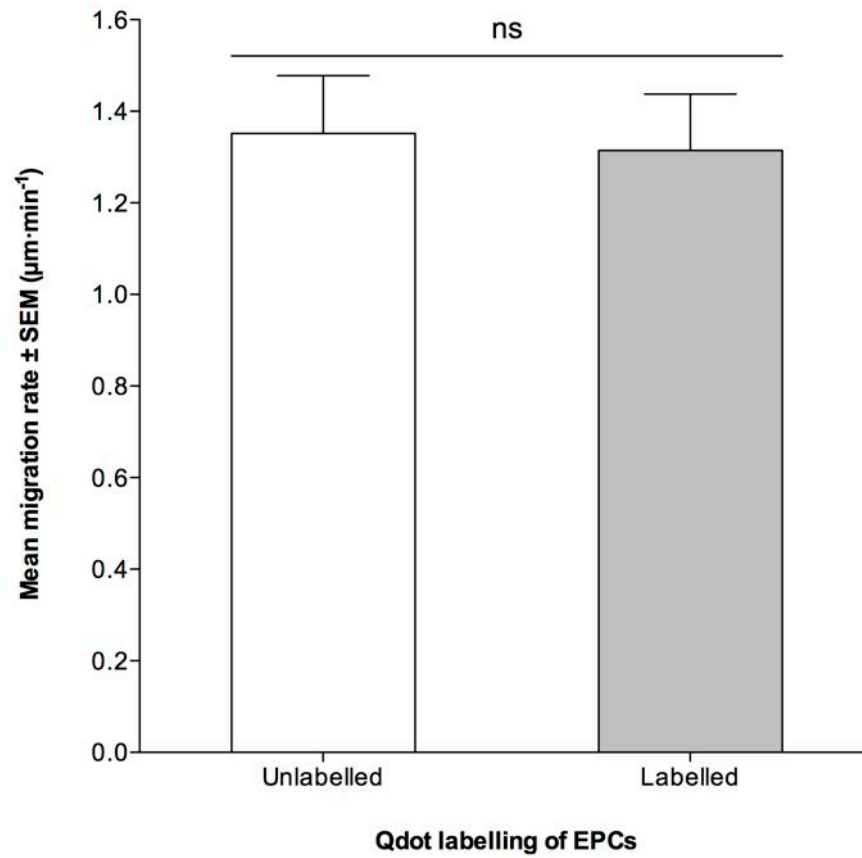


Figure 5.3. Effect of Qdot labelling on EPC migration rate. Four measurements of migration distance were taken at each time-point, data presented as average migration rate \pm SEM, $n=3$.

5.4 Results

The effect of *in vitro* EPC transplantation on EC tubules was investigated by the addition of EPCs at 5 h. Two transplantation methods were used, with a quantity of EPCs equal to either 10% or 50% of the original number of ECs seeded on to the ECMatrix gel. Quantitative analysis of the effect of transplantation on EC tubule recovery was performed by counting tubules nodes and measuring branch lengths, and subsequent changes in endothelial-specific expression determined by qPCR. Additionally, by labelling EPCs with fluorescent Qdots prior to transplantation, localisation of EPCs into the existing EC tubules could be determined.

5.4.1 Node count quantification of tubule formation following transplantation

In the 10% EPC transplantation assay, the greatest number of N1 nodes occurred at 2 h and decreased significantly by 6 h (**Fig. 5.4A**). However, there was no significant difference in N1 nodes between 6 h (10.1 ± 1.1) and 8 h (9.7 ± 0.7), following the transplantation of EPCs at 5 h. A progressive decrease was then seen between 10 h and 14 h and by 14 h no N1 nodes were present. The maximum number of both N2 (7.2 ± 0.6) and N3 nodes (2.7 ± 0.3) was observed at 4 h (1 h prior to transplantation) whilst N4 nodes were maximal at 6 h (1.2 ± 0.2 ; 1 h after transplantation). N4 nodes were infrequent and only evident at 6 h (0.3 ± 0.1) and no N5+ nodes were observed at any point throughout the assay. When the transplantation quantity was increased to 50% EPCs, as with 10%, the maximum number of N1 nodes (24.2 ± 0.6) was observed at 2 h and decreased progressively between 2 h and 8 h (**Fig. 5.4B**). However, unlike 10% transplantation, an increase in N1 nodes was observed between 8 h (6.6 ± 0.4) and 10 h (8.9 ± 0.6) and between 10 h and 14 h (9.6 ± 0.5) the mean number of N1 nodes did not decrease significantly. The greatest number of N2 nodes was again recorded at 4 h (7.6 ± 0.5) though N3 nodes were maximal at 8 h (7.7 ± 0.5 ; 3 h post-transplantation). The mean number of N4 nodes, first evident at 4 h, increased significantly from 4 h (0.5 ± 0.2) to 6 h (3.0 ± 0.5).

N4 nodes then decreased progressively between 8 h (2.9 ± 0.4) and 14 h (0.5 ± 0.1). N5+ nodes, which were not seen in the 10% transplantation assay, were first identified at 6 h (1.9 ± 0.4), 1 h after 50% EPC transplantation. There was no significant difference between 6 h and 10 h (1.9 ± 0.3), with a slight reduction in N5+ nodes between 10 h and 12 h (1.2 ± 0.2) and a significant decrease was seen at 14 h.

5.4.2 Branch length quantification of tubule formation following transplantation

The mean branch length in both the 10% and 50% transplantation assays increased from 2 h (1.5 ± 0.1 in both assays) to 6 h (5.5 ± 0.1 and 5.3 ± 0.1 , respectively), at which time-point (1 h post-transplantation) the maximum branch length for each transplantation method was recorded (**Fig. 5.5**). The mean branch length measured at this time in the 50% transplantation assay was significantly greater than that measured in the 10% transplantation assay. In both assays a reduction in the mean branch length was observed between 6 h and 14 h (0.9 ± 0.1 and 0.0 ± 0.0 in 10% and 50%, respectively) with significantly lower branch lengths recorded at each time-point in the 10% assay compared to 50% transplantation.

5.4.3 Localisation of transplanted EPCs

When 10% EPCs were transplanted at 5 h, based on visual inspection, fluorescent signals were observed to be randomly distributed throughout the EC tubule network, co-localised with the existing tubules (**Fig. 5.6**). Following transplantation with 50% EPCs, however, new tubules composed entirely of Qdot-labelled EPCs were observed to form between 6 h and 14 h, with only some co-localisation of transplanted EPCs with existing EC tubules (**Fig. 5.6**). By visual examination, these new tubules were morphologically comparable to tubules formed by ECs prior to transplantation, as well as to the tubule networks formed by EPCs and ECs separately (SEE **3.4.2**), correlating with the node count and branch length data.

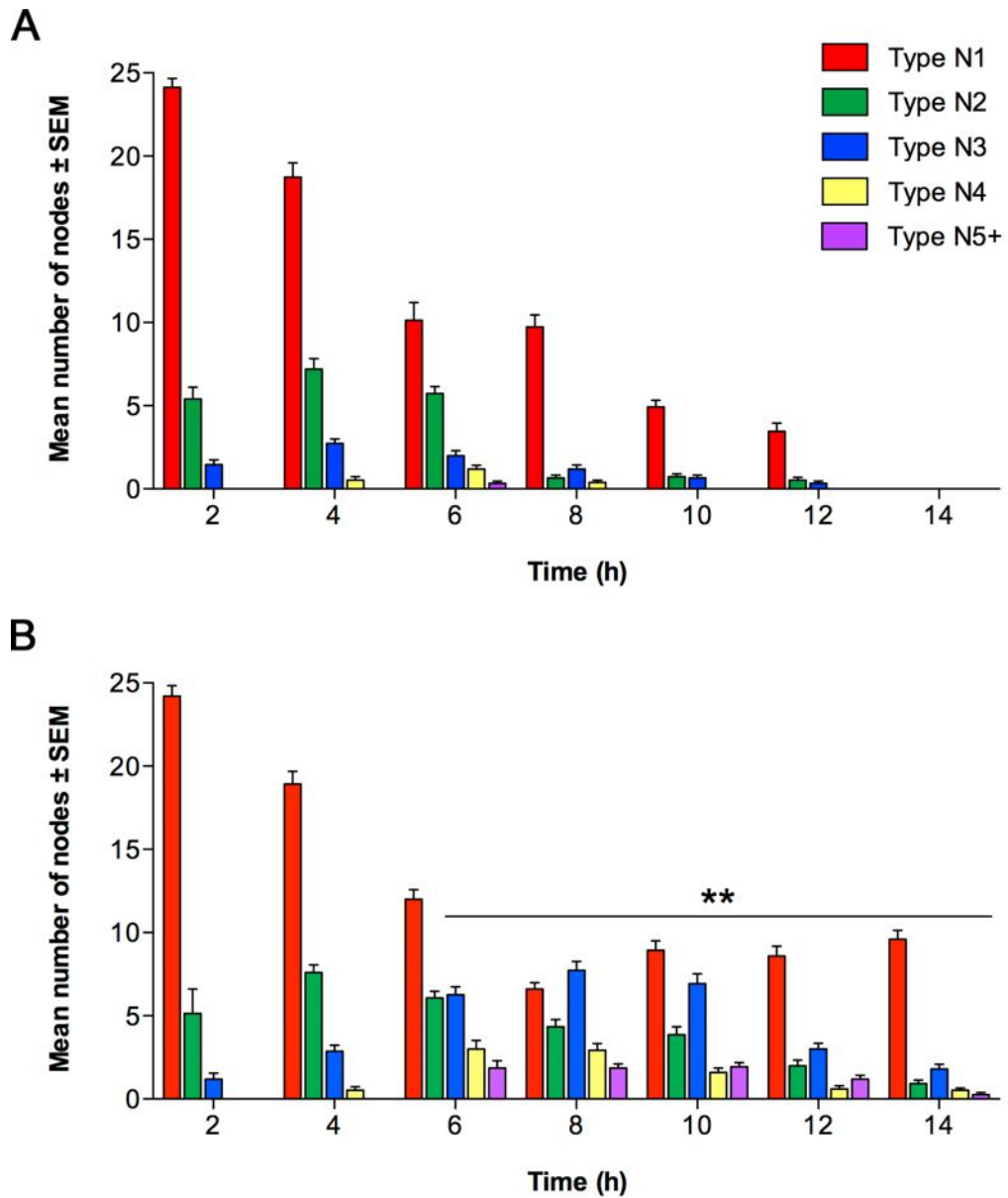


Figure 5.4. Quantification of tubule formation following (A) 10% and (B) 50% EPC transplantation at 5 h, determined by node counting. Data presented as mean number of node type ± SEM ($n = 3$) from five random fields of view at each time-point. Significant differences between transplantation methods at each time-points are indicated (** $P < 0.01$).

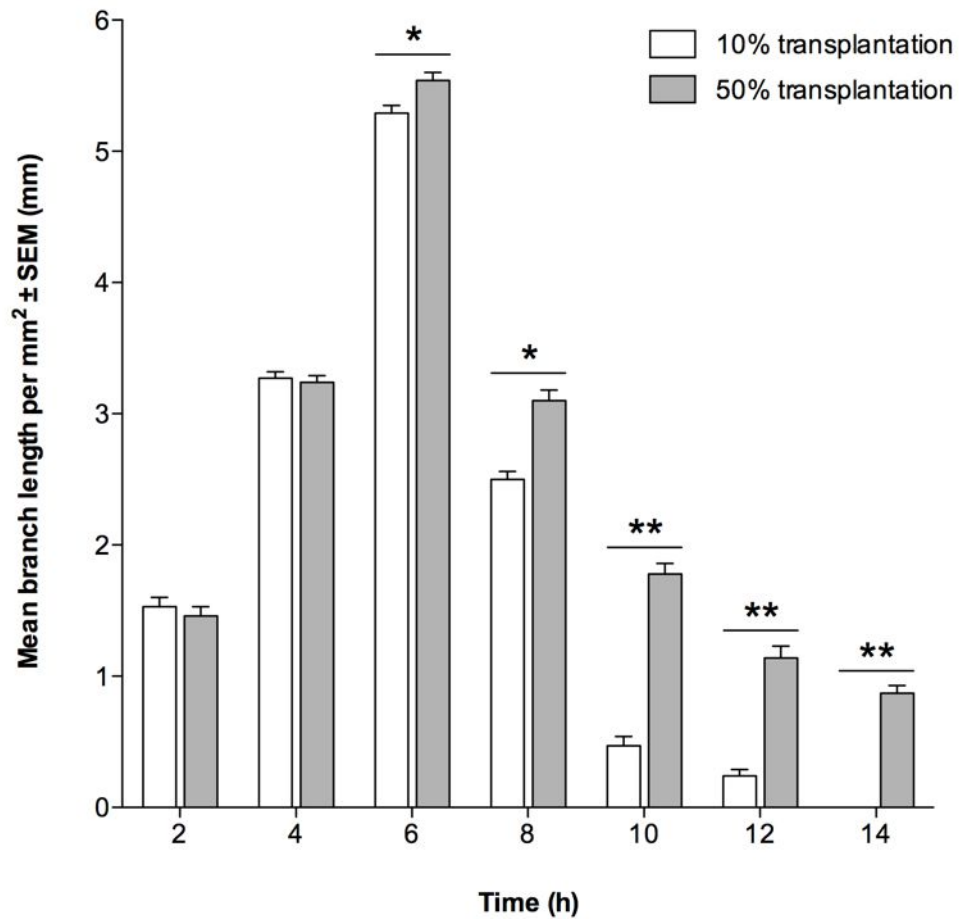


Figure 5.5. Quantification of tubule formation following EPC transplantation, determined by branch measurement. Data presented as mean length per mm² of assay ± SEM ($n = 3$) from five random fields of view at each time-point. Significant differences between transplantation methods are indicated (* $P < 0.05$, ** $P < 0.01$).

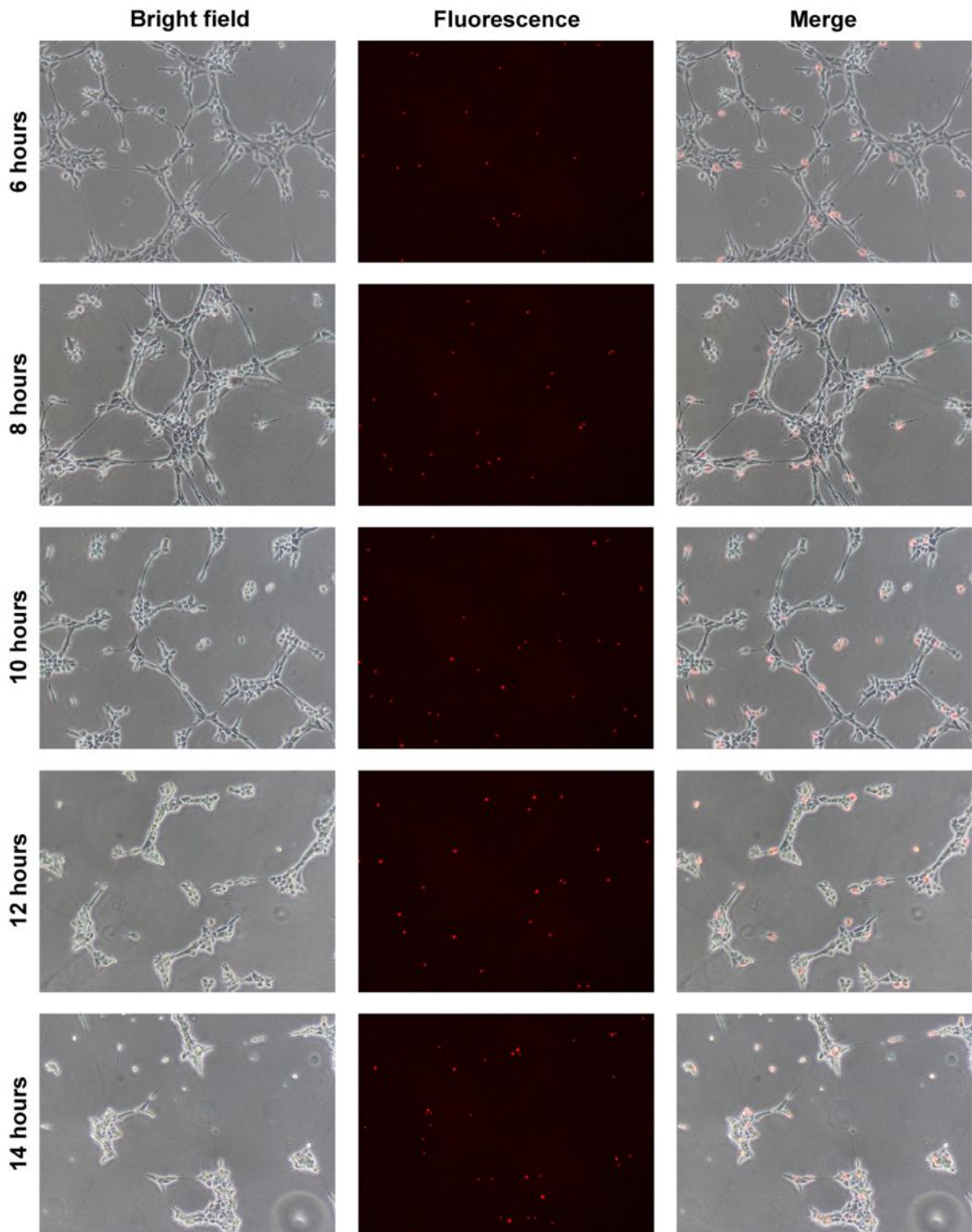


Figure 5.6. In vitro localisation of Qdot-labelled EPCs following 10% transplantation. Transplantation of 8×10^3 EPCs into EC tubules performed at 5 h. Microscopy performed at 2 h intervals with fluorescent detection of Qdots (red) at 655 nm. Scale bar = 50 μm .

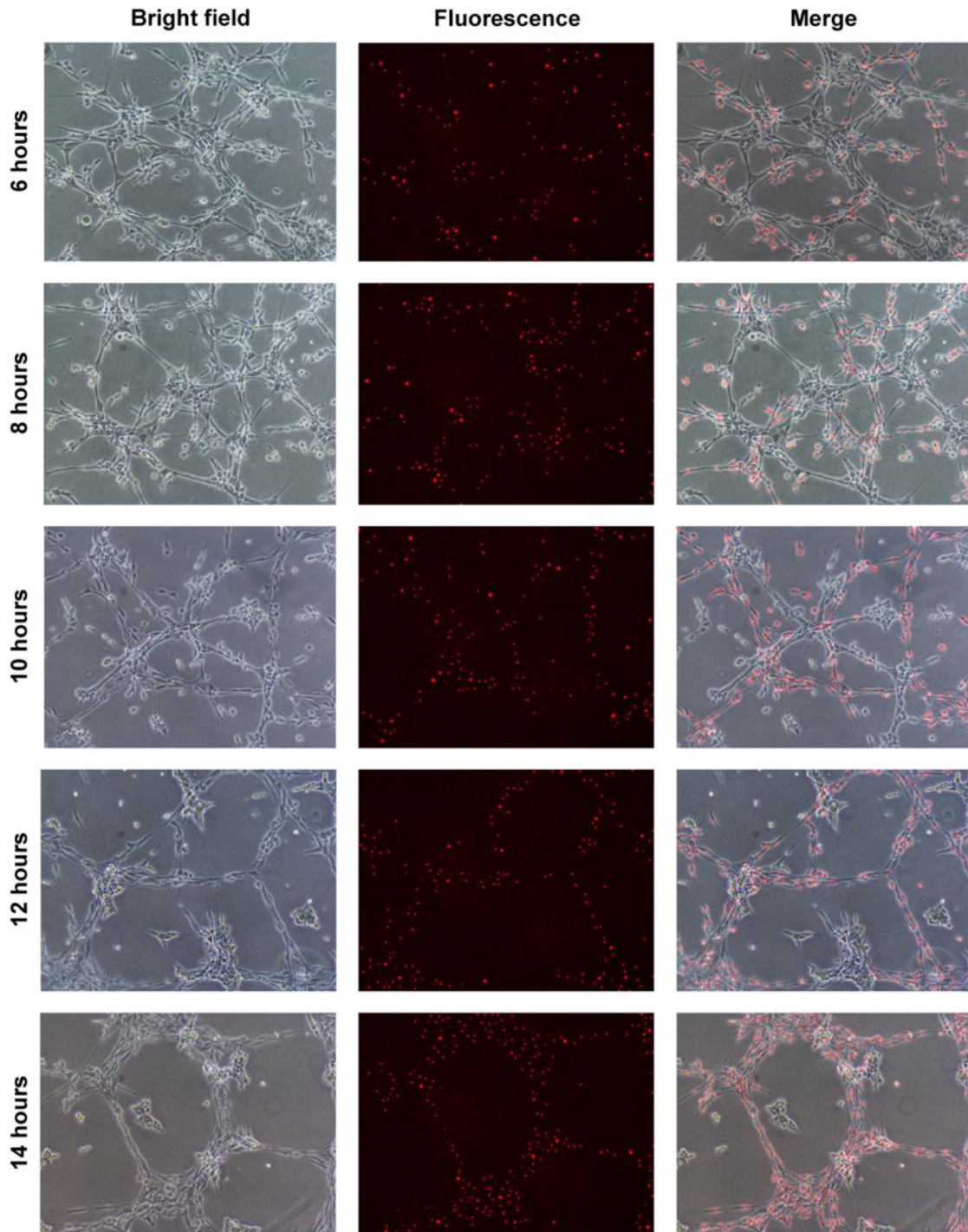


Figure 5.7. In vitro localisation of Qdot-labelled EPCs following 50% transplantation. Transplantation of 4×10^4 EPCs into EC tubules performed at 5 h. Microscopy performed at 2 h intervals with fluorescent detection of Qdots (red) at 655 nm. Scale bar = 50 μm .

5.4.4 qPCR analysis of mRNA expression following EPC transplantation

The effect of EPC transplantation on *VEGFR2*, *VE-cadherin* and *CD31* expression in tubule-forming ECs was investigated using qPCR analysis. As previously, cells were recovered from ECMatrix gel by gel depolymerisation and centrifugation. Prior to transplantation, expression patterns of all three genes were equivalent to ECs grown on ECMatrix gel without transplantation (SEE 3.4.1.1).

Following 50% transplantation at 5 h, *VEGFR2* expression increased significantly compared to 10% transplantation which, conversely, decreased between 4 h and 6 h (Fig. 5.8). Whilst the number of transcripts in both transplantation methods decreased continually from the time of transplantation until 14 h, expression of *VEGFR2* in the 50% transplantation assay was significantly greater at each time-point after transplantation than the expression observed in the 10% assay (a 1.5-fold increase or greater at each time-point; $P < 0.05$).

Unlike *VEGFR2*, the level of *VE-cadherin* expression at 6 h was not different between transplantation quantities, or when compared to the previous time-point (Fig. 5.9). However, as with *VEGFR2*, expression was significantly different between transplantation quantities from 8 h until the end of the assay (a 1.5-fold increase or greater at each time-point; $P < 0.05$). Expression in the 10% assay decreased significantly at every time-point following transplantation (by, on average, 1.4-fold; $P < 0.05$), except between 12 h and 14 h when no difference was observed.

A decrease in *VE-cadherin* was also seen in the 50% assay following transplantation but was only statistically significant between 10 h and 12 h (1.2 fold decrease; $P < 0.05$). Following both 10% and 50% transplantation, the expression of *CD31* was observed to increase

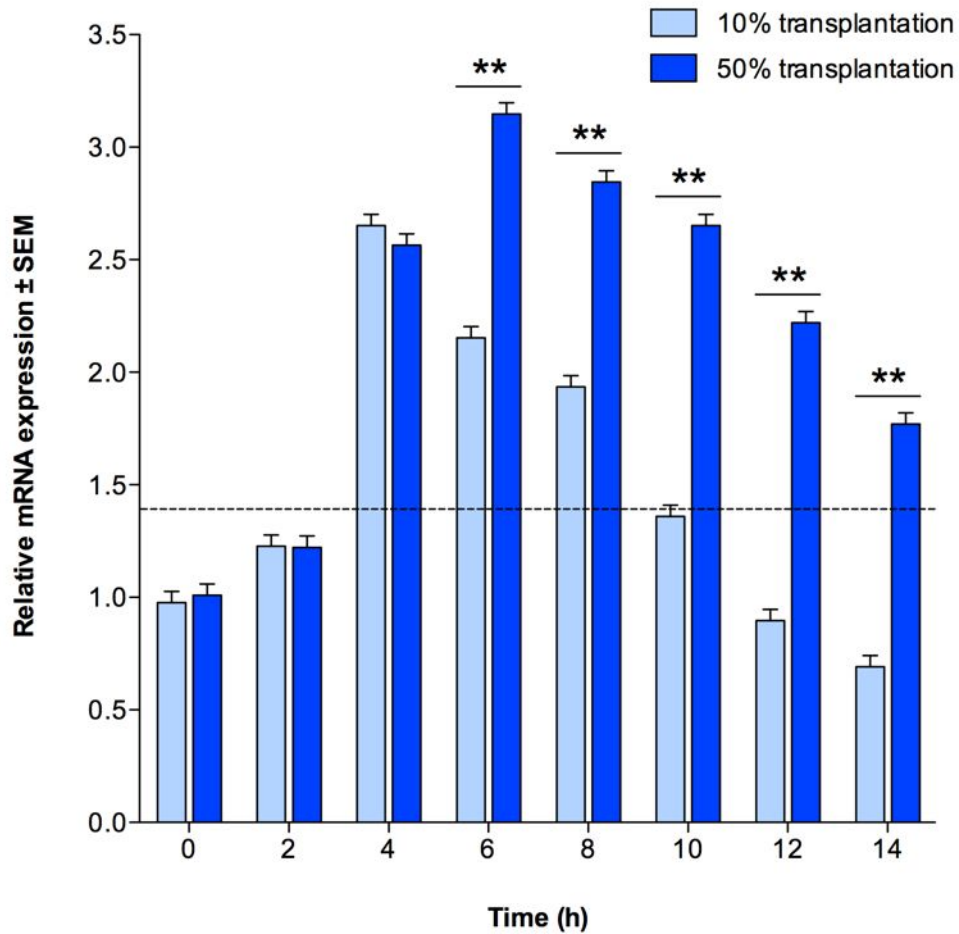


Figure 5.8. Relative expression of VEGFR2 in 10% and 50% EPC transplantation assays, determined by qPCR analysis. Transplantation performed at 5 h. Gene expression normalised to β -actin, data presented as mean expression \pm SEM ($n = 3$) relative to 60% confluent ECs. Expression in 60% confluent EPCs indicated by dotted (----) line. Significant differences between transplantation quantities are indicated (** $P < 0.01$).

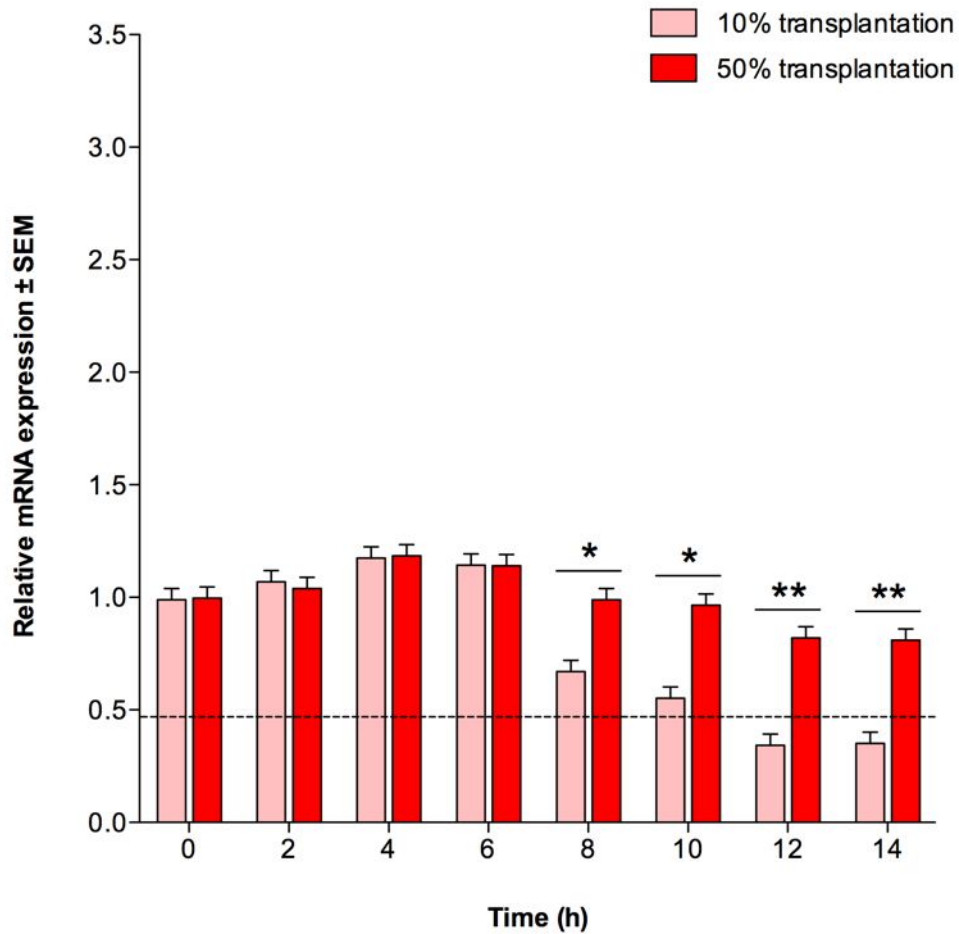


Figure 5.9. Relative expression of VE-cadherin in 10% and 50% EPC transplantation assays, determined by qPCR analysis. Transplantation performed at 5 h. Gene expression normalised to β -actin, data presented as mean expression \pm SEM ($n = 3$) relative to 60% confluent ECs. Expression in 60% confluent EPCs indicated by dotted (----) line. Significant differences between transplantation quantities are indicated (* $P < 0.05$, ** $P < 0.01$).

significantly (by, on average, 1.6-fold, $P < 0.05$; **Fig. 5.10**). However, by 8 h expression in both assays had decreased by 1.2-fold, and continued to do so until 14 h. The decreases in expression at each time-point were determined to be statistically significant in both transplantation assays ($P < 0.05$), except between 10 h and 12 h in the 10% assay when no significant difference in expression was seen. These were also the only time-points at which *CD31* expression was observed to be significant different between 10% and 50% transplantation (1.8- and 1.3-fold, respectively).

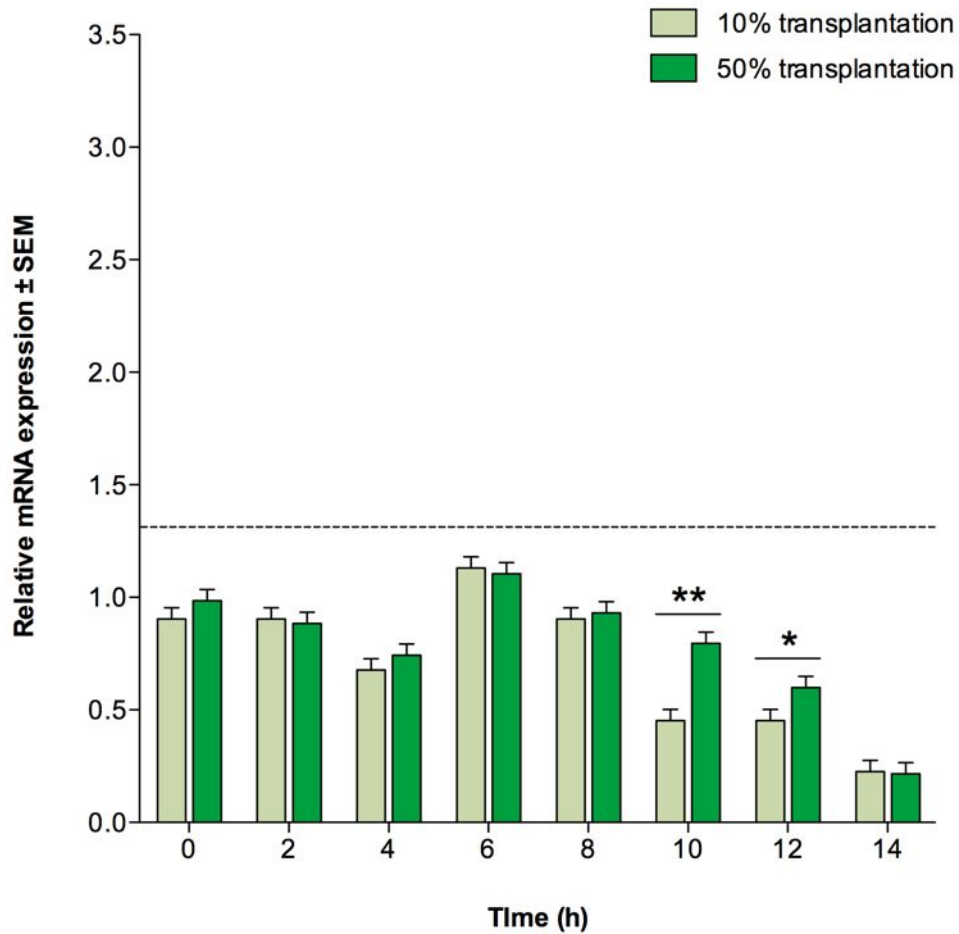


Figure 5.10. Relative expression of CD31 in 10% and 50% EPC transplantation assays, determined by qPCR analysis. Transplantation performed at 5 h. Gene expression normalised to β -actin, data presented as mean expression \pm SEM ($n = 3$) relative to 60% confluent ECs. Expression in 60% confluent EPCs indicated by dotted (----) line. Significant differences between transplantation quantities are indicated (* $P < 0.05$, ** $P < 0.01$).

5.5 Discussion

The capacity of EPCs to form tubule structures *in vitro* has been previously demonstrated, as well as their ability to incorporate into existing endothelial networks and effect significant changes to the morphology and structure of the vasculature (Zhang, L *et al.*, 2006; Wilhelm *et al.*, 2007). EPCs were investigated as a potential tool for therapeutic angiogenic transplantation by exploring the effect that transplantation of MFLM-4 EPCs had on pre-existing tubules formed by MCEC-1 ECs *in vitro*. Two methods of transplantation were assessed, using quantities of EPCs equivalent to 10% or 50% of the original quantity of ECs seeded on to the ECMatrix gel.

The effect of EPC transplantation on tubule formation, as determined by node counting and branch length measurement, was variable, depending on the relative quantity of cells used. When EC tubules were transplanted with 50% EPCs, complexity of the tubule network was significantly different to non-transplanted tubules: the numbers of N3, N4 and N5+ nodes were significantly greater after 5 h and mean branch length was increased at each time-point following, compared to controls. As well as increasing complexity of the network, 50% transplantation also resulted in significantly increased tubule longevity with nodes of all five types and branches being evident at 14 h, compared to control assays in which the network regressed after 12 h. In contrast, transplantation of EC tubules with 10% EPCs had little effect on tubule complexity or longevity, showing no significant differences either node counts or branch length measurements. The increased tubule longevity resulting from 50% EPC transplantation is consistent with the understanding of the involvement of EPCs in specific vascular remodelling during angiogenesis, and the observed beneficial effects of large-scale *in vivo* EPC mobilisation on vascular repair (Brunner *et al.*, 2008).

Whilst rates of cell turnover vary widely according to cellular morphology and function, the regulation of the balance of cell formation and cell loss throughout the body is important (Hooper, 1956). Although the rates of individual EC turnover are low, the endothelium undergoes frequent repair (due to shear damage from blood flow) and remodelling (as a result of angiogenesis). EPCs have also been shown to have a role in the repair of defects in the endothelial layer of blood vessels, and it has been demonstrated that the continual release of EPCs into the circulation is important for the maintenance of vascular wall integrity throughout adult life (Dimmeler & Zeiher, 2004; Op den Buijs *et al.*, 2004). The absence of a significant effect on *in vitro* tubule formation after 10% EPC transplantation may correlate with these findings because, whilst EPC numbers increase during a prolonged angiogenic response, their low number in the peripheral blood of healthy adults may illustrate the active supplementation of normal EC turnover by EPCs. In addition, as aging EPCs exhibit a limited capacity for regeneration of the ischaemic endothelium (Dimmeler & Vasa-Nicotera, 2003) it may be that regular low level BM release of EPCs is more beneficial than intermittent large-scale mobilisation for maintenance of the endothelium. In terms of demonstrating this *in vitro*, it may simply be that the effect of 10% transplantation (i.e. repair of damage rather than tubule network augmentation) is too modest to be evident in the tubule formation assay.

As with tubule formation, localisation of EPCs following transplantation (assessed using Qdot labelling and fluorescent microscopy) was differentially affected by relative transplantation quantity. Whilst 50% transplantation assays showed increased tubule formation following transplantation, Qdot-labelled EPCs did not incorporate solely into existing EC tubules but also into separate additional tubules formed throughout the existing network. These new tubules appeared to consist entirely of transplanted EPCs. Conversely, following 10% transplantation, Qdot-labelled EPCs were found to be randomly distributed throughout the

existing EC tubule network and did not form exclusive EPC tubules. Hence, EPC behaviour following transplantation appears to be affected by the ratio of cell types present. Previous investigations have suggested transplanted EPCs work in conjunction with ECs by localising to existing vessels (as seen with 10% transplantation) rather than by forming entirely new vessels (as with 50% transplantation) (Vasa *et al.*, 2001; Hill *et al.*, 2003; Rauscher *et al.*, 2003). One reason could be the affinity of the two cell types for each other following angiogenic stimulation. If EPCs have a greater homeotypic affinity than heterotypic affinity they are likely to form tubules composed almost entirely of EPCs upon introduction to ECMatrix gel, given a sufficient local density of EPCs. When the relative density of EPCs is lower, such as during 10% transplantation, only then may transplanted EPCs adhere to cells for which they have a lower affinity, resulting in incorporation into EC tubules. To verify this 'critical density' at which EPC behaviour shifts from heterotypic to homotypic, and to aid calculation of the optimum amount of EPCs for beneficial transplantation, further investigations using additional transplantation quantities between 10% and 50% would be needed. In addition to the homo- and heterotypic affinity of the transplanted cells, the local environment generated by the host tissue is also important and may modulate the EPC response after transplantation. For example, evidence suggests that a hostile vascular environment, such as the conditions of low nitric oxide (NO) bioavailability, hyperglycemia and oxidative stress found in diabetic patients, may negatively influence the differentiation and function of recruited EPCs (Fadini *et al.*, 2005). Furthermore, in tumour angiogenesis particularly, host-secreted VEGF has been shown to influence vessel growth by inducing fenestrations in the microvascular endothelium (Roberts, WG & Palade, 1997).

As with the functional readout of tubule formation, significant alteration in endothelial-specific gene expression was only observed with 50% EPC transplantation. The prolongation

effect of EPCs, illustrated by node counts and branch lengths, is reflected in the rate of decrease of *VEGFR2*, *VE-cadherin* and *CD31* mRNA expression being less than in the non-transplanted assay. This suggests a delay in downregulation of endothelial expression with assay progression. No significant difference in expression was observed when EC tubules were transplanted with 10% EPCs, further supporting the tubule quantification data showing no significant effect on tubule complexity or longevity. However, a limitation of this investigation is that it is unclear whether the changes in endothelial gene expression observed following transplantation represent an interactive or additive effect of EPCs (i.e. whether the expressional changes simply reflect the addition of the EPC population or a true effect of EPC transplantation on the endothelial expression in existing ECs). Ultimately, further investigation into the EPC- and EC-specific gene expression of *VEGFR2*, *VE-cadherin* and *CD31*, perhaps using allele-specific PCR that could be used to distinguish between the gene expression profiles of the two co-cultured cell types, would be useful in elucidating the exact nature of the observed EPC transplantation effect.

That said, the outcomes of the two transplantation experiments may be representative of two potential *in vivo* scenarios. First, 10% transplantation simulates the low level, continuing replenishment of maintenance EPCs into the circulation. The phenotypic change in EPCs following 10% transplantation was minor and their effect on existing tubules non-significant.

However, in 50% transplantation, EPC gene expression changed dramatically and an obvious effect on EC tubule formation and longevity was observed, suggesting a transition from quiescent circulating EPCs to a more active, angiogenic phenotype. This active phenotype may be beneficial in a second scenario in which a large population of EPCs are mobilised (either naturally or by drug administration) in response to a greater vascular trauma, requiring

a larger, more efficient EPC replenishment. Indeed, beneficial effects of EPCs have been demonstrated following the administration of exogenous cytokines, such as stromal cell-derived factor (SDF)-1 (Hattori *et al.*, 2001) and G-CSF (Powell *et al.*, 2005), to increase the release of BM-resident EPCs into the circulation. In these studies the increase in mobilised EPCs is contributing, at least in part, to resultant angiogenic recovery (an effect that may be reflected here in the 50% transplantation) although it should be noted that the cell numbers used were far in excess of those used in this investigation.

EPCs have demonstrated a transitional phenotype when transplanted *in vitro*, with differing responses in 10% and 50% transplantation assays. The effect of EPCs on existing tubules following transplantation has also been shown to be differential. These differences are likely linked to factors which are themselves directly influenced by a change in transplantation cell density, such as intracellular contact and paracrine signalling. A multitude of factors can affect EPC behaviour both *in vitro* and *in vivo*, such as migration and cell adhesion, and it is certain that these will significantly affect the benefit of using EPCs for therapeutic transplantation (Liew *et al.*, 2006). It is therefore important to better understand the mechanisms by which EPCs are directed to and recruited into sites of neovascularisation before beginning *in vivo* transplantation experiments.

CHAPTER 6:

PLATELETS IN ENDOTHELIAL PROGENITOR CELL RECRUITMENT

6.1 Introduction

EPC homing may be due to the endothelial release of cytokines or chemokines (which are numerous and difficult to study) or by cellular interactions. One candidate for such an interaction is the formation of platelet bridges. Platelets are small (1-4 μm diameter) circulating cell fragments produced by membrane budding or cytoplasmic fragmentation of megakaryocytes (Ihizumi *et al.*, 1977; Shaklai & Tavassoli, 1978). The main role of platelets is in haemostasis, by their involvement in the primary stages of thrombotic plug formation, preventing sustained blood loss following vascular injury (Davì & Patrono, 2007). In their normal state they consist of a relatively smooth cell membrane surrounded by a thick exterior coat, called the glycocalyx, which is in turn covered in multiple protruding glycoprotein receptors which regulate platelet activation and adhesion (Cooper *et al.*, 1976). The major classes of glycoprotein involved in the platelet's haemostatic role are the glycoprotein (GP) Ib-IX-V complex and GPIIb/IIIa, also known as $\alpha\text{IIb}\beta_3$ integrin. Following vascular damage, which exposes collagen and bound vWF, GPIb-IX immediately binds to vWF and adhesion is subsequently stabilised by the collagen-binding platelet receptors GPVI and $\alpha_2\beta_1$ integrin. This in turn activates $\alpha\text{IIb}\beta_3$, which binds fibrinogen and fibronectin at the site of damage to stabilise the primary platelet plug (Varga-Szabo *et al.*, 2008). Binding of GPIb-IX and $\alpha\text{IIb}\beta_3$ also trigger a conformational change in the platelet cytoskeleton, resulting in a stellate phenotype by actin-mediated growth of filopodia, and the secretion of molecules contained

within vesicular organelles called granules (Mistry *et al.*, 2000). Platelets contain α -granules, lysosomes and dense granules which store a wide variety of adhesion molecules (e.g. P-selectin), growth factors (e.g. transforming growth factor [TGF]- β and thrombospondin) and cytokines (e.g. platelet factor 4 [PF4] and stromal cell-derived factor [SDF]-1) (Weber, 2005). Granules also include adenosine diphosphate (ADP) which activates platelets further and generate thromboxane A₂ (TXA₂) *via* cyclooxygenase which gives full activation. Platelet granules are vital for normal platelet function and degranulation is an important aspect of many platelet-involved processes, augmenting and regulating platelet and cell behaviour in coagulation, inflammation, immunity and wound healing (Blair & Flaumenhaft, 2009).

In addition to their primary role in haemostasis, the involvement of platelets in the recruitment of certain circulating cell types, including leukocytes (Nash, GB, 1994) and blood-resident EPCs (de Boer *et al.*, 2006; May *et al.*, 2008), has also been widely discussed. Whilst the exact mechanisms of EPC homing remain undefined, localisation of EPCs to the endothelium appears essential for their involvement in angiogenesis. Since platelets circulate in proximity to the vessel wall, and are amongst the first cells to bind to the exposed subendothelium following vascular damage, it is suggested that they might play a vital role in either attracting or binding EPCs to the activated endothelium at angiogenic sites (Lev *et al.*, 2006).

At present, interactions between platelets and EPCs are only broadly defined, although platelets are thought to exert both physical and biochemical effects on circulating EPCs (Silvestre, Jean-Sebastien *et al.*, 2008). Adherent platelets express surface ligands for a wide range of adhesion receptors and secrete potent chemokines which are potential mediators of specific platelet-EPC binding (Langer, HF & Gawaz, 2008). For example, platelets secrete

SDF-1 α which has been shown to significantly increase the migration of progenitor cells in areas of endothelial denudation *in vitro* (Massberg *et al.*, 2006). Furthermore, when co-cultured with washed platelets over a period of days, dramatic increases in the functional properties of EPCs have been demonstrated (i.e. increased numbers of EPC colony forming units (CFU), upregulated cell proliferation and greater transmembrane migration), suggesting an augmentation of EPC activity that may arise from platelet-released growth factors such as PDGF and platelet-associated bFGF (Pintucci *et al.*, 2002; Leshem-Lev *et al.*, 2010).

Further suggesting an interaction between platelets and EPCs, human bone marrow CD34⁺ cells (of which a significant subset may be defined as having an EPC phenotype) have been shown to express antigens characteristic for platelets (e.g. CD41, CD52 and CXCR4), likely linked to the binding of activated platelets or platelet microparticles to CD34⁺ cell membranes, transferring these antigens to the EPC surface (Janowska-Wieczorek *et al.*, 2001). This supports the view that platelets may act as 'bridging' structures that can physically support the recruitment of circulating EPCs by providing a direct tether between EPCs and the activated endothelium (Langer, HF & Gawaz, 2008). For example, using human umbilical cord blood isolates as a source of EPCs, it has been shown that platelet aggregates can bring about the tethering, rolling and adhesion of EPCs under flow conditions (de Boer *et al.*, 2006). Adhesion molecules purported to be involved in the platelet-EPC binding interaction include platelet (P)-selectin, the β 1 and β 2 families of integrins, and platelet GPIIb (Hidalgo *et al.*, 2002; Vajkoczy *et al.*, 2003; Daub *et al.*, 2006; Massberg *et al.*, 2006). P-selectin has been shown to be expressed on both platelets and endothelial cells (Koedam *et al.*, 1992; Semenov *et al.*, 1999). In light of this, to clarify the roles of EPC- and platelet-bound P-selectin in adhesion, parallel assays were carried out in which either: (i) EPCs only or (ii)

EPCs and platelets were treated with the blocking antibody. P-selectin is just one of the potential mediators of platelet-EPC binding that will be investigated in this study (**Fig. 6.1**).

In addition to investigations focussed on the positive effect of platelet presence on EPC behaviour and recruitment, recent studies have also illustrated the effects of platelet impairment on EPC function. For example, in co-incubations of platelets and PBMCs, platelets from patients with several defined cardiovascular risk factors (including diabetes mellitus) failed to augment EPC adhesion and migration to the significant extent observed with healthy platelets (Abou-Saleh *et al.*, 2009). This not only confirms a positive influence of normal platelets on EPC adhesion but also illustrates that disease-impaired platelets lack significant factors that would ordinarily enhance EPC function.

Data have also been generated which show that whilst EPCs do adhere to activated platelets, EPCs can actually have an inhibitory effect on platelet function through the local production of prostacyclin (PGI₂) (Abou-Saleh *et al.*, 2009). These findings, which clearly demonstrate a reciprocal interaction between platelets and EPCs, continue to support the 'platelet bridge' hypothesis but suggest the dominant interaction is that of EPCs on platelets, not of platelets on EPCs as otherwise reported, and that EPCs may in fact play a central role in the regulation of platelet activity.

Having demonstrated the beneficial angiogenic effects of EPCs *in vitro* in a platelet-free environment (SEE 5.4), this investigation aimed to investigate the potential interactions between platelet and EPCs before moving to an *in vivo* transplantation model in which

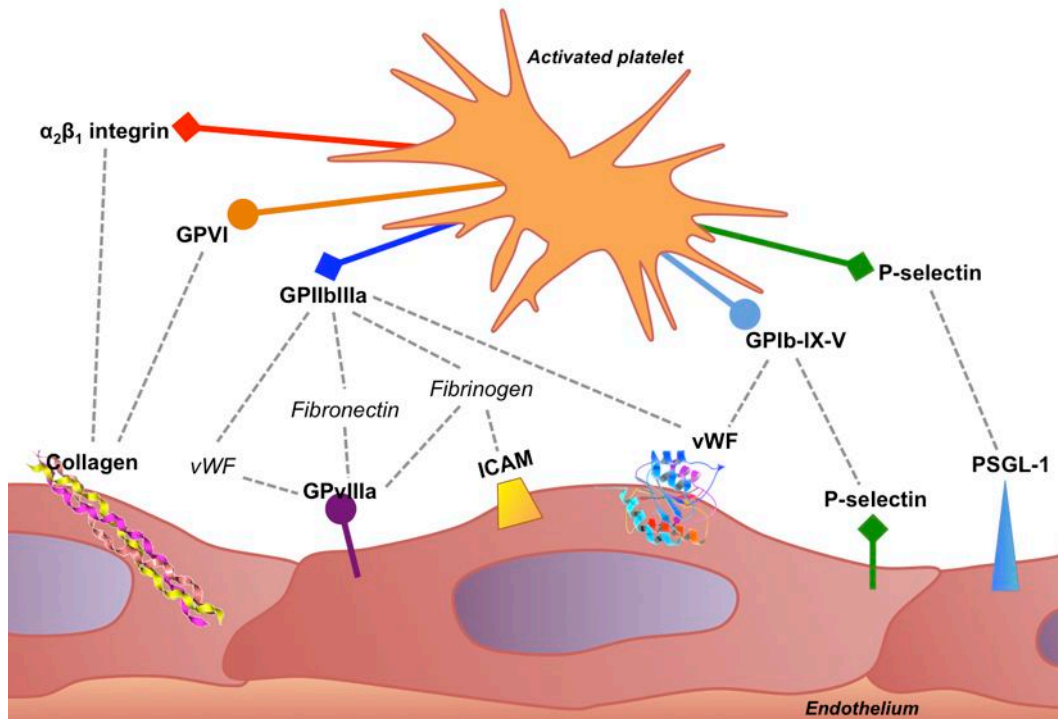


Figure 6.1. Potential mediators of platelet-endothelial binding. Activated platelets express a variety of adhesion molecules and receptors, including $\alpha_2\beta_1$ integrin, GPVI, GPIIb/IIIa, GP-IX-V and P-selectin, that may be involved in the 'platelet bridge' forming between the activated endothelium and circulating EPCs.

platelets would be present. Methods to investigate the adhesion interactions between isolated cells and various cellular or protein substrates and broadly fall into two categories: (i) static assays in which cells are seeded into the system and left to settle on the chosen adhesion surface unaided or (ii) flow-based assays wherein isolated cells are actively perfused across the substrate under flow to test adhesion under conditions of fluid shear stress. By virtue of their simplicity, static assays are easier to perform and allow much greater throughput. However, static assays may not accurately replicate potentially complex binding interactions as they occur *in vivo*. In contrast, flow-based assays, which can be more difficult and time-consuming to set up, can produce data of much greater physiological relevance, by better reflecting the shear-mediated dynamics of cell adhesion in the vasculature (Butler *et al.*, 2009), which is particularly important in the context of angiogenesis (Nash, G & Egginton, 2007). Furthermore, using video microscopy and image analysis, flow-based assays allow the different stages of adhesion (e.g. capture, rolling, stabilisation and migration) to be observed and quantified, in a way that might not be possible in a more simplified static assay (Bahra *et al.*, 1998; Luu *et al.*, 1999). Whether a static or flow-based system is used, the involvement of specific molecules in the platelet-EPC binding mechanism can be explored by selective inhibition of particular receptor-ligand interactions using targeted antibodies or blocking peptides or the modification of cell-wide receptor expression and, in the case of platelets, bioreactivity (i.e. activation and degranulation) using biochemical pre-treatment. For example, sulphated dextran (DxSO₄) binds selectins and competitively inhibits normal selectin binding (Nash, GB *et al.*, 2001) and can be used within an *in vitro* assay system.

Here, platelet-EPC binding was principally investigated using an *in vitro* flow adhesion assay, a closed system consisting of a glass microslide (on to which a platelet monolayer was immobilised) through which a suspension of cultured EPCs was perfused at a constant flow

rate by an electronic syringe pump. The number of adherent EPCs, as well as the dynamics of adhesion, were observed and recorded throughout the period of cell perfusion. Experiments were also carried out using a modified cell-based aggregation assay, a relatively simple non-static assay in which a mixed suspension of washed platelets and EPCs was gently stirred and the resulting cellular aggregates analysed. A variety of inhibition experiments were carried out using both the aggregation and flow adhesion assay systems, inhibiting potential mediators of platelet-EPC binding such as $\alpha\text{IIb}\beta\text{3}$, GPVI and P-selectin.

To maximise data output from the flow adhesion assay system, the spreading of adherent EPCs was also investigated by continued observation of platelet-bound cells after perfusion. Spreading is an important part of stable cell adhesion. When a cell contacts an adhesive surface it spreads, by reorganisation of the cytoskeleton and a subsequent change in cell shape, exerting traction forces against the surface and forming new bonds as the contacted area expands (Reinhart-King *et al.*, 2005). In addition to physical anchorage, spreading is also integral to cell growth and survival. ECs proliferate more rapidly *in vitro* as they become flatter in shape, and the degree of cell spreading can influence their ability to enter the cell cycle (Ingber, 1990). Furthermore, when EC spreading is actively prevented (by the use of non-adherable substrate coatings such as Teflon[®]) an increased incidence of cell apoptosis is observed (Re *et al.*, 1994). Perhaps of more specific interest to this investigation, spreading of adherent cells may aid the physical incorporation of EPCs into sites of angiogenesis, one of the proposed mechanisms for their beneficial effect when used as a transplantation therapy (De Palma *et al.*, 2003; Silva *et al.*, 2005). As previously discussed, the angiogenic benefit of EPCs is also suggested to be due to the release of potent pro-angiogenic factors at the site of neovascularisation (Kushner *et al.*, 2010). By stabilising adherent EPCs, cell spreading may facilitate this cytokine release mechanism by ensuring the continued localisation of EPCs in

the required area; persistence of cells, perhaps owing to the spreading and stabilisation of incorporated cells, has been observed following EPC transplantation and is considered important for a beneficial outcome (Ziebart *et al.*, 2008). To further understand the efficacy of EPCs as an angiogenic therapy, it is important to understand the role of platelets in the recruitment of EPCs to the endothelium, and their effects on spreading and the physical stabilisation of adherent cells.

6.2 Hypothesis & objectives

It was hypothesised that a binding mechanism exists between platelets and EPCs which facilitates capture of flowing EPCs from the peripheral circulation and tethers them to the activated endothelium at sites of angiogenesis. In this manner, platelets may facilitate the beneficial angiogenic effects of EPCs by improving cell persistence and prolonging the stimulatory effects of EPC chemokine release. Moreover, it was suggested that platelets may also influence the subsequent incorporation of EPCs by affecting their rate of spreading and migration across the surface of the endothelium.

Using *in vitro* aggregation and flow adhesion assays, the experiments described in this chapter aimed to:

1. Establish the existence of a specific platelet-EPC binding mechanism to recruit EPCs to immobilised platelets under flow, using ECs and MEFs for comparison;
2. Investigate potential mediators of this binding by selective inhibition of platelet- and cell surface-bound adhesion molecules;
3. Ascertain the effect of platelets on the subsequent spreading and migration of EPCs captured from flow;
4. Determine the effect of platelet activation on EPC adhesion and spreading by inhibition or induction of platelet activation.

6.3 Methods

6.3.1 Cell dissociation treatment

It was necessary to determine an appropriate method for dissociating cells from culture which would preserve their structural and functional integrity. It was important to ensure that the chosen cell dissociation solution did not have an adverse effect on the ability of EPCs or ECs to adhere. For example, prolonged exposure of cells to trypsin (which is used for cell dissociation in routine cell culture) is associated with reduced cell viability and has been shown to have cytotoxic effects (Masson-Pévet *et al.*, 1976; Heng, Boon C *et al.*, 2009), as well as cleaving surface molecules and glycoprotein receptors important for cell adhesion (Vernay *et al.*, 1978; Giancotti *et al.*, 1985).

Trypsin is a serine protease, usually of bovine or porcine origin, which cleaves peptides on the C-terminal side of arginine and lysine residues (Olsen *et al.*, 2004). Dispase is a neutral protease isolated from bacteria that cleaves bonds between leucine and phenylalanine residues (Weimer *et al.*, 2006). Both trypsin and dispase are both routinely used in cell culture to break down cell adhesion proteins and separate cell monolayers from culture flasks and hence were chosen as possible methods for preparing cells for adhesion assays. EPCs and ECs were removed from culture flasks using either 0.25% trypsin-EDTA or 1 mg·ml⁻¹ dispase II solution (both from Sigma-Aldrich, Dorset, UK) and *in vitro* flow adhesion assays, using platelet-coated microslides, were performed in parallel under standard conditions (SEE 2.8.4). Adherent cells in each assay were then counted (Fig. 6.2).

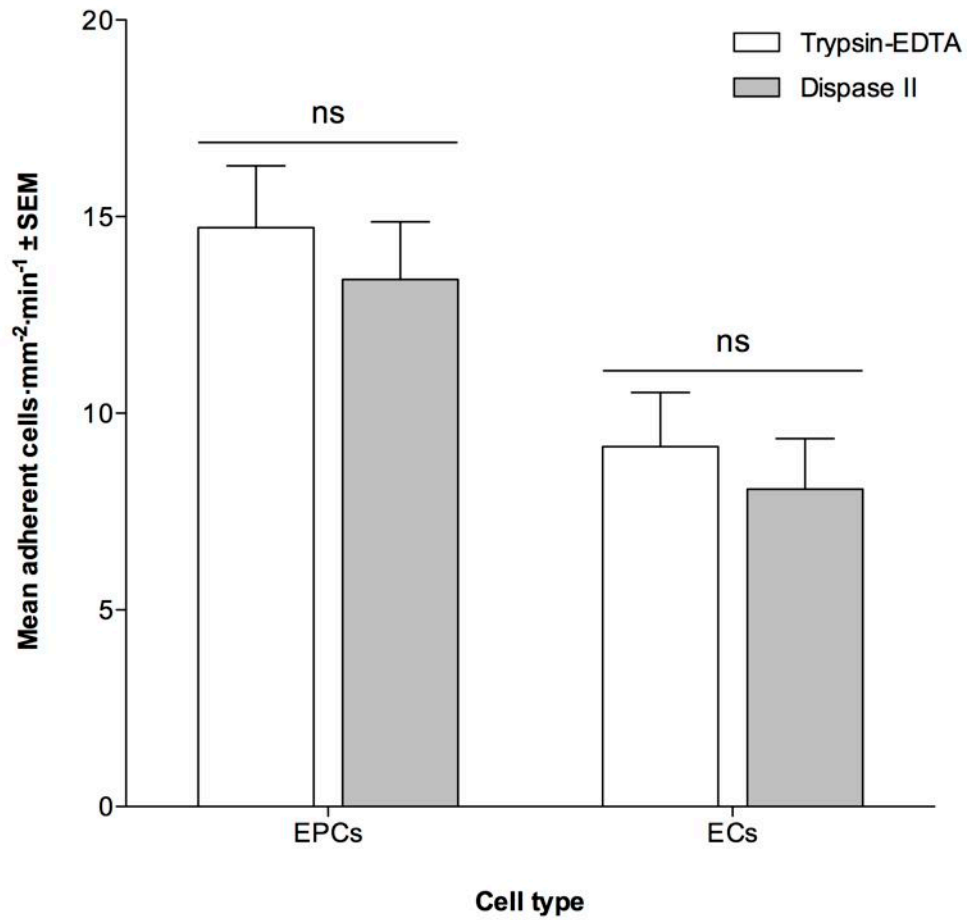


Figure 6.2. The effect of cell dissociation solution on cell adhesion under flow conditions. Platelet-coated microslides were perfused with $2 \times 10^6 \cdot \text{ml}^{-1}$ of either EPCs or ECs, suspended in 0.15% PBSA, at a wall shear stress of 0.025 Pa for 5 min. After perfusion microslides were washed to remove non-adhered cells. Data presented as mean adherent cells per mm² of microslide per min of perfusion \pm SEM, $n=4$; ns, no significant difference between treatments.

No significant difference was observed between cell dissociation treatments with regard to adhesion of EPCs or ECs. This suggests that any effect of trypsin-EDTA and dispase on cell surface adhesion molecules is similar, and that any adverse effects on subsequent binding assays would be comparable regardless of the choice of dissociation treatment. Based on these findings, as trypsin-EDTA caused no greater reduction in adhesion than dispase and was already used in routine cell culture, it was decided that it would also be used for preparing cells for *in vitro* aggregation and flow adhesion assays.

6.4 Results

6.4.1 *In vitro* cell aggregation assay

The interactions between EPCs and platelets were first investigated using an *in vitro* cell-based aggregation assay. Assays were performed with MFLM-4 EPCs and MCEC-1 ECs, as well as with CF-1 MEFs as a non-endothelial control, and the number of platelet-cell aggregates analysed using Coulter size distribution (**Fig. 6.3**).

When mixed with platelets, EPCs, ECs and MEFs all exhibited aggregation to some extent. This was illustrated by increased numbers of 16-42 μm particles, which reflected aggregates larger than single cells. Overall, at each time-point recorded, platelet-mediated EPC aggregation was significantly greater than that seen in ECs or MEFs ($P < 0.05$). Within all three cell types, aggregation was observed to increase at each time-point but not all increases were determined to be statistically significant. The number of platelet-EPC aggregates increased significantly between 5 min (8341 ± 834), 10 min (20354 ± 1168) and 15 min (32367 ± 1693 ; $P < 0.05$). Similarly, platelet-EC aggregates increased significantly between 5 min (2002 ± 489) and 10 min (5105 ± 1324 ; $P < 0.05$) but only moderately between 10 min and 15 min (7508 ± 1805 ; n.s.). The number of platelet-MEF aggregates increased between 5 min (501 ± 289) and 10 min (1835 ± 37 ; n.s.) and again between 10 min and 15 min (3504 ± 578 ; $P < 0.05$). Of the three cell types assayed, MEFs showed the least aggregation.

6.4.1.1 Blockade of selectin-mediated adhesion

Having determined the level of *in vitro* aggregation of untreated EPCs and ECs to platelets, and the preference of platelets to bind to endothelial lineage cells (compared to fibroblast controls), blockade experiments were undertaken to study possible binding mechanisms. Initially, the selectin family of cell surface adhesion molecules was non-specifically blocked

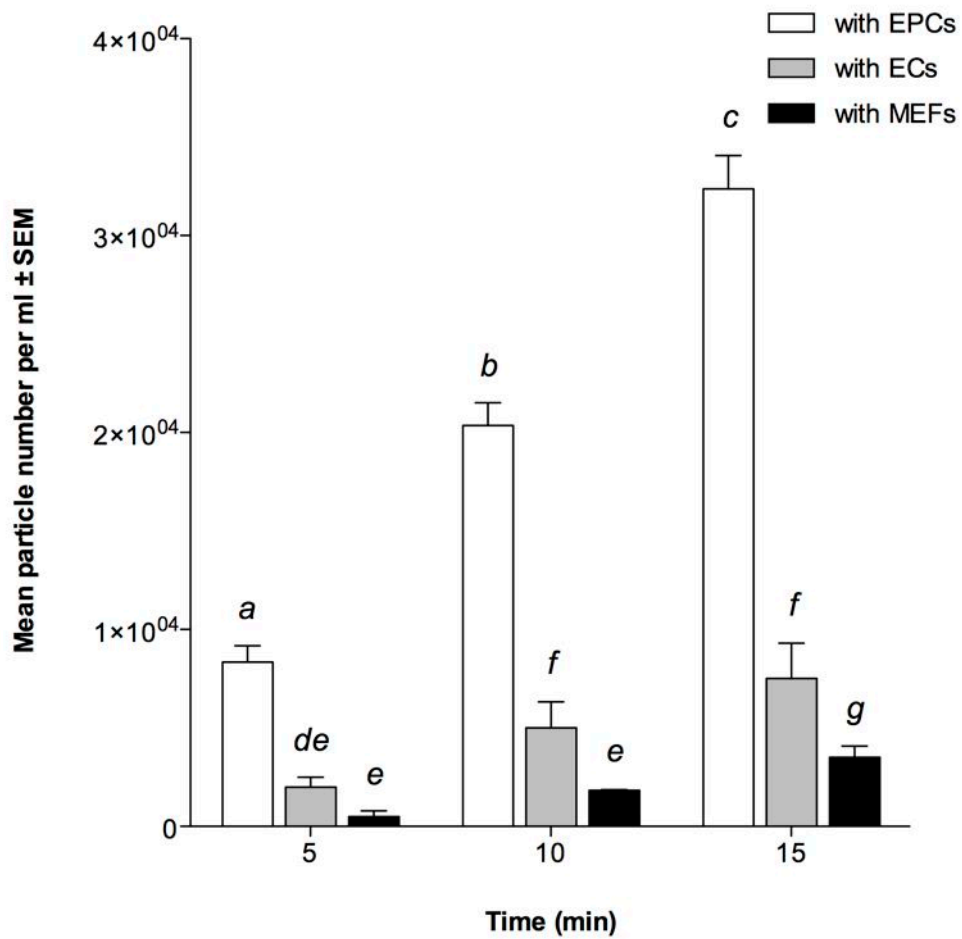


Figure 6.3. In vitro aggregation of EPCs, ECs and MEFs. After mixing 1×10^7 platelets with 1×10^6 cells, aggregate particles of 16-42 μm diameter were counted every 5 min using the Coulter Multisizer II system. Data presented as mean number of particles per ml of platelet-cell suspension \pm SEM ($n=3$). Columns with different letters as superscripts are significantly different from each other ($P < 0.05$).

by incubation of EPCs and ECs with DxSO_4 (**Fig. 6.4**). When treated with DxSO_4 both EPCs and ECs exhibited significantly less aggregation at each time-point than assays performed with untreated cells ($P < 0.01$). Conversely, the cell suspension treated with non-sulphated dextran exhibited platelet-cell aggregation equivalent to untreated cells, confirming the absence of an effect of the dextran carrier on selectin adhesion (data not shown). Although aggregation in DxSO_4 assays was significantly different to assays without DxSO_4 treatment, the number of platelet-cell aggregates was not observed to change significantly when DxSO_4 concentration was increased. There were no significant differences in the number of particles counted at each time-point for either cell line, suggesting the effect of DxSO_4 on aggregation was the same across the range of concentrations tested.

After non-specific selectin blockade, selective inhibition of a particular selectin subtype, P-selectin, was performed using a monoclonal blocking antibody (**Fig. 6.5**). Significantly less aggregation was observed, compared to untreated cells, in both EPC and EC assays ($P < 0.01$). The number of platelet-cell aggregates of both cell lines did not increase with time.

6.4.1.2 Inhibition of $\alpha\text{IIb}\beta_3$ integrin or platelet activation

First, blockade of platelet $\alpha\text{IIb}\beta_3$ integrin (GPIIb/IIIa) was performed using abciximab, to prevent binding *via* this receptor during the *in vitro* aggregation assay (**Fig. 6.6**). When treated with abciximab, neither aggregation of EPCs or ECs was observed to be significantly different to aggregation in control assays. The patterns of aggregation, shown by the number of 16-42 μm particles counted at each time-point, were the same as untreated controls: significant increases in platelet-EPC aggregates were seen at each time-point ($P < 0.05$) whilst only between 10 min and 15 min was the increase in EC aggregation determined to be statistically significant.

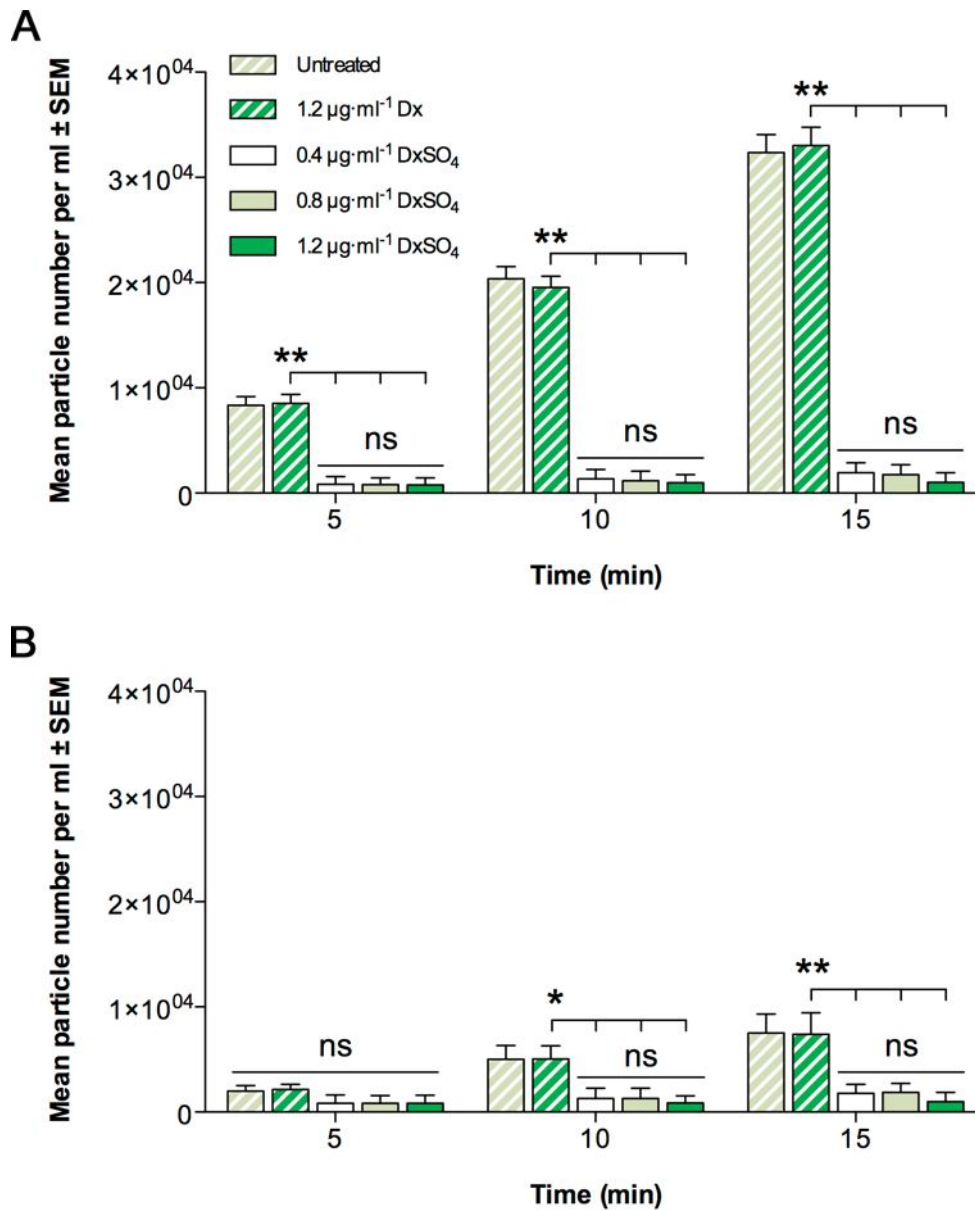


Figure 6.4. In vitro aggregation following non-specific selectin blockade. Performed by incubation of (A) EPCs and (B) ECs with 0.4, 0.8 or 1.2 $\mu\text{g}\cdot\text{ml}^{-1}$ DxSO₄ for 1 h at 37°C prior to assay. Control assays carried out with 1.2 $\mu\text{g}\cdot\text{ml}^{-1}$ dextran only (not shown). Data presented as mean number of 16-42 μm particles per ml \pm SEM (n=4), analysed by Coulter Multisizer II. Significant differences are indicated (* P <0.05, ** P <0.01 vs. untreated); ns, no significant difference from controls.

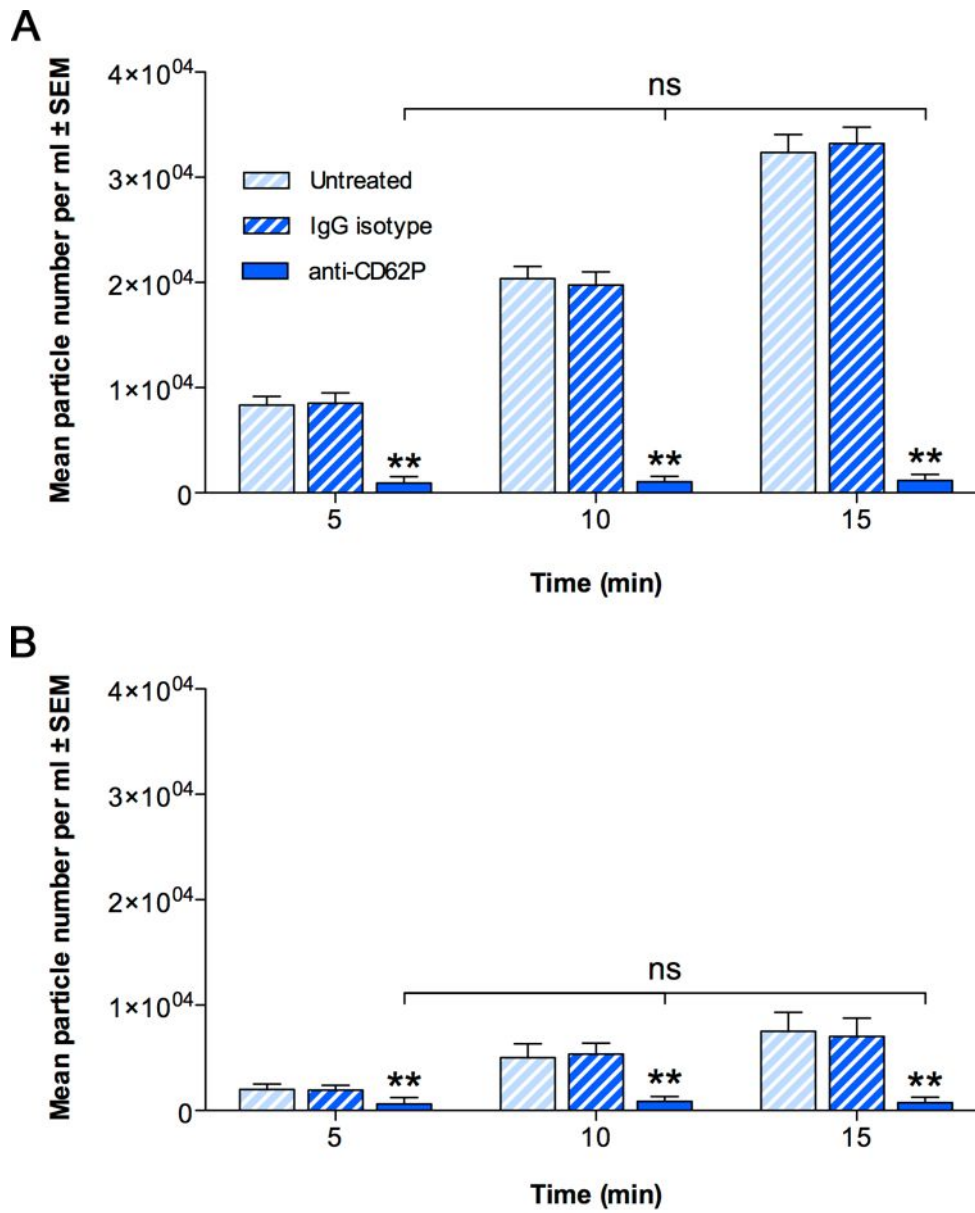


Figure 6.5. The effect of P-selectin blockade on in vitro aggregation of EPCs and ECs. Performed by incubation of cells and platelets with $10 \mu\text{g}\cdot\text{m}^{-1}$ rat anti-mouse CD62P antibody for 1 h at 37°C prior to assay. Control assays carried out with IgG isotype antibody (not shown). Data presented as mean number of $16\text{-}42 \mu\text{m}$ particles per ml \pm SEM ($n=4$). Significant differences are indicated (** $P<0.01$ vs. untreated); ns, no significant difference between time-points.

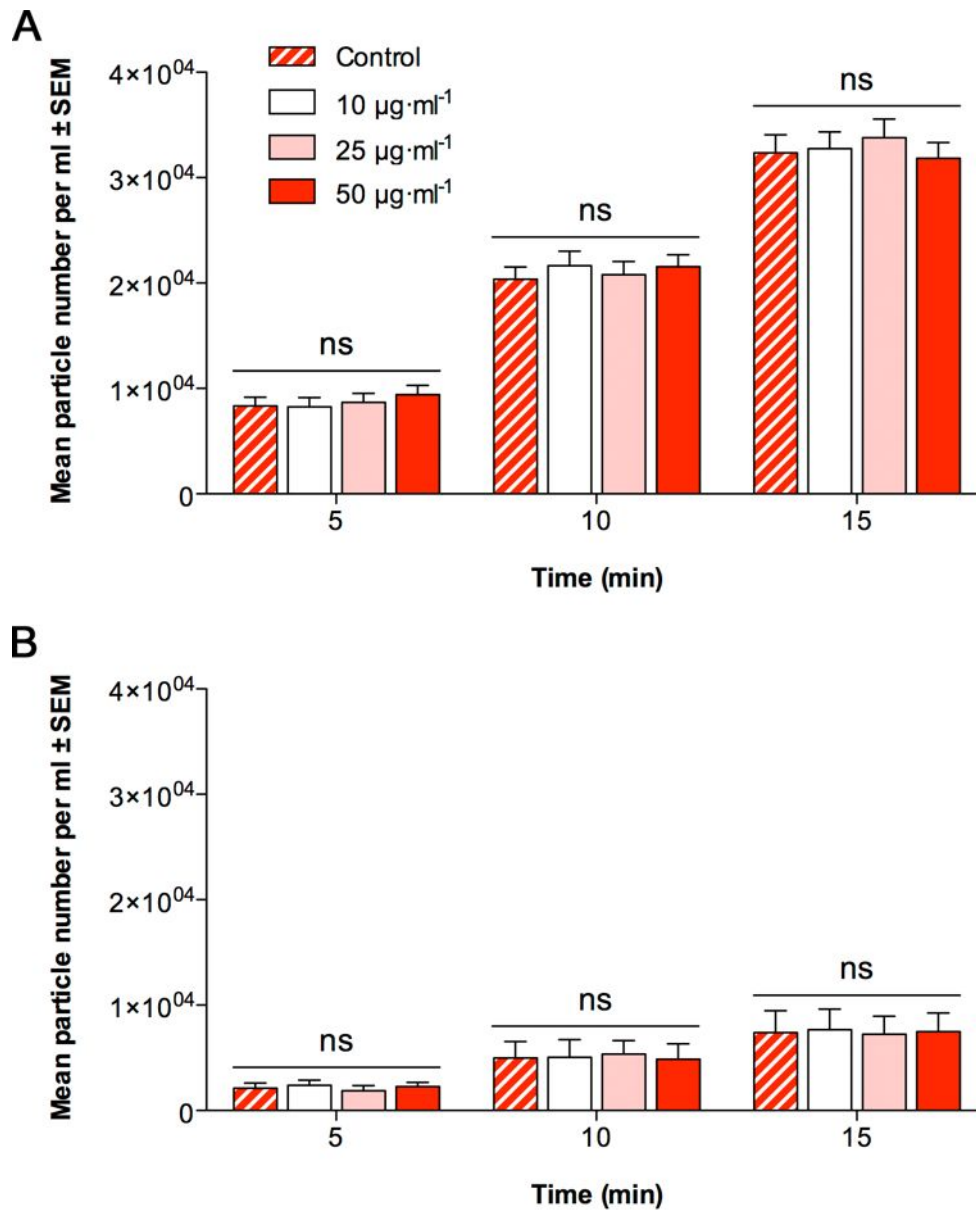


Figure 6.6. In vitro platelet-cell aggregation following blockade of $\alpha\text{IIb}\beta_3$ integrin with abciximab. Assay performed with (A) EPCs or (B) ECs after inhibition of binding via $\alpha\text{IIb}\beta_3$ integrin by treatment with 5, 10 or 15 $\mu\text{g}\cdot\text{ml}^{-1}$ abciximab for 45 min at 37°C. Data presented as mean number of 16-42 μm particles per ml \pm SEM ($n=4$); ns, no significant difference from controls.

Next, activation *via* ADP and TXA₂ production were blocked using a combined treatment of clopidogrel and aspirin (**Fig. 6.7**). Treatment of platelets with combined clopidogrel and aspirin did not have a significant effect on platelet-cell aggregation in assays of either EPCs or ECs. At each time-point the numbers of platelet-EPC and platelet-EC aggregates were equivalent to those observed in untreated control assays, with the same significant increases in aggregation between all time-points for EPCs and between 10 min and 15 min for ECs.

6.4.2 *In vitro* flow adhesion assay

Following investigations of cell aggregation, further studies into platelet-EPC interactions were carried out using an *in vitro* flow adhesion assay. Freshly isolated murine platelets were immobilised on glass capillary microslides, over which cells were perfused for 5 min. After washing unbound cells from the microslide, adherent cells were counted to quantify adhesion to platelets from flow. Initially, EPCs and ECs were perfused across immobilised platelets across a range of wall shear stresses (**Fig. 6.8**). Flow adhesion of MEFs was also investigated, as with *in vitro* aggregation, as a non-endothelial cell type.

At a wall shear stress of 0.025 Pa, EPCs exhibited significantly greater adhesion to immobilised platelets (15.69 ± 0.51) than ECs (7.77 ± 0.24) or MEFs (6.02 ± 0.19 ; $P < 0.01$). However, when wall shear stress was increased to 0.05 Pa, EPC adhesion was significantly reduced (1.03 ± 0.28 ; $P < 0.01$) compared to adhesion at 0.025 Pa, with no significant

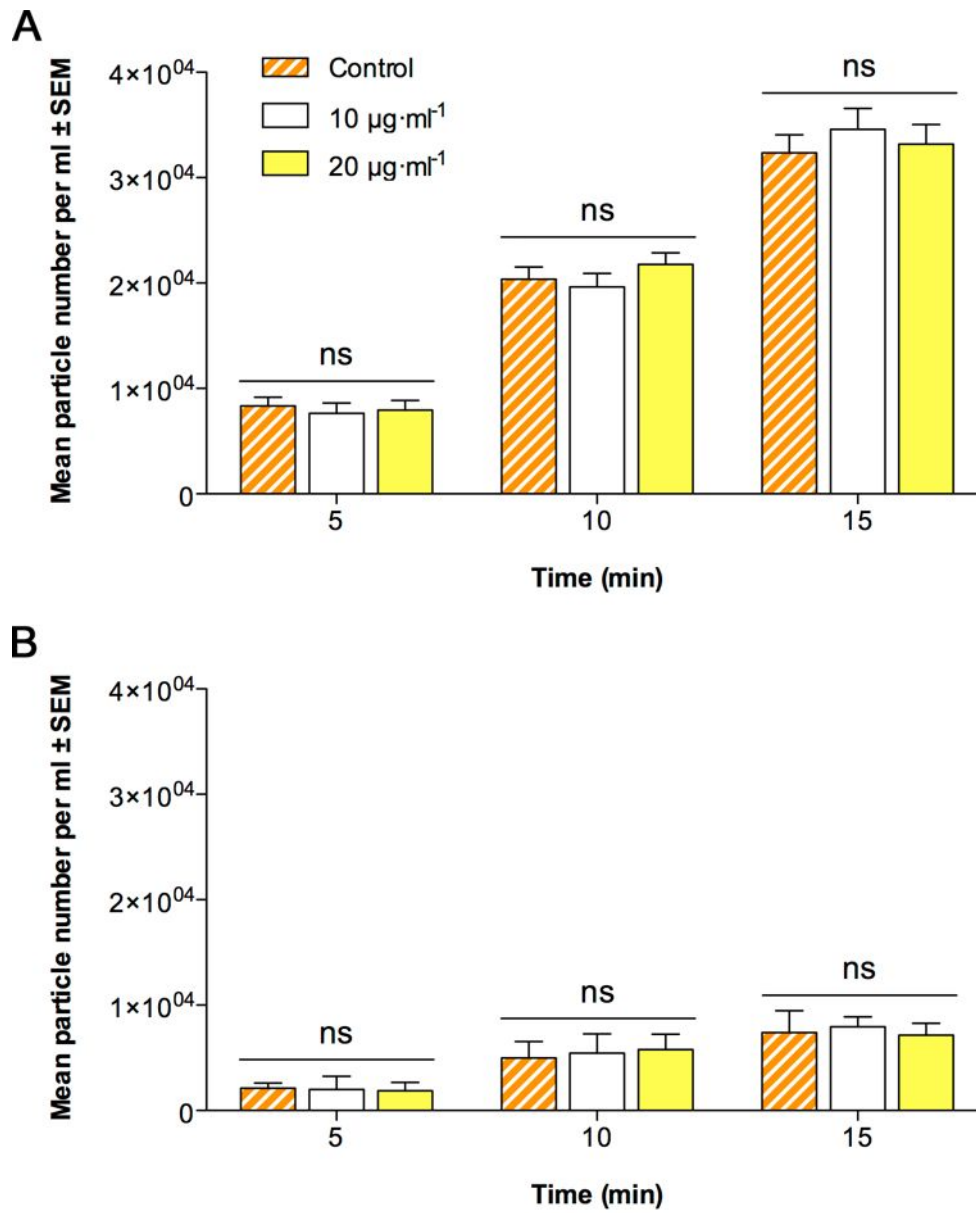


Figure 6.7. In vitro aggregation following clopidogrel/aspirin treatment. Assay performed with (A) EPCs or (B) ECs after incubation of platelets with 10 or 20 $\mu\text{g}\cdot\text{ml}^{-1}$ each of combined clopidogrel and aspirin for 45 min at 37°C. Data presented as mean number of platelet-cell aggregates per ml \pm SEM ($n=4$); ns, no significant difference from controls.

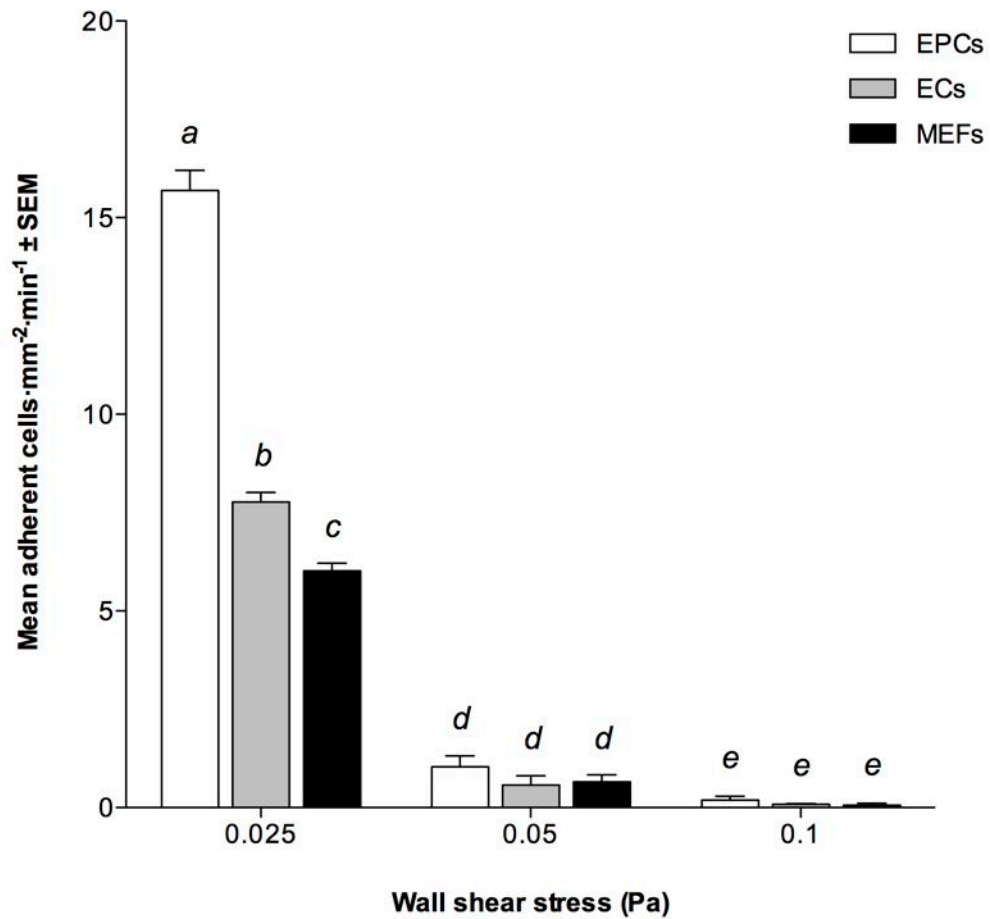


Figure 6.8. In vitro adhesion of EPCs, EC and MEFs to platelets under flow conditions. 2×10^6 cells suspended in 0.15% PBSA perfused for 5 min at wall shear stress of 0.025, 0.05 or 0.1 Pa. Quantification from fourteen random fields of view along the centre-line of the microslide. Data presented as mean adherent cells per mm² of microslide per min of perfusion \pm SEM, $n=3$; columns with different letters as superscripts are significantly different from each other ($P < 0.01$).

differences between adherent EPCs and the number of adherent ECs (0.58 ± 0.23) or MEFs (0.66 ± 0.18 ; n.s.). When wall shear stress was further increased to 0.1 Pa, adhesion of all three cell types was reduced to negligible levels (0.19 ± 0.1 , 0.09 ± 0.02 and 0.06 ± 0.05 for EPCs, ECs and MEFs, respectively) and consequently no significant differences were seen between cell types.

With the adhesion of EPCs and ECs to platelets under flow conditions having been demonstrated, the strength of attachment was investigated by increasing the flow rate of PBSA wash buffer for 10 min after cell adhesion and counting the remaining adherent cells (**Fig. 6.9**). Once adhered to immobilised platelets, neither EPCs or ECs appeared to be significantly affected by increasing wall shear stress. When PBSA buffer was perfused across adherent cells at 0.025 Pa (the wall shear stress previously shown to give maximum adherence across the range tested) negligible detachment of either cell type was observed. Similarly, when wall shear stress was increased to 0.2 Pa or 0.6 Pa, the number of adherent cells was not significantly different from the number observed prior to washing, or from the number of adherent cells after washing at 0.025 Pa.

6.4.2.1 Blockade of selectin-mediated adhesion

Similarly to those performed using the *in vitro* aggregation assay, selectin blockade experiments were carried out using the flow adhesion system. First, DxSO_4 was used for non-specific inhibition of selectin-mediated adhesion (**Fig. 6.10**). The binding of both EPCs and ECs to platelets from flow showed dose-dependent decreases when treated with DxSO_4 , compared to both untreated controls and those treated with non-sulphated dextran. Firstly, there was no significant difference between the number of adherent EPCs (14.7 ± 1.7) or the number of adherent ECs (8.1 ± 1.4) in untreated assays compared to the number of

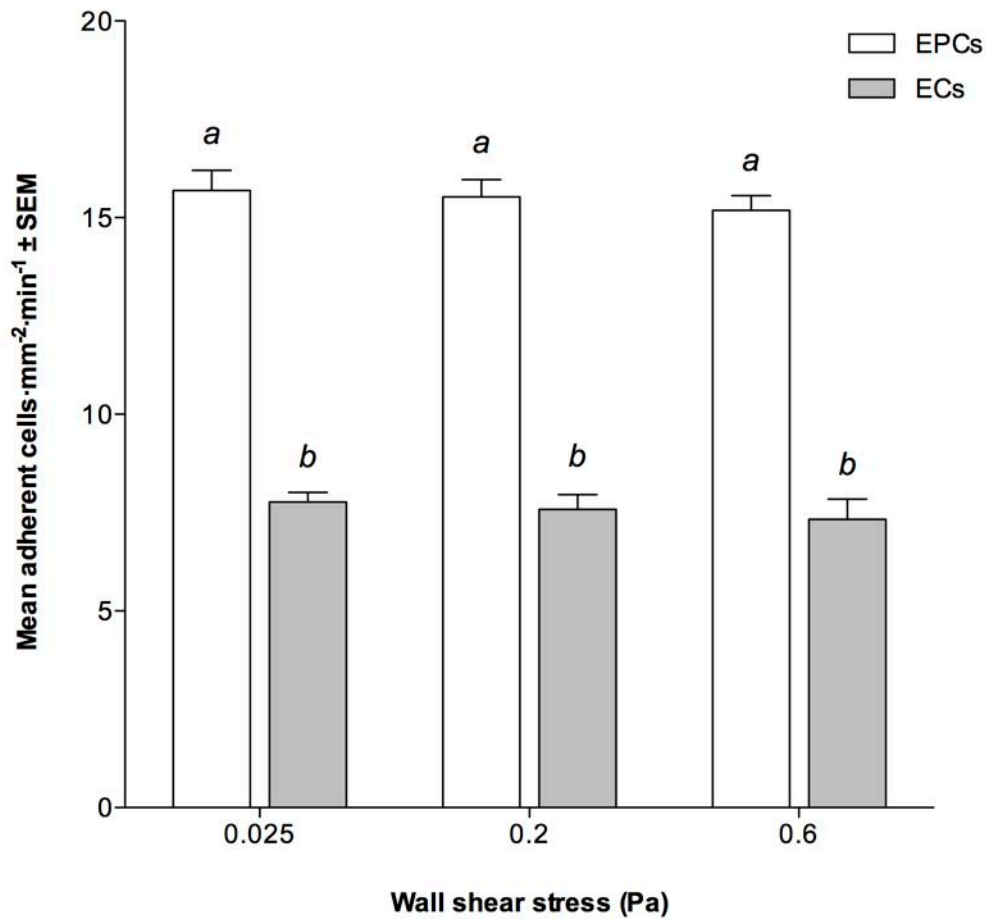


Figure 6.9. In vitro flow adhesion of EPCs and ECs with increasing shear stress. Adherent cells subjected to wall shear stress of 0.025, 0.2 or 0.6 Pa after washing stage of flow adhesion assay. Data from fourteen fields of view, presented as mean adherent cells per mm² of microslide per min of perfusion ± SEM, n=3; columns with different letters as superscripts are significantly different from each other (P<0.01).

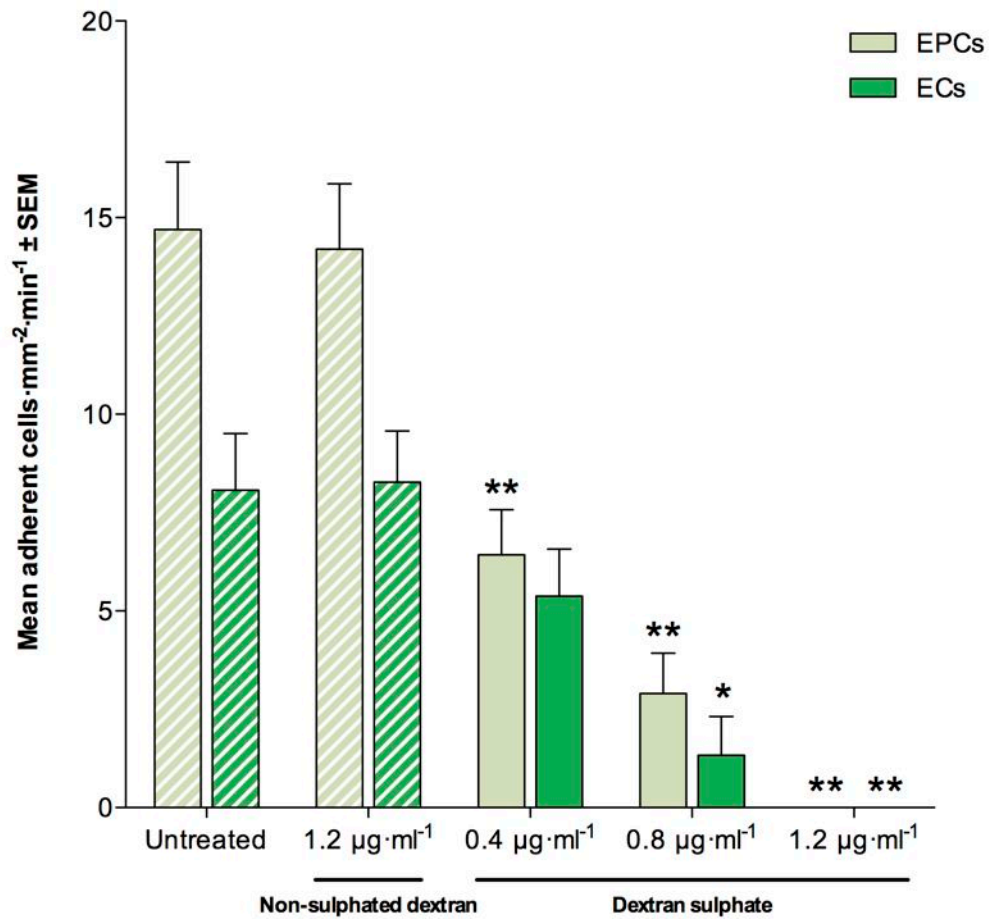


Figure 6.10. In vitro flow adhesion of EPCs and ECs following selectin blockade. Performed by incubation with dextran sulphate for 1 h at 37°C prior to perfusion of 2×10^6 cells for 5 min at wall shear stress of 0.025 Pa. Control assays with untreated cells or with $1.2 \mu\text{g}\cdot\text{ml}^{-1}$ dextran only (striped columns). Data as adherent cells per mm^2 per min (mean \pm SEM, $n=4$) with significant differences indicated (* $P < 0.05$, ** $P < 0.01$ vs. untreated cell type control).

EPCs (14.2 ± 1.6) or ECs (8.3 ± 1.3) adhered from flow in assays treated with dextran only. However, when treated with $0.4 \mu\text{g}\cdot\text{ml}^{-1}$ DxSO_4 a reduction in adhesion was observed for both EPCs (6.4 ± 1.1 ; $P < 0.01$) and ECs (5.4 ± 1.2 ; n.s.). As DxSO_4 concentration was increased to $0.8 \mu\text{g}\cdot\text{ml}^{-1}$, further decreases in adhesion were observed for both EPCs (2.9 ± 1.0 ; $P < 0.01$) and ECs (1.3 ± 1.0 ; $P < 0.05$) compared to controls. At a final concentration of $1.2 \mu\text{g}\cdot\text{ml}^{-1}$ no adhesion of either cell type was seen.

As previously performed using *in vitro* aggregation, an anti-CD62P antibody was used to inhibit P-selectin binding (**Fig. 6.11**). There were no significant differences observed in the number of adherent EPCs (15.7 ± 0.5) or ECs (7.8 ± 0.4) treated with IgG isotype antibody, when compared to the same cell type in untreated control experiments. When cells only were treated with $5 \mu\text{g}\cdot\text{ml}^{-1}$ blocking antibody, slight reductions in the number of adherent EPCs (14.0 ± 1.1) and ECs (6.1 ± 0.5) was observed compared to controls (n.s.). However when the antibody concentration was increased to $10 \mu\text{g}\cdot\text{ml}^{-1}$, significant decreases were observed for both EPCs (6.7 ± 0.7 ; $P < 0.01$) and ECs (5.0 ± 0.8 ; $P < 0.05$). Following dual blockade, when both platelets and cells were treated with $10 \mu\text{g}\cdot\text{ml}^{-1}$ antibody, the greatest decreases in adhesion of EPCs (0.8 ± 0.4) and ECs (1.5 ± 0.4) were observed, compared to controls ($P < 0.01$).

6.4.2.2 Inhibition of GPVI binding

Prior to platelet isolation, mice were antibody-treated to shed GPVI from the platelet surface (SEE 2.8.3) and a 70% reduction of surface GPVI was confirmed by flow cytometry (**Fig. 6.12A**). The shedding of platelet GPVI had no significant effect on the number of adherent EPCs (14.7 ± 0.9) or ECs (8.1 ± 0.3) compared to control assays performed using EPCs (15.7 ± 0.4) or ECs (7.7 ± 0.2) with control platelets (**Fig. 6.12B**).

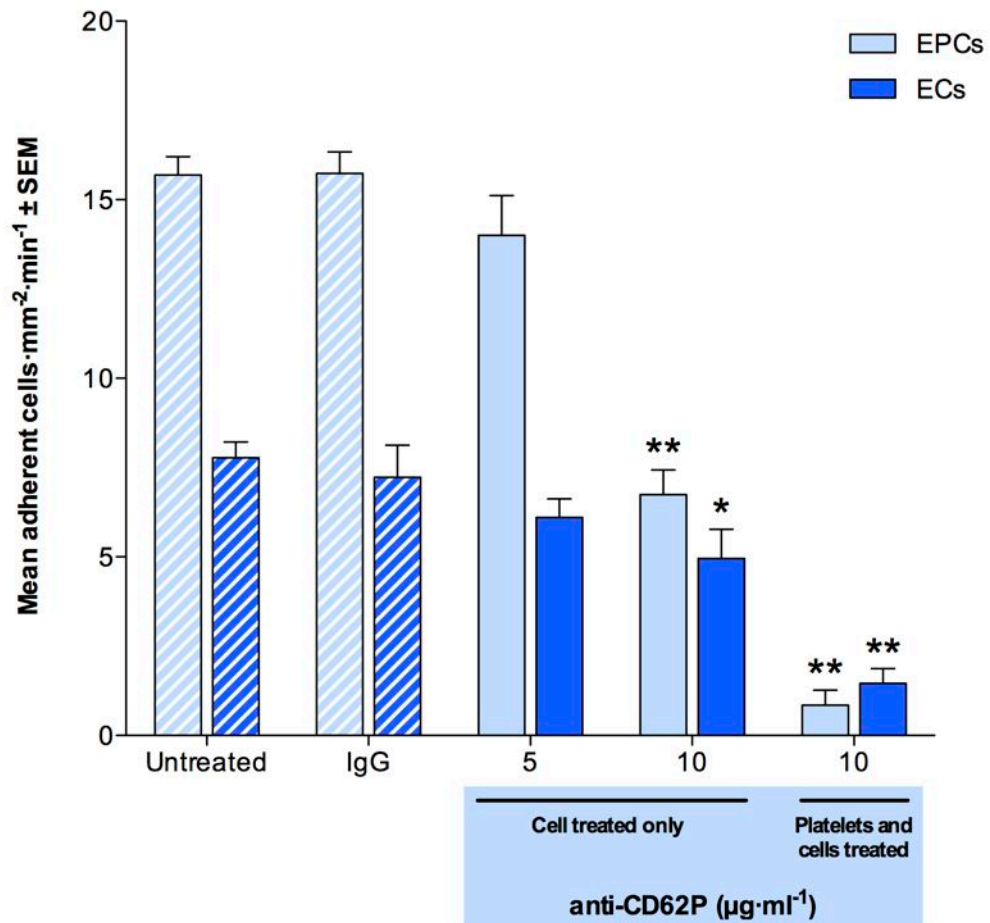


Figure 6.11. The effect of P-selectin blockade on in vitro flow adhesion of EPCs and ECs. By treatment of cells with 5 or 10 $\mu\text{g}\cdot\text{ml}^{-1}$, or cells and platelets with 10 $\mu\text{g}\cdot\text{ml}^{-1}$ blocking antibody. Control assays with untreated cells or IgG isotype antibody (striped columns). Data as adherent cells per mm^2 per min (mean \pm SEM, $n=4$); * $P<0.05$, ** $P<0.01$ vs. untreated cell type control.

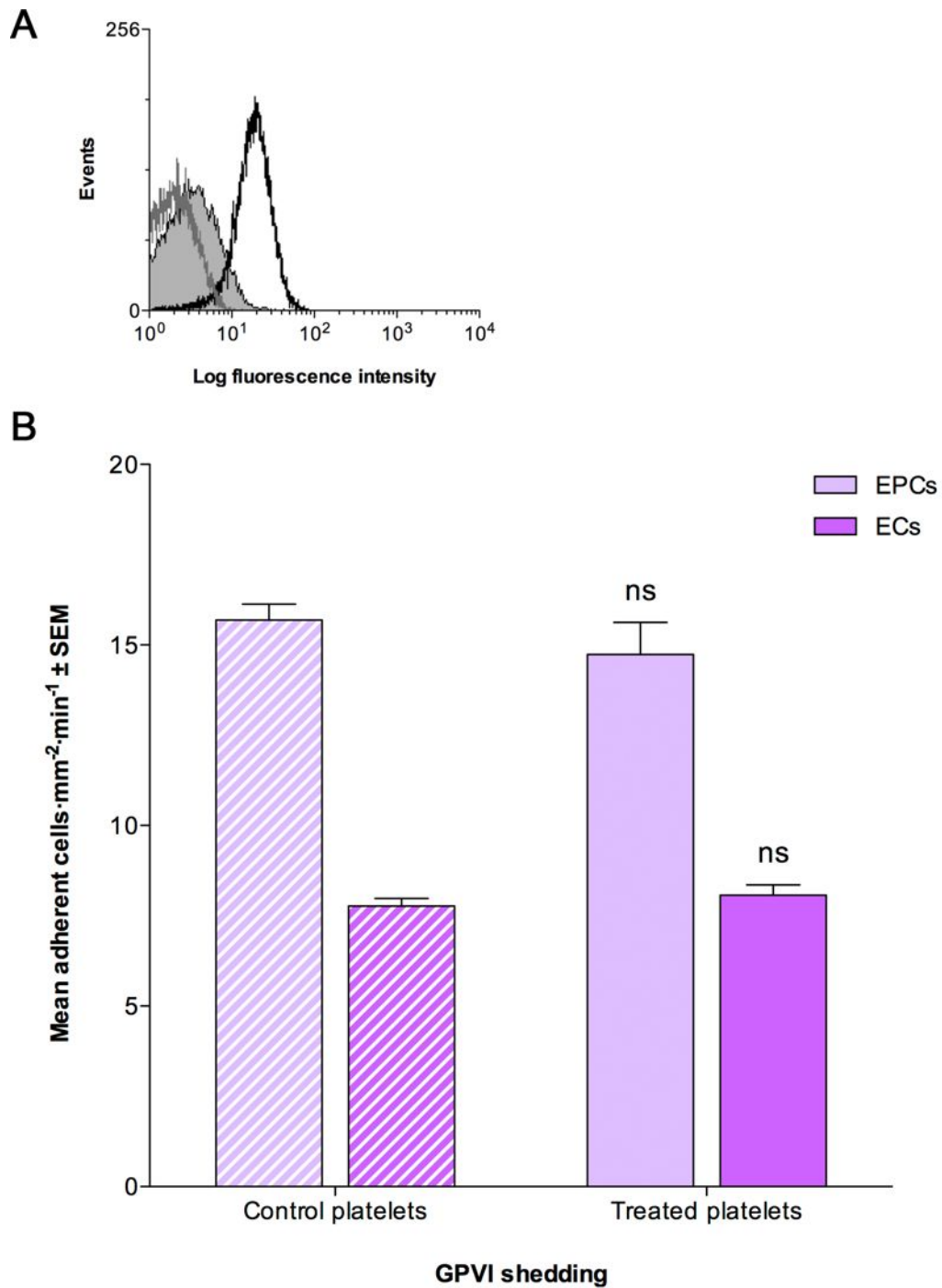


Figure 6.12. In vitro flow adhesion of EPCs and ECs following platelet GPVI shedding. (A) 70% GPVI shedding (shaded grey) compared to untreated (black) was confirmed by flow cytometry, with IgG isotype control (outlined grey) (B) Control assays performed using control platelets (striped columns). Data presented as adherent cells per mm² per min (mean ± SEM, n=4); ns, no significant difference vs. same cell type control.

6.4.2.3 Inhibition of platelet activation

As with *in vitro* aggregation assays, the inhibition of $\alpha\text{IIb}\beta\text{3}$ binding by abciximab treatment had no effect on platelet-cell binding, as determined by adhesion of EPCs and ECs from flow (**Fig. 6.13**). There were no significant differences between the numbers of adherent cells, of either cell type, in assays using abciximab at any concentration and those in control assays using untreated platelets. Similarly, a combined of platelets with clopidogrel and aspirin prior to cell perfusion had no significant effect on flow adhesion of either EPCs or ECs compared to control (**Fig. 6.14**).

6.4.3 Adherent cell spreading assay

To further understand the influence of platelets on EPCs during and after recruitment from flow, cell spreading assays were carried out. In addition to control assays using standard PBSA buffer and an immobilised platelet monolayer, assays were also performed in the presence of thrombin and prostacyclin, as well as using microslides pre-coated with murine P-selectin instead of immobilised platelets. The numbers of adherent EPCs in thrombin assays (16.1 ± 0.5) and assays performed using immobilised P-selectin (14.9 ± 0.6) were not significantly from untreated control assays (15.7 ± 0.5) (**Fig. 6.15**). However, a significant reduction in EPC adhesion was observed with prostacyclin treatment (6.5 ± 0.3 ; $P < 0.01$). In control assays, the mean cell area of adherent EPCs ($284 \pm 18 \mu\text{m}^2$) was seen to increase significantly over the 3 h period of observation following binding to immobilised platelets from flow ($619 \pm 14 \mu\text{m}^2$; $P < 0.01$) (**Fig. 6.16**). When stimulated by thrombin, the area of adherent cells increased at a similar rate, although with increased cell area compared to controls at 110 min ($530 \pm 30 \mu\text{m}^2$), 140 min ($596 \pm 38 \mu\text{m}^2$), 160 min ($634 \pm 23 \mu\text{m}^2$) and 170 min ($656 \pm 20 \mu\text{m}^2$; all $P < 0.05$). At 180 min the area of thrombin-stimulated EPCs ($651 \pm 21 \mu\text{m}^2$) was not significantly different from untreated cells. In contrast to both control

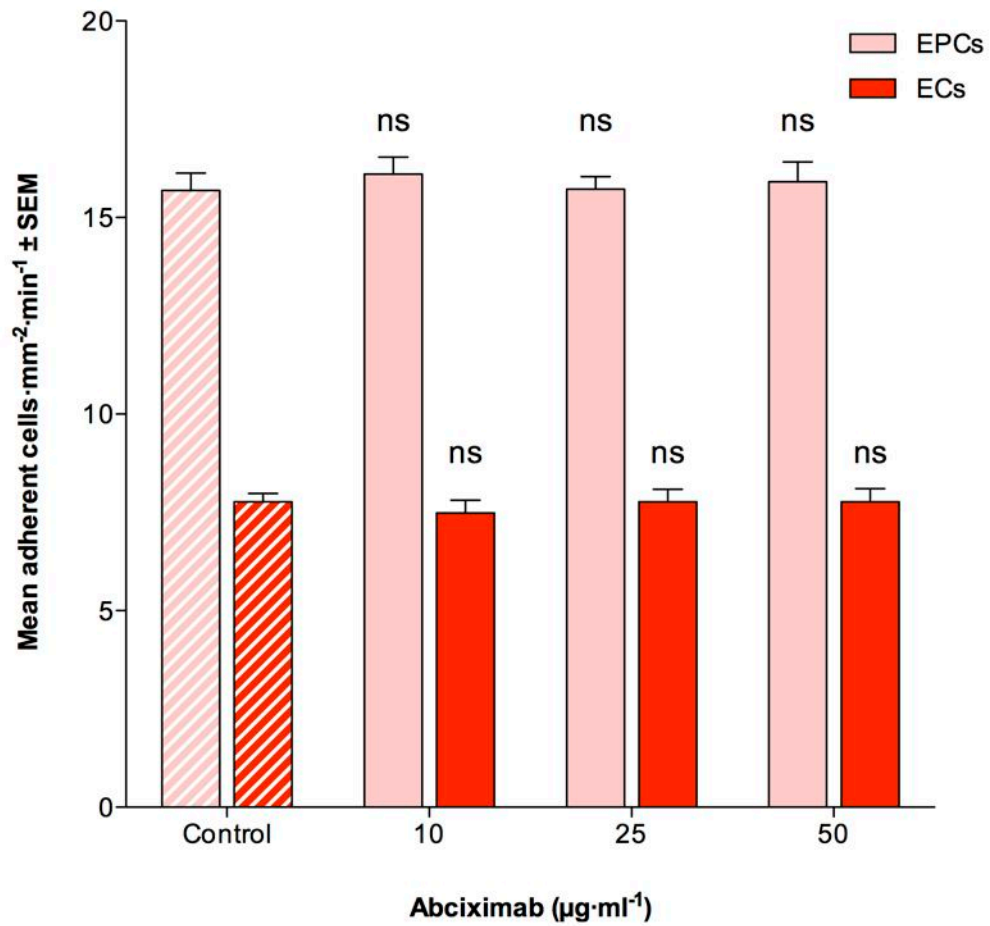


Figure 6.13. The effect of abciximab on in vitro flow adhesion of EPCs and ECs. Platelet $\text{aIIb}\beta 3$ blockade by 10, 25 or 50 $\mu\text{g}\cdot\text{ml}^{-1}$ abciximab for 45 min prior to platelet immobilisation. Control assays performed using untreated platelets (striped columns). Data presented as mean adherent cells per mm^2 per min (mean \pm SEM, $n=4$); ns, no significant difference from same cell type control.

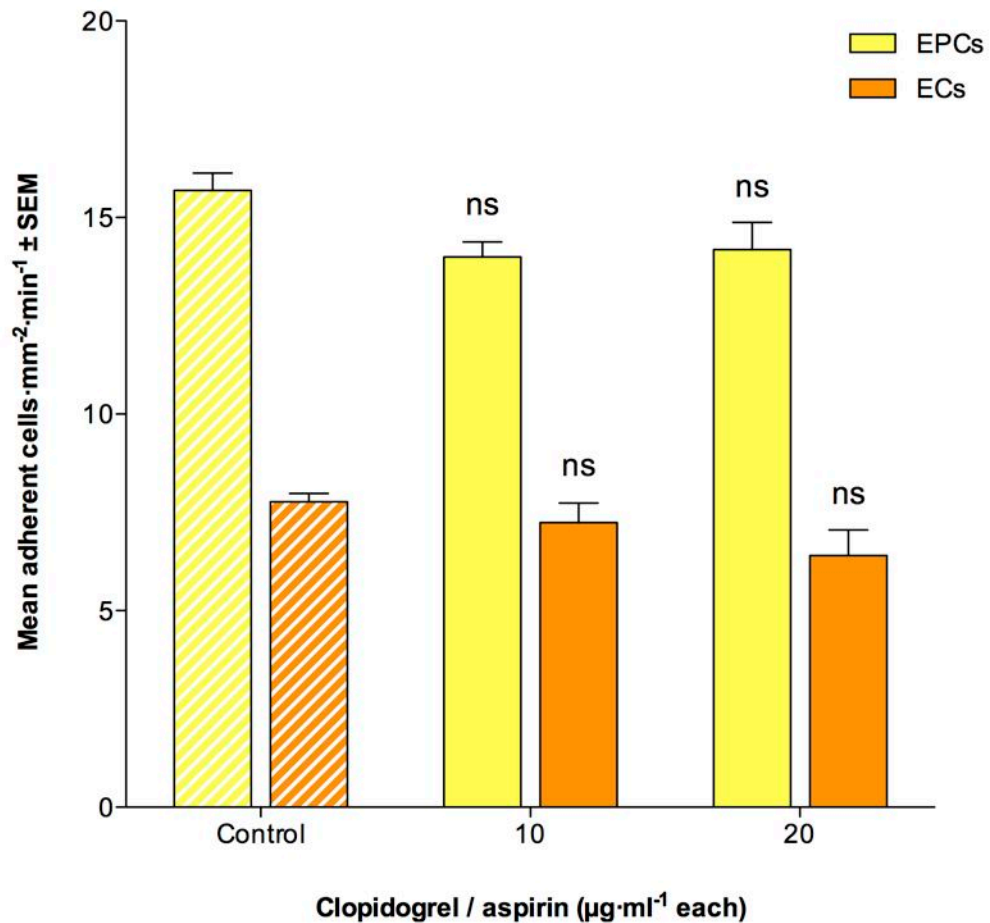


Figure 6.14. The effect of clopidogrel/aspirin on in vitro flow adhesion of EPCs and ECs. Combined treatment of platelets with 10 or 20 µg·ml⁻¹ each of clopidogrel and aspirin for 45 min prior to immobilisation. Control assays using untreated platelets (striped columns). Data presented as mean adherent cells per mm² per min (±SEM, n=4); ns, no significant difference from same cell type control.

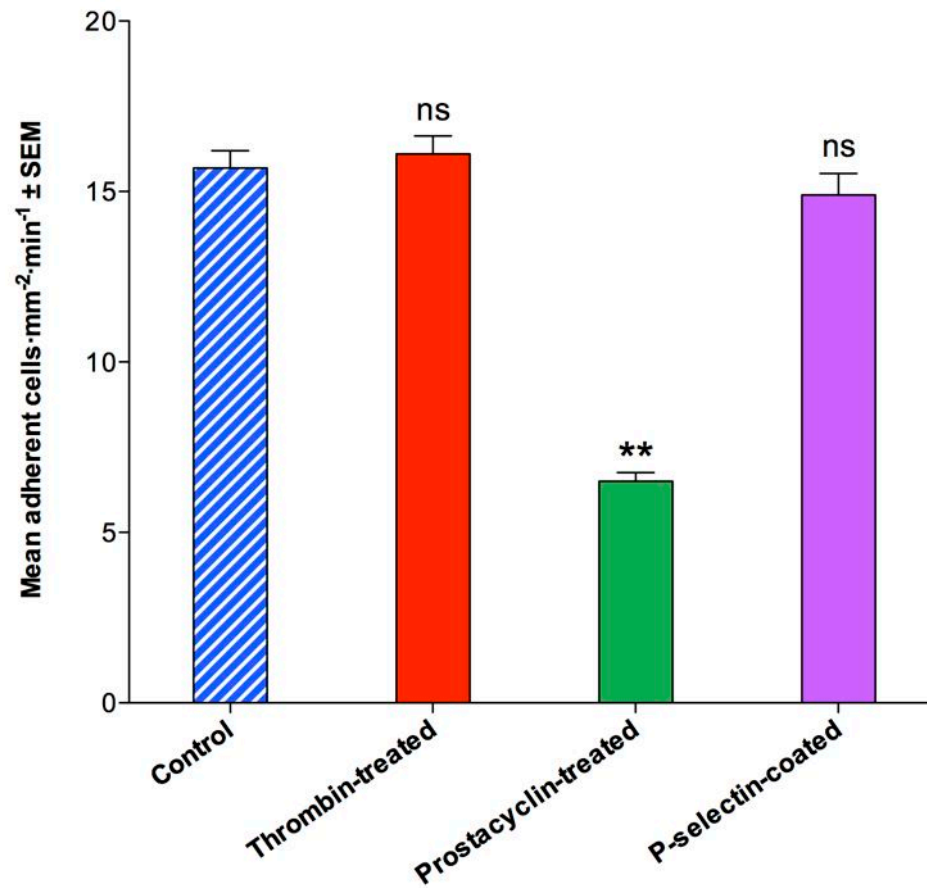


Figure 6.15. In vitro flow adhesion of EPCs prior to adherent cell spreading assays. Performed by perfusion of 2×10^6 thrombin- or prostacyclin-treated EPCs over a murine platelet monolayer or 2×10^6 untreated EPCs over purified P-selectin for 5 min at wall shear stress of 0.025 Pa. Control assays performed using platelet monolayer and untreated cells (striped column). Data presented as adherent cells per mm² per min (mean ± SEM, n=4) with significant differences indicated (** $P < 0.01$ vs. control; ns, no significant difference).

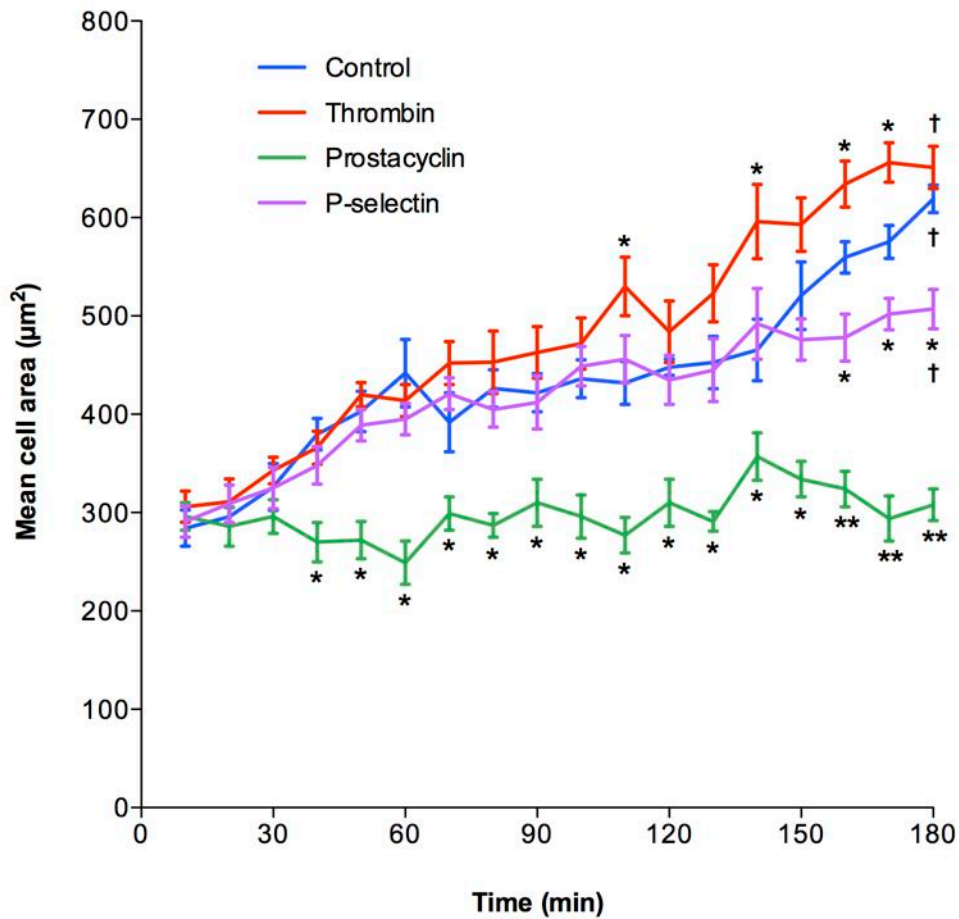


Figure 6.16. Spreading of adherent EPCs following in vitro flow adhesion assays. Performed on immobilised platelets with 0.15% PBSA (control), $1 \text{ U}\cdot\text{ml}^{-1}$ thrombin or $10 \text{ }\mu\text{g}\cdot\text{ml}^{-1}$ prostacyclin, or with P-selectin-coated microspheres and PBSA only. Data presented as mean cell area (mean \pm SEM, $N = 30$ cells, $n = 4$ replicates) with significant differences indicated (* $P < 0.05$, ** $P < 0.01$ vs. control at same time-point; † $P < 0.01$ vs. cell area at 10 mins).

and thrombin-treated assays, cell area did not increase significantly over time when EPCs were perfused with PBSA and prostacyclin. With prostacyclin, area was significantly different from control EPCs between 40 min and 180 min ($P < 0.05$). In assays performed using microslides coated with P-selectin, the rate of EPC spreading was comparable with assays using immobilised platelets, although cell area was significantly less than that of control EPCs at 160 min ($478 \pm 24 \mu\text{m}^2$), 170 min ($502 \pm 15 \mu\text{m}^2$) and 180 min ($507 \pm 20 \mu\text{m}^2$; all $P < 0.05$).

In addition to the measurement of spreading cell area, migration of individual EPCs was determined at each time-point (**Fig 6.17A**) and polar plots of final cell positions produced (**Fig. 6.17B**). Traces of EPC migration were generated using individual cell positions at each time-point and were similar in all four assays: for every cell the path of migration followed the direction of flow, and the apparent degree of path tortuosity was similar for the majority of cells under all conditions. EPC migration was also assessed quantitatively using two criteria: (i) net distance travelled and (ii) lateral movement during migration. The net cell migration distance was not significantly different between control EPCs ($21.7 \pm 0.7 \mu\text{m}$) and those treated with thrombin ($23.3 \pm 1.1 \mu\text{m}$), although a significant decrease in migration distance was observed in the presence of prostacyclin ($17.9 \pm 0.6 \mu\text{m}$, $P < 0.05$). Mean EPC migration distance on microslides coated with P-selectin ($22.5 \pm 0.3 \mu\text{m}$) was similar to that in control assays (n.s.). The amount of lateral movement during migration was measured by the angle of deviation from the axis of flow. As with migration distance, the maximum angular deviation was not significantly different between control ($\pm 55^\circ$), thrombin ($\pm 48^\circ$) and P-selectin ($\pm 51^\circ$) assays. Conversely, in assays of prostacyclin-treated EPCs, in which the lowest migration distance was observed, the maximum angle of deviation was determined to be significantly greater than in control or other assays ($\pm 69^\circ$; $P < 0.05$).

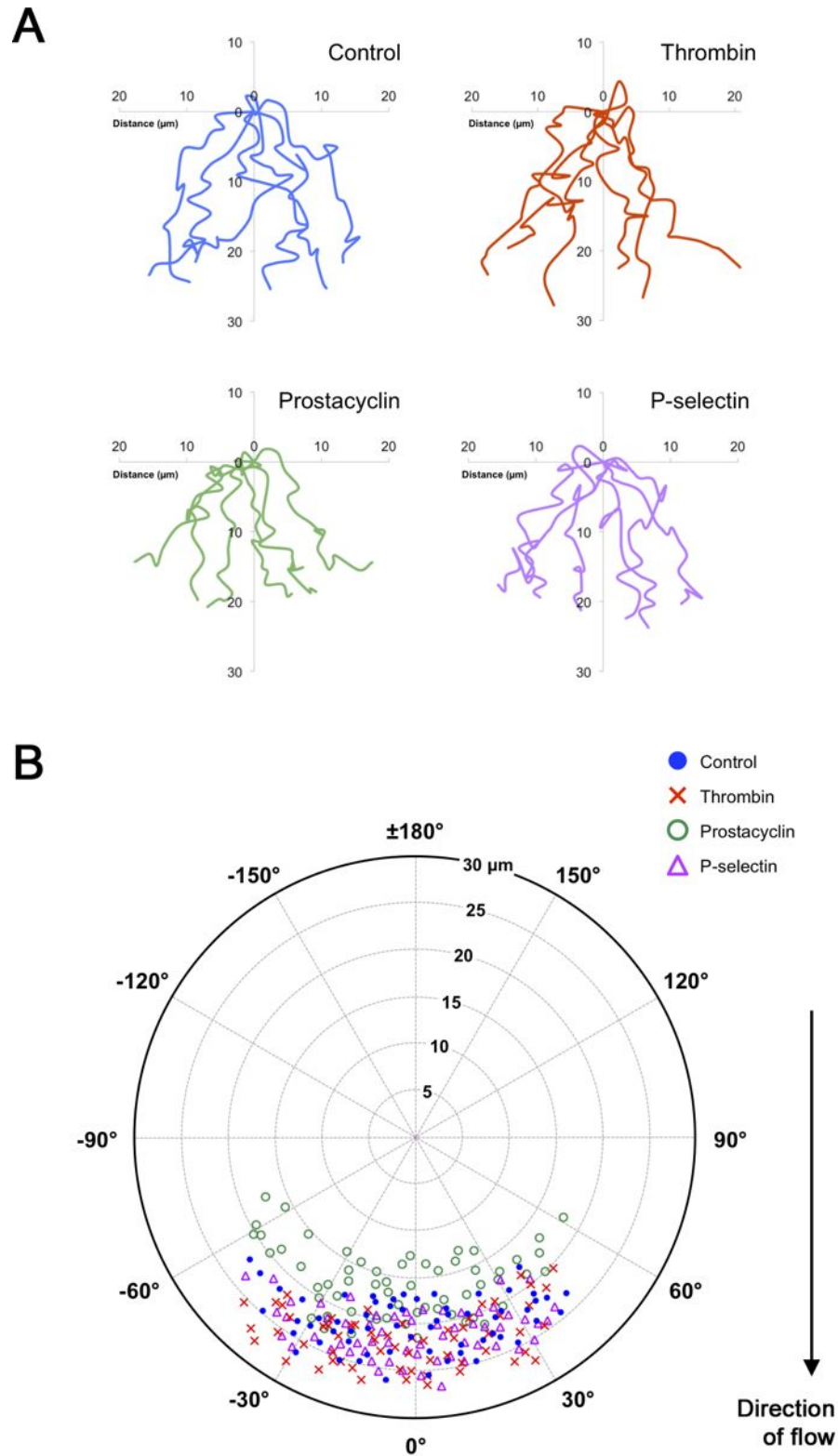


Figure 6.17. EPC migration during adherent cell spreading assays. (A) Traces showing the path of migration of six random cells from each of control, thrombin, prostacyclin and P-selectin assays, observed over 3 h and presented relative to their starting position. **(B)** Polar plot showing final cell position of sixty random cells from each assay, presented as distance (μm) from origin and angle of deviation from axis of flow (0°).

6.5 Discussion

Circulating EPCs are implicated in the angiogenic response to endothelial damage and the maintenance of vascular integrity, while increasing evidence suggests a positive role for platelets in EPC recruitment during angiogenesis (Ding *et al.*, 2007). It is proposed that platelets may adhere to the vessel wall, forming a bridge between circulating EPCs and the activated endothelium, aiding localisation of EPCs to the site of neovascularisation (de Boer *et al.*, 2006).

Here, platelet-EPC binding was first investigated using a simple *in vitro* cell-based aggregation assay, whereby a mixed preparation of murine platelets and EPCs was gently stirred and the extent of particulate aggregation determined. Then, using a flow-based adhesion assay, EPC recruitment was studied under flow conditions, by adhesion of perfused cells to platelets immobilised to glass microslides. Adherent cell spreading assays were also carried out to investigate the behaviour of cells after recruitment, given that increased spreading after adhesion might aid persistence of adhered EPCs at sites of angiogenesis.

The amount of platelet-cell aggregation observed over the 15 min aggregation assay period was significantly greater in EPCs than in ECs or MEFs, suggesting the existence of a mechanism for platelet-endothelial binding, and a preferential binding to EPCs in particular. That platelet-mediated cell aggregation, at least when studied in this manner, is more specific to endothelial phenotypes than other cell types, considering the negligible aggregation observed with fibroblasts, is also suggested. This correlates with the established role of platelets as thrombotic agents, given that a critical stage in the platelet attachment to damaged endothelium is the formation of tethering bonds between platelet glycoprotein receptor Iba and the A1 domain of surface vWF (Mody *et al.*, 2005), and that vWF has been

identified on the EPC surface (Rafii, 2000). Furthermore, CD31, which is found on both the EPC and platelet surfaces, has been shown to mediate adhesion interactions by homophilic contact and heterophilic binding with platelet $\alpha_v\beta_3$ integrin (Piali *et al.*, 1995).

When perfused through capillaries, as in the aggregation assay, EPCs exhibited far greater adhesion to immobilised platelets compared to ECs and MEFs, although attachment was rare at wall shear stresses above 0.025 Pa. Shear stress has a significant effect on cell behaviour *in vivo* and endothelial tubule formation *in vitro* (Tressel *et al.*, 2007), and adhesion of EPCs to platelets from flow appears to be sensitive to changes in shear stress. Mean shear stress has been shown to vary greatly between vascular beds, from high shear stress of around 1.2 Pa in the common carotid artery to relatively low shear stresses of 0.4 to 0.5 Pa in the femoral and brachial arteries (Dammers *et al.*, 2003). Shear stresses are also low in post-capillary venules, importance sites of angiogenesis, demonstrating shear stresses of around 0.2 Pa (Zhao, Y *et al.*, 2001). Furthermore, fluid shear stresses around tissue islands in the developing chick CAM (similar to the intravascular pillars generated during intussusceptive angiogenesis) have been measured at less than 0.1 Pa (Lee, GS *et al.*, 2010). In other flowing cell recruitment models, such as adhesion of flowing isolated leukocytes to immobilised selectins, efficient binding has been demonstrated at wall shear stresses between 0.05 and 0.1 Pa (Lawrence & Springer, 1991; Buttrum *et al.*, 1993). In this study, EPC recruitment was only observed at shear stresses below 0.05 Pa, with the greatest number of adherent cells at 0.025 Pa, shear stresses lower than those at which leukocytes have been shown to adhere. However, different forces acting upon these different cell types may be important. The force exerted on a cell adhering to the endothelium is directly related to the shear stress generated as blood flows through the vessel: as shear stress increases, the force acting on the cell also increases. Furthermore, the force increases with increasing cell size (Tees & Goetz, 2003). Therefore,

flowing blood generating the same shear stress will exert a reduced force on a relatively small cell such as a neutrophil (10-12 μm diameter) compared to a larger cell such as an EPC (16-18 μm diameter). In addition, owing to its larger size, the centroid of a flowing EPC cannot approach as close to the endothelium as the smaller neutrophil, increasing its velocity as it effectively travels within a faster moving layer of fluid further from the wall. The increased force acting on the EPC, compounded by its travelling relatively fast, reduces the amount of sustained contact between the EPC and the endothelium and increases the likelihood of breaking any formed bond, which in turn reduces the likelihood of successful binding for a given shear stress compared to a smaller cell. Indeed, changes in cell size (and the differential forces experienced) have been shown to significantly influence flow adhesion across a particle diameter range of 5-20 μm , the typical range of sizes of circulating cells that may adhere to the endothelium (Patil *et al.*, 2001).

Correlating data from aggregation and flow adhesion assays suggest that selectins, and the P-selectin subtype in particular, mediate the attachment of EPCs to the endothelium. When platelet P-selectin was blocked using sulphated dextran or anti-CD62P antibody the number of platelet-EPC aggregates or adherent EPCs (in the aggregation and flow adhesion assays, respectively) was markedly reduced. However, perhaps the most obvious illustration of the role of P-selectin comes from the adhesion assays performed using a recombinant P-selectin substrate: there was no difference in the amount of adhesion, cell spreading or migration of EPCs compared to control assays using an immobilised platelet monolayer. In addition to clearly demonstrating the importance of P-selectin, these flow assays also suggest that other specific surface receptors or granule contents of the platelet may not be required for EPC attachment. At least, albumin co-immobilised with P-selectin was adequate to replicate the function of any other necessary constituent of the platelet. It should also be noted that

albumin alone did not support adhesion of flowing EPCs. This has important implications for the platelet-EPC mechanism. In other flowing cell recruitment models, such as leukocyte migration, capture occurs primarily through rolling adhesion, mediated by selectins, which is subsequently stabilised by integrin-activating chemokine signals from the endothelium (Butler *et al.*, 2009). However, in this model EPCs were observed to bind efficiently and, interestingly, became immediately adherent without rolling adhesion. Stabilised adhesion was evident since, after initial adhesion at 0.025 Pa, EPCs remained attached and stationary on immobilised platelets even when shear stress was increased to 0.6 Pa. Based on this observation, and the similar capability of P-selectin/albumin in EPC recruitment from flow, it appears that an additional activating mechanism after the initial selectin-mediated attachment is not required for firm adhesion to occur. It is possible that constitutively active integrins are expressed on the EPC surface which immediately stabilise the platelet-EPC bond upon selectin-mediated attachment, negating the rolling adhesion observed with leukocytes. This raises the question as to the ligand(s) on platelets that support any integrin-mediated stable adhesion, although again, it should be noted that surface-immobilised albumin or P-selectin itself must be able to fulfil this role judging from the experiments with purified proteins.

A potential candidate for this ligand would be a protein, such as fibrinogen or vWF, which can bind to an active integrin, $\alpha\text{IIb}\beta\text{3}$, on the platelets. This possibility was investigated in both aggregation and flow adhesion assays, by adding abciximab, a blocking antibody against $\alpha\text{IIb}\beta\text{3}$. However, antibody inhibition of $\alpha\text{IIb}\beta\text{3}$ binding had no effect on either platelet-EPC aggregation or adhesion of EPCs to platelets from flow, demonstrating that $\alpha\text{IIb}\beta\text{3}$ is not necessary for EPC attachment, nor a vital component of the immediate stationary adhesion mechanism requiring P-selectin.

If, as our data suggests, the presence of P-selectin is required for EPC recruitment but activation of $\alpha\text{IIb}\beta\text{3}$ is not, the degree of platelet activation required for the binding mechanism is unclear. Upon activation, platelets exocytose their intracellular alpha granules, which contain a variety of coagulation proteins, cell-activating cytokines and growth factors, inflammatory regulators and adhesion molecules including P-selectin, as well as dense granules containing ADP (Rendu & Brohard-Bohn, 2001). Full platelet activation typically involves the binding of ADP, released from dense granules, to P2Y_{12} receptors on the platelet's surface and the production of thromboxane A₂ (TXA₂) by the action of cyclooxygenase 1 (COX1) on arachidonic acid. Here, combined treatment of the platelets with clopidogrel (which blocks P2Y_{12} receptors) and aspirin (which inhibits COX1 activity) has demonstrated that neither ADP binding nor TXA₂ production are not required for EPC binding. This suggests that full platelet activation *via* this pathway was not required for EPC adhesion. This is also consistent with the lack of a role for $\alpha\text{IIb}\beta\text{3}$, which is activated and required for platelet-platelet aggregation in response to ADP and thromboxane.

Although ADP and TXA₂ do not play a role in the EPC binding mechanism, there is evidence that the platelets used in the flow adhesion model are activated at the time of EPC recruitment. Perhaps the most obvious indication is the shape change of the platelets and significant presence of P-selectin on the platelet monolayer (itself indicated by the effect of P-selectin blockade on the extent of EPC adhesion) which is greatly upregulated with platelet activation and degranulation. Interestingly, EPC adhesion was not significantly affected by the presence of thrombin, although EPC spreading tended to increase slightly. It has been previously shown that whilst platelets immobilised on glass microslides are activated to a certain degree, expressing P-selectin and capturing flowing neutrophils by rolling adhesion, they can be activated further to induce stationary adhesion by the addition of thrombin (Stone

& Nash, 1999). Thrombin is a blood coagulation factor which promotes platelet aggregation by cleavage of the protease-activated receptor PAR1 on the platelet membrane (Vu *et al.*, 1991). Here, if platelets were not already activated to a significant extent, thrombin would be expected to greatly increase EPC adhesion by the upregulation of P-selectin upon platelet activation. However, little increase in adhesion was observed following the addition of thrombin, suggesting that no further increase in platelet activation was required to capture EPCs. There were also visual similarities between platelet monolayers in the control and thrombin-treated assays: in both assays platelets were observed to have stellate morphologies with pronounced surface contours, characteristic of an activated phenotype. Thus, platelet activation beyond that occurring during adhesion to the substrate was not required for adhesion. It is possible that a thrombin-induced response in platelets encouraged EPC spreading (even though not necessary for adhesion) or that thrombin acted directly on the EPCs to increase their spreading following adhesion. To investigate this, additional thrombin-treated assays were performed using microslides coated with immobilised P-selectin. The extent of EPC spreading following adhesion to immobilised P-selectin in the presence of thrombin was not significantly different from untreated controls, and did not demonstrate the significantly increased cell area seen in the later stages of thrombin-treated assays performed on a platelet monolayer. This suggested that the effect of thrombin on EPC spreading seen previously was the result of its action upon the platelets to which the cells were bound rather than directly on the cells themselves, as no effect on cell area was seen when platelets are absent from the system.

In contrast to thrombin, addition of PGI₂ was observed to cause a marked reduction in the number of platelet-adherent EPCs and resulted in no increase in cell area after attachment. PGI₂ can silence cell or platelet receptor activity by signalling an increase in cyclic adenosine

monophosphate (cAMP) production (Mandl *et al.*, 1988; Fisch *et al.*, 1997). During isolation from whole blood platelets are kept in a state of agonist insensitivity using a relatively high concentration of PGI₂, which is rapidly reversed upon washing allowing platelet activation (Vargas *et al.*, 1982). However in the continued presence of PGI₂, here EPC adhesion was dramatically reduced, most likely as a result of downregulation of platelet surface P-selectin. Furthermore, in contrast to the platelet monolayers observed in control and thrombin-treated assays, platelets immobilised on glass microslides in the presence of PGI₂ demonstrated a much more inactive morphology, with a spherical shape showing less vivid surface folds. Thus 'inactive' platelets could not support efficient adhesion of EPCs. Lack of spreading of the EPCs that did adhere could again have occurred because of a change in the platelet surface (such as a reduction in P-selectin expression) or may have arisen from effects of PGI₂ on the EPCs. To test this, as with thrombin, PGI₂ assays were performed with immobilised P-selectin replacing the platelet monolayer. In these assays, unlike the previous PGI₂-treated platelet monolayer assays, the number of adherent EPCs was not observed to be significantly reduced compared to untreated controls, nor was EPC spreading affected. Again, this suggests the effect that PGI₂ has on EPC adhesion and spreading, as with thrombin, is the result of its effect on the platelet monolayer (which was absent in the P-selectin-coated assays) and not on the cells directly.

In conclusion, platelets have demonstrated the ability to bind EPCs in suspension or to capture them from flow, in both cases through presentation of P-selectin. In studying the therapeutic potential of EPC transplantation, it was considered important to investigate the mechanisms by which they might be physically recruited before progressing to a comparable *in vivo* model. Our data suggests that the platelet may act to promote EPC recruitment simply as a 'bearer' of P-selectin rather than *via* more complex activation-dependent mechanisms

requiring interaction between the EPC and other platelet constituents. On this basis, it was considered appropriate to investigate the roles of platelets and P-selectin in an *in vivo* EPC transplantation model.

CHAPTER 7:

IN VIVO TRANSPLANTATION OF ENDOTHELIAL PROGENITOR CELLS

7.1 Introduction

Comparisons made between *in vitro* and *in vivo* models of transplantation may prove vital to the development of efficient angiogenic therapies involving EPCs. Having demonstrated that EPCs have the capacity to recover the complexity and longevity of EC tubules when transplanted *in vitro*, and that a preferential binding mechanism exists between platelets and EPCs, we investigated the recruitment of EPCs to angiogenically active tissues *in vivo*. As previously discussed, the angiogenic treatments that currently show the greatest therapeutic potential are those that involve the injection of an excess quantity of donor progenitor cells. However, a search of the available literature revealed a variety of models and regimes that are used to demonstrate and assess the beneficial effects of cell transplantation (**Table 7.1**). These studies vary in the precise donor cell population used, the animal model chosen, the method of cell administration and the criteria used to quantify the outcome of transplantation.

Model	Animal	Cell	Quantity	Administration	Time	Analysis
Hindlimb ischaemia	Mouse	Liver progenitor cells	1×10^5	i.v. injection, 24 h post	2 weeks	Laser Doppler perfusion analysis of limb (Aicher <i>et al.</i> , 2007)
Hindlimb ischaemia	Mouse, rabbit	CD34 ⁺ BM cells	5×10^5	Tail vein injection, 2 days post	1-6 weeks	Localisation of fluorescent cells (Asahara <i>et al.</i> , 1997)
Hindlimb ischaemia	Mouse	VEGFR2 ⁺ BMCs	1×10^4	Route unreported, 2 days post	4 weeks	Cell incorporation, CD31 and lectin staining (Asahara <i>et al.</i> , 1997)
Hindlimb ischaemia	Mouse	Murine Sca-1 ⁺ Lin ⁻ BM MNCs	1×10^5	i.v. injection, 24 h post	2 weeks	Laser Doppler flow imaging, capillary density (Chavakis <i>et al.</i> , 2005)

Model	Animal	Cell	Quantity	Administration	Time	Analysis
Historical myocardial infarction	Human	Human BM stem cells	$8-10 \times 10^9$	Coronary artery injection	Day 0, 3 and 6 months	Left ventricular haemodynamics by ECG (Chen, S-I <i>et al.</i> , 2004)
Hindlimb ischaemia	Mouse	CD31 ⁺ c-kit ⁺ BM MNCs	2×10^6	Tail vein injection, 40 days post	Over 35 days	Laser Doppler perfusion analysis, capillary density (Cheng, XW <i>et al.</i> , 2007)
Spinal cord injury	Rat	MSCs	2.5×10^5	Injection to injury epicentre, 1 week post	8 weeks	Basso-Beattie-Bresnahan scores and motor evoked potentials (Cho <i>et al.</i> , 2009)
Myocardial infarction	Mouse	BM-derived EPCs	5×10^5	Directly into peri-infarct areas, immediate	2 weeks	Left ventricular function by ECG, capillary density myocardial cell proliferation, infarct size (Cho, H-J <i>et al.</i> , 2007)
Myocardial infarction	Rat	MNCs and MSCs	1×10^6	Injection into infarct border, 24 hours post	1 and 30 days	ECG, capillary density (de Macedo Braga <i>et al.</i> , 2008)
Irradiation with Matrigel plug	Mouse	CD34 ⁺ MNCs from cord blood	8×10^5	i.v. injection, 1 day post; s.c. Matrigel injection, 6 weeks post	10 days after Matrigel plug	ICC of Matrigel for CD31, CD11b and vWF (Droetto <i>et al.</i> , 2004)
Atherosclerosis	Mouse	Spleen EPCs	1×10^6	3 twice-weekly i.v. injections from age 10 weeks	8 weeks	Atherosclerotic lesion size (George <i>et al.</i> , 2005)
Hindlimb ischaemia	Mouse	EPCs	5×10^6	Directly into muscle, immediate	Days 0, 10 and 21	Laser Doppler perfusion analysis, capillary density, proliferation and apoptosis assays (Hu, Z <i>et al.</i> , 2008)
Hindlimb ischaemia	Mouse	ESCs and ESC-derived ECs	5×10^4	i.v., i.a. and i.m. injection, immediate	Over 2 weeks	Bioluminescence and Laser Doppler imaging, CD31 and green fluorescent protein (Huang <i>et al.</i> , 2010)
Hindlimb ischaemia	Rat	MNCs from cord blood	1×10^6	Direct i.m. injection, 4 weeks post	4 weeks	Regional perfusion by near-infrared spectroscopy, capillary density (Ikeda <i>et al.</i> , 2004)
Myocardial infarction	Mouse	MSCs	$2-5 \times 10^6$	Tail vein injection, 1, 8 and 15 days post	1, 2 and 3 weeks	ECG, cell engraftment imaging (Iso <i>et al.</i> , 2007)
Tumour	Mouse	CD34+ PB MNCs	$1-2 \times 10^6$	i. v. injection, immediate	Unreported	Imaging of cell homing (Jin <i>et al.</i> , 2006)
Hindlimb ischaemia	Mouse	PB MNC outgrowths	5×10^5	Intracardiac injection, 1 day post	Over 4 weeks	Laser Doppler imaging, capillary density (Kalka <i>et al.</i> , 2000)
Hindlimb ischaemia	Mouse	ESC-derived ECs	1×10^6	Injected along femoral artery, time not reported	1 and 2 weeks	Laser Doppler perfusion analysis, CD31 and lectin staining (Kane <i>et al.</i> , 2010)
Historical myocardial infarction	Human	CD34+ cells from PBs	7×10^6	Unreported	1 day	ECG to assess myocardium, quantitative coronary angiography (Kang <i>et al.</i> , 2004)
Myocardial ischaemia	Rat	PB MNCs	1×10^6	i.v. injection, 3 h post	1 week	Imaging of labelled cells, capillary density, left ventricular function by ECG (Kawamoto, A <i>et al.</i> , 2001)
Myocardial ischaemia	Rat	CD34+ PB MNCs	1×10^5	Directly into ischaemic zone, 10 min post	4 weeks	Cell incorporation, ECG for left ventricular function, capillary density (Kawamoto, Atsuhiko <i>et al.</i> , 2003)
Myocardial ischaemia	Pig	CD31+ PB MNCs	1×10^7	Injected into left ventricle, 4 weeks post	4 weeks	Cell incorporation imaging, left ventricular ejection fraction, capillary density (Kawamoto, Atsuhiko <i>et al.</i> , 2003)
Hindlimb ischaemia	Mouse	MNCs outgrowths	Unreported	Route not reported, on day of surgery	Over 2 weeks	Laser Doppler blood flow analysis (Kebir <i>et al.</i> , 2010)
Hindlimb ischaemia	Mouse	PB MNC outgrowths	Unreported	Systemic injection, 1 day post	Over 3 weeks	Cell homing by tissue digestion and FACS, laser Doppler perfusion analysis (Kränkel <i>et al.</i> , 2008)
Hindlimb ischaemia	Human	MSCs and MNCs from BM	Unreported	Direct i.m. Injection, time unreported	2 and 4 weeks, 2-10 months	Vital sign monitoring, blood pressure, heart rate, exercise treadmill test (Lasala <i>et al.</i> , 2010)
Hindlimb ischaemia	Mouse	PB MNCs	5×10^5	Immediate intracardiac puncture	Over 3 weeks	EPC homing by counting labelled cells, Laser Doppler imaging, capillary density (Lee, S-P <i>et al.</i> , 2006)
Myocardial ischaemia	Mouse	ESC-derived ECs	5×10^5	Injection at peri-infarct zone, 10 min post	4 to 8 weeks	Bioluminescence imaging, left ventricular functional analysis by ECG, capillary density (Li, Z <i>et al.</i> , 2007)

Model	Animal	Cell	Quantity	Administration	Time	Analysis
Myocardial infarction	Rat	MSCs	6×10^6	Injection into infarct border, immediate	Over 6 weeks	Scar tissue size, cell survival, infarct size, capillary density (Li, W <i>et al.</i> , 2007)
Left ventricular cryoinjury	Mouse	CD133 ⁺ cells BM and cord blood	5×10^5	Injection into necrosis border, immediate	4 weeks	Measurement of scar size, capillary density (Ma <i>et al.</i> , 2006)
Myocardial infarction	Human	CD133 ⁺ cells from BM	1×10^6	Infused into left anterior descending artery or right coronary artery	1 month, every 3 months	Coronary angiography to assess progression of vascular lesions; left ventricular dimensions (Manginas <i>et al.</i> , 2007)
Tumour	Mouse	ESC-derived EPCs	1×10^6	Co-injection with tumoral cells	After tumour identification	Cell incorporation by immunofluorescence imaging (Marchetti <i>et al.</i> , 2002)
Hindlimb ischaemia	Rat	CD34 ⁺ MNCs from cord blood	3×10^5	Direct i.m. injection, immediate	2 weeks	Capillary density, imaging of labelled transplanted cells (Murohara <i>et al.</i> , 2000)
Myocardial ischaemia	Mouse	Induced pluripotent EPCs	2×10^5	Intramyocardial injection, 30 min post	Unreported	Ventricular ejection fraction (Nelson <i>et al.</i> , 2009)
Atherosclerosis	Mouse	MNCs	1×10^6 per injection	Three i.v. and i.p. injections every 2 weeks	Unreported	Cell localisation (Rauscher <i>et al.</i> , 2003)
Tumour	Mouse	CD34 ⁺ MNCs from cord blood	0.5×10^6	Tail vein injection, 3 days post	9 days	Cells for incorporation into capillaries, total capillaries, tumour volume (Le Ricousse-Roussanne <i>et al.</i> , 2004)
Myocardial infarction	Rat	PB MNCs	1×10^6	Injection into marginal zones, 4 weeks post	2 months	Left ventricular dimensions and function by ECG, infarct size, apoptosis and collagen in infarct areas (Schuh <i>et al.</i> , 2008)
Myocardial infarction	Pig	MSCs	2×10^8	Intramyocardial injections, 2 days post	Over 8 weeks	MRI scanning for left ventricular dimensions and function, perfusion imaging, infarct area measurements (Schuleri <i>et al.</i> , 2008)
Myocardial ischaemia	Dog	MSCs from BM	1×10^8	Intramyocardial injection, immediate	Immediate, 30 and 60 days	Coronary angiography, ECG, vascular density (Silva <i>et al.</i> , 2005)
Hindlimb ischaemia	Mouse	BM-derived MNCs	1×10^6	i.v. injection, immediate	4 weeks	Microangiopathy and capillary density, Laser Doppler perfusion imaging of hindlimb (Silvestre, Jean-Sébastien <i>et al.</i> , 2003)
Historical myocardial infarction	Human	CD133 ⁺ cells from BM	1.5×10^6	Unreported	3-9 months	Left ventricular function, infarct tissue perfusion (Stamm <i>et al.</i> , 2003)
Focal cerebral infarction	Mouse	CD34 ⁺ Flk ^{+/-} cells cord blood	5×10^5	Tail vein injection, 2 days post	Over 2 weeks	Cell proliferation, carbon black perfusion to quantify viable and non-viable tissue (Taguchi <i>et al.</i> , 2004)
Myocardial infarction	Rat	Cardiac progenitor cells	$0.8-1 \times 10^5$	Injected proximal to occlusion, immediate	1 hour to 1 month	Ventricular function and haemodynamic measurements, cell incorporation, myocardial regeneration (Tillmanns <i>et al.</i> , 2008)
SCID	Mouse	MSC outgrowths	$0.5-1 \times 10^6$	Left ventricular injection	30 mins, 4-60 days	Identification of incorporated cells (Toma <i>et al.</i> , 2002)
Atherosclerosis	Mouse	Flk ⁺ Sca-1 ⁺ c-kit ⁺ MNCS	2×10^7 per day	Tail vein injection on 3 consecutive days	7, 14 and 45 days	Tension recording of aortic ring preparations, staining for cell incorporation (Wassmann <i>et al.</i> , 2006)
Neointima formation following carotid artery injury	Mouse	Spleen-derived MNCs or EPCs	1×10^6	Tail vein injection, immediate and 24 hours post	Unreported	Localisation of fluorescent cells (Werner <i>et al.</i> , 2003)
Wound healing	Mouse	BM-derived MSCs	1×10^6	Intradermal injection and applied to wound bed, immediate	Over 4 weeks	Capillary density, histological scores for regeneration and cell infiltration (Wu, Y <i>et al.</i> , 2007)
Hindlimb ischaemia	Mouse	PB CD34 ⁺ cells	1.5×10^5	i.v. injection, immediate	Over 4 weeks	Laser Doppler perfusion imaging, histological assessment of cell incorporation (Yamaguchi <i>et al.</i> , 2003)
Chick embryo	Chicken	Flk ⁺ E-cadherin ⁻ ESC-derived cells	$1-2 \times 10^5$	Injected into heart of embryo	2-3 days	Immunofluorescent staining for cell localisation (Yamashita <i>et al.</i> , 2000)

Model	Animal	Cell	Quantity	Administration	Time	Analysis
Hindlimb ischaemia	Mouse	CD133 ⁺ MNCs	5×10 ⁵	Tail vein injection, 1 day post	Over 3 weeks	Capillary density, Laser Doppler analysis (Yang, C <i>et al.</i> , 2004)
Myocardial infarction	Mouse	PB CD34 ⁺ cells	1×10 ⁶	Tail vein injection, 16 hours post	60 days	Immunofluorescence of differentiation markers in infarct areas (Yeh <i>et al.</i> , 2003)
Hindlimb ischaemia	Mouse	BM-EPCs	1×10 ⁶	Cardiac puncture, 1 day post	15 hours	EPC homing by counting labelled cells (Yoon <i>et al.</i> , 2006)
Cerebral artery occlusion	Rat	BM stromal cells	3×10 ⁶	Tail vein injection, 1 day post	2 weeks	Histological and immunofluorescent staining (Zacharek <i>et al.</i> , 2007)

Table 7.1. Comparison of in vivo cell transplantation regimes.
BM, bone marrow; i.a., intraarterial; i.m., intramuscular; i.v., intravenous; MNC, mononuclear cell; MSC, mesenchymal stem cells; PB, peripheral blood; s.c., subcutaneous.

However, although they differed in many details, this brief survey did reveal certain similarities between regimes in recent transplantation studies. For example, it was clear that the most common stimulation model (used in 37 of the 53 studies analysed) was one typified by ischaemia, either hindlimb ischaemia or myocardial infarction prior to cell administration. Furthermore, over 60% of these transplantation experiments were performed in mice, organisms considered to be well-suited to the physiologically relevant generalisation of findings to other organisms, such as humans (Kellogg & Shaffer, 1993). The range of cell quantities used throughout the analysed studies was also wide, with a relatively high mean number of transplanted cells ($\sim 1.9 \times 10^8$). However, the modal average of transplanted cells, i.e. the most commonly used transplantation quantity, was two orders of magnitude less than this (1×10^6): cell quantities in the millions, rather than tens or hundreds of millions, are most common. The transplantation study survey also revealed the use of many different cell types, although almost all were deemed to have ‘progenitor’ phenotypes such as peripheral and cord blood mononuclear cells and bone-marrow derived EPCs. Further disparities between regimes were seen in the routes of cell administration, which could be broadly defined as either indirect vascular infusion or direct intramuscular injection. The timescales used in many contemporary transplantation studies was generally long, measured in weeks and

months. This was often because the main aim of these investigations was to quantify the beneficial outcome of cell transplantation (for example, by improved hindlimb blood perfusion or increased capillary density) which occurs on a physiological timescale, i.e. at a relatively slow rate. These timescales were less well-suited to our *in vivo* experiments, in which we were interested in the initial recruitment of transplanted EPCs and the potential mediating role of platelets.

It was clear that there is currently no single defined transplantation regime that uncovers a mechanism for *in vivo* EPC recruitment and produces a clear beneficial effect as a result of transplantation. Therefore, the transplantation protocol presented here (SEE 2.9.3) was based on the most common (and validated) methods available in the scientific literature, adapted to suit the particular aims of this study.

Angiogenesis can be induced in a number of ways but it was clear from the above survey that one of the most common *in vivo* models involved the surgical occlusion or removal of the FA to cause ischaemia in the hindlimb of mice or rats. Occlusion of blood flow leads to hypoxia and the deprivation of other important nutrients. A mismatch between metabolic delivery and demand is a key stimulus for angiogenesis (Adair *et al.*, 1990). Furthermore, occlusion causes a pressure gradient between the ischaemic and non-ischaemic regions, which leads to increased shear stress in collateral vessels, which respond through shear stress responsive elements to upregulate angiogenesis-associated genes (Topper & Gimbrone, 1999). To get a broader view of EPC recruitment response to different stimuli it was decided that cell transplantation would be performed following both acute (30 min) and chronic (2 and 7 days) hindlimb ischaemia. In addition, transplantation would also be carried out in a model of extirpation-induced overload which, unlike hindlimb ischaemia, provides a mechanical

stimulus for angiogenesis without the changes in blood flow and shear stress commonly associated with ischaemia (Badr *et al.*, 2003).

Together with the demonstration of the localisation of circulating EPCs to angiogenic regions, this *in vivo* study aimed to determine whether platelets play a substantial role in EPC recruitment following transplantation. Whilst the relationship between platelets and angiogenic EPCs has been demonstrated *in vitro* (Langer, H *et al.*, 2006; Lev *et al.*, 2006), and the role of platelet-derived growth factors in EPC transplantation have been investigated *in vivo* (Kim, JY *et al.*, 2010), there are limited data regarding the physical influence of platelets on *in vivo* angiogenesis. For example, the vascularisation of tissue-engineered bone constructs using a platelet-leukocyte gel, prepared using separated blood components, has been demonstrated (Geuze *et al.*, 2009), although the animal (goat) and transplantation model (bone graft) are quite different to those used in the current experiments. One particular study with similarity to this investigation examined cell incorporation and resulting capillary density following the implantation of combined PBMCs and platelets into the ischaemic rat hindlimb (Iba *et al.*, 2002). However, unlike our transplantation models, that study was focussed on exogenously-applied platelets and their effects on cell transplantation, rather than the role of existing platelets resident in the circulation.

For our experiments, it was important to be able to reduce the normal circulating platelet count in the blood and observe the effect this has on the localisation of transplanted EPCs. In many investigations necessitating a reduction in platelet count, antibodies specifically targeted towards platelet antigens are used for systemic platelet depletion. In particular, targeting of the GPIIb/IIIa receptor has been shown to induce the formation of circulating platelet microaggregates which are quickly cleared from the blood, drastically reducing the platelet

count to cause a rapid and irreversible thrombocytopenia (Bergmeier *et al.*, 2000). This method of platelet depletion has been used successfully in a wide variety of studies, from those looking at the role of platelets in the responses of the heart and lungs to vascular injury (Russ *et al.*, 2008; Looney *et al.*, 2009), as well as in the protection of the liver from continued damage following viral infection (Iannacone *et al.*, 2005). Other methods of systemic platelet depletion, such as the continuous removal of circulating platelets from patients undergoing heart surgery by means of an automated blood cell separator, have also been previously demonstrated (Morioka *et al.*, 1996). However, although this method was shown to reduce platelet count to a level considered appropriate to the study being made (by 27%), this level of depletion was not adequate to investigate the effect of platelet absence in EPC recruitment. Furthermore, such blood-separating equipment is primarily designed for human use (i.e. for large-scale donation of platelets *via* apheresis), removing a relatively large volume (220 ml) of platelet concentrate during separation (Buchholz *et al.*, 1997). Therefore it was decided that continuous platelet depletion would not be feasible for the small scale of our mouse transplantation model, and it was decided that antibody-mediated platelet depletion was better suited to our investigation.

7.2 Hypothesis & objectives

It was hypothesised that circulating EPCs would specifically target and bind to sites of neovascularisation following *in vivo* transplantation into a murine model in which EC activation had been induced in the muscles of the hindlimb. Furthermore, it was believed that EPC recruitment might be influenced, at least in part, by the presence of blood platelets, that may capture transplanted EPCs and localise them to the activated endothelium.

By *in vivo* transplantation of EPCs into murine models of hindlimb angiogenesis, the experiments described in this chapter aimed to:

1. Demonstrate preferential *in vivo* localisation of EPCs to sites of angiogenic stimulation following transplantation;
2. Establish the role of platelets in recruitment of transplanted EPCs using a platelet-depleted murine model of angiogenic stimulation;
3. Investigate EPC recruitment patterns in transplantation models with different angiogenic stimuli.

7.3 Methods

7.3.1 Optimisation of percutaneous sciatic nerve stimulation.

To maximise the endothelial insult in the acute ischaemia transplantation model, electrical stimulation was performed concurrently with FA ligation in order to vigorously exercise the ischaemic hindlimb by inducing frequent muscle contractions. Indirect stimulation of the exposed skeletal muscles was initially performed by percutaneous stimulation of the sciatic nerve. The electrical parameters used (5-10 V, 10 Hz, 0.3 ms pulse duration) resulted in a muscle activity pattern that has been shown to be very effective in inducing angiogenesis over a matter of days without having an effect on sympathetic nerve fibres (Kjellmer, 1965; Hansen-Smith *et al.*, 1996). However, in an effort to further increase the angiogenic stimulus, parallel experiments were also performed with electrical stimulation at 40 Hz. This induced muscle tetani and thereby maximised tissue responsiveness to activity (due to muscle fatigue and increased production of reactive oxygen species (ROS) upon cessation of stimulus) and the subsequent recruitment of transplanted EPCs compared.

Following 30 min ischaemic stimulation, 2×10^6 Qdot-labelled EPCs were injected *via* a CCA cannula. After a further 15 min, the hindlimb muscles *m. tibialis anterior*, *m. extensor digitorum longus* and *m. soleus* were digested and analysed by flow cytometry to identify recruited EPCs. Although the total numbers of transplanted EPCs localised to the muscle were observed to be different for each of the three muscle types (and will be discussed in greater detail later in this chapter), EPC localisation was not significantly affected by the change in stimulation frequency (**Fig. 7.1**). This suggests that an increased electrical frequency did not bring about an increased endothelial damage in the ischaemic hindlimb, or at least not one resolved by the functional readout of recruited EPC localisation. Based on these findings, that in this model no additional benefit comes from the increased frequency, and to utilise the

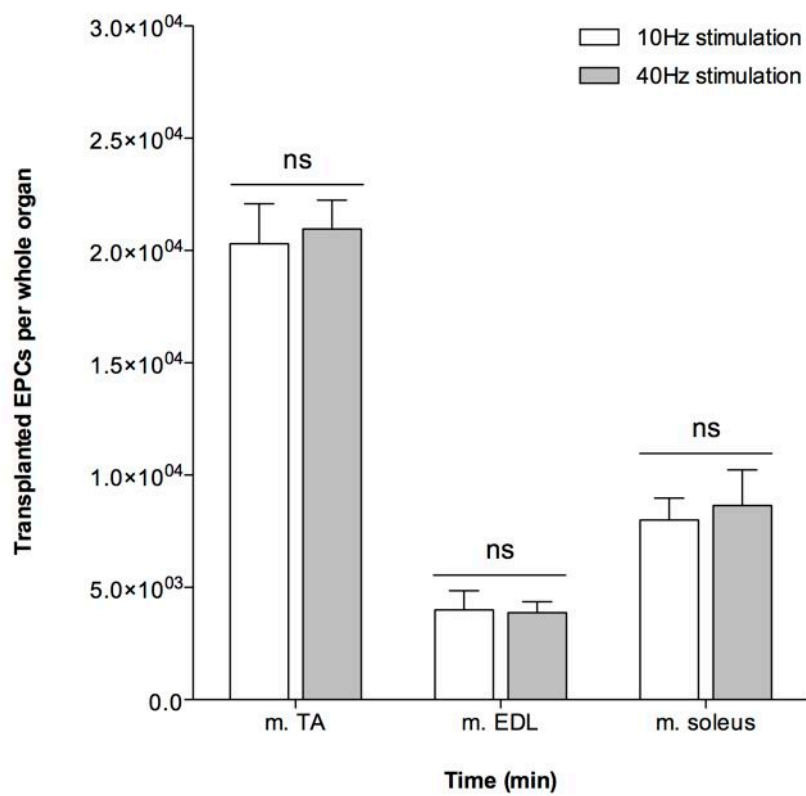


Figure 7.1. Optimisation of percutaneous sciatic nerve stimulation. Electrical stimulation of ischaemic hindlimb was performed at 10 or 40 Hz for 30 min before EPC transplantation and flow cytometric analysis of digested hindlimb muscles. Data presented as total number of transplanted EPCs per whole muscle (mean \pm SEM, $n=5$); ns, no significant difference between frequencies. m. TA, tibialis anterior; m. EDL, extensor digitorum longus.

functional hyperaemia to enhance delivery without the potential for tissue damage, stimulation parameters were set as described in Chapter 2 (SEE 2.9.3.3). Furthermore, chronic electronic stimulation has also been demonstrated to stimulate angiogenesis in ischaemic skeletal muscle (Hudlicka *et al.*, 1994), but with the attendant possibility of endothelial damage if the applied stimulus is too strenuous (Egginton *et al.*, 1993). Interestingly these findings do offer an approximation of the exercise therapy that may be undertaken (or required) by patients with peripheral vascular disease (PVD). For the treatment of PVD, mild exercise has been shown to improve cardiovascular efficiency, through the stimulation of pro-angiogenic mechanisms which increase muscle vascularity and alleviate PVD symptoms (Priebe *et al.*, 1991; Chinsomboon *et al.*, 2009).

7.3.2 Route of administration of anti-GPIIb α platelet depletion antibody

To investigate the role of platelets in the recruitment of transplanted EPCs, a platelet-depleting anti-GPIIb α antibody was used to remove circulating platelets from the mouse prior to transplantation. Two routes of antibody administration were tested: (i) intraperitoneal injection and (ii) intraarterial perfusion *via* a CCA cannula. In parallel experiments, 50 μ g antibody was administered and allowed to take effect over 1 h before whole blood was collected from the IVC and a platelet count performed (Fig. 7.2).

Compared to untreated control animals, in which an average platelet count of $5.3 \pm 1.1 \times 10^8$ per ml was recorded, those treated with anti-GPIIb α antibody by intraperitoneal injection showed a decrease in platelet count ($1.8 \pm 0.45 \times 10^8$ per ml; $P < 0.05$). However, animals treated by intraarterial infusion exhibited a much greater decrease compared to controls, equating to a nearly complete removal of circulating platelets ($2.0 \pm 0.15 \times 10^7$ per ml; $P < 0.01$). Interestingly, intraperitoneal administration has been previously shown to deplete circulating

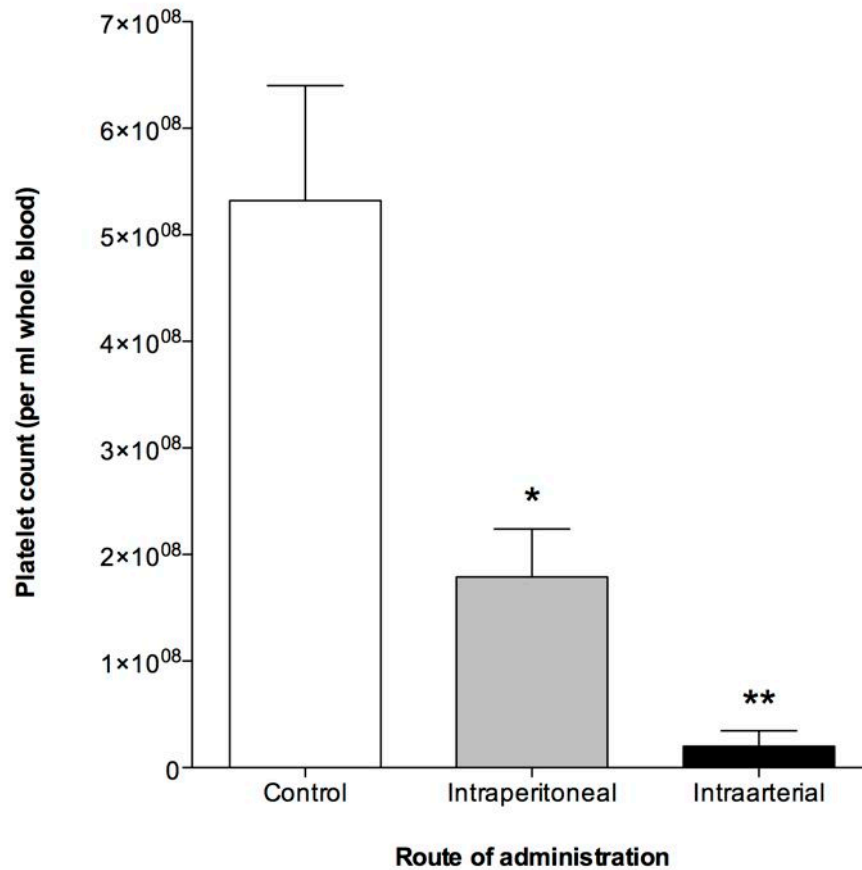


Figure 7.2. Systemic platelet depletion by anti-GPIIb α antibody. $2 \mu\text{g}\cdot\text{m}^{-1}$ antibody administered by intraperitoneal injection or via common carotid artery cannula. Platelets were isolated from whole blood after 1 h and counted using Coulter Multisizer II analysis. Data presented as mean number of platelets per ml of whole blood (\pm SEM; $n=5$); * $P<0.05$, ** $P<0.01$ vs. untreated control.

platelets by >95%, as was seen here following intraarterial infusion (96.2%), although a greater amount of antibody (100 µg) was administered 24 h before blood sampling (Nieswandt *et al.*, 2000). For our purposes intraarterial infusion, which produced a more complete depletion after a much shorter time period, was chosen as the route of antibody administration for subsequent experiments, to minimise surgical duration and stability of the animal preparation. With this in mind, it should be noted that the timescale of antibody administration and its effect was carefully considered before performing platelet-depleted EPC transplantation experiments. The supplied preparation of anti-GPIIb/IIIa antibody is suggested by the manufacturer (Emfret Analytics) to achieve maximal platelet depletion after 1 h and hence at least 1 h had to be left between antibody administration and EPC transplantation. Furthermore, it was decided that platelet depletion should be performed after carrying out the surgical procedures necessary to perform transplantation (i.e. CCA cannulation, exposure of the dorsal hindlimb, FA ligation) due to the risk to the animal of excessive bleeding once depleted of platelets.

7.4 Results

The *in vivo* recruitment of transplanted EPCs was investigated using a murine model of hindlimb angiogenesis, with a variety of acute and chronic stimuli. Furthermore, in order to assess the effect of platelets in EPC recruitment, systemic platelet depletion was also performed prior to transplantation in the acute ischaemia model. Following transplantation with fluorescently labelled EPCs, the muscles of both the stimulated (ipsilateral) and unstimulated (contralateral) hindlimbs, as well as the major abdominal viscera as control tissue, were harvested and digested with collagenase. The tissue digests were then analysed by flow cytometry to identify populations of recruited EPCs in each muscle and organ.

7.4.1 EPC recruitment in abdominal viscera

Prior to the analysis of hindlimb muscles, the number of EPCs localised in the major abdominal organs was investigated in order to establish a baseline level of recruitment in unstimulated tissues (i.e. those not specifically targeted by the applied angiogenic stimuli). After EPC transplantation, flow cytometric analysis was performed on digests of heart, lung, liver, spleen, ileum and kidney from each of the angiogenic models (**Fig. 7.3**). Fluorescent signals from each organ digest were adjusted for levels of background fluorescence by subtracting the mean values recorded in digests of organs taken from non-transplanted mice (data not shown). The number of transplanted EPCs found in the viscera was not significantly different between the heart, spleen, ileum or kidney. However, a significantly greater number of EPCs was localised in the liver (approximately six-fold greater compared to the other organs) and a greater number still (almost ten-fold greater) was identified in the lung ($P < 0.01$). Within each organ type, however, there were no significant differences observed in the number of transplanted EPCs between models using different angiogenic stimuli.

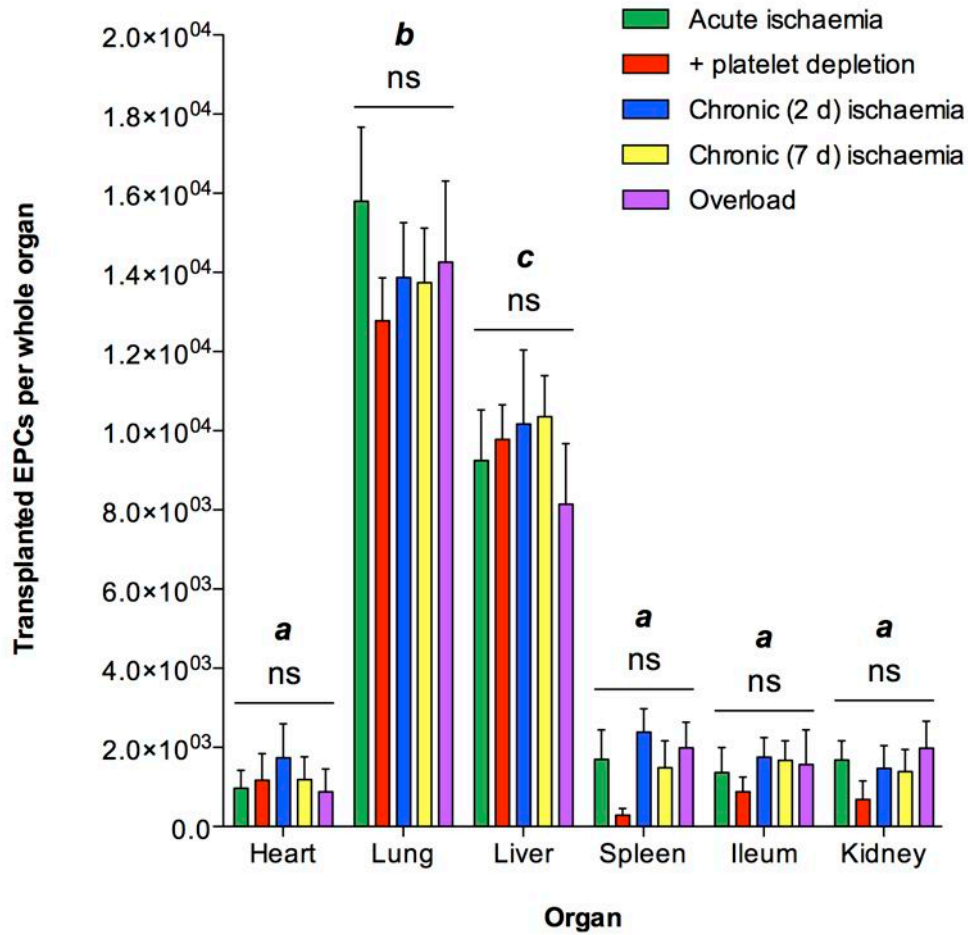


Figure 7.3. Recruitment of EPCs in abdominal viscera following in vivo transplantation. Organ digests were analysed by flow cytometry to identify fluorescent transplanted EPCs in models of acute ischaemia (\pm platelet depletion), chronic ischaemia (2 days and 7 days) or synergistic muscle overload. Data presented as mean number of EPCs per whole organ \pm SEM ($n=8$) adjusted for background fluorescence; ns, no significant difference between models; organs with different letters as superscripts are significantly different from each other ($P<0.01$).

7.4.2 Acute ischaemia

In the first transplantation model, FA ligation was simultaneously performed with percutaneous sciatic nerve stimulation to produce an acute ischaemic insult lasting for 30 min. Following EPC transplantation, digests of harvested hindlimb muscles were analysed by flow cytometry to identify fluorescent EPCs within the *m. tibialis anterior*, *m. extensor digitorum longus* and *m. soleus* (Fig. 7.4).

A greater number of transplanted EPCs was observed in the *m. tibialis anterior* of the ipsilateral limb compared to the contralateral limb (20300 ± 1675 vs. 12250 ± 1549 , respectively; $P < 0.01$). However there was no significant difference observed in EPC recruitment between the ipsilateral and contralateral limbs when systemic platelet depletion was performed prior to transplantation (14342 ± 1389 vs. 11837 ± 1829 , n.s.). Compared to the non-depleted hindlimb, the number of EPCs recruited to the ipsilateral *m. tibialis anterior* was lower in the absence of platelets, a statistically significant reduction ($P < 0.05$).

In the ipsilateral *m. extensor digitorum longus* there was a slight increase in EPC recruitment compared to the contralateral, although it was not determined to be statistically significant (4156 ± 1294 vs. 1820 ± 874 , n.s.). Similarly, and as with the *m. tibialis anterior*, there was no significant difference between the number of transplanted EPCs identified in the ipsilateral and contralateral *m. extensor digitorum longus* muscles in the absence of platelets (2073 ± 758 vs. 1960 ± 456 , n.s.). Hence, in the ipsilateral *m. extensor digitorum longus* there was no significant effect evident as a result of platelet depletion.

The pattern of EPCs recruitment in the *m. soleus* was similar to that seen in the *m. extensor digitorum longus*. A slight increase in the number of EPCs was identified in the ipsilateral

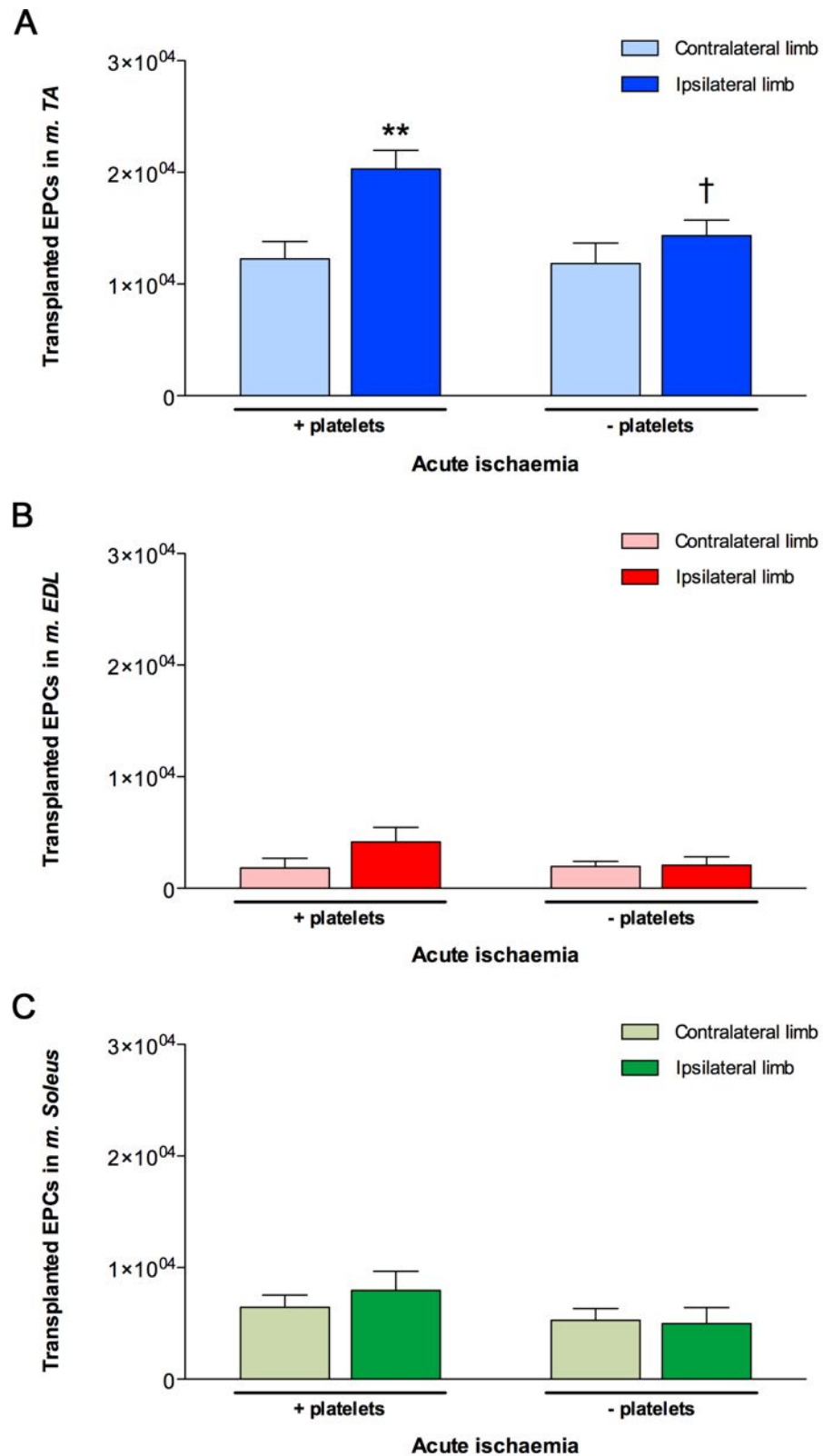


Figure 7.4. In vivo recruitment of transplanted EPCs following acute hindlimb and platelet depletion. Localisation of fluorescent EPCs in (A) *m. tibialis anterior*, (B) *m. extensor digitorum longus* and (C) *m. soleus* analysed by flow cytometry. Data presented as number of EPCs per muscle (mean ± SEM; n=8); ** $P < 0.01$ vs. contralateral, † $P < 0.05$ vs. ipsilateral with platelets.

m. soleus, compared to the contralateral (7956 ± 1713 vs. 6450 ± 1084 , n.s.), and there was no observed difference in the number of recruited EPCs in the ipsilateral and contralateral muscles in the platelet depleted model (4982 ± 1442 vs. 5267 ± 1054 , n.s.). Again, as with the *m. extensor digitorum longus*, EPC recruitment in the *m. soleus* was not significantly affected by the systemic removal of platelets.

7.4.3 Chronic ischaemia

The second angiogenic stimulus used to induce EPC recruitment following transplantation was chronic hindlimb ischaemia. This was performed over 2 or 7 days by permanent ligation of the FA, performed by recovery surgery under anaesthesia. Transplantation of fluorescent EPCs was then performed as previously, with flow cytometric analysis of the harvested hindlimb muscles (**Fig. 7.5**).

Following 2 days of ischemia, a significantly greater number of EPCs was recruited to the ipsilateral *m. tibialis anterior*, a two-fold increase compared to the contralateral muscles (25184 ± 1521 vs. 11675 vs. 1467 ; $P < 0.01$). At 7 days, there was no significant difference between the ipsilateral and contralateral *m. tibialis anterior* muscles (13782 ± 1411 vs. 11783 ± 1686 , n.s.), corresponding to a significant decrease in recruitment to the ipsilateral *m. tibialis anterior* from the number identified in the same muscle at 2 days ($P < 0.05$).

A significant difference was observed between the *m. extensor digitorum longus* of the two hindlimbs after 2 days of ischaemia, with more transplanted EPCs being recruited to the ipsilateral muscle than the contralateral (5964 ± 1073 vs. 2076 ± 978 ; $P < 0.05$). As with the *m. tibialis anterior*, the number of EPCs identified in the *m. extensor digitorum longus*

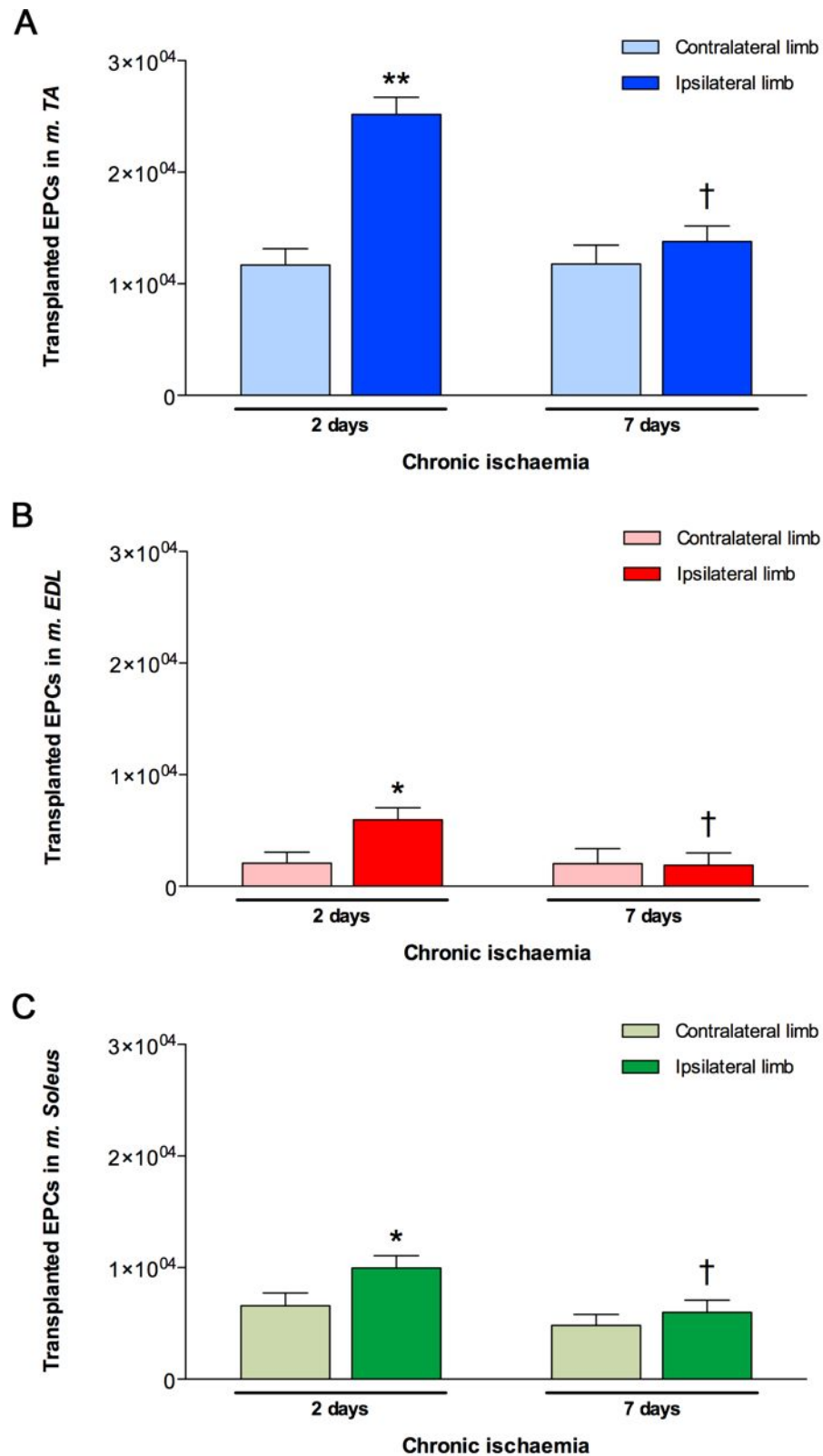


Figure 7.5. In vivo recruitment of transplanted EPCs following chronic hindlimb ischaemia. Localisation of fluorescent EPCs in (A) *m. tibialis anterior*, (B) *m. extensor digitorum longus* and (C) *m. soleus* analysed by flow cytometry. Data as number of EPCs per muscle (mean ± SEM; n=8); * $P < 0.05$ and ** $P < 0.01$ vs. contralateral, † $P < 0.05$ vs. ipsilateral at 2 days.

following transplantation was significantly reduced compared to 2 days ischaemia ($P < 0.05$), resulting in no significant difference in recruitment between the ipsilateral and contralateral muscles after 7 days of ischaemia (1897 ± 1087 vs. 2017 ± 1365 , n.s.).

Recruitment of EPCs to the 2 day ischaemic *m. soleus* was determined to be statistically significant between the ipsilateral and contralateral limbs, with more EPCs identified in the ipsilateral muscle (9956 ± 1102 vs. 6564 ± 1143 ; $P < 0.05$). Following 7 days of ischaemia, the number of EPCs recruited to the *m. soleus* was significantly lower than that observed at 2 days ($P < 0.05$) with no significant difference between the ipsilateral and contralateral muscles (5978 ± 1103 vs. 4786 ± 987 , n.s.).

7.4.4 Overload of synergistic muscles by unilateral extirpation

The third EPC transplantation model required the extirpation of the ipsilateral *m. tibialis anterior* to induce overload of the remaining synergistic hindlimb muscles. For this reason, only ipsilateral *m. extensor digitorum longus* and *m. soleus* muscles were available for flow cytometric analysis of recruited EPCs (**Fig. 7.6**).

After transplantation of EPCs into the overload model, a significantly greater number were identified in the ipsilateral *m. extensor digitorum longus* (a greater than two-fold increase) compared to the contralateral muscle (8647 ± 1654 vs. 4086 ± 913 ; $P < 0.05$). In contrast, recruitment of EPCs to the ipsilateral *m. soleus* was not significantly different from the contralateral (7526 ± 1846 vs. 5867 ± 1106 , n.s.), although there was a trend towards increased numbers of EPCs.

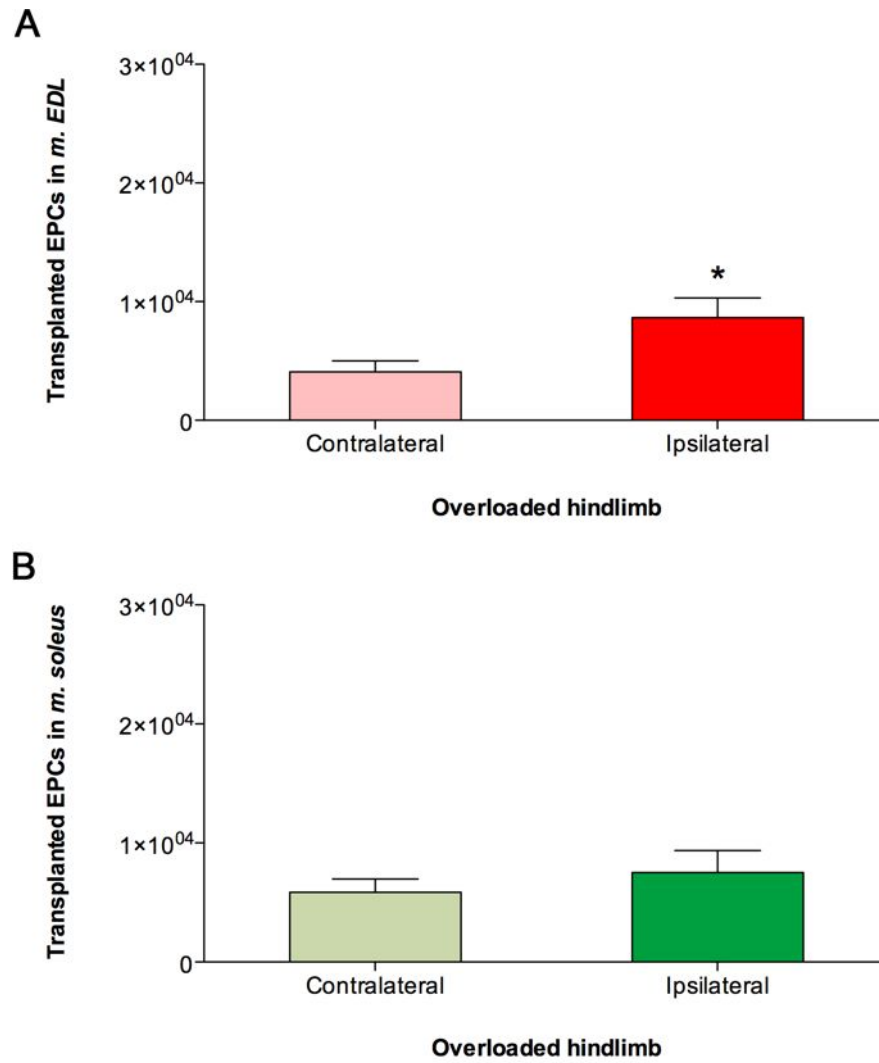


Figure 7.6. In vivo recruitment of transplanted EPCs following synergistic hindlimb muscle overload. Localisation of fluorescent EPCs in (A) *m. extensor digitorum longus* and (B) *m. soleus* analysed by flow cytometry. Data presented as number of EPCs per muscle (mean \pm SEM; $n=8$); * $P<0.05$ vs. contralateral.

7.5 Discussion

The preferential recruitment of EPCs to skeletal muscle with activated endothelium was investigated by *in vivo* transplantation into mice following a variety of angiogenic stimuli, including acute ischaemia, chronic ischaemia and extirpation-induced overload. These stimuli represented a reasonable model of exercise without the volitional component (i.e. of voluntary movement by the animal) which is difficult to standardise when working with animals, especially in chronic models that are observed over extended periods of time. In addition, continuing on from the study of platelet-EPC binding *in vitro*, the role of platelets in EPC recruitment *in vivo* was investigated by systemic platelet depletion prior to transplantation.

Firstly, in each of the transplantation models investigated, a proportion of the transplanted EPCs was found in the harvested viscera. The number of organ-bound EPCs did not vary significantly between the heart, spleen, ileum and kidney, and all analysed organs appeared largely unaffected by the different pre-transplantation stimuli, with the numbers of cells likely reflecting blood perfusion levels. However, a relatively large quantity of EPCs were localised to the liver, with a far greater number still found in the lung. Whilst this may suggest an active and preferential recruitment of transplanted EPCs to these organs in particular, these findings may be alternatively explained by taking the vascular nature of these tissues into consideration. The liver is a highly vascular organ, having an relatively dense capillary bed to provide sufficient blood flow to supply its high nutrient and oxygen requirements, and to allow adequate cleansing of toxins from the circulation. It has also been identified as a site of particle clearance (Weinstock & Brain, 1988). The blood elimination half-life of radiolabelled nanoparticles (0.1 to 1 μm diameter) injected into C57BL/6 mice has been determined to be between 1.4 and 4.9 min, depending on particle size; in general, larger particles were

removed from the circulation faster than smaller particles and a large proportion (around 60%) were later found localised in the liver (Simon *et al.*, 1995). These findings are corroborated by a previous study in which nanoparticles (0.25 to 0.3 μm) were shown to be rapidly cleared from the blood (3 to 5 min half-life) and were mainly deposited (60%) in the liver 10 min after administration (Rolland *et al.*, 1989).

Furthermore, assuming transplanted EPCs were not specifically targeted to the liver for recruitment, and even discounting the propensity of the liver for cell clearance, the increased amount of blood in the liver (compared to other less-vascular organs such as the spleen and kidney) could simply result in a greater number of EPCs being present (but not necessarily bound) in the liver when the animal was sacrificed and the organs harvested. Given the relatively low infusion rate of cells through the CCA cannula ($1.7 \mu\text{l}\cdot\text{s}^{-1}$) and the relatively high heart rate of the mouse ($594 \pm 9 \text{ beat}\cdot\text{min}^{-1}$ (Mattson, 2001)), an approximately even distribution of transplanted EPCs throughout the circulation is assumed in the moments after injection. Subsequently, as the blood volume contained within the wildtype C57BL/6 liver is approximately 8% of the animal's 1.2 ml total blood volume (Goossens *et al.*, 1988) it may be expected that as many as 1.6×10^5 cells (8% of the total transplanted quantity) would be found there at harvesting. In practice the actual number of cells found in the liver (between 8415 and 10256 across the five transplantation models) was far less than would be expected by this estimate, and certainly far less than would be observed if liver-specific recruitment was occurring.

Similarly to the liver, the lung is an organ with a relatively dense vasculature, which enables efficient gas transfer between inhaled air and erythrocytes in the blood. Alveolar macrophages are important in the efficient removal of apoptotic cells, making the lung an

essential part of the resolution of inflammation (Borges *et al.*, 2009). Furthermore, especially in terms of cell-based transplantation, the pulmonary capillaries have been shown known to be point of clearance of a significant number of circulating particles from the blood (Rajvanshi *et al.*, 1999).

It is clear from the flow cytometric data that the different acute and chronic angiogenic stimuli had no effect on EPC recruitment to the viscera, i.e. that they were confirmed to be essentially local events. Although the number of transplanted EPCs identified in each organ was shown to vary, the extent of EPC localisation was not significantly different between transplantation models in any of the organs analysed. This suggests that, unlike the hindlimb muscles, the responses of the viscera to each stimulus (whether a sign of targeted recruitment or simply an artefactual accumulation of EPCs) are not influenced by the different systemic responses induced by the various insults, representing normal haemodynamic delivery, rather than homing.

In the proposed 'platelet bridge' model, circulating EPCs are sequestered to the regions of angiogenesis in the muscles of the stimulated hindlimb and, in the presence of blood platelets, become tethered to the endothelium (Lev *et al.*, 2006). Once bound in this way, EPCs are suggested to influence the angiogenic process through either the release of endogenous pro-angiogenic factors or by their physical incorporation into the growing vessel (Silva *et al.*, 2005; Kushner *et al.*, 2010). Here, in transplanted wildtype mice that contained normal levels of blood platelets (5.3×10^8 platelets/ml) EPCs were found to be preferentially recruited to the *m. tibialis anterior* following acute ischaemia combined with electrically-stimulated activity of the hindlimb muscles. When platelets were removed from the animal prior to transplantation using a depletion antibody (which reduced blood platelet count by

96%), the increased ipsilateral recruitment was almost completely ablated, reducing it to a level comparable to that seen in the contralateral limb. A similar trend was also seen in both the *m. extensor digitorum longus* and *m. soleus* muscles (in which a higher number of EPCs in the ipsilateral muscle was reduced to a level similar to that in the contralateral following platelet depletion), although the initial differences between the ipsilateral and contralateral limbs in the wildtype mice were not determined to be statistically significant. However, the data from the *m. tibialis anterior* do confirm the importance of platelets in the binding of circulating EPCs during angiogenesis, suggesting that although EPCs may home to angiogenic sites under the influence of chemokine gradients established by an activated endothelium, they may not persist in these regions without platelets to physically tether them in place.

This study has showed that *in vivo* transplantation of EPCs likely leads to homing and preferential recruitment of cells to angiogenic tissues. Further to this, analysis of digested hindlimb muscles identified a different extent of EPC recruitment across the three muscle types, which varied depending on the angiogenic stimulus applied. Following transplantation in the acute ischaemia model, significantly increased EPC recruitment was only evident in the *m. tibialis anterior*. In the overload model only the *m. extensor digitorum longus* showed an increased number of bound EPCs (relative to the *m. soleus* as the *m. tibialis anterior* was removed). In contrast, following 2 days of chronic ischaemia, significantly increased recruitment of transplanted EPCs was observed in all three muscles. The 7 day chronic ischaemia model was the only one in which there was no significant difference observed between the ipsilateral and contralateral limbs, although only the ipsilateral *m. extensor digitorum longus* and *m. soleus* muscles were available for analysis due to the necessary extirpation of the ipsilateral *m. tibialis anterior*. This may be due to macrophage-mediated clearance of EPCs from the hindlimb muscles at a time-point between 2 days (at which time

EPCs were identified in the hindlimb) and 7 days. Macrophage infiltration and subsequent transplanted cell clearance has been demonstrated in a canine model of subendocardial and subepicardial injection of EPCs for the treatment of MI (Mitchell *et al.*, 2010). Furthermore, an EPC clearance half-life was established (2.5-3 days) in this study, which could explain the reduced recruitment observed in our murine hindlimb model at 7 days.

The patterns of recruitment demonstrated in our different transplantation models suggest that there may be something inherent in the nature of the different angiogenic stimuli that might differentially influence the recruitment of circulating EPCs. For example, it may be that the recruitment of EPCs is dependent, at least to a certain degree, on muscle fibre type. This is possible because it was in the muscles (rather than the viscera) that differential recruitment patterns were observed. It is known, for example, that the muscles of the hindlimb differ in fibre type composition (**Fig. 7.7**). The *m. tibialis anterior* is a mostly glycolytic muscle, consisting largely of fibre type II, with some mixed and a small amount of oxidative (type IIa and I) fibres (Augusto *et al.*, 2004). The *m. extensor digitorum longus* is composed of mixed fibre types, but with more type IIb than type IIa or type I fibres (Rosenblatt *et al.*, 1996). In contrast, the *m. soleus* is a mostly oxidative muscle, comprising only type IIa and I fibres (Totsuka *et al.*, 2003).

The localisation patterns observed in our investigation suggest a correlation between EPC recruitment and type IIb fibres. Following both acute and 2 day chronic ischaemia, as well as extirpation-induced overload, the two muscles that exhibited the most significant EPC localisation compared to the contralateral limb were the *m. tibialis anterior* and the *m. extensor digitorum longus*; both muscles contain a high proportion of type IIb fibres. The response of different muscle fibre types to angiogenic stimuli has been documented and this

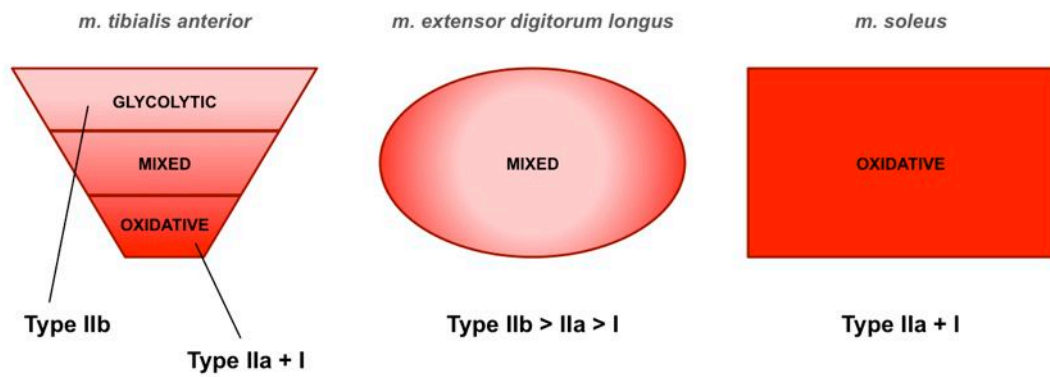


Figure 7.7. Fibre type composition of murine hindlimb muscles. The proportion of glycolytic and oxidative muscle fibres vary between the three muscles analysed in this study.

observed relationship may simply be due, for example, to type IIb muscle fibres being more significantly affected by the hypoxic conditions in the ischaemic transplantation models. Specifically, type IIb fibres (which have a low myosin and mitochondrial content) have been shown to be preferentially affected by reperfusion injury which causes them to fatigue more quickly under ischaemic conditions (Chan *et al.*, 2004). Simply put, it may be that the glycolytic muscles (*m. tibialis anterior* and *m. extensor digitorum longus*) of the mouse hindlimb are more dramatically affected by the insult of the ischaemic model than the oxidative *m. soleus*. Whilst a similar observation has been made in the rat hindlimb (Pette, 2002), other data from appropriate mouse models are not available. This greater sensitivity to ischaemia may in turn produce a greater angiogenic response in the activated ECs to which the transplanted EPCs respond and bind, increasing the apparent preference of EPCs for those muscle types. However, this reasoning does not fully explain the recruitment patterns seen across all of our transplantation models: in the overload model (which is not typified by ischaemia but rather by increased metabolic demand through hypertrophy of the remaining synergistic muscle) the *m. extensor digitorum longus* also demonstrated increased EPC recruitment compared to both its contralateral control and the ipsilateral *m. soleus*. However, the proportional change in recruitment with overload (111.6%) was far less than with chronic ischaemia (187.3%), although similar to acute ischaemia (128.4%).

An alternative transplantation model that employs a stimulus other than ischaemia to induce an angiogenic response may be useful in clarifying these findings. For example, angiogenesis can be induced in skeletal muscle by oral administration of prazosin, an α_1 -adrenergic receptor antagonist, which increases blood flow and capillary wall shear stress (Zhou *et al.*, 1998). Prazosin had been used in conjunction with synergistic muscle extirpation (as performed in our overload transplantation model) to investigate the mechanisms of

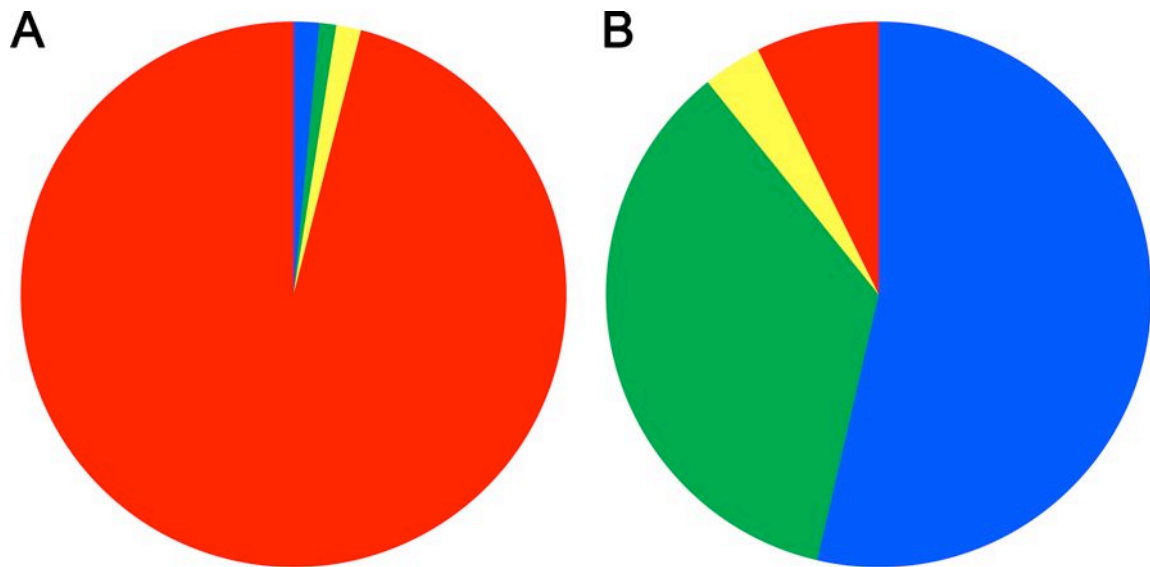
angiogenesis that occur in response to different mechanical stimuli (Egginton *et al.*, 2001; Williams, JL *et al.*, 2006). Hence, performing EPC transplantation using this shear stress model, in which ischaemia is not a major contributing factor, may further elucidate the relationships between EPC recruitment, ischaemia and type IIb muscle fibres. However, it must be noted that the increased shear stresses inherent to prazosin-induced angiogenesis may differentially influence platelet binding (and hence platelet-mediated EPC recruitment) as the adhesive bonds involved are influenced by changes in shear flow (Weiss *et al.*, 1978; Furukawa *et al.*, 2000). Similarly, leukocyte recruitment (which occurs by similar mechanisms to those proposed in our platelet-EPC model) has been shown to be differentially influenced by flow rates by the conditioning of the endothelium to shear stress (Sheikh *et al.*, 2005). In addition, our flow adhesion data suggests that high shear conditions (such as those induced by prazosin) are not best suited to binding of EPCs from flow. Instead perhaps, the prazosin model could be employed as a negative control for EPC transplantation, namely angiogenesis without EPC recruitment.

Whilst a greater understanding of the factors modulating the response to different stimuli is needed, the demonstration of a preferential, platelet-mediated recruitment of EPCs to angiogenically stimulated tissues *in vivo* dramatically increases the evidence for a potential of EPCs for therapeutic angiogenesis.

In terms of the proportional number of cells localised in different regions of the transplanted animal, the raw data do not adequately illustrate the extent of preferential recruitment of EPCs to the stimulated ipsilateral muscles. Averaged across the different transplantation models, 2.2% of the 2×10^6 injected EPCs were localised in the digested limb muscles, with 1.3% being found in the ipsilateral limb and 0.9% in the contralateral limb. In

comparison, 1.4% of the transplanted EPCs were identified in the six analysed organs. In absolute terms, the difference in cell recruitment between the ipsilateral muscles and the viscera was not substantial and may be taken to suggest that binding of EPCs in the stimulated regions of the hindlimb was not indicative of a preferential recruitment. Furthermore, over 96% of the injected cells were unaccounted for in our digestion analysis. It is logical to assume that a number of transplanted EPCs were lost to other tissues that were not included in our analysis, or that a certain proportion of the transplanted cells were still present in the blood at the time of tissue harvesting. However, as flow cytometry of exsanguinated blood taken at the time of tissue harvesting showed negligible levels of fluorescently-labelled EPCs (data not shown) the obvious conclusion is further non-specific localisation of EPCs to the remainder of the animal. Again, when taken as an absolute value, this significant loss of transplanted EPCs from the circulation to 'unintended' tissues suggests a low efficiency of cell delivery and a minimal homing of EPCs to angiogenic regions. However, if the numbers of EPCs found throughout the body are expressed proportionally to the mass of each analysed tissue, correlations between angiogenic stimulation and EPC binding become more evident (**Fig. 7.8**).

Although the total number of EPCs identified in the ipsilateral muscles ($\sim 2.7 \times 10^4$) was comparable to the total number found in the viscera ($\sim 2.9 \times 10^4$), there is a significant difference in mass between the hindlimb muscles and the organs. When this is taken into consideration, it dramatically alters the apparent distribution of transplanted cells. The relatively low combined mass of the *m. tibialis anterior*, *m. extensor digitorum longus* and *m. soleus* (51.7 mg) and the relatively high combined mass of the six analysed organs (769 mg) means that the proportional number of recruited EPCs is actually much lower in the viscera (38.1 cells \cdot mg $^{-1}$) than in the stimulated hindlimb muscles (513.5 cells \cdot mg $^{-1}$).



Region	Absolute cell number (A)	Proportional cell number (B)	%
■ Ipsilateral hindlimb	30229 ± 1774	585 ± 106	53.6
■ Contralateral hindlimb	20065 ± 297	388 ± 28	35.6
■ Viscera	28277 ± 294	38 ± 3	3.5
■ Remainder of animal	1921429 *	80 *	7.3

Figure 7.8. Proportional recruitment of EPCs following in vivo transplantation. Distribution of EPCs throughout the ipsilateral and contralateral hindlimb muscles, combined viscera and, by inference, the remainder of the animal, plotted using (A) absolute numbers of localised cells in each region and (B) EPC recruitment proportional to tissue mass. *derived values.

Furthermore, when spread across the entire remaining mass of the animal (2.4×10^4 mg), the large number of 'missing' EPCs (1.9×10^6) actually represents a far less significant proportion of transplanted cells ($79.7 \text{ cells} \cdot \text{mg}^{-1}$) than those recruited to the ipsilateral hindlimb. This is particularly interesting as it suggests that systemic clearance of a high percentage of the injected EPCs does not dramatically affect the efficiency of EPC recruitment to sites of angiogenesis. Of course to confirm that the level of visceral sequestration of EPCs seen here is not significant enough to detrimentally affect the outcome of EPC transplantation, further investigation into the functional effect of EPC transplantation would be necessary by, for example, the determination of improved limb perfusion by Laser Doppler flow imaging.

However, regardless of their end-point effect, we have demonstrated that EPCs will readily and preferentially bind at sites of angiogenesis *in vivo*. Furthermore, the importance of platelet presence in the recruitment of EPCs is evident from our depleted transplantation model. Whilst further investigations into the long-term beneficial outcome of EPC administration are necessary to define an effective cell-based transplantation regime, our data clearly suggest a potential for EPCs as a therapeutic tool for *in vivo* angiogenic treatment.

CHAPTER 8:

FINAL CONCLUSIONS

This investigation has described the endothelial phenotype of EPCs using a combination of gene expression and protein expression analysis, clarifying the position of naïve EPCs in the endothelial lineage. Furthermore, the significant angiogenic activity shown by EPCs, deemed to be much greater than fully differentiated mature ECs by the quantification of tubule formation *in vivo*, confirmed the suggested potential of EPCs to be used therapeutically for the treatment of conditions characterised by limited or impaired vascularity.

The mechanisms by which EPCs are thought to exert a beneficial angiogenic effect are numerous, including direct incorporation of cells into sites of neovascularisation and paracrine secretion of pro-angiogenic factors. However, regardless of the exact mechanism of action, it is clear from the literature that regimes involving the transplantation of donor cells show the greatest promise for the development of an angiogenic therapy involving EPCs. Whilst EPCs have a significant inherent potential for angiogenic activity they are only found in very limited circulating numbers in the adult and can be difficult to culture and expand to sufficient quantities *in vitro*. This problem has led to the suggestion of using highly proliferative pluripotent stem cells (either ESCs or iPSCs) to manufacture donor cells for transplantation, through the targeted differentiation of stem cells to produce defined populations of EPC-like cells in large quantities. As described here, ESCs can indeed be treated in such a way to produce cells with a genetic and proteomic profile, as well as an

angiogenic potential, identical to natural EPCs. Unfortunately, although there is evidence in the literature that EPCs (as well as a full range of cell types) can be produced from reprogrammed somatic cells, this investigation did not succeed in producing similarly angiogenic cells from iPSCs.

Through *in vitro* transplantation of EPCs into EC tubules grown on a gel matrix, it was possible to demonstrate the beneficial effects of EPCs in a simplified model of vascular growth. In addition, EPCs were observed to have a transitional phenotype depending on the quantity transplanted. This suggests the existence of a graded response of EPCs to vascular trauma, with cumulative upregulation in the angiogenic activity of each EPC (combined with an increase of cells from the BM) ensuring an efficient and controlled level of natural cell activity appropriate to the response required. It also offers the suggestion that EPC transplantation can eventually be modulated to suit particular pathophysiological conditions, by adjusting the regime to provide a tailored therapy depending on specific requirements for revascularisation. Although it was not tested following stem cell differentiation, one may assume that the EPC-equivalent angiogenic activity demonstrated by ESC-derived cells would result in the same tubule-enhancing effects. This would be an ideal next stage for this study, to further aid the understanding of the relationship between endothelial differentiation and angiogenic activity, and the development of stem cell sources for angiogenic treatments.

Using a combination of *in vitro* and *in vivo* experiments, this investigation also illustrated the role of platelets in the recruitment of EPCs following transplantation, demonstrating the importance of the purported 'platelet bridge' in the adhesion of EPCs from flow. Furthermore, P-selectin was identified as an important mediator in the primary adhesion mechanism. The subsequent steps involved in stabilisation of the platelet-EPC bond are still unclear, however,

and further studies are needed to identify additional factors involved in the formation of the platelet-EPC bridge. In addition, being shown to play a significant role, further investigations into P-selectin specifically would be beneficial in fully understanding its role in EPC recruitment. A useful model for this would be the P-selectin-deficient mouse (P-sel^{-/-}; C57BL/6J-*Selep*) in which P-selectin is absent on both the platelet and endothelial cell surface (Bullard *et al.*, 1995). Performing EPC transplantation experiments using this model would enable: (i) P-selectin inhibition experiments performed in this study using *in vitro* flow assays to be repeated in a comparable *in vivo* model and (ii) a better understanding of the radiometric involvement of platelet- and cell-surface P-selectin by the use of (P-selectin-positive) donor platelets and EPCs in the P-selectin-deficient environment.

Here, the recruitment of EPCs was illustrated using a tissue digestion and flow cytometry method that enabled localisation of transplanted EPCs to selected tissues. This allowed the preferential recruitment of EPCs between the ipsilateral and contralateral muscles of our hindlimb models to be determined. However, the method was limited by the choice of tissues harvested and lacks sensitivity compared to other possible techniques. For example, whole-body imaging of fluorescently labelled cells has been demonstrated using the Xenogen IVIS Imaging System (Xenogen Corporation, California, USA) to observe EPC presence at sites of wound healing following *in vivo* transplantation of EPC-seeded polymeric scaffolds (Kim, KL *et al.*, 2009). As a pilot study for a potential future experiment, an experiment was performed in which Qdot-labelled EPCs were directly transplanted into the murine hindlimb by intramuscular injection (**Fig. 8.1**). Using the IVIS imaging system, the fluorescence resolution of the system was sufficient to detect the presence of EPCs within the muscle,

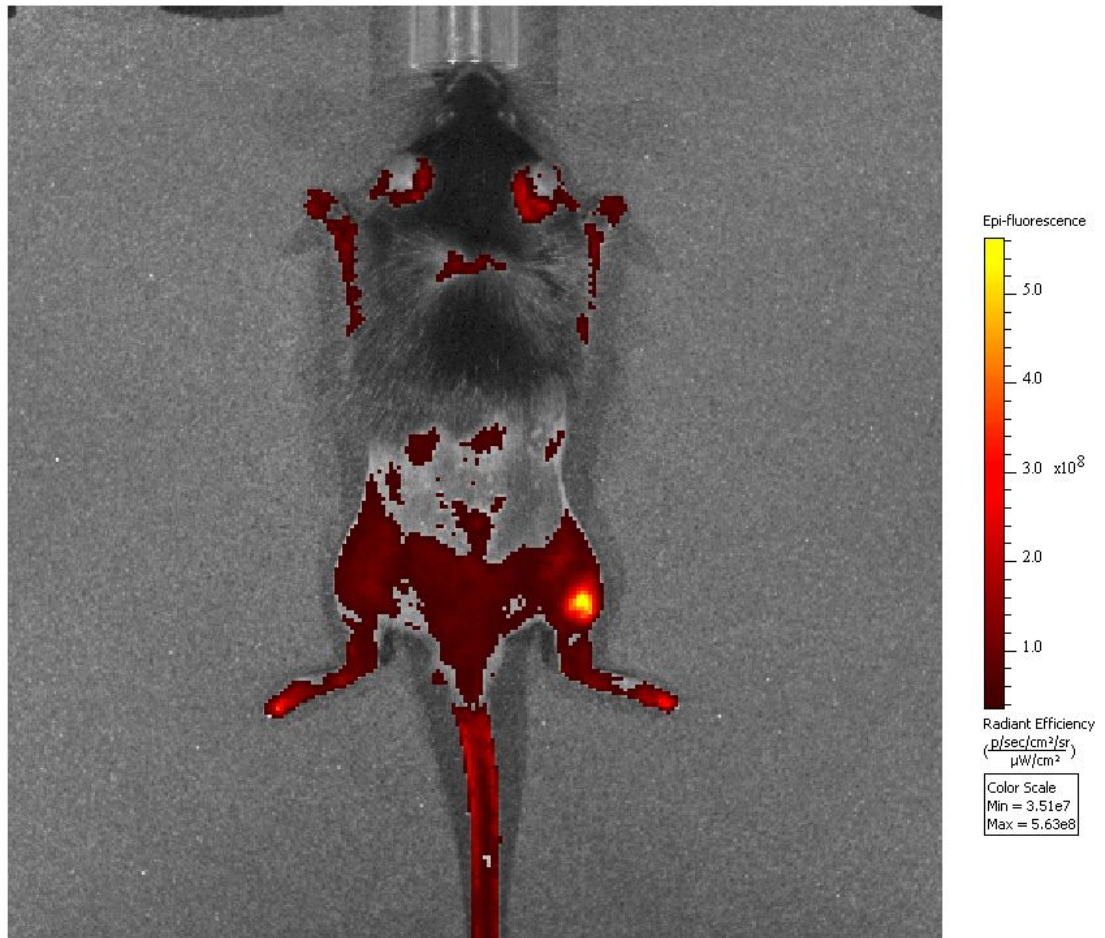


Figure 8.1. In vivo fluorescence microscopy of the murine hindlimb following EPC transplantation. 1×10^6 Qdot-labelled EPCs were injected via intramuscular injection and detected at 615 nm. Presence of EPCs indicated by level of epi-fluorescence (yellow).

offering the potential to adapt the system to perform further investigations into EPC transplantation. For our purposes, this *in vivo* imaging system would allow detection of transplanted cells throughout the whole animal and, because imaging can be performed on live animals, the persistence of adhered cells could be observed in subject-matched experiments over a prolonged time-course, something not possible using our current technique.

Similarly to the IVIS system, another technique that could benefit future studies is intravital microscopy, the live video-recording of the *in vivo* environment using epifluorescent microscopy. Intravital microscopy has been previously used to study leukocyte adhesion and migration behavior in the microvessels of the cremaster muscle under various *in vivo* flow conditions (Nolan *et al.*, 2008) and the migration of HSCs between the BM vascular niche and the blood circulation following induced mobilisation using G-CSF (Ross *et al.*, 2008). Preliminary experiments performed using intravital microscopy during this investigation have shown binding of transplanted EPCs in the exposed murine ileal endothelium following ischaemia (**Fig. 8.2**). This technique could therefore be used in our murine transplantation models to observe the adhesion of EPCs to a wide range of angiogenically active tissues following transplantation, providing an alternative readout of EPC recruitment to the flow cytometric analysis performed in this study. Furthermore, it may also be useful in corroborating the kinetics of EPC adhesion (i.e. stable non-rolling adhesion) observed in our *in vitro* flow adhesion assays.

Considering the primary focus of this study (that is, the initial binding events that occur immediately following transplantation) another interesting future direction for this study would be the investigation of the long-term outcomes of EPC transplantation. Whilst we have

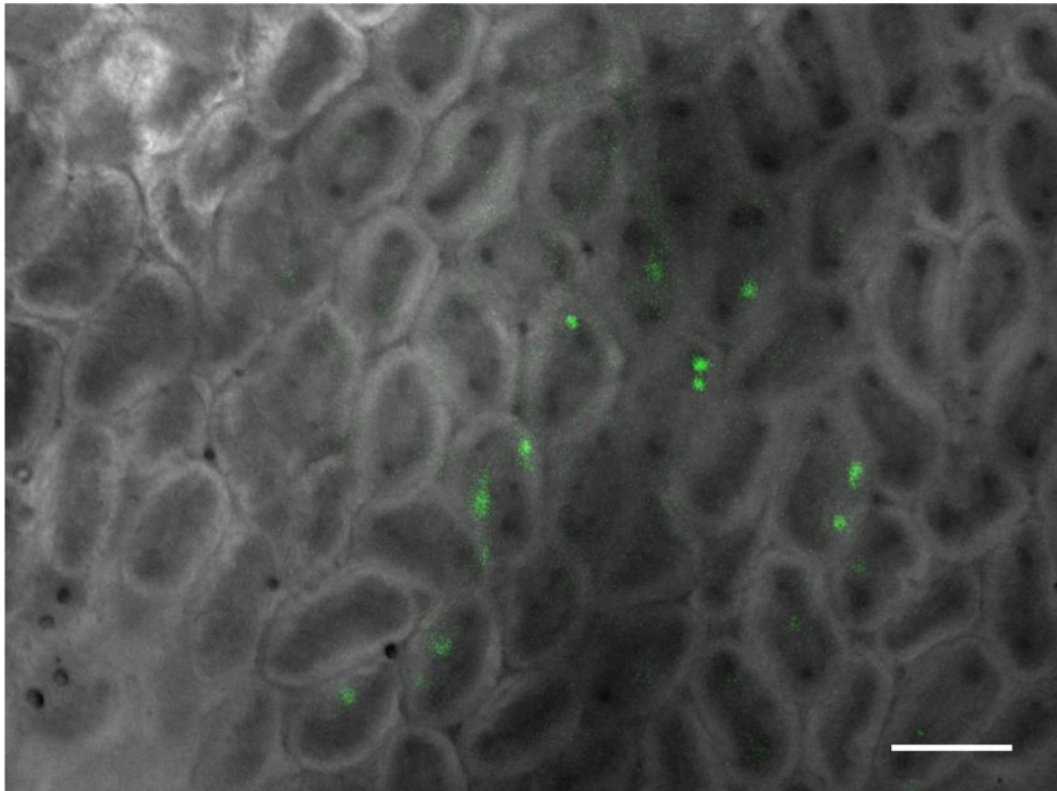


Figure 8.2. Intravital microscopy of the murine ileum following EPC transplantation. Prior to transplantation of 2×10^6 EPCs, cells were labelled with $10 \mu\text{M}$ carboxyfluorescein succinimidyl ester (CFSE) for 30 min. Intravital microscopy was used to image CFSE-labelled cells (green) at 517 nm. Scale bar = $50 \mu\text{m}$.

demonstrated: (i) a potential for EPC involvement in EC tubule repair *in vitro*, (ii) clarified aspects of the platelet-EPC adhesion mechanism and (iii) illustrated the binding of EPCs to sites of angiogenesis *in vivo*, the functional effects of transplantation were beyond the scope of this study. As evident by our survey of current transplantation regimes, many methods exist to quantify the functional outcome of cell transplantation, one of the the most common being Laser Doppler perfusion analysis to quantify the improvement of blood flow during angiogenesis (Hu, Z *et al.*, 2008; Kane *et al.*, 2010). By observing the hindlimb perfusion rates of EPC-transplanted animals over a relatively long time-course, it would be possible to make further physiologically relevant conclusions about the benefits of EPCs for angiogenic therapy, beyond our demonstration of a positive effect on tubule formation *in vitro*. Furthermore, correlations between therapeutic benefit and the persistence of transplanted cells, as suggested by the differential recruitment patterns seen following acute and chronic ischaemia stimulation, may be further elucidated.

Another interesting avenue of further study would be the transcriptional regulation of the differentiation and proliferation of EPCs, which are integral parts of the angiogenic EPC response and occur following recruitment to the stimulated endothelium. One candidate for such regulation is proline-rich homeodomain (PRH; also known as haematopoietically expressed homeobox [Hex]). PRH regulates many aspects of embryonic development through the activation and repression of transcription of its target genes, and is required for the correct formation of the haematopoietic and vascular systems (Soufi & Jayaraman, 2008). Preliminary experiments during this investigation have shown that *PRH* gene expression is variable during endothelial maturation (**Fig. 8.3**). High levels of *PRH* expression were detected in naïve ESCs, with expression decreasing to negligible levels over the course of 7 days of directed differentiation. In EPCs, expression was seen to increase with culture confluency (and hence,

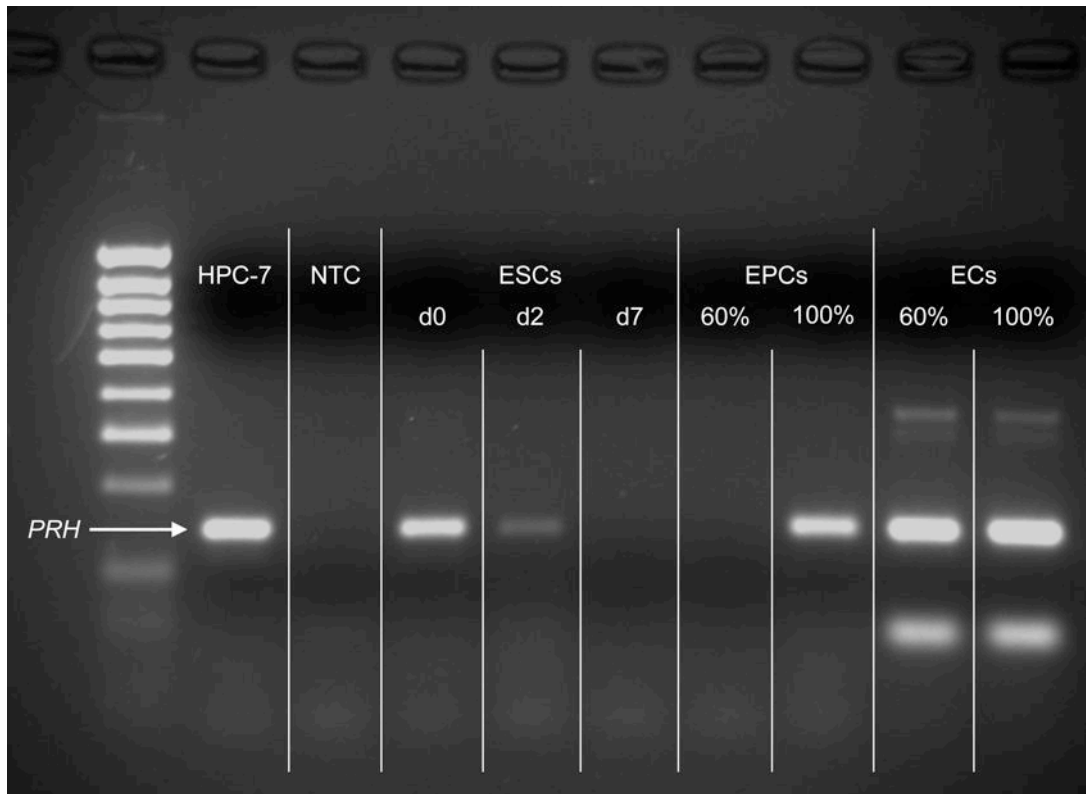


Figure 8.3. Analysis of PRH expression in ESCs, EPCs and ECs performed by RT-PCR. RT-PCR was carried out to detect PRH in D3 ESCs from day (D)0, D2 and D7 of directed differentiation using ECCM, and in MFLM-4 EPCs and MCEC-1 ECs at 60% and 100% culture confluence. Haematopoietic progenitor cells (HPC-7), which have been previously shown to express high levels of PRH, were used as a positive control. NTC, non-template negative control.

as previously discussed, EPC maturation) and in ECs, *PRH* levels were determined to be high once more. These findings suggest a relationship between *PRH* and endothelial maturation that could be explored to further understand EPC behaviour and the derivation of donor cells from ESCs. Furthermore, as it has previously been demonstrated that overexpression or knockdown of *PRH* directly affects leukaemic and tumour cell survival through the *PRH*-mediated modulation of VEGF and VEGFR signalling (Noy *et al.*, 2010), further investigation into the transcriptional role of *PRH* and VEGF(R) in the survival of transplanted EPCs may be beneficial.

Ultimately, in terms of the future of EPC transplantation, it is clear that there are many questions still to be answered and a wide variety of possible experiments remaining to be performed. However, within the scope of this study we conclude that EPC transplantation, especially when combined with the selective manipulation of pluripotent stem cells and the naïve precursor phenotype, has abundant potential for development into a viable and efficacious therapeutic angiogenic treatment.

REFERENCES

- Abou-Saleh H, Yacoub D, Théorêt J-F, Gillis M-A, Neagoe P-E, Labarthe B, Thérroux P, Sirois MG, Tabrizian M, Thorin E & Merhi Y** (2009). Endothelial progenitor cells bind and inhibit platelet function and thrombus formation. *Circulation* 120(22): 2230-9.
- Adair TH, Gay WJ & Montani JP** (1990). Growth regulation of the vascular system: evidence for a metabolic hypothesis. *Am J Physiol* 259(3 Pt 2): R393-404.
- Adams RH & Alitalo K** (2007). Molecular regulation of angiogenesis and lymphangiogenesis. *Nat Rev Mol Cell Biol* 8(6): 464-78.
- Aicher A, Rentsch M, Sasaki K-i, Ellwart JW, Fändrich F, Siebert R, Cooke JP, Dimmeler S & Heeschen C** (2007). Nonbone marrow-derived circulating progenitor cells contribute to postnatal neovascularization following tissue ischemia. *Circulation Research* 100(4): 581-9.
- Akeson AL, Brooks SK, Thompson FY & Greenberg JM** (2001). In vitro model for developmental progression from vasculogenesis to angiogenesis with a murine endothelial precursor cell line, MFLM-4. *Microvascular Research* 61(1): 75-86.
- Akeson AL, Wetzel B, Thompson FY, Brooks SK, Paradis H, Gendron RL & Greenberg JM** (2000). Embryonic vasculogenesis by endothelial precursor cells derived from lung mesenchyme. *Dev Dyn* 217(1): 11-23.
- Algire GH & Merwin RM** (1955). Vascular patterns in tissues and grafts within transparent chambers in mice. *Angiology* 6(4): 311-8.
- Allen J, Khan S, Serrano MC & Ameer G** (2008). Characterization of porcine circulating progenitor cells: toward a functional endothelium. *Tissue Engineering Part A* 14(1): 183-94.
- Altman SA, Randers L & Rao G** (1993). Comparison of trypan blue dye exclusion and fluorometric assays for mammalian cell viability determinations. *Biotechnol Prog* 9(6): 671-4.
- Aplin AC, Fogel E & Nicosia RF** (2010). MCP-1 promotes mural cell recruitment during angiogenesis in the aortic ring model. *Angiogenesis* 13(3): 219-26.
- Arfors KE, Lundberg C, Lindbom L, Lundberg K, Beatty PG & Harlan JM** (1987). A monoclonal antibody to the membrane glycoprotein complex CD18 inhibits polymorphonuclear leukocyte accumulation and plasma leakage in vivo. *Blood* 69(1): 338-40.
- Arnautova I, George J, Kleinman HK & Benton G** (2009). The endothelial cell tube formation assay on basement membrane turns 20: state of the science and the art. *Angiogenesis* 12(3): 267-74.
- Arnautova I & Kleinman HK** (2010). In vitro angiogenesis: endothelial cell tube formation on gelled basement membrane extract. *Nat Protoc* 5(4): 628-35.

- Arroyo JA & Winn VD** (2008). Vasculogenesis and angiogenesis in the IUGR placenta. *Seminars in Perinatology* 32(3): 172-7.
- Asahara T, Murohara T, Sullivan A, Silver M, van der Zee R, Li T, Witzenbichler B, Schatteman G & Isner JM** (1997). Isolation of putative progenitor endothelial cells for angiogenesis. *Science* 275(5302): 964-7.
- Auerbach R, Lewis R, Shinnars B, Kubai L & Akhtar N** (2003). Angiogenesis assays: a critical overview. *Clin Chem* 49(1): 32-40.
- Augusto V, Padovani CR & Campos GER** (2004). Skeletal muscle fiber types in C57BL/6J mice. *Braz J Morphol Sci* 21(2): 89-94.
- Badr I, Brown MD, Egginton S, Hudlická O, Milkiewicz M & Verhaeg J** (2003). Differences in local environment determine the site of physiological angiogenesis in rat skeletal muscle. *Exp Physiol* 88(5): 565-8.
- Bagheri-Yarmand R, Vadlamudi RK, Wang RA, Mendelsohn J & Kumar R** (2000). Vascular endothelial growth factor up-regulation via p21-activated kinase-1 signaling regulates heregulin-beta1-mediated angiogenesis. *J Biol Chem* 275(50): 39451-7.
- Bagley RG, Rouleau C, St Martin T, Boutin P, Weber W, Ruzek M, Honma N, Nacht M, Shankara S, Kataoka S, Ishida I, Roberts BL & Teicher BA** (2008). Human endothelial precursor cells express tumor endothelial marker 1/endothelialin/CD248. *Molecular Cancer Therapeutics* 7(8): 2536-46.
- Bahra P, Rainger GE, Wautier JL, Nguyet-Thin L & Nash GB** (1998). Each step during transendothelial migration of flowing neutrophils is regulated by the stimulatory concentration of tumour necrosis factor-alpha. *Cell Adhes Commun* 6(6): 491-501.
- Baker M** (2007). Scientific definition by political request.
- Balasubramanian V, Grabowski E, Bini A & Nemerson Y** (2002). Platelets, circulating tissue factor, and fibrin colocalize in ex vivo thrombi: real-time fluorescence images of thrombus formation and propagation under defined flow conditions. *Blood* 100(8): 2787-92.
- Barbee KA, Mundel T, Lal R & Davies PF** (1995). Subcellular distribution of shear stress at the surface of flow-aligned and nonaligned endothelial monolayers. *Am J Physiol* 268(4 Pt 2): H1765-72.
- Barber CL & Iruela-Arispe ML** (2006). The ever-elusive endothelial progenitor cell: identities, functions and clinical implications. *Pediatr Res* 59(4 Pt 2): 26R-32R.
- Beeres SLMA, Atsma DE, van Ramshorst J, Schaliij MJ & Bax JJ** (2008). Cell therapy for ischaemic heart disease. *Heart* 94(9): 1214-26.
- Beilmann M, Birk G & Lenter MC** (2004). Human primary co-culture angiogenesis assay reveals additive stimulation and different angiogenic properties of VEGF and HGF. *Cytokine* 26(4): 178-85.
- Bendeck MP** (2004). Macrophage matrix metalloproteinase-9 regulates angiogenesis in ischemic muscle. *Circulation Research* 94(2): 138-9.
- Bentz K, Molcanyi M, Hess S, Schneider A, Hescheler J, Neugebauer E & Schaefer U** (2006). Neural differentiation of embryonic stem cells is induced by signalling from non-neural niche cells. *Cell Physiol Biochem* 18(4-5): 275-86.

- Bergmeier W, Rackebrandt K, Schröder W, Zirngibl H & Nieswandt B** (2000). Structural and functional characterization of the mouse von Willebrand factor receptor GPIb-IX with novel monoclonal antibodies. *Blood* 95(3): 886-93.
- Bernstein A, MacCormick R & Martin GS** (1976). Transformation-defective mutants of avian sarcoma viruses: the genetic relationship between conditional and nonconditional mutants. *Virology* 70(1): 206-9.
- Blair P & Flaumenhaft R** (2009). Platelet alpha-granules: basic biology and clinical correlates. *Blood Reviews* 23(4): 177-89.
- Blau HM, Pavlath GK, Hardeman EC, Chiu CP, Silberstein L, Webster SG, Miller SC & Webster C** (1985). Plasticity of the differentiated state. *Science* 230(4727): 758-66.
- Boettcher M, Gloe T & de Wit C** (2009). Semiautomatic Quantification of Angiogenesis. *J Surg Res.*
- Bordoni V, Alonzi T, Zanetta L, Khouri D, Conti A, Corazzari M, Bertolini F, Antoniotti P, Pisani G, Tognoli F, Dejana E & Tripodi M** (2007). Hepatocyte-conditioned medium sustains endothelial differentiation of human hematopoietic-endothelial progenitors. *Hepatology* 45(5): 1218-28.
- Borges VM, Vandivier RW, McPhillips KA, Kench JA, Morimoto K, Groshong SD, Richens TR, Graham BB, Muldrow AM, Van Heule L, Henson PM & Janssen WJ** (2009). TNFalpha inhibits apoptotic cell clearance in the lung, exacerbating acute inflammation. *Am J Physiol Lung Cell Mol Physiol* 297(4): L586-95.
- Bouvier CA, Gaynor E & Cintron JR** (1970). Circulating endothelium as an indication of vascular injury. *Thromb Diath Haemorrh* 40(Suppl.): 163-8.
- Boyer LA, Lee TI, Cole MF, Johnstone SE, Levine SS, Zucker JP, Guenther MG, Kumar RM, Murray HL, Jenner RG, Gifford DK, Melton DA, Jaenisch R & Young RA** (2005). Core transcriptional regulatory circuitry in human embryonic stem cells. *Cell* 122(6): 947-56.
- Braddock M, Schwachtgen J-L, Houston P, Dickson MC, Lee MJ & Campbell CJ** (1998). Fluid Shear Stress Modulation of Gene Expression in Endothelial Cells. *News Physiol Sci* 13: 241-46.
- Brown MA, Wallace CS, Angelos M & Truskey GA** (2009). Characterization of umbilical cord blood-derived late outgrowth endothelial progenitor cells exposed to laminar shear stress. *Tissue Engineering Part A* 15(11): 3575-87.
- Brunner S, Engelmann MG & Franz W-M** (2008). Stem cell mobilisation for myocardial repair. *Expert Opin Biol Ther* 8(11): 1675-90.
- Buchholz DH, Squires JE, Herman JH, Ng AT, Anderson JK & Hedberg SL** (1997). Plateletpheresis in 90- to 110-pound donors using the CS-3000 blood cell separator. *Transfusion* 37(7): 715-8.
- Bullard DC, Qin L, Lorenzo I, Quinlin WM, Doyle NA, Bosse R, Vestweber D, Doerschuk CM & Beaudet AL** (1995). P-selectin/ICAM-1 double mutant mice: acute emigration of neutrophils into the peritoneum is completely absent but is normal into pulmonary alveoli. *J Clin Invest* 95(4): 1782-8.
- Burri PH & Djonov V** (2002). Intussusceptive angiogenesis--the alternative to capillary sprouting. *Mol Aspects Med* 23(6S): S1-27.
- Burri PH & Tarek MR** (1990). A novel mechanism of capillary growth in the rat pulmonary microcirculation. *Anat Rec* 228(1): 35-45.

- Bustin S** (2000). Absolute quantification of mRNA using real-time reverse transcription polymerase chain reaction assays. *J Mol Endocrinol* 25(2): 169-93.
- Butler LM, Mcgettrick HM & Nash GB** (2009). Static and dynamic assays of cell adhesion relevant to the vasculature. *Methods Mol Biol* 467: 211-28.
- Butler LM, Rainger GE & Nash GB** (2009). A role for the endothelial glycosaminoglycan hyaluronan in neutrophil recruitment by endothelial cells cultured for prolonged periods. *Exp Cell Res* 315(19): 3433-41.
- Buttrum SM, Hatton R & Nash GB** (1993). Selectin-mediated rolling of neutrophils on immobilized platelets. *Blood* 82(4): 1165-74.
- Cardillo C, Kilcoyne CM, Cannon RO & Panza JA** (2000). Interactions between nitric oxide and endothelin in the regulation of vascular tone of human resistance vessels in vivo. *Hypertension* 35(6): 1237-41.
- Carlevaro MF, Albini A, Ribatti D, Gentili C, Benelli R, Cermelli S, Cancedda R & Cancedda FD** (1997). Transferrin promotes endothelial cell migration and invasion: implication in cartilage neovascularization. *J Cell Biol* 136(6): 1375-84.
- Carlson TH, Kolman MR & Piepkorn M** (1995). Activation of antithrombin III isoforms by heparan sulphate glycosaminoglycans and other sulphated polysaccharides. *Blood Coagul Fibrinolysis* 6(5): 474-80.
- Carmeliet P** (2000). Mechanisms of angiogenesis and arteriogenesis. *Nat Med* 6(4): 389-95.
- Chan RK, Austen WG, Ibrahim S, Ding GY, Verna N, Hechtman HB & Moore FD** (2004). Reperfusion injury to skeletal muscle affects primarily type II muscle fibers. *J Surg Res* 122(1): 54-60.
- Chavakis E, Aicher A, Heeschen C, Sasaki K-i, Kaiser R, El Makhfi N, Urbich C, Peters T, Scharffetter-Kochanek K, Zeiher AM, Chavakis T & Dimmeler S** (2005). Role of beta2-integrins for homing and neovascularization capacity of endothelial progenitor cells. *J Exp Med* 201(1): 63-72.
- Chen S-l, Fang W-w, Ye F, Liu Y-H, Qian J, Shan S-j, Zhang J-j, Chunhua RZ, Liao L-m, Lin S & Sun J-p** (2004). Effect on left ventricular function of intracoronary transplantation of autologous bone marrow mesenchymal stem cell in patients with acute myocardial infarction. *Am J Cardiol* 94(1): 92-5.
- Chen WV & Soriano P** (2003). Gene trap mutagenesis in embryonic stem cells. *Meth Enzymol* 365: 367-86.
- Chen X, Vega VB & Ng H-H** (2008). Transcriptional regulatory networks in embryonic stem cells. *Cold Spring Harb Symp Quant Biol* 73: 203-9.
- Cheng C, Helderma F, Tempel D, Segers D, Hierck B, Poelmann R, van Tol A, Duncker DJ, Robbers-Visser D, Ursem NTC, van Haperen R, Wentzel JJ, Gijzen F, van der Steen AFW, de Crom R & Krams R** (2007). Large variations in absolute wall shear stress levels within one species and between species. *Atherosclerosis* 195(2): 225-35.
- Cheng XW, Kuzuya M, Nakamura K, Maeda K, Tsuzuki M, Kim W, Sasaki T, Liu Z, Inoue N, Kondo T, Jin H, Numaguchi Y, Okumura K, Yokota M, Iguchi A & Murohara T** (2007). Mechanisms underlying the impairment of ischemia-induced neovascularization in matrix metalloproteinase 2-deficient mice. *Circulation Research* 100(6): 904-13.

- Chin MH, Mason MJ, Xie W, Volinia S, Singer M, Peterson C, Ambartsumyan G, Aimiwu O, Richter L, Zhang J, Khvorostov I, Ott V, Grunstein M, Lavon N, Benvenisty N, Croce CM, Clark AT, Baxter T, Pyle AD, Teitell MA, Pelegriani M, Plath K & Lowry WE** (2009). Induced pluripotent stem cells and embryonic stem cells are distinguished by gene expression signatures. *Cell Stem Cell* 5(1): 111-23.
- Chinsomboon J, Ruas J, Gupta RK, Thom R, Shoag J, Rowe GC, Sawada N, Raghuram S & Arany Z** (2009). The transcriptional coactivator PGC-1 α mediates exercise-induced angiogenesis in skeletal muscle. *Proc Natl Acad Sci USA* 106(50): 21401-6.
- Chiu J-J, Lee P-L, Chen C-N, Lee C-I, Chang S-F, Chen L-J, Lien S-C, Ko Y-C, Usami S & Chien S** (2004). Shear stress increases ICAM-1 and decreases VCAM-1 and E-selectin expressions induced by tumor necrosis factor-[α] in endothelial cells. *Arteriosclerosis, Thrombosis, and Vascular Biology* 24(1): 73-9.
- Cho H-J, Lee N, Lee JY, Choi YJ, Li M, Wecker A, Jeong J-O, Curry C, Qin G & Yoon Y-S** (2007). Role of host tissues for sustained humoral effects after endothelial progenitor cell transplantation into the ischemic heart. *J Exp Med* 204(13): 3257-69.
- Cho S-R, Kim YR, Kang H-S, Yim SH, Park C-I, Min YH, Lee BH, Shin JC & Lim J-B** (2009). Functional recovery after the transplantation of neurally differentiated mesenchymal stem cells derived from bone marrow in a rat model of spinal cord injury. *Cell Transplant*.
- Cho S-W, Moon S-H, Lee S-H, Kang S-W, Kim J, Lim JM, Kim H-S, Kim B-S & Chung H-M** (2007). Improvement of postnatal neovascularization by human embryonic stem cell derived endothelial-like cell transplantation in a mouse model of hindlimb ischemia. *Circulation* 116(21): 2409-19.
- Choi K-D, Yu J, Smuga-Otto K, Salvagiotto G, Rehrauer W, Vodyanik M, Thomson J & Slukvin I** (2009). Hematopoietic and endothelial differentiation of human induced pluripotent stem cells. *Stem Cells* 27(3): 559-67.
- Chomczynski P & Sacchi N** (1987). Single-step method of RNA isolation by acid guanidinium thiocyanate-phenol-chloroform extraction. *Anal Biochem* 162(1): 156-9.
- Chung JW, Park JH, Han JK, Choi BI & Han MC** (1995). Hepatocellular carcinoma and portal vein invasion: results of treatment with transcatheter oily chemoembolization. *AJR Am J Roentgenol* 165(2): 315-21.
- Conway H, Joslin D & Stark RB** (1951). Observations on the development of circulation in skin grafts. I. Technique of adaptation of the transparent chamber technique to study of the circulation in skin grafts. *Plast Reconstr Surg (1946)* 8(3): 194-203.
- Cooper HA, Mason RG & Brinkhous KM** (1976). The platelet: membrane and surface reactions. *Annu Rev Physiol* 38: 501-35.
- Dahlbäck B & Villoutreix BO** (2005). The anticoagulant protein C pathway. *FEBS Letters* 579(15): 3310-6.
- Dammers R, Stiff F, Tordoir JHM, Hameleers JMM, Hoeks APG & Kitslaar PJEHM** (2003). Shear stress depends on vascular territory: comparison between common carotid and brachial artery. *J Appl Physiol* 94(2): 485-9.
- Daub K, Langer H, Seizer P, Stellos K, May AE, Goyal P, Bigalke B, Schönberger T, Geisler T, Siegel-Axel D, Oostendorp RAJ, Lindemann S & Gawaz M** (2006). Platelets induce differentiation of human CD34+ progenitor cells into foam cells and endothelial cells. *FASEB J* 20(14): 2559-61.

- Davì G & Patrono C** (2007). Platelet activation and atherothrombosis. *N Engl J Med* 357(24): 2482-94.
- Davies PF, Spaan JA & Krams R** (2005). Shear stress biology of the endothelium. *Ann Biomed Eng* 33(12): 1714-8.
- Davis TA, Black AT, Kidwell WR & Lee KP** (1997). Conditioned medium from primary porcine endothelial cells alone promotes the growth of primitive human haematopoietic progenitor cells with a high replating potential: evidence for a novel early haematopoietic activity. *Cytokine* 9(4): 263-75.
- de Boer HC, Verseyden C, Ulfman LH, Zwaginga JJ, Bot I, Biessen EA, Rabelink TJ & van Zonneveld AJ** (2006). Fibrin and activated platelets cooperatively guide stem cells to a vascular injury and promote differentiation towards an endothelial cell phenotype. *Arteriosclerosis, Thrombosis, and Vascular Biology* 26(7): 1653-9.
- de Macedo Braga LMG, Lacchini S, Schaan BDA, Rodrigues B, Rosa K, De Angelis K, Borges LF, Irigoyen MC & Nardi NB** (2008). In situ delivery of bone marrow cells and mesenchymal stem cells improves cardiovascular function in hypertensive rats submitted to myocardial infarction. *J Biomed Sci* 15(3): 365-74.
- De Palma M, Venneri MA, Roca C & Naldini L** (2003). Targeting exogenous genes to tumor angiogenesis by transplantation of genetically modified hematopoietic stem cells. *Nat Med* 9(6): 789-95.
- Demir R, Kaufmann P, Castellucci M, Erben T & Kotowski A** (1989). Fetal vasculogenesis and angiogenesis in human placental villi. *Acta Anat (Basel)* 136(3): 190-203.
- Dewey CF, Bussolari SR, Gimbrone MA & Davies PF** (1981). The dynamic response of vascular endothelial cells to fluid shear stress. *J Biomech Eng* 103(3): 177-85.
- Di Cera E, Dang QD & Ayala YM** (1997). Molecular mechanisms of thrombin function. *Cell Mol Life Sci* 53(9): 701-30.
- Dimmeler S** (2010). Regulation of Bone Marrow-Derived Vascular Progenitor Cell Mobilization and Maintenance. *Arteriosclerosis, Thrombosis, and Vascular Biology* 30(6): 1088-93.
- Dimmeler S, Haendeler J, Rippmann V, Nehls M & Zeiher AM** (1996). Shear stress inhibits apoptosis of human endothelial cells. *FEBS Lett* 399(1-2): 71-4.
- Dimmeler S & Vasa-Nicotera M** (2003). Aging of progenitor cells: limitation for regenerative capacity? *Journal of the American College of Cardiology* 42(12): 2081-2.
- Dimmeler S & Zeiher AM** (2004). Vascular repair by circulating endothelial progenitor cells: the missing link in atherosclerosis? *J Mol Med* 82(10): 671-7.
- Ding D-C, Shyu W-C, Lin S-Z & Li H** (2007). The role of endothelial progenitor cells in ischemic cerebral and heart diseases. *Cell transplantation* 16(3): 273-84.
- Djonov V, Baum O & Burri PH** (2003). Vascular remodeling by intussusceptive angiogenesis. *Cell Tissue Res* 314(1): 107-17.
- Donovan D, Brown NJ, Bishop ET & Lewis CE** (2001). Comparison of three in vitro human 'angiogenesis' assays with capillaries formed in vivo. *Angiogenesis* 4(2): 113-21.

- Droetto S, Viale A, Primo L, Jordaney N, Bruno S, Pagano M, Piacibello W, Bussolino F & Aglietta M** (2004). Vasculogenic potential of long term repopulating cord blood progenitors. *FASEB J* 18(11): 1273-5.
- Dunk C & Ahmed A** (2001). Vascular endothelial growth factor receptor-2-mediated mitogenesis is negatively regulated by vascular endothelial growth factor receptor-1 in tumor epithelial cells. *Am J Pathol* 158(1): 265-73.
- Durcova-Hills G, Tang F, Doody G, Tooze R, Surani M & Volff J** (2008). Reprogramming Primordial Germ Cells into Pluripotent Stem Cells. *PLoS ONE* 3(10): e3531.
- Egginton S** (2002). Temperature and angiogenesis: the possible role of mechanical factors in capillary growth. *Comp Biochem Physiol, Part A Mol Integr Physiol* 132(4): 773-87.
- Egginton S & Gerritsen M** (2003). Lumen formation: in vivo versus in vitro observations. *Microcirculation (New York, NY : 1994)* 10(1): 45-61.
- Egginton S, Hudlicka O & Glover M** (1993). Fine structure of capillaries in ischaemic and non ischaemic rat striated muscle. Effect of torbafylline. *International journal of microcirculation, clinical and experimental / sponsored by the European Society for Microcirculation* 12(1): 33-44.
- Egginton S, Zhou AL, Brown MD & Hudlická O** (2001). Unorthodox angiogenesis in skeletal muscle. *Cardiovascular Research* 49(3): 634-46.
- Erdbruegger U, Haubitz M & Woywodt A** (2006). Circulating endothelial cells: a novel marker of endothelial damage. *Clin Chim Acta* 373(1-2): 17-26.
- Evans MJ & Kaufman MH** (1981). Establishment in culture of pluripotential cells from mouse embryos. *Nature* 292(5819): 154-6.
- Facucho-Oliveira JM, Alderson J, Spikings EC, Egginton S & St John JC** (2007). Mitochondrial DNA replication during differentiation of murine embryonic stem cells. *Journal of Cell Science* 120(Pt 22): 4025-34.
- Fadini GP, Agostini C & Avogaro A** (2005). Endothelial progenitor cells and vascular biology in diabetes mellitus: current knowledge and future perspectives. *Curr Diabetes Rev* 1(1): 41-58.
- Feng Q, Lu S-J, Klimanskaya I, Gomes I, Kim D, Chung Y, Honig GR, Kim K-S & Lanza R** (2010). Hemangioblastic derivatives from human induced pluripotent stem cells exhibit limited expansion and early senescence. *Stem Cells* 28(4): 704-12.
- Fisch A, Tobusch K, Veit K, Meyer J & Darius H** (1997). Prostacyclin receptor desensitization is a reversible phenomenon in human platelets. *Circulation* 96(3): 756-60.
- Fox A, Smythe J, Fisher N, Tyler MPH, McGrouther DA, Watt SM & Harris AL** (2008). Mobilization of endothelial progenitor cells into the circulation in burned patients. *The British journal of surgery* 95(2): 244-51.
- Friis T, Kjaer Sørensen B, Engel A-M, Rygaard J & Houen G** (2003). A quantitative ELISA-based coculture angiogenesis and cell proliferation assay. *APMIS* 111(6): 658-68.
- Fukushima K, Murata M, Hachisuga M, Tsukimori K, Seki H, Takeda S, Kato K & Wake N** (2008). Gene expression profiles by microarray analysis during matrigel-induced tube formation in a human extravillous trophoblast cell line: comparison with endothelial cells. *Placenta* 29(10): 898-904.

- Furukawa KS, Ushida T, Sugano H, Tamaki T, Ohshima N & Tateishi T** (2000). Effect of shear stress on platelet adhesion to expanded polytetrafluoroethylene, a silicone sheet, and an endothelial cell monolayer. *ASAIO J* 46(6): 696-701.
- Gai H, Leung EL-H, Costantino PD, Aguila JR, Nguyen DM, Fink LM, Ward DC & Ma Y** (2009). Generation and characterization of functional cardiomyocytes using induced pluripotent stem cells derived from human fibroblasts. *Cell Biol Int* 33(11): 1184-93.
- Garmy-Susini B & Varner JA** (2005). Circulating endothelial progenitor cells. *Br J Cancer* 93(8): 855-8.
- George J, Afek A, Abashidze A, Shmilovich H, Deutsch V, Kopolovich J, Miller H & Keren G** (2005). Transfer of endothelial progenitor and bone marrow cells influences atherosclerotic plaque size and composition in apolipoprotein E knockout mice. *Arteriosclerosis, Thrombosis, and Vascular Biology* 25(12): 2636-41.
- Gerhardt H, Golding M, Fruttiger M, Ruhrberg C, Lundkvist A, Abramsson A, Jeltsch M, Mitchell C, Alitalo K, Shima D & Betsholtz C** (2003). VEGF guides angiogenic sprouting utilizing endothelial tip cell filopodia. *The Journal of Cell Biology* 161(6): 1163-77.
- Geuze RE, Wegman F, Oner FC, Dhert WJA & Alblas J** (2009). Influence of endothelial progenitor cells and platelet gel on tissue-engineered bone ectopically in goats. *Tissue Eng Part A* 15(11): 3669-77.
- Giancotti FG, Tarone G, Knudsen K, Damsky C & Comoglio PM** (1985). Cleavage of a 135 kD cell surface glycoprotein correlates with loss of fibroblast adhesion to fibronectin. *Exp Cell Res* 156(1): 182-90.
- Gill M, Dias S, Hattori K, Rivera ML, Hicklin D, Witte L, Girardi L, Yurt R, Himel H & Rafii S** (2001). Vascular trauma induces rapid but transient mobilization of VEGFR2(+)AC133(+) endothelial precursor cells. *Circulation Research* 88(2): 167-74.
- Gillespie DL, Villavicencio JL, Gallagher C, Chang A, Hamelink JK, Fiala LA, O'Donnell SD, Jackson MR, Pikoulis E & Rich NM** (1997). Presentation and management of venous aneurysms. *J Vasc Surg* 26(5): 845-52.
- Goldstein LJ, Gallagher KA, Bauer SM, Bauer RJ, Baireddy V, Liu Z-J, Buerk DG, Thom SR & Velazquez OC** (2006). Endothelial progenitor cell release into circulation is triggered by hypoxia-induced increases in bone marrow nitric oxide. *Stem Cells* 24(10): 2309-18.
- Goodwin AM** (2007). In vitro assays of angiogenesis for assessment of angiogenic and anti-angiogenic agents. *Microvascular Research* 74(2-3): 172-83.
- Goossens PL, Marchal G & Milon G** (1988). Early influx of Listeria-reactive T lymphocytes in liver of mice genetically resistant to listeriosis. *J Immunol* 141(7): 2451-5.
- Gotoh N, Kambara K, Jiang XW, Ohno M, Emura S, Fujiwara T & Fujiwara H** (2000). Apoptosis in microvascular endothelial cells of perfused rabbit lungs with acute hydrostatic edema. *J Appl Physiol* 88(2): 518-26.
- Gulati R, Jevremovic D, Peterson TE, Chatterjee S, Shah V, Vile RG & Simari RD** (2003). Diverse origin and function of cells with endothelial phenotype obtained from adult human blood. *Circulation Research* 93(11): 1023-5.
- Guzman RJ, Abe K & Zarins CK** (1997). Flow-induced arterial enlargement is inhibited by suppression of nitric oxide synthase activity in vivo. *Surgery* 122(2): 273-9; discussion 79-80.

- Hall AP** (2006). Review of the pericyte during angiogenesis and its role in cancer and diabetic retinopathy. *Toxicol Pathol* 34(6): 763-75.
- Hansen-Smith FM, Hudlicka O & Egginton S** (1996). In vivo angiogenesis in adult rat skeletal muscle: early changes in capillary network architecture and ultrastructure. *Cell Tissue Res* 286(1): 123-36.
- Hansson GK** (2005). Inflammation, atherosclerosis, and coronary artery disease. *N Engl J Med* 352(16): 1685-95.
- Hattori K, Heissig B, Tashiro K, Honjo T, Tateno M, Shieh JH, Hackett NR, Quitariano MS, Crystal RG, Rafii S & Moore MA** (2001). Plasma elevation of stromal cell-derived factor-1 induces mobilization of mature and immature hematopoietic progenitor and stem cells. *Blood* 97(11): 3354-60.
- Hayashi H, Nakagami H, Takami Y, Sato N, Saito Y, Nishikawa T, Mori M, Koriyama H, Tamai K, Morishita R & Kaneda Y** (2007). Involvement of gamma-secretase in postnatal angiogenesis. *Biochemical and Biophysical Research Communications* 363(3): 584-90.
- Heeschen C, Aicher A, Lehmann R, Fichtlscherer S, Vasa M, Urbich C, Mildner-Rihm C, Martin H, Zeiher AM & Dimmeler S** (2003). Erythropoietin is a potent physiologic stimulus for endothelial progenitor cell mobilization. *Blood* 102(4): 1340-6.
- Heng BC, Cowan CM & Basu S** (2009). Comparison of Enzymatic and Non-Enzymatic Means of Dissociating Adherent Monolayers of Mesenchymal Stem Cells. *Biol Proced Online*.
- Heng BC, Liu H, Rufaihah AJ & Cao T** (2006). Human embryonic stem cell (hES) colonies display a higher degree of spontaneous differentiation when passaged at lower densities. *In Vitro Cell Dev Biol Anim* 42(3-4): 54-7.
- Henrich D, Hahn P, Wahl M, Wilhelm K, Dernbach E, Dimmeler S & Marzi I** (2004). Serum derived from multiple trauma patients promotes the differentiation of endothelial progenitor cells in vitro: possible role of transforming growth factor-beta1 and vascular endothelial growth factor165. *Shock* 21(1): 13-6.
- Hidalgo A, Weiss LA & Frenette PS** (2002). Functional selectin ligands mediating human CD34(+) cell interactions with bone marrow endothelium are enhanced postnatally. *J Clin Invest* 110(4): 559-69.
- Hilaire G & Duron B** (1999). Maturation of the mammalian respiratory system. *Physiol Rev* 79(2): 325-60.
- Hill JM, Zalos G, Halcox JPJ, Schenke WH, Waclawiw MA, Quyyumi AA & Finkel T** (2003). Circulating endothelial progenitor cells, vascular function, and cardiovascular risk. *N Engl J Med* 348(7): 593-600.
- Hirschi KK, Ingram DA & Yoder MC** (2008). Assessing identity, phenotype, and fate of endothelial progenitor cells. *Arteriosclerosis, Thrombosis, and Vascular Biology* 28(9): 1584-95.
- Hogg N, Henderson R, Leitinger B, McDowall A, Porter J & Stanley P** (2002). Mechanisms contributing to the activity of integrins on leukocytes. *Immunol Rev* 186: 164-71.
- Hombach-Klonisch S, Panigrahi S, Rashedi I, Seifert A, Alberti E, Pocar P, Kurpisz M, Schulze-Osthoff K, Mackiewicz A & Los M** (2008). Adult stem cells and their trans-differentiation potential-perspectives and therapeutic applications. *J Mol Med*.

- Hong H, Takahashi K, Ichisaka T, Aoi T, Kanagawa O, Nakagawa M, Okita K & Yamanaka S** (2009). Suppression of induced pluripotent stem cell generation by the p53-p21 pathway. *Nature* 460(7259): 1132-5.
- Hooper C** (1956). Cell turnover in epithelial populations. *J Histochem Cytochem* 4(6): 531-40.
- Hordijk P** (2003). Endothelial signaling in leukocyte transmigration. *Cell Biochem Biophys* 38(3): 305-22.
- Hristov M & Weber C** (2004). Endothelial progenitor cells: characterization, pathophysiology, and possible clinical relevance. *J Cell Mol Med* 8(4): 498-508.
- Hu X-B, Feng F, Wang Y-C, Wang L, He F, Dou G-R, Liang L, Zhang H-W, Liang Y-M & Han H** (2009). Blockade of Notch signaling in tumor-bearing mice may lead to tumor regression, progression, or metastasis, depending on tumor cell types. *Neoplasia* 11(1): 32-8.
- Hu Z, Zhang F, Yang Z, Yang N, Zhang D, Zhang J & Cao K** (2008). Combination of simvastatin administration and EPC transplantation enhances angiogenesis and protects against apoptosis for hindlimb ischemia. *J Biomed Sci* 15(4): 509-17.
- Huang NF, Niiyama H, Peter C, De A, Natkunam Y, Fleissner F, Li Z, Rollins MD, Wu JC, Gambhir SS & Cooke JP** (2010). Embryonic stem cell-derived endothelial cells engraft into the ischemic hindlimb and restore perfusion. *Arteriosclerosis, Thrombosis, and Vascular Biology* 30(5): 984-91.
- Hudlicka O, Brown M & Egginton S** (1992). Angiogenesis in skeletal and cardiac muscle. *Physiol Rev* 72(2): 369-417.
- Hudlicka O, Brown MD, Egginton S & Dawson JM** (1994). Effect of long-term electrical stimulation on vascular supply and fatigue in chronically ischemic muscles. *J Appl Physiol* 77(3): 1317-24.
- Iannacone M, Sitia G, Isogawa M, Marchese P, Castro MG, Lowenstein PR, Chisari FV, Ruggeri ZM & Guidotti LG** (2005). Platelets mediate cytotoxic T lymphocyte-induced liver damage. *Nat Med* 11(11): 1167-9.
- Iba O, Matsubara H, Nozawa Y, Fujiyama S, Amano K, Mori Y, Kojima H & Iwasaka T** (2002). Angiogenesis by implantation of peripheral blood mononuclear cells and platelets into ischemic limbs. *Circulation* 106(15): 2019-25.
- Ichida JK, Blanchard J, Lam K, Son EY, Chung JE, Egli D, Loh KM, Carter AC, Di Giorgio FP, Koszka K, Huangfu D, Akutsu H, Liu DR, Rubin LL & Eggan K** (2009). A small-molecule inhibitor of tgf-Beta signaling replaces sox2 in reprogramming by inducing nanog. *Cell Stem Cell* 5(5): 491-503.
- Ihizumi T, Hattori A, Sanada M & Muto M** (1977). Megakaryocyte and platelet formation: a scanning electron microscope study in mouse spleen. *Arch Histol Jpn* 40(4): 305-20.
- Iida M, Heike T, Yoshimoto M, Baba S, Doi H & Nakahata T** (2005). Identification of cardiac stem cells with FLK1, CD31, and VE-cadherin expression during embryonic stem cell differentiation. *FASEB J* 19(3): 371-8.
- Ikeda Y, Fukuda N, Wada M, Matsumoto T, Satomi A, Yokoyama S-I, Saito S, Matsumoto K, Kanmatsuse K & Mugishima H** (2004). Development of angiogenic cell and gene therapy by transplantation of umbilical cord blood with vascular endothelial growth factor gene. *Hypertens Res* 27(2): 119-28.

- Ingber DE** (1990). Fibronectin controls capillary endothelial cell growth by modulating cell shape. *Proc Natl Acad Sci USA* 87(9): 3579-83.
- Ingram DA, Caplice NM & Yoder MC** (2005). Unresolved questions, changing definitions, and novel paradigms for defining endothelial progenitor cells. *Blood* 106(5): 1525-31.
- Iso Y, Spees JL, Serrano C, Bakondi B, Pochampally R, Song Y-H, Sobel BE, Delafontaine P & Prockop DJ** (2007). Multipotent human stromal cells improve cardiac function after myocardial infarction in mice without long-term engraftment. *Biochemical and Biophysical Research Communications* 354(3): 700-6.
- Iwami Y, Masuda H & Asahara T** (2004). Endothelial progenitor cells: past, state of the art, and future. *J Cell Mol Med* 8(4): 488-97.
- Jain RK** (2003). Molecular regulation of vessel maturation. *Nat Med* 9(6): 685-93.
- Janowska-Wieczorek A, Majka M, Kijowski J, Baj-Krzyworzeka M, Reza R, Turner AR, Ratajczak J, Emerson SG, Kowalska MA & Ratajczak MZ** (2001). Platelet-derived microparticles bind to hematopoietic stem/progenitor cells and enhance their engraftment. *Blood* 98(10): 3143-9.
- Jin H, Aiyer A, Su J, Borgstrom P, Stupack D, Friedlander M & Varner J** (2006). A homing mechanism for bone marrow-derived progenitor cell recruitment to the neovasculature. *Journal of Clinical Investigation* 116(3): 652-62.
- Jo H, Dull RO, Hollis TM & Tarbell JM** (1991). Endothelial albumin permeability is shear dependent, time dependent, and reversible. *Am J Physiol* 260(6 Pt 2): H1992-6.
- Jodon de Villeroché V, Avouac J, Ponceau A, Ruiz B, Kahan A, Boileau C, Uzan G & Allanore Y** (2010). Enhanced late-outgrowth circulating endothelial progenitor cell levels in rheumatoid arthritis and correlation with disease activity. *Arthritis Res Ther* 12(1): R27.
- Kabrun N, Bühring HJ, Choi K, Ullrich A, Risau W & Keller G** (1997). Flk-1 expression defines a population of early embryonic hematopoietic precursors. *Development* 124(10): 2039-48.
- Kado M, Lee J-K, Hidaka K, Miwa K, Murohara T, Kasai K, Saga S, Morisaki T, Ueda Y & Kodama I** (2008). Paracrine factors of vascular endothelial cells facilitate cardiomyocyte differentiation of mouse embryonic stem cells. *Biochemical and Biophysical Research Communications* 377(2): 413-8.
- Kadokama T, Nishimura K, Hoshino Y, Sasajima T & Sumpio BE** (2007). Effects of different types of fluid shear stress on endothelial cell proliferation and survival. *J Cell Physiol* 212(1): 244-51.
- Kahn D & Westerhoff HV** (1993). The regulatory strength: how to be precise about regulation and homeostasis. *Acta Biotheor* 41(1-2): 85-96.
- Kalka C, Masuda H, Takahashi T, Kalka-Moll WM, Silver M, Kearney M, Li T, Isner JM & Asahara T** (2000). Transplantation of ex vivo expanded endothelial progenitor cells for therapeutic neovascularization. *Proc Natl Acad Sci USA* 97(7): 3422-7.
- Kanayasu-Toyoda T, Yamaguchi T, Oshizawa T & Hayakawa T** (2003). CD31 (PECAM-1)-bright cells derived from AC133-positive cells in human peripheral blood as endothelial-precursor cells. *J Cell Physiol* 195(1): 119-29.
- Kane NM, Meloni M, Spencer HL, Craig MA, Strehl R, Milligan G, Houslay MD, Mountford JC, Emanuelli C & Baker AH** (2010). Derivation of Endothelial Cells From Human Embryonic Stem

- Cells by Directed Differentiation. Analysis of MicroRNA and Angiogenesis In Vitro and In Vivo. *Arteriosclerosis, Thrombosis, and Vascular Biology*: 1-44.
- Kang H-J, Kim H-S, Zhang S-Y, Park K-W, Cho H-J, Koo B-K, Kim Y-J, Soo Lee D, Sohn D-W, Han K-S, Oh B-H, Lee M-M & Park Y-B** (2004). Effects of intracoronary infusion of peripheral blood stem-cells mobilised with granulocyte-colony stimulating factor on left ventricular systolic function and restenosis after coronary stenting in myocardial infarction: the MAGIC cell randomised clinical trial. *Lancet* 363(9411): 751-6.
- Karumbayaram S, Novitch BG, Patterson M, Umbach JA, Richter L, Lindgren A, Conway AE, Clark AT, Goldman SA, Plath K, Wiedau-Pazos M, Kornblum HI & Lowry WE** (2009). Directed differentiation of human-induced pluripotent stem cells generates active motor neurons. *Stem Cells* 27(4): 806-11.
- Kawamoto A & Asahara T** (2007). Role of progenitor endothelial cells in cardiovascular disease and upcoming therapies. *Catheterization and cardiovascular interventions : official journal of the Society for Cardiac Angiography & Interventions* 70(4): 477-84.
- Kawamoto A, Gwon HC, Iwaguro H, Yamaguchi JI, Uchida S, Masuda H, Silver M, Ma H, Kearney M, Isner JM & Asahara T** (2001). Therapeutic potential of ex vivo expanded endothelial progenitor cells for myocardial ischemia. *Circulation* 103(5): 634-7.
- Kawamoto A, Tkebuchava T, Yamaguchi J-I, Nishimura H, Yoon Y-S, Milliken C, Uchida S, Masuo O, Iwaguro H, Ma H, Hanley A, Silver M, Kearney M, Losordo DW, Isner JM & Asahara T** (2003). Intramyocardial transplantation of autologous endothelial progenitor cells for therapeutic neovascularization of myocardial ischemia. *Circulation* 107(3): 461-8.
- Kebir A, Harhoury K, Guillet B, Liu JW, Foucault-Bertaud A, Lamy E, Kaspi E, Elganfoud N, Vely F, Sabatier F, Sampol J, Pisano P, Kruithof EKO, Bardin N, Dignat-George F & Blot-Chaubaud M** (2010). CD146 Short Isoform Increases the Proangiogenic Potential of Endothelial Progenitor Cells In Vitro and In Vivo. *Circulation Research*: 1-20.
- Kellogg E & Shaffer H** (1993). Model Organisms in Evolutionary Studies. *Systematic Biology* 42(4): 409-14.
- Kim JY, Song S-H, Kim KL, Ko J-J, Im J-E, Yie SW, Ahn YK, Kim D-K & Suh W** (2010). Human cord blood-derived endothelial progenitor cells and their conditioned media exhibit therapeutic equivalence for diabetic wound healing. *Cell Transplant* 19(12): 1635-44.
- Kim KL, Han DK, Park K, Song S-H, Kim JY, Kim J-M, Ki HY, Yie SW, Roh C-R, Jeon E-S, Kim D-K & Suh W** (2009). Enhanced dermal wound neovascularization by targeted delivery of endothelial progenitor cells using an RGD-g-PLLA scaffold. *Biomaterials* 30(22): 3742-8.
- Kim S & von Recum HA** (2009). Endothelial progenitor populations in differentiating embryonic stem cells I: Identification and differentiation kinetics. *Tissue Engineering Part A* 15(12): 3709-18.
- Kiran MS, Viji RI, Kumar SV, Prabhakaran AA & Sudhakaran PR** (2011). Changes in expression of VE-cadherin and MMPs in endothelial cells: Implications for angiogenesis. *Vascular cell* 3(1): 6.
- Kjellmer I** (1965). On the competition between metabolic vasodilatation and neurogenic vasoconstriction in skeletal muscle. *Acta Physiol Scand* 63: 450-9.
- Klintman D, Li X & Thorlacius H** (2004). Important role of P-selectin for leukocyte recruitment, hepatocellular injury, and apoptosis in endotoxemic mice. *Clin Diagn Lab Immunol* 11(1): 56-62.

- Koedam JA, Cramer EM, Briend E, Furie B, Furie BC & Wagner DD** (1992). P-selectin, a granule membrane protein of platelets and endothelial cells, follows the regulated secretory pathway in AtT-20 cells. *J Cell Biol* 116(3): 617-25.
- Kono T, Kubo H, Shimazu C, Ueda Y, Takahashi M, Yanagi K, Fujita N, Tsuruo T, Wada H & Yamashita JK** (2006). Differentiation of lymphatic endothelial cells from embryonic stem cells on OP9 stromal cells. *Arteriosclerosis, Thrombosis, and Vascular Biology* 26(9): 2070-6.
- Kränkel N, Katare R, Siragusa M, Barcelos L, Campagnolo P, Mangialardi G, Fortunato O, Spinetti G, Tran N, Zacharowski K, Wojakowski W, Mroz I, Herman A, Manning Fox J, MacDonald P, Schanstra J, Bascands J, Ascione R, Angelini G, Emanuelli C & Madeddu P** (2008). Role of kinin B2 receptor signaling in the recruitment of circulating progenitor cells with neovascularization potential. *Circulation Research* 103(11): 1335-43.
- Krause DS, Ito T, Fackler MJ, Smith OM, Collector MI, Sharkis SJ & May WS** (1994). Characterization of murine CD34, a marker for hematopoietic progenitor and stem cells. *Blood* 84(3): 691-701.
- Krishnaswamy G, Kelley J, Yerra L, Smith JK & Chi DS** (1999). Human endothelium as a source of multifunctional cytokines: molecular regulation and possible role in human disease. *J Interferon Cytokine Res* 19(2): 91-104.
- Kubo A, Chen V, Kennedy M, Zahradka E, Daley GQ & Keller G** (2005). The homeobox gene *HEX* regulates proliferation and differentiation of hemangioblasts and endothelial cells during ES cell differentiation. *Blood* 105(12): 4590-7.
- Kubota Y, Kleinman HK, Martin GR & Lawley TJ** (1988). Role of laminin and basement membrane in the morphological differentiation of human endothelial cells into capillary-like structures. *The Journal of Cell Biology* 107(4): 1589-98.
- Kushner E, Van Guilder G, MacEneaney O, Greiner J, Cech J, Stauffer B & Desouza C** (2010). Ageing and endothelial progenitor cell release of proangiogenic cytokines. *Age Ageing* 39(2): 268-72.
- Langer H, May AE, Daub K, Heinzmann U, Lang P, Schumm M, Vestweber D, Massberg S, Schönberger T, Pfisterer I, Hatzopoulos AK & Gawaz M** (2006). Adherent platelets recruit and induce differentiation of murine embryonic endothelial progenitor cells to mature endothelial cells in vitro. *Circulation Research* 98(2): e2-10.
- Langer HF & Chavakis T** (2009). Leukocyte-endothelial interactions in inflammation. *J Cell Mol Med* 13(7): 1211-20.
- Langer HF & Gawaz M** (2008). Platelet-vessel wall interactions in atherosclerotic disease. *Thromb Haemost* 99(3): 480-6.
- Langer HF & Gawaz M** (2008). Platelets in regenerative medicine. *Basic Res Cardiol* 103(4): 299-307.
- Lasala GP, Silva JA, Gardner PA & Minguell JJ** (2010). Combination Stem Cell Therapy for the Treatment of Severe Limb Ischemia: Safety and Efficacy Analysis. *Angiology*: 1-6.
- Laufs U, Werner N, Link A, Endres M, Wassmann S, Jürgens K, Miche E, Böhm M & Nickenig G** (2004). Physical training increases endothelial progenitor cells, inhibits neointima formation, and enhances angiogenesis. *Circulation* 109(2): 220-6.
- Lawley TJ & Kubota Y** (1989). Induction of morphologic differentiation of endothelial cells in culture. *J Invest Dermatol* 93(2 Suppl): 59S-61S.

- Lawrence MB & Springer TA** (1991). Leukocytes roll on a selectin at physiologic flow rates: distinction from and prerequisite for adhesion through integrins. *Cell* 65(5): 859-73.
- Le Ricousse-Roussanne S, Barateau V, Contreres J-O, Boval B, Kraus-Berthier L & Tobelem G** (2004). Ex vivo differentiated endothelial and smooth muscle cells from human cord blood progenitors home to the angiogenic tumor vasculature. *Cardiovasc Res* 62(1): 176-84.
- Lee G, Papapetrou EP, Kim H, Chambers SM, Tomishima MJ, Fasano CA, Ganat YM, Menon J, Shimizu F, Viale A, Tabar V, Sadelain M & Studer L** (2009). Modelling pathogenesis and treatment of familial dysautonomia using patient-specific iPSCs. *Nature* 461(7262): 402-6.
- Lee GS, Filipovic N, Miele LF, Lin M, Simpson DC, Giney B, Konerding MA, Tsuda A & Mentzer SJ** (2010). Blood flow shapes intravascular pillar geometry in the chick chorioallantoic membrane. *J Angiogenesis Res* 2: 11.
- Lee PC, Salyapongse AN, Bragdon GA, Shears LL, Watkins SC, Edington HD & Billiar TR** (1999). Impaired wound healing and angiogenesis in eNOS-deficient mice. *Am J Physiol* 277(4 Pt 2): H1600-8.
- Lee S-P, Youn S-W, Cho H-J, Li L, Kim T-Y, Yook H-S, Chung J-W, Hur J, Yoon C-H, Park K-W, Oh B-H, Park Y-B & Kim H-S** (2006). Integrin-linked kinase, a hypoxia-responsive molecule, controls postnatal vasculogenesis by recruitment of endothelial progenitor cells to ischemic tissue. *Circulation* 114(2): 150-9.
- Lee Y, McIntire LV & Zygorakis K** (1994). Analysis of endothelial cell locomotion: Differential effects of motility and contact inhibition. *Biotechnol Bioeng* 43(7): 622-34.
- Lengerke C, Grauer M, Niebuhr NI, Riedt T, Kanz L, Park I-H & Daley GQ** (2009). Hematopoietic development from human induced pluripotent stem cells. *Ann N Y Acad Sci* 1176: 219-27.
- Leshem-Lev D, Omelchenko A, Perl L, Kornowski R, Battler A & Lev EI** (2010). Exposure to platelets promotes functional properties of endothelial progenitor cells. *J Thromb Thrombolysis* 30(4): 398-403.
- Lev EI, Estrov Z, Aboulfatova K, Harris D, Granada JF, Alviar C, Kleiman NS & Dong J-f** (2006). Potential role of activated platelets in homing of human endothelial progenitor cells to subendothelial matrix. *Thromb Haemost* 96(4): 498-504.
- Levy AP, Levy NS, Wegner S & Goldberg MA** (1995). Transcriptional regulation of the rat vascular endothelial growth factor gene by hypoxia. *J Biol Chem* 270(22): 13333-40.
- Li W, Ma N, Ong L-L, Nesselmann C, Klopsch C, Ladilov Y, Furlani D, Piechaczek C, Moebius JM, Lützw K, Lendlein A, Stamm C, Li R-K & Steinhoff G** (2007). Bcl-2 engineered MSCs inhibited apoptosis and improved heart function. *Stem Cells* 25(8): 2118-27.
- Li Y, Zheng J, Bird IM & Magness RR** (2003). Effects of pulsatile shear stress on nitric oxide production and endothelial cell nitric oxide synthase expression by ovine fetoplacental artery endothelial cells. *Biol Reprod* 69(3): 1053-9.
- Li Z, Wu JC, Sheikh AY, Kraft D, Cao F, Xie X, Patel M, Gambhir SS, Robbins RC, Cooke JP & Wu JC** (2007). Differentiation, survival, and function of embryonic stem cell derived endothelial cells for ischemic heart disease. *Circulation* 116(11 Suppl): I46-54.
- Lian Q, Zhang Y, Zhang J, Zhang HK, Wu X, Zhang Y, Lam FF-Y, Kang S, Xia JC, Lai W-H, Au K-W, Chow YY, Siu C-W, Lee C-N & Tse H-F** (2010). Functional mesenchymal stem cells derived from

- human induced pluripotent stem cells attenuate limb ischemia in mice. *Circulation* 121(9): 1113-23.
- Liang C-C, Park AY & Guan J-L** (2007). In vitro scratch assay: a convenient and inexpensive method for analysis of cell migration in vitro. *Nat Protoc* 2(2): 329-33.
- Lidington EA, Rao RM, Marelli-Berg FM, Jat PS, Haskard DO & Mason JC** (2002). Conditional immortalization of growth factor-responsive cardiac endothelial cells from H-2K(b)-tsA58 mice. *Am J Physiol, Cell Physiol* 282(1): C67-74.
- Liew A, Barry F & O'Brien T** (2006). Endothelial progenitor cells: diagnostic and therapeutic considerations. *Bioessays* 28(3): 261-70.
- Lim YC, Snapp K, Kansas GS, Camphausen R, Ding H & Lusinskas FW** (1998). Important contributions of P-selectin glycoprotein ligand-1-mediated secondary capture to human monocyte adhesion to P-selectin, E-selectin, and TNF-alpha-activated endothelium under flow in vitro. *J Immunol* 161(5): 2501-8.
- Livak K** (2001). Analysis of Relative Gene Expression Data Using Real-Time Quantitative PCR and the 2- $\Delta\Delta$ CT Method. *Methods* 25(4): 402-08.
- Looney MR, Nguyen JX, Hu Y, Van Ziffle JA, Lowell CA & Matthay MA** (2009). Platelet depletion and aspirin treatment protect mice in a two-event model of transfusion-related acute lung injury. *J Clin Invest* 119(11): 3450-61.
- Lowry WE, Richter L, Yachechko R, Pyle AD, Tchieu J, Sridharan R, Clark AT & Plath K** (2008). Generation of human induced pluripotent stem cells from dermal fibroblasts. *Proc Natl Acad Sci USA* 105(8): 2883-8.
- Luu NT, Rainger GE & Nash GB** (1999). Kinetics of the different steps during neutrophil migration through cultured endothelial monolayers treated with tumour necrosis factor-alpha. *J Vasc Res* 36(6): 477-85.
- Ma N, Ladilov Y, Moebius JM, Ong L, Piechaczek C, Dávid A, Kaminski A, Choi Y-H, Li W, Egger D, Stamm C & Steinhoff G** (2006). Intramyocardial delivery of human CD133+ cells in a SCID mouse cryoinjury model: Bone marrow vs. cord blood-derived cells. *Cardiovascular Research* 71(1): 158-69.
- Madri JA, Pratt BM & Tucker AM** (1988). Phenotypic modulation of endothelial cells by transforming growth factor-beta depends upon the composition and organization of the extracellular matrix. *J Cell Biol* 106(4): 1375-84.
- Malek A & Izumo S** (1992). Physiological fluid shear stress causes downregulation of endothelin-1 mRNA in bovine aortic endothelium. *Am J Physiol* 263(2 Pt 1): C389-96.
- Malek AM, Alper SL & Izumo S** (1999). Hemodynamic shear stress and its role in atherosclerosis. *JAMA* 282(21): 2035-42.
- Malek AM & Izumo S** (1996). Mechanism of endothelial cell shape change and cytoskeletal remodeling in response to fluid shear stress. *Journal of Cell Science* 109 (Pt 4): 713-26.
- Mamdouh Z, Mikhailov A & Muller WA** (2009). Transcellular migration of leukocytes is mediated by the endothelial lateral border recycling compartment. *J Exp Med* 206(12): 2795-808.

- Mandl J, Mucha I, Bánhegyi G, Mészáros G, Faragó A, Spolarics Z, Machovich R, Antoni F & Garzó T** (1988). cAMP dependent inhibition of thromboxane A₂, prostacyclin and PGF₂ alpha synthesis in mouse hepatocytes. *Prostaglandins* 36(6): 761-72.
- Manginas A, Goussetis E, Koutelou M, Karatasakis G, Peristeri I, Theodorakos A, Leontiadis E, Plessas N, Theodosaki M, Graphakos S & Cokkinos DV** (2007). Pilot study to evaluate the safety and feasibility of intracoronary CD133(+) and CD133(-) CD34(+) cell therapy in patients with nonviable anterior myocardial infarction. *Catheterization and cardiovascular interventions : official journal of the Society for Cardiac Angiography & Interventions* 69(6): 773-81.
- Marchetti S, Gimond C, Iljin K, Bourcier C, Alitalo K, Pouyssegur J & Pagès G** (2002). Endothelial cells genetically selected from differentiating mouse embryonic stem cells incorporate at sites of neovascularization in vivo. *Journal of Cell Science* 115(Pt 10): 2075-85.
- Marino J, Cook P & Miller K** (2003). Accurate and statistically verified quantification of relative mRNA abundances using SYBR Green I and real-time RT-PCR. *J Immunol Methods* 283(1-2): 291-306.
- Martin T, Harding K & Jiang W** (1999). Regulation of angiogenesis and endothelial cell motility by matrix-bound fibroblasts. *Angiogenesis* 3(1): 69-76.
- Massberg S, Konrad I, Schürzinger K, Lorenz M, Schneider S, Zohlnhoefer D, Hoppe K, Schiemann M, Kennerknecht E, Sauer S, Schulz C, Kerstan S, Rudelius M, Seidl S, Sorge F, Langer H, Peluso M, Goyal P, Vestweber D, Emambokus NR, Busch DH, Frampton J & Gawaz M** (2006). Platelets secrete stromal cell-derived factor 1alpha and recruit bone marrow-derived progenitor cells to arterial thrombi in vivo. *J Exp Med* 203(5): 1221-33.
- Masson-Pévet M, Jongasma HJ & De Bruijne J** (1976). Collagenase- and trypsin-dissociated heart cells: a comparative ultrastructural study. *J Mol Cell Cardiol* 8(10): 747-57.
- Mattson DL** (2001). Comparison of arterial blood pressure in different strains of mice. *Am J Hypertens* 14(5 Pt 1): 405-8.
- May AE, Seizer P & Gawaz M** (2008). Platelets: inflammatory firebugs of vascular walls. *Arteriosclerosis, Thrombosis, and Vascular Biology* 28(3): s5-10.
- Mayadas TN, Johnson RC, Rayburn H, Hynes RO & Wagner DD** (1993). Leukocyte rolling and extravasation are severely compromised in P selectin-deficient mice. *Cell* 74(3): 541-54.
- Mazur P** (1970). Cryobiology: the freezing of biological systems. *Science* 168(934): 939-49.
- McGann LE** (1979). Optimal temperature ranges for control of cooling rate. *Cryobiology* 16(3): 211-6.
- Milkiewicz M, Ispanovic E, Doyle JL & Haas TL** (2006). Regulators of angiogenesis and strategies for their therapeutic manipulation. *The International Journal of Biochemistry & Cell Biology* 38(3): 333-57.
- Mistry N, Cranmer SL, Yuan Y, Mangin P, Dopheide SM, Harper I, Giuliano S, Dunstan DE, Lanza F, Salem HH & Jackson SP** (2000). Cytoskeletal regulation of the platelet glycoprotein Ib/IX-von willebrand factor interaction. *Blood* 96(10): 3480-9.
- Mitchell AJ, Sabondjian E, Sykes J, Deans L, Zhu W, Lu X, Feng Q, Prato FS & Wisenberg G** (2010). Comparison of initial cell retention and clearance kinetics after subendocardial or subepicardial injections of endothelial progenitor cells in a canine myocardial infarction model. *J Nucl Med* 51(3): 413-7.

- Miyakawa AA, de Lourdes Junqueira M & Krieger JE** (2004). Identification of two novel shear stress responsive elements in rat angiotensin I converting enzyme promoter. *Physiol Genomics* 17(2): 107-13.
- Mody NA, Lomakin O, Doggett TA, Diacovo TG & King MR** (2005). Mechanics of transient platelet adhesion to von Willebrand factor under flow. *Biophysical Journal* 88(2): 1432-43.
- Montero-Balaguer M, Swirsding K, Orsenigo F, Cotelli F, Mione M & Dejana E** (2009). Stable vascular connections and remodeling require full expression of VE-cadherin in zebrafish embryos. *PLoS ONE* 4(6): e5772.
- Morioka K, Muraoka R, Chiba Y, Ihaya A, Kimura T, Noguti H & Uesaka T** (1996). Leukocyte and platelet depletion with a blood cell separator: effects on lung injury after cardiac surgery with cardiopulmonary bypass. *J Thorac Cardiovasc Surg* 111(1): 45-54.
- Mukai N, Akahori T, Komaki M, Li Q, Kanayasu-Toyoda T, Ishii-Watabe A, Kobayashi A, Yamaguchi T, Abe M, Amagasa T & Morita I** (2008). A comparison of the tube forming potentials of early and late endothelial progenitor cells. *Exp Cell Res* 314(3): 430-40.
- Muller WA, Berman ME, Newman PJ, DeLisser HM & Albelda SM** (1992). A heterophilic adhesion mechanism for platelet/endothelial cell adhesion molecule 1 (CD31). *J Exp Med* 175(5): 1401-4.
- Murohara T, Ikeda H, Duan J, Shintani S, Sasaki Ki, Eguchi H, Onitsuka I, Matsui K & Imaizumi T** (2000). Transplanted cord blood-derived endothelial precursor cells augment postnatal neovascularization. *Journal of Clinical Investigation* 105(11): 1527-36.
- Murphy JB** (1913). Transplantability of tissues to the embryo of foreign species: Its bearing n questions of tissue specificity and tumor immunity. *J Exp Med* 17(4): 482-93.
- Muthukkaruppan VR, Kubai L & Auerbach R** (1982). Tumor-induced neovascularization in the mouse eye. *J Natl Cancer Inst* 69(3): 699-708.
- Nagy A** (2003). Manipulating the mouse embryo: a laboratory manual. 764.
- Narazaki G, Uosaki H, Teranishi M, Okita K, Kim B, Matsuoka S, Yamanaka S & Yamashita JK** (2008). Directed and systematic differentiation of cardiovascular cells from mouse induced pluripotent stem cells. *Circulation* 118(5): 498-506.
- Nash G & Egginton S** (2007). Modelling the Effects of the Haemodynamic Environment on Endothelial Cell Responses Relevant to Angiogenesis.
- Nash GB** (1994). Adhesion between neutrophils and platelets: a modulator of thrombotic and inflammatory events? *Thromb Res* 74 Suppl 1: S3-11.
- Nash GB, Abbitt KB, Tate K, Jetha KA & Egginton S** (2001). Changes in the mechanical and adhesive behaviour of human neutrophils on cooling in vitro. *Pflugers Arch* 442(5): 762-70.
- Nelson TJ, Martinez-Fernandez A, Yamada S, Perez-Terzic C, Ikeda Y & Terzic A** (2009). Repair of acute myocardial infarction by human stemness factors induced pluripotent stem cells. *Circulation* 120(5): 408-16.
- Nesbitt WS, Mangin P, Salem HH & Jackson SP** (2006). The impact of blood rheology on the molecular and cellular events underlying arterial thrombosis. *J Mol Med* 84(12): 989-95.

- Nicosia R** (2009). The Aortic Ring Model of Angiogenesis: A Quarter Century of Search and Discovery. *J Cell Mol Med.*
- Nicosia RF, McCormick JF & Bielunas J** (1984). The formation of endothelial webs and channels in plasma clot culture. *Scan Electron Microsc*(Pt 2): 793-9.
- Nieswandt B, Bergmeier W, Rackebrandt K, Gessner JE & Zirngibl H** (2000). Identification of critical antigen-specific mechanisms in the development of immune thrombocytopenic purpura in mice. *Blood* 96(7): 2520-7.
- Niwa A, Umeda K, Chang H, Saito M, Okita K, Takahashi K, Nakagawa M, Yamanaka S, Nakahata T & Heike T** (2009). Orderly hematopoietic development of induced pluripotent stem cells via Flk-1(+) hemoangiogenic progenitors. *J Cell Physiol* 221(2): 367-77.
- Nolan SL, Kalia N, Nash GB, Kamel D, Heeringa P & Savage COS** (2008). Mechanisms of ANCA-mediated leukocyte-endothelial cell interactions in vivo. *J Am Soc Nephrol* 19(5): 973-84.
- Noy P, Williams H, Sawasdichai A, Gaston K & Jayaraman PS** (2010). PRH/Hhex Controls Cell Survival through Coordinate Transcriptional Regulation of Vascular Endothelial Growth Factor Signaling. *Molecular and Cellular Biology* 30(9): 2120-34.
- Ogunrinade O, Kameya GT & Truskey GA** (2002). Effect of fluid shear stress on the permeability of the arterial endothelium. *Ann Biomed Eng* 30(4): 430-46.
- Ohno-Matsui K, Uetama T, Yoshida T, Hayano M, Itoh T, Morita I & Mochizuki M** (2003). Reduced retinal angiogenesis in MMP-2-deficient mice. *Invest Ophthalmol Vis Sci* 44(12): 5370-5.
- Okrainec K, Banerjee DK & Eisenberg MJ** (2004). Coronary artery disease in the developing world. *American Heart Journal* 148(1): 7-15.
- Olsen JV, Ong S-E & Mann M** (2004). Trypsin cleaves exclusively C-terminal to arginine and lysine residues. *Mol Cell Proteomics* 3(6): 608-14.
- Op den Buijs J, Musters M, Verrips T, Post JA, Braam B & van Riel N** (2004). Mathematical modeling of vascular endothelial layer maintenance: the role of endothelial cell division, progenitor cell homing, and telomere shortening. *Am J Physiol Heart Circ Physiol* 287(6): H2651-8.
- Osakada F, Jin Z-B, Hirami Y, Ikeda H, Danjyo T, Watanabe K, Sasai Y & Takahashi M** (2009). In vitro differentiation of retinal cells from human pluripotent stem cells by small-molecule induction. *J Cell Sci* 122(Pt 17): 3169-79.
- Paleolog E** (2005). It's all in the blood: circulating endothelial progenitor cells link synovial vascularity with cardiovascular mortality in rheumatoid arthritis? *Arthritis Res Ther* 7(6): 270-2.
- Pan Y, Yuan D, Zhang J, Xu P, Chen H & Shao C** (2009). Cadmium-induced adaptive response in cells of Chinese hamster ovary cell lines with varying DNA repair capacity. *Radiat Res* 171(4): 446-53.
- Papaoiannou TG & Stefanadis C** (2005). Vascular wall shear stress: basic principles and methods. *Hellenic J Cardiol* 46(1): 9-15.
- Park I-H, Zhao R, West JA, Yabuuchi A, Huo H, Ince TA, Lerou PH, Lensch MW & Daley GQ** (2008). Reprogramming of human somatic cells to pluripotency with defined factors. *Nature* 451(7175): 141-6.

- Pascal LE, True LD, Campbell DS, Deutsch EW, Risk M, Coleman IM, Eichner LJ, Nelson PS & Liu AY** (2008). Correlation of mRNA and protein levels: cell type-specific gene expression of cluster designation antigens in the prostate. *BMC Genomics* 9: 246.
- Passaniti A, Taylor RM, Pili R, Guo Y, Long PV, Haney JA, Pauly RR, Grant DS & Martin GR** (1992). A simple, quantitative method for assessing angiogenesis and antiangiogenic agents using reconstituted basement membrane, heparin, and fibroblast growth factor. *Lab Invest* 67(4): 519-28.
- Patil S, Newman DK & Newman PJ** (2001). Platelet endothelial cell adhesion molecule-1 serves as an inhibitory receptor that modulates platelet responses to collagen. *Blood* 97(6): 1727-32.
- Patrick CW & McIntire LV** (1995). Shear stress and cyclic strain modulation of gene expression in vascular endothelial cells. *Blood Purif* 13(3-4): 112-24.
- Pearson JD** (2010). Endothelial progenitor cells--an evolving story. *Microvascular Research* 79(3): 162-8.
- Peichev M, Naiyer AJ, Pereira D, Zhu Z, Lane WJ, Williams M, Oz MC, Hicklin DJ, Witte L, Moore MA & Rafii S** (2000). Expression of VEGFR-2 and AC133 by circulating human CD34(+) cells identifies a population of functional endothelial precursors. *Blood* 95(3): 952-8.
- Perry AR & Linch DC** (1996). The history of bone-marrow transplantation. *Blood Rev* 10(4): 215-9.
- Pette D** (2002). The adaptive potential of skeletal muscle fibers. *Can J Appl Physiol* 27(4): 423-48.
- Petzold T, Orr AW, Hahn C, Jhaveri KA, Parsons JT & Schwartz MA** (2009). Focal adhesion kinase modulates activation of NF-kappaB by flow in endothelial cells. *Am J Physiol, Cell Physiol* 297(4): C814-22.
- Pfaffl M** (2001). A new mathematical model for relative quantification in real-time RT-PCR. *Nucleic Acids Res* 29(9): e45.
- Piali L, Hammel P, Uherek C, Bachmann F, Gisler RH, Dunon D & Imhof BA** (1995). CD31/PECAM-1 is a ligand for alpha v beta 3 integrin involved in adhesion of leukocytes to endothelium. *The Journal of Cell Biology* 130(2): 451-60.
- Pintucci G, Froum S, Pinnell J, Mignatti P, Rafii S & Green D** (2002). Trophic effects of platelets on cultured endothelial cells are mediated by platelet-associated fibroblast growth factor-2 (FGF-2) and vascular endothelial growth factor (VEGF). *Thromb Haemost* 88(5): 834-42.
- Pique JM, Whittle BJ & Esplugues JV** (1989). The vasodilator role of endogenous nitric oxide in the rat gastric microcirculation. *Eur J Pharmacol* 174(2-3): 293-6.
- Ponce ML** (2009). Tube formation: an in vitro matrigel angiogenesis assay. *Methods Mol Biol* 467: 183-8.
- Poon RT, Ng IO, Lau C, Zhu LX, Yu WC, Lo CM, Fan ST & Wong J** (2001). Serum vascular endothelial growth factor predicts venous invasion in hepatocellular carcinoma: a prospective study. *Ann Surg* 233(2): 227-35.
- Povsic TJ, Zavodni KL, Vainorius E, Kherani JF, Goldschmidt-Clermont PJ & Peterson ED** (2009). Common endothelial progenitor cell assays identify discrete endothelial progenitor cell populations. *Am Heart J* 157(2): 335-44.

- Powell TM, Paul JD, Hill JM, Thompson M, Benjamin M, Rodrigo M, McCoy JP, Read EJ, Khuu HM, Leitman SF, Finkel T & Cannon RO** (2005). Granulocyte colony-stimulating factor mobilizes functional endothelial progenitor cells in patients with coronary artery disease. *Arterioscler Thromb Vasc Biol* 25(2): 296-301.
- Prager E, Sunder-Plassmann R, Hansmann C, Koch C, Holter W, Knapp W & Stockinger H** (1996). Interaction of CD31 with a heterophilic counterreceptor involved in downregulation of human T cell responses. *J Exp Med* 184(1): 41-50.
- Priebe M, Davidoff G & Lampman RM** (1991). Exercise testing and training in patients with peripheral vascular disease and lower extremity amputation. *West J Med* 154(5): 598-601.
- Prokopi M, Pula G, Mayr U, Devue C, Gallagher J, Xiao Q, Boulanger CM, Westwood N, Urbich C, Willeit J, Steiner M, Breuss J, Xu Q, Kiechl S & Mayr M** (2009). Proteomic analysis reveals presence of platelet microparticles in endothelial progenitor cell cultures. *Blood* 114(3): 723-32.
- Rafii S** (2000). Circulating endothelial precursors: mystery, reality, and promise. *J Clin Invest* 105(1): 17-9.
- Rajvanshi P, Fabrega A, Bhargava KK, Kerr A, Pollak R, Blanchard J, Palestro CJ & Gupta S** (1999). Rapid clearance of transplanted hepatocytes from pulmonary capillaries in rats indicates a wide safety margin of liver repopulation and the potential of using surrogate albumin particles for safety analysis. *J Hepatol* 30(2): 299-310.
- Rauscher FM, Goldschmidt-Clermont PJ, Davis BH, Wang T, Gregg D, Ramaswami P, Phippen AM, Annex BH, Dong C & Taylor DA** (2003). Aging, progenitor cell exhaustion, and atherosclerosis. *Circulation* 108(4): 457-63.
- Re F, Zanetti A, Sironi M, Polentarutti N, Lanfrancone L, Dejana E & Colotta F** (1994). Inhibition of anchorage-dependent cell spreading triggers apoptosis in cultured human endothelial cells. *J Cell Biol* 127(2): 537-46.
- Rehman J, Li J, Orschell CM & March KL** (2003). Peripheral blood "endothelial progenitor cells" are derived from monocyte/macrophages and secrete angiogenic growth factors. *Circulation* 107(8): 1164-9.
- Reinhart-King CA, Dembo M & Hammer DA** (2005). The dynamics and mechanics of endothelial cell spreading. *Biophysical Journal* 89(1): 676-89.
- Reininger AJ, Heijnen HFG, Schumann H, Specht HM, Schramm W & Ruggeri ZM** (2006). Mechanism of platelet adhesion to von Willebrand factor and microparticle formation under high shear stress. *Blood* 107(9): 3537-45.
- Rendu F & Brohard-Bohn B** (2001). The platelet release reaction: granules' constituents, secretion and functions. *Platelets* 12(5): 261-73.
- Ribatti D** (2004). The first evidence of the tumor-induced angiogenesis in vivo by using the chorioallantoic membrane assay dated 1913. *Leukemia* 18(8): 1350-1.
- Richards M & Bongso A** (2006). Propagation of human embryonic stem cells on human feeder cells. *Methods Mol Biol* 331: 23-41.
- Ririe KM, Rasmussen RP & Wittwer CT** (1997). Product differentiation by analysis of DNA melting curves during the polymerase chain reaction. *Anal Biochem* 245(2): 154-60.

- Risau W** (1997). Mechanisms of angiogenesis. *Nature* 386(6626): 671-4.
- Roberts N, Jahangiri M & Xu Q** (2005). Progenitor cells in vascular disease. *J Cell Mol Med* 9(3): 583-91.
- Roberts WG & Palade GE** (1997). Neovasculature induced by vascular endothelial growth factor is fenestrated. *Cancer Research* 57(4): 765-72.
- Rolland A, Collet B, Le Verge R & Toujas L** (1989). Blood clearance and organ distribution of intravenously administered polymethacrylic nanoparticles in mice. *J Pharm Sci* 78(6): 481-4.
- Rosenblatt JD, Parry DJ & Partridge TA** (1996). Phenotype of adult mouse muscle myoblasts reflects their fiber type of origin. *Differentiation* 60(1): 39-45.
- Ross EA, Freeman S, Zhao Y, Dhanjal TS, Ross EJ, Lax S, Ahmed Z, Hou TZ, Kalia N, Egginton S, Nash G, Watson SP, Frampton J & Buckley CD** (2008). A novel role for PECAM-1 (CD31) in regulating haematopoietic progenitor cell compartmentalization between the peripheral blood and bone marrow. *PLoS ONE* 3(6): e2338.
- Rossi-Schneider TR, Verli FD, Marinho SA, Yurgel LS & De Souza MAL** (2010). Study of intussusceptive angiogenesis in inflammatory regional lymph nodes by scanning electron microscopy. *Microsc Res Tech* 73(1): 14-9.
- Roy A, Krzykwa E, Lemieux R & Néron S** (2001). Increased efficiency of gamma-irradiated versus mitomycin C-treated feeder cells for the expansion of normal human cells in long-term cultures. *J Hematother Stem Cell Res* 10(6): 873-80.
- Russ M, Seliger B, Hauptmann S, Marty R, Bukur J, Eriksson U, Schubert S, Werdan K & Buerke M** (2008). Abstract 5261: Platelet-Depletion Ameliorates Cardiac Function and Disease Severity in Experimental Autoimmune Myocarditis. *Circulation* 118(18_MeetingAbstracts): S_516-a EP -.
- Salven P, Mustjoki S, Alitalo R, Alitalo K & Rafii S** (2003). VEGFR-3 and CD133 identify a population of CD34+ lymphatic/vascular endothelial precursor cells. *Blood* 101(1): 168-72.
- Sambrook J, F. Fritsch E & Maniatis T** (1989). Molecular cloning: a laboratory manual. 1659.
- Schaper J, König R, Franz D & Schaper W** (1976). The endothelial surface of growing coronary collateral arteries. Intimal margination and diapedesis of monocytes. A combined SEM and TEM study. *Virchows Arch A Pathol Anat Histol* 370(3): 193-205.
- Schenke-Layland K, Rhodes KE, Angelis E, Butylkova Y, Heydarkhan-Hagvall S, Gekas C, Zhang R, Goldhaber JI, Mikkola HK, Plath K & MacLellan WR** (2008). Reprogrammed mouse fibroblasts differentiate into cells of the cardiovascular and hematopoietic lineages. *Stem Cells* 26(6): 1537-46.
- Schmittgen T & Zakrajsek B** (2000). Effect of experimental treatment on housekeeping gene expression: validation by real-time, quantitative RT-PCR. *J Biochem Biophys Methods* 46(1-2): 69-81.
- Schuh A, Liehn E, Sasse A, Hristov M, Sobota R, Kelm M, Merx M & Weber C** (2008). Transplantation of endothelial progenitor cells improves neovascularization and left ventricular function after myocardial infarction in a rat model. *Basic Res Cardiol* 103(1): 69-77.
- Schuleri KH, Amado LC, Boyle AJ, Centola M, Saliaris AP, Gutman MR, Hatzistergos KE, Oskouei BN, Zimmet JM, Young RG, Heldman AW, Lardo AC & Hare JM** (2008). Early improvement in

- cardiac tissue perfusion due to mesenchymal stem cells. *Am J Physiol Heart Circ Physiol* 294(5): H2002-11.
- Semenov AV, Romanov YA, Loktionova SA, Tikhomirov OY, Khachikian MV, Vasil'ev SA & Mazurov AV** (1999). Production of soluble P-selectin by platelets and endothelial cells. *Biochemistry Mosc* 64(11): 1326-35.
- Shaklai M & Tavassoli M** (1978). Demarcation membrane system in rat megakaryocyte and the mechanism of platelet formation: a membrane reorganization process. *J Ultrastruct Res* 62(3): 270-85.
- Shantsila E, Watson T & Lip G** (2007). Endothelial Progenitor Cells in Cardiovascular Disorders. *Journal of the American College of Cardiology* 49(7): 741-52.
- Sheikh S, Rahman M, Gale Z, Luu NT, Stone PCW, Matharu NM, Rainger GEL & Nash GB** (2005). Differing mechanisms of leukocyte recruitment and sensitivity to conditioning by shear stress for endothelial cells treated with tumour necrosis factor-alpha or interleukin-1beta. *Br J Pharmacol* 145(8): 1052-61.
- Shi Q, Rafii S, Wu MH, Wijelath ES, Yu C, Ishida A, Fujita Y, Kothari S, Mohle R, Sauvage LR, Moore MA, Storb RF & Hammond WP** (1998). Evidence for circulating bone marrow-derived endothelial cells. *Blood* 92(2): 362-7.
- Shintani S, Murohara T, Ikeda H, Ueno T, Honma T, Katoh A, Sasaki K, Shimada T, Oike Y & Imaizumi T** (2001). Mobilization of endothelial progenitor cells in patients with acute myocardial infarction. *Circulation* 103(23): 2776-9.
- Shirota T, Yasui H, Shimokawa H & Matsuda T** (2003). Fabrication of endothelial progenitor cell (EPC)-seeded intravascular stent devices and in vitro endothelialization on hybrid vascular tissue. *Biomaterials* 24(13): 2295-302.
- Shmelkov SV, Meeus S, Moussazadeh N, Kermani P, Rashbaum WK, Rabbany SY, Hanson MA, Lane WJ, St Clair R, Walsh KA, Dias S, Jacobson JT, Hempstead BL, Edelberg JM & Rafii S** (2005). Cytokine preconditioning promotes codifferentiation of human fetal liver CD133+ stem cells into angiomyogenic tissue. *Circulation* 111(9): 1175-83.
- Sieveking DP, Buckle A, Celermajer DS & Ng MKC** (2008). Strikingly different angiogenic properties of endothelial progenitor cell subpopulations: insights from a novel human angiogenesis assay. *Journal of the American College of Cardiology* 51(6): 660-8.
- Silva GV, Litovsky S, Assad JAR, Sousa ALS, Martin BJ, Vela D, Coulter SC, Lin J, Ober J, Vaughn WK, Branco RVC, Oliveira EM, He R, Geng Y-J, Willerson JT & Perin EC** (2005). Mesenchymal stem cells differentiate into an endothelial phenotype, enhance vascular density, and improve heart function in a canine chronic ischemia model. *Circulation* 111(2): 150-6.
- Silvestre J-S, Gojova A, Brun V, Potteaux S, Esposito B, Duriez M, Clergue M, Le Ricousse-Roussanne S, Barateau V, Merval R, Groux H, Tobelem G, Levy B, Tedgui A & Mallat Z** (2003). Transplantation of bone marrow-derived mononuclear cells in ischemic apolipoprotein E-knockout mice accelerates atherosclerosis without altering plaque composition. *Circulation* 108(23): 2839-42.
- Silvestre J-S, Mallat Z, Tedgui A & Lévy BI** (2008). Post-ischaemic neovascularization and inflammation. *Cardiovascular Research* 78(2): 242-9.

- Simon BH, Ando HY & Gupta PK** (1995). Circulation time and body distribution of ¹⁴C-labeled amino-modified polystyrene nanoparticles in mice. *J Pharm Sci* 84(10): 1249-53.
- Sirker AA, Astroulakis ZMJ & Hill JM** (2009). Vascular progenitor cells and translational research: the role of endothelial and smooth muscle progenitor cells in endogenous arterial remodelling in the adult. *Clin Sci* 116(4): 283-99.
- Song Z, Cai J, Liu Y, Zhao D, Yong J, Duo S, Song X, Guo Y, Zhao Y, Qin H, Yin X, Wu C, Che J, Lu S, Ding M & Deng H** (2009). Efficient generation of hepatocyte-like cells from human induced pluripotent stem cells. *Cell Res* 19(11): 1233-42.
- Soufi A & Jayaraman P-S** (2008). PRH/Hex: an oligomeric transcription factor and multifunctional regulator of cell fate. *Biochem J* 412(3): 399-413.
- Stamm C, Westphal B, Kleine H-D, Petzsch M, Kittner C, Klinge H, Schümichen C, Nienaber CA, Freund M & Steinhoff G** (2003). Autologous bone-marrow stem-cell transplantation for myocardial regeneration. *Lancet* 361(9351): 45-6.
- Staton CA, Reed MWR & Brown NJ** (2009). A critical analysis of current in vitro and in vivo angiogenesis assays. *Int J Exp Pathol* 90(3): 195-221.
- Stein I, Neeman M, Shweiki D, Itin A & Keshet E** (1995). Stabilization of vascular endothelial growth factor mRNA by hypoxia and hypoglycemia and coregulation with other ischemia-induced genes. *Mol Cell Biol* 15(10): 5363-8.
- Steiner S, Niessner A, Ziegler S, Richter B, Seidinger D, Pleiner J, Penka M, Wolzt M, Huber K, Wojta J, Minar E & Kopp CW** (2005). Endurance training increases the number of endothelial progenitor cells in patients with cardiovascular risk and coronary artery disease. *Atherosclerosis* 181(2): 305-10.
- Stone PC & Nash GB** (1999). Conditions under which immobilized platelets activate as well as capture flowing neutrophils. *Br J Haematol* 105(2): 514-22.
- Struijk PC, Stewart PA, Fernando KL, Mathews VJ, Loupas T, Steegers EAP & Wladimiroff JW** (2005). Wall shear stress and related hemodynamic parameters in the fetal descending aorta derived from color Doppler velocity profiles. *Ultrasound Med Biol* 31(11): 1441-50.
- Stump MM, Jordan GL, Debakey ME & Halpert B** (1963). Endothelial grown from circulating blood on isolated intravascular dacron hub. *Am J Pathol* 43: 361-7.
- Suchting S, Freitas C, le Noble F, Benedito R, Bréant C, Duarte A & Eichmann A** (2007). The Notch ligand Delta-like 4 negatively regulates endothelial tip cell formation and vessel branching. *Proc Natl Acad Sci USA* 104(9): 3225-30.
- Suchting S, Heal P, Tahtis K, Stewart LM & Bicknell R** (2005). Soluble Robo4 receptor inhibits in vivo angiogenesis and endothelial cell migration. *FASEB J* 19(1): 121-3.
- Sun X, Cheng L, Duan H & Lu G** (2009). Effects of an endothelial cell-conditioned medium on the hematopoietic and endothelial differentiation of embryonic stem cells. *Cell Biol Int* 33(11): 1201-5.
- Taguchi A, Soma T, Tanaka H, Kanda T, Nishimura H, Yoshikawa H, Tsukamoto Y, Iso H, Fujimori Y, Stern DM, Naritomi H & Matsuyama T** (2004). Administration of CD34+ cells after stroke enhances neurogenesis via angiogenesis in a mouse model. *Journal of Clinical Investigation* 114(3): 330-8.

- Takahashi K & Yamanaka S** (2006). Induction of pluripotent stem cells from mouse embryonic and adult fibroblast cultures by defined factors. *Cell* 126(4): 663-76.
- Takahashi T, Ueno H & Shibuya M** (1999). VEGF activates protein kinase C-dependent, but Ras-independent Raf-MEK-MAP kinase pathway for DNA synthesis in primary endothelial cells. *Oncogene* 18(13): 2221-30.
- Tanaka Y, Fujii K, Hübscher S, Aso M, Takazawa A, Saito K, Ota T & Eto S** (1998). Heparan sulfate proteoglycan on endothelium efficiently induces integrin-mediated T cell adhesion by immobilizing chemokines in patients with rheumatoid synovitis. *Arthritis Rheum* 41(8): 1365-77.
- Taylor CR & Weibel ER** (1981). Design of the mammalian respiratory system. I. Problem and strategy. *Respiration physiology* 44(1): 1-10.
- Tees DFJ & Goetz DJ** (2003). Leukocyte adhesion: an exquisite balance of hydrodynamic and molecular forces. *News Physiol Sci* 18: 186-90.
- Thum T, Fleissner F, Klink I, Tsikas D, Jakob M, Bauersachs J & Stichtenoth DO** (2007). Growth hormone treatment improves markers of systemic nitric oxide bioavailability via insulin-like growth factor-1. *J Clin Endocrinol Metab* 92(11): 4172-9.
- Thum T, Hoerber S, Froese S, Klink I, Stichtenoth DO, Galuppo P, Jakob M, Tsikas D, Anker SD, Poole-Wilson PA, Borlak J, Ertl G & Bauersachs J** (2007). Age-dependent impairment of endothelial progenitor cells is corrected by growth-hormone-mediated increase of insulin-like growth-factor-1. *Circulation Research* 100(3): 434-43.
- Tillmanns J, Rota M, Hosoda T, Misao Y, Esposito G, Gonzalez A, Vitale S, Parolin C, Yasuzawa-Amano S, Muraski J, De Angelis A, Lecapitaine N, Siggins RW, Loredi M, Bearzi C, Bolli R, Urbanek K, Leri A, Kajstura J & Anversa P** (2008). Formation of large coronary arteries by cardiac progenitor cells. *Proc Natl Acad Sci USA* 105(5): 1668-73.
- Tolnai S** (1975). A method for viable cell count. *Methods in Cell Science* 1(1): 37-38.
- Toma C, Pittenger MF, Cahill KS, Byrne BJ & Kessler PD** (2002). Human mesenchymal stem cells differentiate to a cardiomyocyte phenotype in the adult murine heart. *Circulation* 105(1): 93-8.
- Topper JN & Gimbrone MA** (1999). Blood flow and vascular gene expression: fluid shear stress as a modulator of endothelial phenotype. *Mol Med Today* 5(1): 40-6.
- Totsuka Y, Nagao Y, Horii T, Yonekawa H, Imai H, Hatta H, Izaike Y, Tokunaga T & Atomi Y** (2003). Physical performance and soleus muscle fiber composition in wild-derived and laboratory inbred mouse strains. *J Appl Physiol* 95(2): 720-7.
- Tressel SL, Huang R-P, Tomsen N & Jo H** (2007). Laminar shear inhibits tubule formation and migration of endothelial cells by an angiopoietin-2 dependent mechanism. *Arteriosclerosis, Thrombosis, and Vascular Biology* 27(10): 2150-6.
- Urbich C & Dimmeler S** (2004). Endothelial progenitor cells functional characterization. *Trends Cardiovasc Med* 14(8): 318-22.
- Vajkoczy P, Blum S, Lamparter M, Mailhammer R, Erber R, Engelhardt B, Vestweber D & Hatzopoulos AK** (2003). Multistep nature of microvascular recruitment of ex vivo-expanded embryonic endothelial progenitor cells during tumor angiogenesis. *J Exp Med* 197(12): 1755-65.

- van 't Veer C, Hackeng TM, Delahaye C, Sixma JJ & Bouma BN** (1994). Activated factor X and thrombin formation triggered by tissue factor on endothelial cell matrix in a flow model: effect of the tissue factor pathway inhibitor. *Blood* 84(4): 1132-42.
- van der Meer AD, Poot AA, Feijen J & Vermes I** (2010). Analyzing shear stress-induced alignment of actin filaments in endothelial cells with a microfluidic assay. *Biomicrofluidics* 4(1): 11103.
- van Hinsbergh VWM, Engelse MA & Quax PHA** (2006). Pericellular proteases in angiogenesis and vasculogenesis. *Arteriosclerosis, Thrombosis, and Vascular Biology* 26(4): 716-28.
- Varga-Szabo D, Pleines I & Nieswandt B** (2008). Cell adhesion mechanisms in platelets. *Arteriosclerosis, Thrombosis, and Vascular Biology* 28(3): 403-12.
- Vargas JR, Radomski M & Moncada S** (1982). The use of prostacyclin in the separation from plasma and washing of human platelets. *Prostaglandins* 23(6): 929-45.
- Vasa M, Fichtlscherer S, Aicher A, Adler K, Urbich C, Martin H, Zeiher AM & Dimmeler S** (2001). Number and migratory activity of circulating endothelial progenitor cells inversely correlate with risk factors for coronary artery disease. *Circulation Research* 89(1): E1-7.
- Vernay M, Cornic M, Aubery M & Bourrillon R** (1978). Relationship between regeneration of cell surface glycoproteins in trypsin-treated chick embryo fibroblasts and cell adhesion to the substratum. *Experientia* 34(6): 736-7.
- Vestweber D** (1992). Selectins: cell surface lectins which mediate the binding of leukocytes to endothelial cells. *Semin Cell Biol* 3(3): 211-20.
- Vita JA, Treasure CB, Ganz P, Cox DA, Fish RD & Selwyn AP** (1989). Control of shear stress in the epicardial coronary arteries of humans: impairment by atherosclerosis. *Journal of the American College of Cardiology* 14(5): 1193-9.
- Vittet D, Prandini MH, Berthier R, Schweitzer A, Martin-Sisteron H, Uzan G & Dejana E** (1996). Embryonic stem cells differentiate in vitro to endothelial cells through successive maturation steps. *Blood* 88(9): 3424-31.
- Vu TK, Hung DT, Wheaton VI & Coughlin SR** (1991). Molecular cloning of a functional thrombin receptor reveals a novel proteolytic mechanism of receptor activation. *Cell* 64(6): 1057-68.
- Wagner OF, Christ G, Wojta J, Vierhapper H, Parzer S, Nowotny PJ, Schneider B, Waldhäusl W & Binder BR** (1992). Polar secretion of endothelin-1 by cultured endothelial cells. *J Biol Chem* 267(23): 16066-8.
- Wang Y, Dur O, Patrick MJ, Tinney JP, Tobita K, Keller BB & Pekkan K** (2009). Aortic arch morphogenesis and flow modeling in the chick embryo. *Ann Biomed Eng* 37(6): 1069-81.
- Wassmann S, Werner N, Czech T & Nickenig G** (2006). Improvement of endothelial function by systemic transfusion of vascular progenitor cells. *Circulation Research* 99(8): e74-83.
- Weber C** (2005). Platelets and chemokines in atherosclerosis: partners in crime. *Circulation Research* 96(6): 612-6.
- Weimer S, Oertel K & Fuchsbauer H-L** (2006). A quenched fluorescent dipeptide for assaying dispase- and thermolysin-like proteases. *Anal Biochem* 352(1): 110-9.

- Weinstock SB & Brain JD** (1988). Comparison of particle clearance and macrophage phagosomal motion in liver and lungs of rats. *J Appl Physiol* 65(4): 1811-20.
- Weiss HJ, Turitto VT & Baumgartner HR** (1978). Effect of shear rate on platelet interaction with subendothelium in citrated and native blood. I. Shear rate--dependent decrease of adhesion in von Willebrand's disease and the Bernard-Soulier syndrome. *J Lab Clin Med* 92(5): 750-64.
- Welt FGP, Tso C, Edelman ER, Kjelsberg MA, Paolini JF, Seifert P & Rogers C** (2003). Leukocyte recruitment and expression of chemokines following different forms of vascular injury. *Vasc Med* 8(1): 1-7.
- Werner N, Junk S, Laufs U, Link A, Walenta K, Bohm M & Nickenig G** (2003). Intravenous transfusion of endothelial progenitor cells reduces neointima formation after vascular injury. *Circulation Research* 93(2): e17-24.
- Whittingham DG, Leibo SP & Mazur P** (1972). Survival of mouse embryos frozen to -196 degrees and -269 degrees C. *Science* 178(59): 411-4.
- Wilhelm C, Bal L, Smirnov P, Galy-Fauroux I, Clément O, Gazeau F & Emmerich J** (2007). Magnetic control of vascular network formation with magnetically labeled endothelial progenitor cells. *Biomaterials* 28(26): 3797-806.
- Williams JL, Cartland D, Hussain A & Egginton S** (2006). A differential role for nitric oxide in two forms of physiological angiogenesis in mouse. *The Journal of Physiology* 570(Pt 3): 445-54.
- Williams JL, Cartland D, Rudge JS & Egginton S** (2006). VEGF trap abolishes shear stress- and overload-dependent angiogenesis in skeletal muscle. *Microcirculation (New York, NY : 1994)* 13(6): 499-509.
- Williams R, Hilton D, Pease S, Willson T, Stewart C, Gearing D, Wagner E, Metcalf D, Nicola N & Gough N** (1988). Myeloid leukaemia inhibitory factor maintains the developmental potential of embryonic stem cells. *Nature* 336(6200): 684-7.
- Wilmot I, Schnieke AE, McWhir J, Kind AJ & Campbell KH** (1997). Viable offspring derived from fetal and adult mammalian cells. *Nature* 385(6619): 810-3.
- Wittchen ES** (2009). Endothelial signaling in paracellular and transcellular leukocyte transmigration. *Front Biosci* 14: 2522-45.
- Wolfram O, Jentsch-Ullrich K, Wagner A, Hammwöhner M, Steinke R, Franke A, Zupan I, Klein HU & Goette A** (2007). G-CSF-induced mobilization of CD34(+) progenitor cells and proarrhythmic effects in patients with severe coronary artery disease. *Pacing Clin Electrophysiol* 30 Suppl 1: S166-9.
- Wu & Thiagarajan P** (1996). Role of endothelium in thrombosis and hemostasis. *Annu Rev Med* 47: 315-31.
- Wu Y, Chen L, Scott PG & Tredget EE** (2007). Mesenchymal stem cells enhance wound healing through differentiation and angiogenesis. *Stem Cells* 25(10): 2648-59.
- Xiao Q, Kiechl S, Patel S, Oberhollenzer F, Weger S, Mayr A, Metzler B, Reindl M, Hu Y, Willeit J & Xu Q** (2007). Endothelial progenitor cells, cardiovascular risk factors, cytokine levels and atherosclerosis--results from a large population-based study. *PLoS ONE* 2(10): e975.

- Xu C, Inokuma M, Denham J, Golds K, Kundu P, Gold J & Carpenter M** (2001). Feeder-free growth of undifferentiated human embryonic stem cells. *Nat Biotechnol* 19(10): 971-4.
- Yamaguchi J-I, Kusano KF, Masuo O, Kawamoto A, Silver M, Murasawa S, Bosch-Marce M, Masuda H, Losordo DW, Isner JM & Asahara T** (2003). Stromal cell-derived factor-1 effects on ex vivo expanded endothelial progenitor cell recruitment for ischemic neovascularization. *Circulation* 107(9): 1322-8.
- Yamashita J, Itoh H, Hirashima M, Ogawa M, Nishikawa S, Yurugi T, Naito M, Nakao K & Nishikawa S** (2000). Flk1-positive cells derived from embryonic stem cells serve as vascular progenitors. *Nature* 408(6808): 92-6.
- Yanaka K, Spellman SR, McCarthy JB, Oegema TR, Low WC & Camarata PJ** (1996). Reduction of brain injury using heparin to inhibit leukocyte accumulation in a rat model of transient focal cerebral ischemia. I. Protective mechanism. *J Neurosurg* 85(6): 1102-7.
- Yang C, Zhang ZH, Li ZJ, Yang RC, Qian GQ & Han ZC** (2004). Enhancement of neovascularization with cord blood CD133+ cell-derived endothelial progenitor cell transplantation. *Thromb Haemost* 91(6): 1202-12.
- Yang E, Shim JS, Woo H-J, Kim K-W & Kwon HJ** (2007). Aminopeptidase N/CD13 induces angiogenesis through interaction with a pro-angiogenic protein, galectin-3. *Biochemical and Biophysical Research Communications* 363(2): 336-41.
- Ye Z, Zhan H, Mali P, Dowey S, Williams DM, Jang Y-Y, Dang CV, Spivak JL, Moliterno AR & Cheng L** (2009). Human-induced pluripotent stem cells from blood cells of healthy donors and patients with acquired blood disorders. *Blood* 114(27): 5473-80.
- Yeh ETH, Zhang S, Wu HD, Körbling M, Willerson JT & Estrov Z** (2003). Transdifferentiation of human peripheral blood CD34+-enriched cell population into cardiomyocytes, endothelial cells, and smooth muscle cells in vivo. *Circulation* 108(17): 2070-3.
- Ying Q-L, Wray J, Nichols J, Battle-Morera L, Doble B, Woodgett J, Cohen P & Smith A** (2008). The ground state of embryonic stem cell self-renewal. *Nature* 453(7194): 519-23.
- Yoon C-H, Hur J, Oh I-Y, Park K-W, Kim T-Y, Shin J-H, Kim J-H, Lee C-S, Chung J-K, Park Y-B & Kim H-S** (2006). Intercellular adhesion molecule-1 is upregulated in ischemic muscle, which mediates trafficking of endothelial progenitor cells. *Arterioscler Thromb Vasc Biol* 26(5): 1066-72.
- Yu J, Vodyanik MA, Smuga-Otto K, Antosiewicz-Bourget J, Frane JL, Tian S, Nie J, Jonsdottir GA, Ruotti V, Stewart R, Slukvin II & Thomson JA** (2007). Induced pluripotent stem cell lines derived from human somatic cells. *Science* 318(5858): 1917-20.
- Zacharek A, Chen J, Cui X, Li A, Li Y, Roberts C, Feng Y, Gao Q & Chopp M** (2007). Angiopoietin1/Tie2 and VEGF/Flk1 induced by MSC treatment amplifies angiogenesis and vascular stabilization after stroke. *J Cereb Blood Flow Metab* 27(10): 1684-91.
- Zhang H, Li C & Baciuc PC** (2002). Expression of integrins and MMPs during alkaline-burn-induced corneal angiogenesis. *Invest Ophthalmol Vis Sci* 43(4): 955-62.
- Zhang J-J, Yi Z-W, Dang X-Q, He X-J & Wu X-C** (2007). [Mobilization effects of SCF along with G-CSF on bone marrow stem cells and endothelial progenitor cells in rats with unilateral ureteral obstruction]. *Zhongguo Dang Dai Er Ke Za Zhi* 9(2): 144-8.

- Zhang L, Yang R & Han ZC** (2006). Transplantation of umbilical cord blood-derived endothelial progenitor cells: a promising method of therapeutic revascularisation. *Eur J Haematol* 76(1): 1-8.
- Zhang LW & Monteiro-Riviere NA** (2009). Mechanisms of quantum dot nanoparticle cellular uptake. *Toxicol Sci* 110(1): 138-55.
- Zhang W & Chen H** (2001). [The study on the shear stress responsive element in endothelial cells]. *Sheng Wu Yi Xue Gong Cheng Xue Za Zhi* 18(3): 461-5.
- Zhang XW, Liu Q & Thorlacius H** (2001). Inhibition of selectin function and leukocyte rolling protects against dextran sodium sulfate-induced murine colitis. *Scand J Gastroenterol* 36(3): 270-5.
- Zhang Y, Ingram DA, Murphy MP, Saadat-zadeh MR, Mead LE, Prater DN & Rehman J** (2009). Release of proinflammatory mediators and expression of proinflammatory adhesion molecules by endothelial progenitor cells. *Am J Physiol Heart Circ Physiol* 296(5): H1675-82.
- Zhao H-P, Lu G-X & Wang Q-R** (2003). [Bone marrow endothelial cell-conditioned medium promotes hematopoietic differentiation of mouse embryonic stem cells]. *Zhongguo Shi Yan Xue Ye Xue Za Zhi* 11(2): 109-14.
- Zhao Y, Chien S & Weinbaum S** (2001). Dynamic contact forces on leukocyte microvilli and their penetration of the endothelial glycocalyx. *Biophysical Journal* 80(3): 1124-40.
- Zheng W, Wan Y, Ma X, Li X, Yang Z, Yin Q & Yi J** (2010). Isolation of cultured endothelial progenitor cells in vitro from PBMCs and CD133(+) enriched cells. *J Huazhong Univ Sci Technol Med Sci* 30(1): 18-24.
- Zhou A, Egginton S, Hudlická O & Brown MD** (1998). Internal division of capillaries in rat skeletal muscle in response to chronic vasodilator treatment with alpha1-antagonist prazosin. *Cell Tissue Res* 293(2): 293-303.
- Zhu Z, Lu D, Kotanides H, Santiago A, Jimenez X, Simcox T, Hicklin DJ, Bohlen P & Witte L** (1999). Inhibition of vascular endothelial growth factor induced mitogenesis of human endothelial cells by a chimeric anti-kinase insert domain-containing receptor antibody. *Cancer Lett* 136(2): 203-13.
- Ziebart T, Yoon C-H, Trepels T, Wietelmann A, Braun T, Kiessling F, Stein S, Grez M, Ihling C, Muhly-Reinholz M, Carmona G, Urbich C, Zeiher AM & Dimmeler S** (2008). Sustained persistence of transplanted proangiogenic cells contributes to neovascularization and cardiac function after ischemia. *Circulation Research* 103(11): 1327-34.
- Zipper H** (2004). Investigations on DNA intercalation and surface binding by SYBR Green I, its structure determination and methodological implications. *Nucleic Acids Res* 32(12): e103-e03.
- Zou Y, Mirbaha F & Stastny P** (2006). Contact inhibition causes strong downregulation of expression of MICA in human fibroblasts and decreased NK cell killing. *Hum Immunol* 67(3): 183-7.

APPENDIX I:

CULTURE MEDIA, REAGENTS & STOCK SOLUTIONS

All culture media and stock solutions stored at 4°C unless otherwise stated.

EPC culture medium

440 ml	DMEM
50 ml	FBS
5 ml	Penicillin-streptomycin solution (100x)
5 ml	L-glutamine (200 mM)
500 µl	Amphotericin B (25 mg/ml)
250 µl	bFGF (20 µg/ml)

EC culture medium

435 ml	DMEM
50 ml	FBS
5 ml	Penicillin-streptomycin solution (100x)
5 ml	L-glutamine (100x)
5 ml	Heparin (1000 U/ml)
50 µl	Recombinant murine EGF (1 mg/ml)

ESC & iPSC culture medium

415 ml	Knockout DMEM
75 ml	ESC-screened FBS
5 ml	Penicillin-streptomycin solution (100x)
5 ml	L-glutamine (200 mM)
5 ml	Non-essential amino acids (NEAA) (100x)
500 µl	β-mercaptoethanol (0.1 M)*
500 µl	Recombinant murine LIF (10 µg/ml)

***β-mercaptoethanol stock (0.1 M)**

70 µl	β-mercaptoethanol (14.3 M)
10 ml	DMEM

MEF culture medium

415 ml	DMEM
75 ml	FBS
5 ml	Penicillin-streptomycin solution (100x)
5 ml	L-glutamine (200 mM)
5 ml	NEAA (100x)

Cryopreservation medium

6 ml	DMEM
2 ml	FBS
5 ml	DMSO

TAE buffer (50x)

242 g	Tris base
100 ml	EDTA (0.5 M, pH 8.0) [†]
57.1 ml	Acetic acid
842.9 ml	ddH ₂ O

1x working solution produced by diluting 20 ml TAE buffer (50x) in 980 ml ddH₂O.

[†]EDTA stock (0.5 M, pH 8.0)

186.1 g	Disodium EDTA dihydrate
800 ml	ddH ₂ O

Adjusted to pH 8.0 using NaOH.

DNA loading buffer (6x)

40 g	Sucrose
250 mg	Bromophenol blue
250 mg	Xylene cyanol
100 ml	ddH ₂ O

1x working solution produced by 1:6 dilution into PCR product before gel loading.

Antibody blocking solution (stored at room temperature)

200 ml	D-PBS (without calcium)
1.5 g	Glycine (100 mM)
400 mg	Bovine serum albumin
40 mg	Sodium azide

PBSA wash buffer (0.15%)

1 ml	Bovine serum albumin solution (7.5%)
49 ml	D-PBS (with calcium)

Acid-citrate-dextrose (ACD) anticoagulant

12.5 g	Sodium citrate
10 g	Glucose
7.5 g	Citric acid
500 ml	ddH ₂ O

Modified Tyrode's buffer (pH 7.4)

3.913 g	Sodium chloride
2.381 g	HEPES
0.504 g	Sodium bicarbonate
0.109 g	Potassium chloride
0.061 g	Disodium phosphate (12 Hydrate)
0.048 g	Magnesium chloride
500 ml	ddH ₂ O

Add 0.9 mg/ml glucose prior to use. Adjust to pH 7.4 using NaOH.

Gelatin solution (0.1%)

500 mg	Gelatin (from bovine skin, Type B)
500 ml	ddH ₂ O

After being dissolved by magnetic stir-bar, 0.1% gelatin was autoclaved before use.

Paraformaldehyde solution (4% w/v, pH 7.4)

8 g	Paraformaldehyde
200 ml	PBS

Adjusted to pH 7.4 using NaOH. Stored at -20°C.

Ketamine/xylazine anaesthetic

100 µl	Ketamine (100 mg/ml)
50 µl	Xylazine (20 mg/ml)
850 µl	PBS

APPENDIX II:

MULTIPLE mRNA SEQUENCE ALIGNMENTS

Multiple sequence alignments were performed between mRNA transcripts (**transcript**) obtained from NCBI GenBank (<http://www.ncbi.nlm.nih.gov/Genbank>) and the results of RT-PCR product sequencing (**seq result**). Intended regions of amplification are designated by locations of forward (**BLUE**) and reverse (**RED**) primers and consensus between sequences (*) is indicated. Alignments were performed using ClustalW software (European Bioinformatics Institute, Cambridgeshire, UK).

VEGFR2 (NCBI accession NM_010612.2)

```

transcript      TCTGTGGTTCTGCGTGGAGA CCGAGCCGCCTCTGTGGGTTTGCCTGGCGATTTTCTCCA 60
seq result      -----NNNNNNNNNNNNNNNTGC-TGGCGANTTTCTCCN 34
                *** ***** *****

transcript      TCCCCCAAGCTCAGCACACAGAAAGACATACTGACAATTTTGGCAAATACAACCCTTCA 120
seq result      TCCCCCAAGCTCAGCACACAGAAAGACATACTGACAATTTTGGCAAATACAACCCTTCA 94
                *****

transcript      GATTACTTGCAGGGGACAGCGGGACCTGGACTGGCTTTGGCCAATGCTCAGCGTGATTC 180
seq result      GATTACTTGCAGGGGACAGCGGGACCTGGACTGGCTTTGGCCAATGCTCAGCGTGATTC 154
                *****

transcript      TGAGGAAAGGTATTTGGTACTGAATGCGGCGGTGGTGACAGTATCTTCTGCAAACACT 240
seq result      TGAGGAAAGGTATTTGGTACTGAATGCGGCGGTGGTGACAGTATCTTCTGCAAACACT 214
                *****

transcript      CACCATTCCCAGGGTGGTTGGAATGATAC- 270
seq result      CACCATTCCCAGGGTGGTTGGAATGATACA 245
                *****

```

CD31 (NCBI accession NM_008816.2)

```

transcript      ---CGCACCTTGATCTTCCTTCGTTCCATGCC--GAAGGCCCAAAGAAGAGAAATGGCT 56
seq result     NNNNNNNNNNGATCTNNC'TTCCGTTCCATGNCCGAAGGCCCANNGAAGAGAAATGGCT 60
                *****
transcript      GGCTACAACAACGTATTATTTTTTTAATAGTAAAAGGAAATATGTACTTTTCTCACTA 116
seq result     GGCTACAACAACGTATTATTTTTTTAATAGTAAAAGGAAATATGTACTTTTCTCACTA 120
                *****
transcript      ATTTTCTTTATTATTATCCCCACTAAAGAAACGGTTTCCTAAGGCTGAGCTGTTTCCCA 176
seq result     ATTTTCTTTATTATTATCCCCACTAAAGAAACGGTTTCCTAAGGCTGAGCTGTTTCCCA 180
                *****
transcript      GGGTGGGCTAGAGTGGGTGGGCGAGAGCTGCCGACATTTTGTGTACTATACCTAACCTC 236
seq result     GGGTGGGCTAGAGTGGGTGGGCGAGAGCTGCCGACATTTTGTGTACTATACCTAACCTC 240
                *****
transcript      CTGCGCTT---- 244
seq result     CTNNNNNNNNNN 252
                **
    
```

VE-cadherin (NCBI accession NM_009868.4)

```

transcript      -----TC 2
seq result     NNNNNNANNANCTCACTAAAGGGACTAGTCCTGCAGGTTTAAACGAATTCGCCCTTTC 60
                **
transcript      CTCTGCATCCTCACCATCACA GTGATTACCTTGCTGATCATCCTGCGGAGGCGGATCCGG 62
seq result     CTCTGCATCCTCACCATCACAGTGATTACCTTGCTGATCATCCTGCGGAGGCGGATCCGG 120
                *****
transcript      AAGCAGGCGCATGCTCATAGCAAGAGTGCCTGGAGATTCACGAGCAGTTGGTCACTTAC 122
seq result     AAGCAGGCGCATGCTCATAGCAAGAGTGCCTGGAGATTCACGAGCAGTTGGTCACTTAC 180
                *****
    
```

β -actin (NCBI accession NM_007393.3)

```

transcript      CACCACACCTTCTACAATGAGCTGCGTGTGGCCCTGAGGAGCACCTGTGCTGCTCACC 60
seq result     ----NNNNNNNTACAANGAGCTGCGTGTGGCCCTGAGGAGCACCTGTGCTGCTCACC 56
                *****
transcript      GAGGCCCCCTGAACCCTAAGGCCAACCCTGAAAAGATGACCAGATCATGTTTGAGACC 120
seq result     GAGGCCCCCTGAACCCTAAGGCCAACCCTGAAAAGATNNNCCAGATCATGTTTGAGACC 116
                *****
transcript      TTCAACACCCAGCCATGTACGTAGCCATCCAGGCTGTGCTGTCCCTGTATGCCTCTGGT 180
seq result     TTCAACACCCAGCCATGTACGTAGCCATCCAGGCTGTGCTGTCCCTGTATGCCTCNGGT 176
                *****
transcript      CGTACCACAGGCATTGTGATGGACTCCGGAGACGGGGTCA CACCACTGTGCCCATCTAC 240
seq result     CGTACCACAGGCATTGTGATGGACTCCGGAGACGGGGTCA CACCACTGTGCCCATCTAC 234
                *****
    
```

APPENDIX III:

PUBLICATIONS

ORIGINAL ARTICLES ARISING FROM THIS THESIS:

Rae PC, Kelly RD, Egginton S & St John JC (2011). Angiogenic potential of endothelial progenitor cells and embryonic stem cells. *Vascular Cell* 3(1): 11. [Epub ahead of print] **(provided overleaf)**

ABSTRACTS ARISING FROM THIS THESIS:

Rae PC, Nash GB & Egginton S (2011). Platelet-mediated adhesion of endothelial progenitor cells during *in vivo* transplantation. Poster communication; *61st Annual Meeting of the British Microcirculation Society*. William Harvey Research Institute, Barts & the London School of Medicine & Dentistry, UK

Rae PC, Nash GB, St John JC & Egginton S (2010). Adhesion mechanisms underlying capture and immobilisation of flowing endothelial progenitor cells by platelets. Poster communication; *Main Meeting of the Physiology Society*. University of Manchester, UK.

Rae PC, Nash GB, St John JC & Egginton S (2010). The potential role of platelets in endothelial progenitor cell adhesion during angiogenesis. Poster communication; *60th Annual Meeting of the British Microcirculation Society*. Peninsula Medical School, University of Exeter, UK.

Rae PC, Egginton S, St John JC (2009). Endothelial gene expression during *in vitro* tubule formation and progenitor cell transplantation. Poster communication; *59th Annual Meeting of the British Microcirculation Society*. College of Medical & Dental Sciences, University of Birmingham, UK.

OTHER ORIGINAL ARTICLES:

Butler LM, Jeffery HC, Wheat RL, Rae PC, Townsend K, Alkharsah KR, Schulz TF, Nash GB & Blackburn DJ (2011). Kaposi's Sarcoma-associated Herpesvirus infection of endothelial cells inhibits neutrophil recruitment through an IL-6 dependent mechanism – A new paradigm for viral immune evasion. *Journal of Virology* May 4. [Epub ahead of print]

Butler LM, Jeffery HC, Wheat RL, Rae PC, Long HM, Nash GB & Blackburn DJ (2011). Kaposi's Sarcoma-associated Herpesvirus inhibits endothelial cell MHC class II upregulation *via* induction of Suppressor of Cytokine Signalling 3. [In preparation]